Histamine H$_2$- and H$_3$-Receptor Antagonists: Synthesis and Characterization of Radio-labelled and Fluorescent Pharmacological Tools

Dissertation

Zur Erlangung des Doktorgrades der Naturwissenschaften (Dr. rer. nat.)

der Fakultät für Chemie und Pharmazie

der Universität Regensburg

vorgelegt von

Daniela Erdmann

aus Burlafingen

2010

Die vorliegende Arbeit entstand in der Zeit von Mai 2006 bis Dezember 2010 unter der Leitung von Herrn Prof Dr. A. Buschauer und Herrn Prof. Dr. G. Bernhardt am Institut für Pharmazie der Naturwissenschaftlichen Fakultät IV –Chemie und Pharmazie- der Universität Regensburg

Das Promotionsgesuch wurde eingereicht im Dezember 2010.

Tag der mündlichen Prüfung: 16.12.2010

Prüfungsausschuß: Prof. Dr. Dr. W. Wiegrebe   (Vorsitzender)

Prof. Dr. A. Buschauer   (Erstgutachter)

Prof. Dr. G. Bernhardt   (Zweitgutachter)

Prof. Dr. J. Heilmann   (Drittprüfer)

Danksagung

II

Poster Presentations

Erdmann D., Gross D., Mosandl J., Bernhardt G., Seifert R., Elz S., Wolfbeis O.S., Buschauer A., *"Synthesis and pharmacological activity of fluorescent histamine H_2 receptor ligands",* Annual meeting of the German Pharmaceutical Society (DPhG), Erlangen, Germany, October 10-13, 2007

Erdmann D., Gross D., Mosandl J., Bernhardt G., Seifert R., Wolfbeis O.S., Buschauer A., *"Synthesis and pharmacological activity of fluorescent histamine H_2 receptor ligands"(modified version), Annual meeting "Frontiers* in Medicinal Chemistry", University of Regensburg, Germany, March 02 -05, 2008

Erdmann D., Mosandl J., Bernhardt G., Seifert R., Wolfbeis O.S., Buschauer A., *"Pharmacological activity and selectivity of fluorescent histamine H_2 receptor antagonists",* 4th Summer School Medicinal Chemistry, University of Regensburg, Germany, September 29- October 01, 2008

Mosandl J., Erdmann D., Bernhardt G., Seifert R., Elz S., Wolfbeis O.S., Buschauer A., *"A flow cytometric binding assay for the human histamine H_2 receptor (hH_2R)",* 4th Summer School Medicinal Chemistry, University of Regensburg, Germany, September 29- October 01, 2008

Erdmann D., Mosandl J., Bernhardt G., Seifert R., Wolfbeis O.S., Buschauer A., *"Antagonistic activity and selectivity of fluorescent histamine H_2 and H_3 receptor ligands", "Frontiers* in Medicinal Chemistry", University of Heidelberg, Germany, March 15-18, 2009

Erdmann D., Mosandl J., Bernhardt G., Seifert R., Wolfbeis O.S., Buschauer A., *"Antagonistic activity and selectivity of fluorescent histamine H_2 and H_3 receptor ligands"(modified version),* XXXVIIIth Meeting European Histamine Research Society, Fulda, Germany, May 13-16, 2009

Erdmann D., Mosandl J., Nordemann U., Bernhardt G., Wolfbeis O.S., Seifert R., Buschauer A., *"Pharmacological activity and selectivity of fluorescent histamine H_3 receptor ligands",* Annual meeting of the German Pharmaceutical Society (DPhG), Jena, Germany, September 28- October 1, 2009

Erdmann D., Lopuch M., Elz S., Bernhardt G., Buschauer A., *"[^{3}H]UR-DE257: a new radioligand for the histamine H_2 receptor",* 5th Summer School Medicinal Chemistry, University of Regensburg, Germany, September 13- September 15, 2010

Contents

Abbreviations

AA	amino acid(s)
AC	adenylyl cyclase
aq.	aqueous
B_{max}	maximum number of binding sites
Boc	tert- butoxycarbonyl
Bq	Becquerel
bs	broad singulet
BSA	bovine serum albumin
c	concentration
$[Ca^{2+}]_i$	intracellular calcium ion concentration
cAMP	cyclic 3', 5'- adenosine-monophosphate
CDI	carbonyldiimidazole
CH_2Cl_2	methylene chloride
$CHCl_3$ (d)	chloroform (d =deuterated)
Ci	curie
CI	chemical ionization
CNS	central nervous system
COSY	correlated spectroscopy
d	doublet or day (s)
DAG	diacylglycerol
δ	chemical shift
DCC	N,N'-dicyclohexylcarbodiimide
decomp.	decomposition
$CDCl_3$	deuterated chloroform
DMEM	Dulbecco's modified eagle medium
DMF	N,N-dimethylformamide
DMSO	dimethylsulfoxide
$DMSO-d_6$	per-deuterated dimethylsulfoxide
EC_{50}	agonist concentration which induces 50 % of the maximum response
EDTA	ethylendiamineteraacetic acid
EtOAc	ethyl acetate
EI	electron impact ionization
E_{max}	maximal response relative to histamine (1.0)

eq	equivalent(s)
ES	electrospray ionization
EtOH	ethanol
FAB	fast atom bombardment
FBS (=FCS)	fetal bovine serum
Fl-1, Fl-2, Fl-3, Fl-4	fluorescence channels (Flow cytometer)
FLAG	octapeptide epitope for the labelling of proteins
FRET	fluorescence resonance energy transfer
GDP	guanosine diphosphate
GTP	guanosine triphosphate
GPCR	G-protein coupled receptor
gp	guinea pig
gpH_2R	guinea pig H_2 receptor
h	hour(s)
HEK293 cells	human embryonic kidney cells
HMBC	heteronuclear multiple bond correlation
HRMS	high resolution mass spectrometry
HR	histamine receptor
hH_xR	human histamine H_x receptor (x= 1,2,3,4)
$hH_2R\text{-}G_{s\alpha S}$	fusion protein of the hH_2R and short splice varian of G_s
$hH_4R\text{-}RGS19$	fusion protein of the hH_4R and RGS19
His_6	hexahistidine tag for labelling and purification of proteins
HPLC	high performance (pressure) liquid chromatography
HSQC	heteronuclear single quantum coherence
IC_{50}	antagonist concentration causing 50 % inhibition
IP_3	inositol-1,4,5-trisphosphate
IR	infrared spectroscopy
^nJ	coupling constant for geminal (n = 2), vicinal (n = 3), etc. coupling
k	retention (capacity) factor
$K_{b'}$	dissociation constant derived from a functional assay
K_D	dissociation constant derived from a saturation binding experiment
K_i	dissociation constant derived from a competition binding assay
L15	Leibovitz medium without phenol red
k_{ob}	observed/macroscopic association rate constant
k_{off}	dissociation rate constant

k_{on}	association rate constant
logP	logarithm of the n-octanol/water partition coefficient
LSI	liquid secondary ion
m	multiplet
M	molar (mol/L)
MAPK	mitogen- activated protein kinase
MeCN	acetonitrile
MeOH	methanol
MeOH-d_4	per-deuterated methanol
mol	mole (s)
mp	melting point
mRNA	messenger RNA
NEt$_3$	triethylamine
NHS	N-hydroxysuccinimide
PBS	phosphate buffered saline
PFA	paraformaldehyde
PE	petroleum ether
PEI	polyethyleneimine
PET	positron emission tomography
P$_i$	inorganic phosphate
PIP$_2$	phopshatidylinositol-4,5-bisphosphate
PKA	protein kinase A
PKC	protein kinase C
Ph	phenyl
ppm	parts per million
q	quaternary C-atom
qua	quartet
qui	quintet
qs5-HA	chimeric G$_{\alpha q}$ proteins which incorporate a HA epitope
RP	reversed-phase
r^2	coefficient of determination
rt	room temperature
R	inactive state of a GPCR
R*	active state of a GPCR
RGS	regulator of G-protein signalling
rpm	revolutions per minute

s	(1) singulet, (2) second(s)
S.E.M.	standard error of the mean
Sf9	*Spodoptera frugiperda* insect cell line
t	(1) time, (2) triplet
t_0	dead time
TFA	trifluoroacetic acid
THF	tetrahydrofurane
TLC	thin layer chromatography
TM	transmembrane
t_R	retention time
Tris	tris (hydroxymethyl) aminoethane
UV	ultraviolet

Chapter 1

General introduction

1   General introduction

1.1   G-protein coupled receptors

1.1.1   GPCRs as drug targets

G-protein coupled receptors, also known as seven transmembrane receptors (7TMs [1]), represent the largest family of cell surface receptors. This accounts for about 800 genes i.e. 2 % of the human genome[2]. Half of these receptors are chemosensory receptors responding to external signals like pheromones, fragrances or flavors. The residual receptors are addressed by endogenous ligands like peptides, lipids, neurotransmitters or nucleotides. Endogenous ligands have been identified for more than 200 of the GPCRs. "Orphan" receptors within the GPCRs are those of which the endogenous ligand is not known yet. GPCRs influence a lot of important physiological processes, and are involved in a variety of diseases, including asthma, inflammation, pain, obesity, cancer and cardiovascular, metabolic, gastrointestinal and CNS diseases. This makes GPCRs the main class of therapeutic targets, addressed by about 30 % of the currently marketed drugs[2-3]. GPCRs are characterized by seven α-helical transmembrane (TM) domains linked by three alternating intracellular and extracellular loops, with an intracellular carboxy terminus and an extracellular amino terminus. Additionally, upon extracellular ligand binding they can transduce the signal from the extracellular side into the cell via interaction with G-proteins[4]. However, G-protein independent pathways are possible. Therefore, the term seven transmembrane (7TM) receptors seem more appropriate. GPCRs can be divided in five main families termed glutamate, rhodopsin, adhesion, frizzled/taste2 and secretin. The rhodopsin-like family, also referred to as class A GPCRs, constitutes the largest family, containing receptors for odorants, small molecules like biogenic amines, peptides and glycoprotein hormones.

The first insight into the three dimensional architecture of GPCRs was provided by the crystal structure of bovine rhodopsin in 2000[5-6]. Further structures have been resolved recently, such as the human β2-adrenoceptor[6-7] the turkey β1-adrenergic receptor[8], the human adenosine 2A receptor[9] and opsin[10-11]. Except for the opsin structure, all these structures represent the receptors in the inactive state. The most recent structure of opsin might provide more insight into active receptor conformations and could serve as template for GPCR homology models to study GPCR conformations and ligand receptor interactions.

1.1.2 Signal transduction pathway

A GPCR in the active conformation (with agonist bound or in the agonist free, constitutively active form) is able to activate heterotrimeric G-proteins, which transduce the signal into the cell. Binding of the G-protein to the GPCR, induces a conformational change and GDP, which is bound to the G_α-subunit in the inactive state, is released, resulting in the ternary complex "ligand + receptor + G-protein". The ternary complex is characterized through high affinity for agonists. Binding of GTP disrupts this complex. This exchange of GDP by GTP promotes the dissociation of the G_α-subunit from the $G_{\beta\gamma}$- heterodimer and the receptor. Subsequently, effector proteins are activated or inhibited by these G-protein subunits, for instance, enzymes or ion channels. The intrinsic GTPase activity of the G_α-subunit leads to conversion of GTP to GDP and P_i. The G_α-induced signal transduction is terminated and the subunits reassociate allowing new cycles [12-13]. The hydrolysis of GTP is accelerated by regulators of G-protein signalling, for example RGS proteins[14], which are in use in the GTPase assays applied in this work. A scheme of the G-protein cycle is depicted in Figure 1.1.
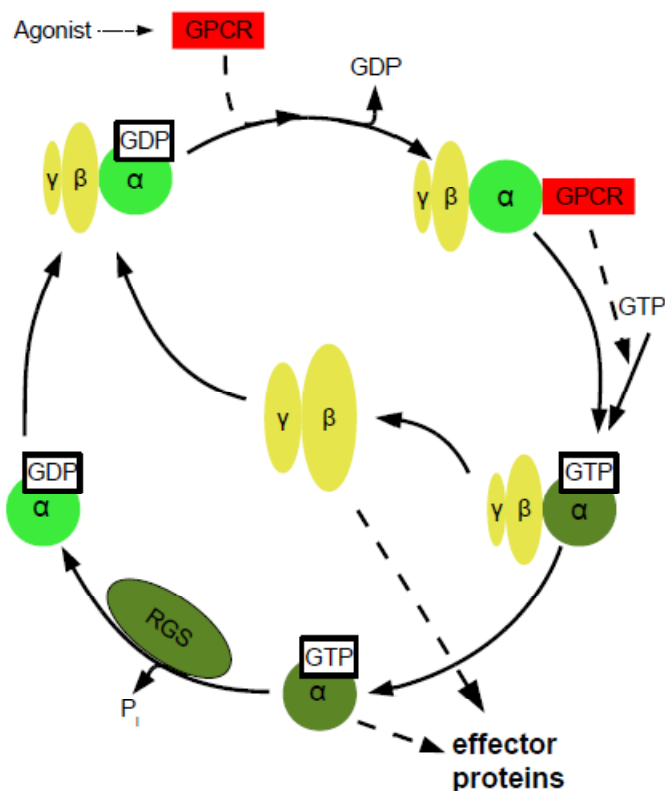
Figure 1.1: G-protein cycle (activation and deactivation) after stimulation by an agonist; adapted from [15].

G-proteins are classified according to their G_{α}-subunits into four main families[12]: $G_{\alpha S}$, $G_{\alpha i}$, $G_{\alpha q}$ and $G_{\alpha 12}$. Receptors of the $G_{\alpha S}$ family stimulate adenylyl cyclase (AC), which leads to increases in intracellular cAMP levels, resulting in the activation of proteinkinase A (PKA), which leads to a variety of cellular responses. Proteins from the $G_{\alpha i}$ family inhibit the adenylylcyclase, whereas $G_{\alpha q}$ proteins stimulate phospholipase Cβ (PLCβ), catalyzing the cleavage of phosphatidylinositol-bisphosphate to diacylglycerol (DAG) and inositol-1,4,5-trisphosphate (IP3). Elevated IP_3 levels result in a release of intracellular calcium from the endoplasmatic reticulum. Calcium ions and DAG can stimulate proteinkinase C (PKC), which in turn activates various intracellular proteins by phosphorylation[16]. The $G_{\beta\gamma}$-heterodimers can also trigger cellular effects, e.g. activation of PLCβ and regulation of ion channels[12].

1.1.3   Models of receptor activation

To explain the interaction between a GPCR, its ligand and the respective G-protein, several models have been proposed as depicted in Figure 1.2. The simplest among these models is the ternary complex model[17], where binding of an agonist to the receptor enables its interaction with the G-protein. In this model four receptor species are considered: unoccupied receptor (R), agonist bound receptor (AR), receptor bound to the G-protein (RG) and the agonist bound to the receptor with the G-protein forming the ternary complex. However, with such a model the phenomen of constitutive activity or inverse agonistic activity can not be explained. Further evaluations resulted in the extended ternary complex model, with 6 possible receptor species[18]. In this model the receptor can adopt an inactive (R) and an active receptor state (R*) [19], independent from ligand binding. Full agonists stabilize the active conformation, whereas inverse agonists can shift the equilibrium to the inactive state. Both effects lead to changes in the basal acitivity of the receptor. In conclusion, partial agonists/partial inverse agonists only partially bind and stabilize the respective receptor state. According to this model neutral (silent) antagonists do not change basal activity and do not differentiate between the two receptor states R and R*[19]. In addition to this approach, the cubic ternary complex model[20-22] comprises possible interactions of inactive receptors with G-proteins (non-signalling complexes). However, these models can not fully describe all observed experimental findings. GPCRs are at present assumed to exist in multiple active and inactive state conformations. There is evidence that different agonists can stabilize different distinct receptor conformations, resulting in diverse biological answers. These observations may play a role in modulating different signal transduction pathways of a receptor by different specific ligands. Furthermore, the assumption that receptors can adopt several inactive

and active states can serve to explain effects such as unsurmountable antagonism[23-24]. To sum up, it should be taken into account that these models are only theoretical approaches and that they can not fully describe reality. Anyway, they are regarded as useful approaches to explain ligand binding and receptor activation.
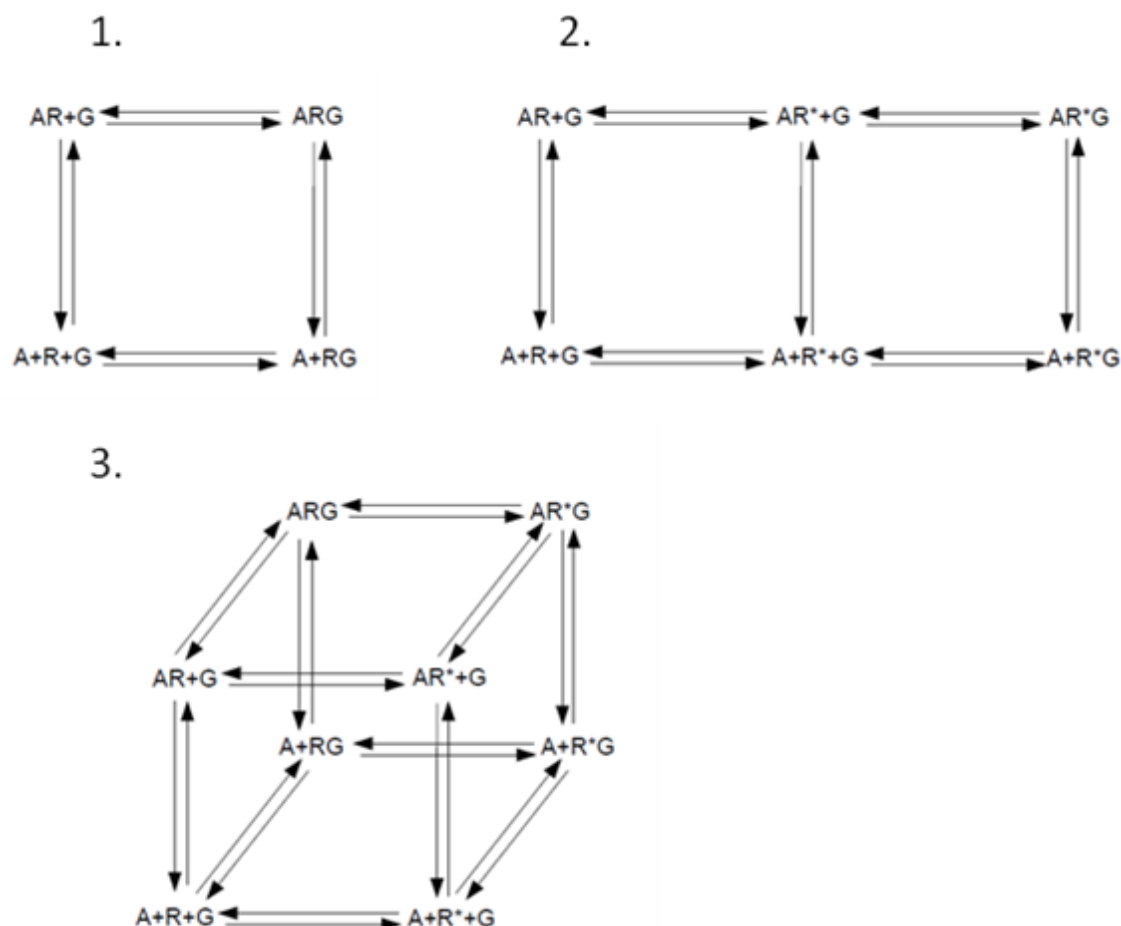
Figure 1.2: Models explaining the interactions between GPCR, agonist and G-protein: R: inactive state of the receptor; R*: active state of the receptor; G: G-protein; A: agonist; **1.** Ternary complex model (no discrimination between R and R*); **2.** Extended ternary complex model: discrimination between R and R*; C, **3.** Cubic ternary complex model: interaction of G with R leading to non-signaling complexes is possible; adapted from[17, 21-22]

1.1.4   GPCR oligmers

It is widely accepted that GPCRs not only exist as monomers, but can form dimers, oligomers and heteromers [25-26]. They are suggested to interact via their extracellular loops, transmembrane helices and intracellular loops, to form covalent and noncovalent interactions. As a result, e.g. for dimers, two binding domains can be created upon a mutual exchange of the transmembrane

domains from both receptors ("domain swapped receptors"[27-28]). Although no clear consensus exists about the role of receptor dimerization, potential roles in receptor transport to the membrane, signal transduction and internalization are proposed[26]. For heterodimers, for example, cross talk and mutual regulations between specific receptor subtypes are assumed, as well as possible alterations in receptor pharmacology[25]. Several techniques are used to investigate putative receptor dimers and oligomers (see chapter 4). One approach is the creation of bivalent ligands to target the respective oligomers and to investigate their function and biological role. These aspects will be discussed in chapter 4 in more detail.

1.2 Histamine receptors

1.2.1 The biogenic amine histamine as an endogeneous agonist

The biogenic amine histamine was first synthesized over a century ago in 1908 by Windhaus and Vogt and isolated from ergot in 1910 by Sir Henry Dale[29] and his colleagues, who investigated its biological activity for the first time[30]. Histamine has two basic centers, with the strongly basic primary amino group in the side chain (pK_a =9.4) and the imidazole ring with lower basicity (pK_a = 5.8). At physiological pH the monocation dominates[31], the tautomeric forms[32] of which are depicted in Figure 1.3.
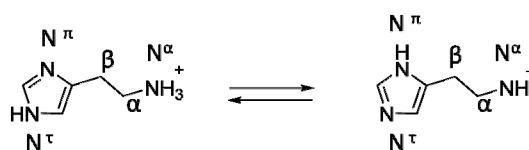
Figure 1.3: Tautomeric forms of histamine (as monocation)

In the body histamine is formed by decarboxylation of L-histidine via the enzyme L-hisitidine decarboxylase and the cofactor pyridoxalphosphate[33]. Histamine has a short half life and is inactivated by two pathways via the enzymes diamine oxidase and histamine N-methyl transferase. In the main metabolic pathway the N^τ nitrogen is methylated by N-methyl transferase, followed by oxidation to the carboxylic acid. The second pathway includes oxidation steps via the enzymes diamine oxidase and xanthin oxidase to imidazole-4-acetic acid and subsequent conjugation to ribose[34] (Scheme 1.1).
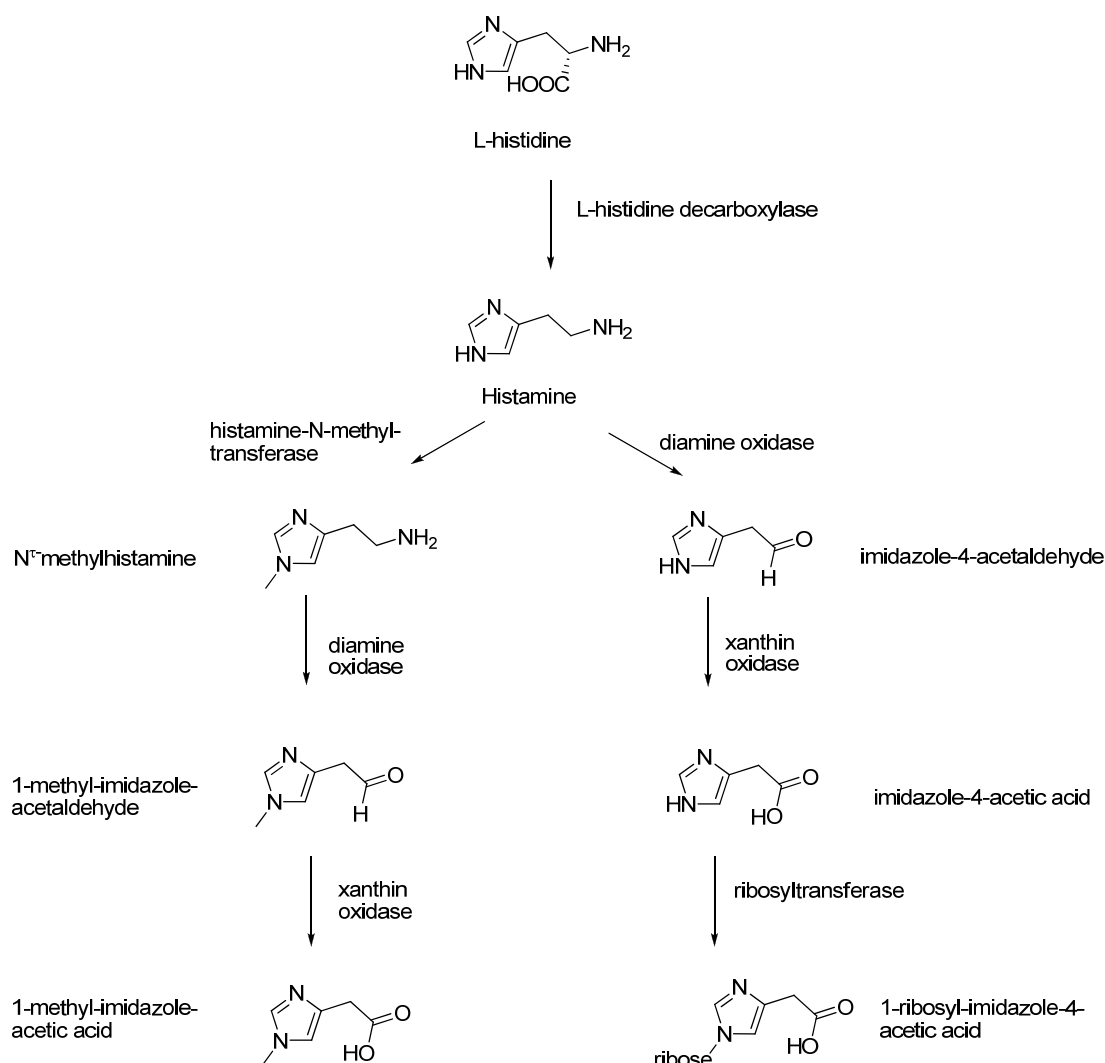
Scheme 1.1: Biosynthesis and metabolism of histamine

Histamine is involved in physiological and pathological processes such as secretion of hormones, regulation of gastic acid secretion, cardiovascular homeostasis, inflammatory reactions, regulation of neurotransmission and brain functions[35-36]. It is distributed all over the body, with high concentrations in the lung, skin and the gastrointestinal tract[30]. Additionally, histamine is located in mast cells, basophils, endothelial cells and in neurons[37]. Histamine in mast cells and basophils is released from secretory granules as response to immunological stimuli. Examples are allergic reactions, where histamine release leads to vasodilatation, smooth muscle contraction and increases in vascular permeability[38]. Histamine can also be released from these cells through destruction of the latter or e.g. by drugs like morphine and muscle relaxants or by toxins. Histamine release from enterochromaffine like cells plays a key role in regulating gastric acid secre-

tion[39]. In the CNS histamine is mainly found in the tuberomamillary nucleus of the posterior hypothalamus[40]. As a neurotransmitter histamine regulates functions like sleep and wakefulness, learning processes or endocrine homeostasis[40]. In cells of the immune system, like macrophages, T-cells, dendritic cells and neutrophils histamine is released without prior storage and regulated by cytokines[38, 41].

Histamine excerts its effects through four histamine receptor subtypes (HR), named H_1R, H_2R, H_3R and H_4R, which belong to class A^4 (rhodopsin like) G-protein coupled receptors.

1.2.2   The H_1-receptor

The first compounds acting as antihistamines were developed in the 1930s by Bovet & Staub, counteracting some pathophysiological actions of histamine on vascular dilation and smooth muscle contraction during anaphylactic responses. In the following many substances with similar effects were identified leading to the discovery of the now called "classical antihistamines", including mepyramine (Neoantergan™), diphenhydramine (Benadryl™), chlorpheniramine or promethazine[30, 42]. These histamine receptors were referred to as H_1-receptors[43] and the "antihistamines" were classified as H_1 receptor antagonists as a consequence of the discovery of an additional histamine receptor subtype (H_2R) in the 1960s. The hH_1R, first cloned in 1993[44], is a GPCR preferentially coupling to $G_{q/11}$ proteins[45]. Histamine stimulates phospholipase C, mainly leading to inositol trisphosphate accumulation and intracellular calcium mobilization[36]. Additionally, activation of (recombinant) H_1R can lead to an increase in intracellular cAMP levels[46]. The H_1R is present in many tissues, e.g. in airway smooth muscle cells, in the cardiovascular system, blood vessels, in the mammalian brain, lymphocytes or the gastrointestinal tract[36, 45]. Upon receptor stimulation the typical symptoms of allergic and inflammatory reactions, such as bronchoconstriction, urticaria or decrease in blood pressure are observed. In the brain the H_1R receptor plays a role in the circadian rhythm (e.g. wakefulness), in cognitive processes, thermoregulation and pain. H_1R antagonists were originally developed for the treatment of allergic diseases. The classical antihistamines (1st generation antagonists, see above) suffered from drawbacks like sedating effects, due to their ability in crossing the blood brain barrier. Newer 2nd generation antagonists, such as cetirizine, or loratadine, are more hydrophilic compounds and lack these side effects[36]. They are successfully applied for diseases like allergic rhinitis, whereas the more lipophilic ones are used as mild sleeping pills or against travel sickness. H_1R agonists are mainly used as pharmacological tools to analyze H_1R function on the cellular level and in organs. The

only agonist used as a drug is betahistine to treat Menières disease[47]. Among the H_1R agonists used as pharmacological tools are small molecules like histamine (non-selective), 2-methyl-histamine or substances with more bulky aromatic groups in 2-position of the imidazole ring, which are more potent agonists e.g. histaprodifens/suprahistaprodifens[48-49] (35 fold increase in potency compared to histamine). Selected H_1R ligands are depicted in Figure 1.4.
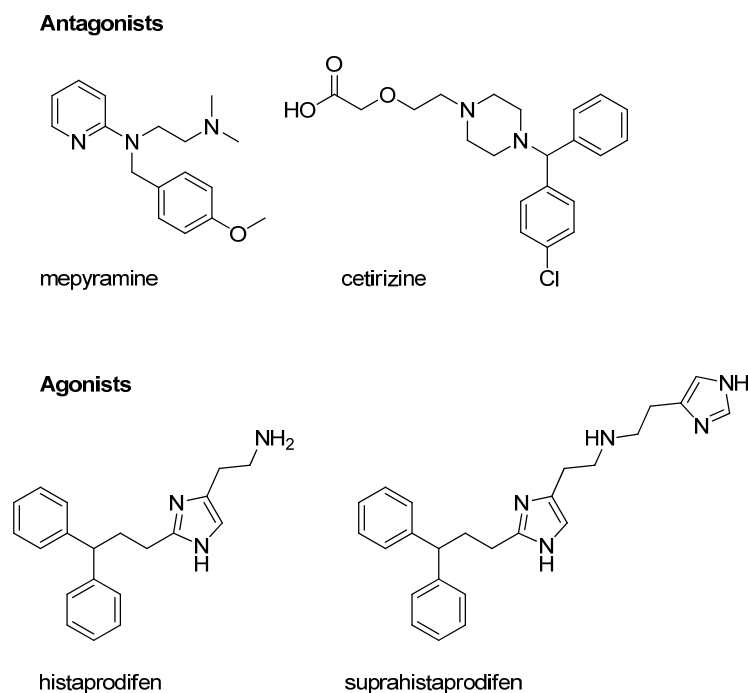
Figure 1.4: Selected H_1R ligands

1.2.3 The H_2-receptor

In the 1940s, as certain effects of histamine could not be prevented by the available antihistamines, such as cardiac chronotropism and gastric acid secretion, the existence of two distinct receptors for histamine action was suggested[43]. In 1972 the development of burimamide[50], the first compound antagonizing the histamine-stimulated gastric acid secretion, confirmed the existence of the second histamine receptor, named H_2 receptor. Starting from burimamide a series of potent H_2R antagonists were discovered such as metiamide[51] and the first marketed drug for the treatment of duodenal ulcer, cimetidine (Tagamet®). Cimetidine and the subsequently discovered "H_2 blockers", e.g. ranitidine (Zantic®) and famotidine (Pepdul®), became for some decades blockbuster drugs in the treatment of gastric and duodenal ulcers (for reviews see [30, 36]). Meanwhile the importance of the H_2R antagonists declined due to the introduction of proton pump inhibitors into therapy.

Cloning of the H_2R, which conists of 359 amino acids and couples to G_s-proteins, was published in 1991[52]. Activation of the H_2R leads to increases in cAMP levels[36, 53]. cAMP can activate protein kinases, which phosphorylate regulatory proteins, leading to calcium influx and intracellular calcium mobilisation, for example in cardiac myocytes (see Figure 1.5). Additionally, coupling to G_q proteins, resulting in increases of the intracellular calcium levels was reported[46, 54]. Expression levels of the H_2R are high in gastric parietal cells[55], in the heart[56], neurons[40], vascular, airway and uterine smooth muscle cells[57] and immune cells[38]. An important physiological function is the control of gastric acid secretion from parietal cells[50]. Other functions are positive chronotropic and inotropic response upon stimulation of cardiac H_2Rs[50] and smooth muscle relaxation for example in blood vessels. Additionally the H_2R has certain effects on immune cells, such as modulation of cytokine production, blocking histamine release from mast cells or induction of cell differentiation[58]. In the CNS H_2R effects are mainly stimulatory. Histamine can inhibit the long – lasting afterhyperpolarization after calcium influx, influencing the accommodation of firing[40].
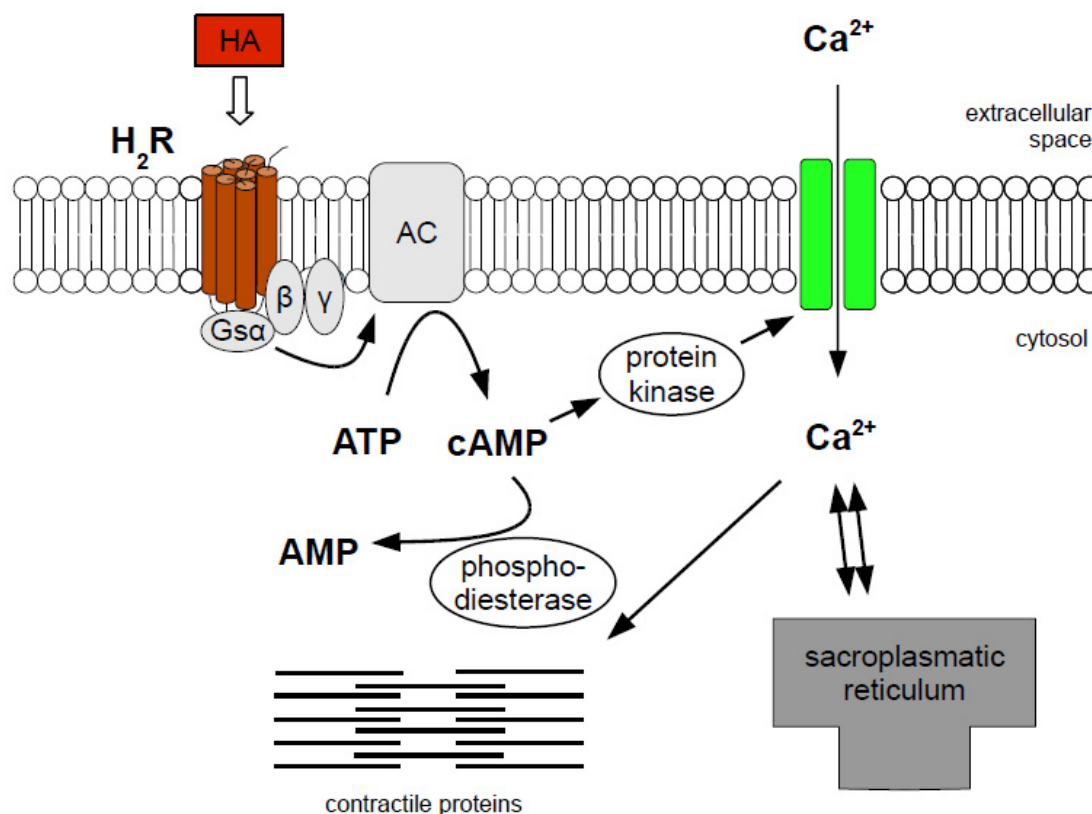
Figure 1.5: H_2R mediated signalling. Cardiac myocyte as example, adapted from [59] and [53]

Thus H_2R agonists are valuable pharmacological tools and possibly useful with respect to therapeutic applications. H_2R agonists are regarded as potential drugs for the treatment of congestive

heart failure[60-61] or as differentiation inducers in leukemia[58]. The endogenous ligand histamine is suggested to bind in its N^τ-tautomeric form to the receptor to amino acids in the transmembrane domains TM3 and TM5. The primary amino group (protonated) interacts with the conserved Asp-98 in TM3. The imidazole N^π –H can form a hydrogen bond with Asp-186 in TM5 and the second imidazole nitrogen (N^τ)interacts with Tyr-182 in TM5[62-63]. Alternatively, Thr-190 may participate in binding instead of Tyr-182[64]. Among the H_2R agonists are amine-type and guanidine-type agonists, such as amthamine, dimaprit[65-66], impromidine or arpromidine and analogues [67-68]. Arpromidine shows up to 400 times the potency of histamine at the gpH_2R. Pharmacokinetic limitations of the guanidine type agonists due to the strongly basic guanidine moiety, like insufficient oral bioavailability and brain penetration, led to the development of the less basic N^G-acylated imidazolylalkylguanidines. They are potent H_2R agonists[69], orally available and capable of penetrating the blood brain barrier (e.g., UR-AK24). Many N^G-acylated imidazolylalkylguanidines are H_3R and H_4R ligands as well. The search for a bioisosteric replacement of the imidazole ring resulted in 2-aminothiazoles, which are highly potent and selective H_2R agonists (e. g. UR-PG267, see Figure 1.6)[70]. Structural variations of this structural motif also led to the synthesis of bivalent ligands, the most potent H_2R agonists known so far (e. g. UR-AK480), which were designed with respect to the investigation of putative receptor dimers.

Regardless of the declining therapeutic relevance of H_2R antagonists, there is a need for more selective ligands (agonists and antagonists) to study the physiological role of the H_2R. Especially many of the previously used standard compounds turned out not to sufficiently discriminate between H_3R and H_4R. Numerous H_2R antagonists used as pharmacological tools resulted from the development of the marketed drugs or from academic research in the H_2R field at its peak, for instance, the radioligands [^{3}H]tiotidine and [^{125}I]iodoaminopotentidine (see Figure 1.6).

Agonists
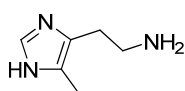
5-methylhistamine
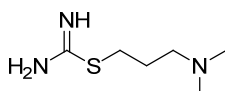
dimaprit
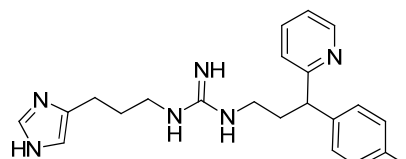
arpromidine
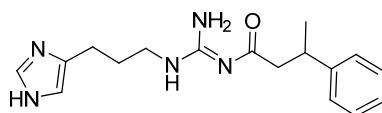
UR-AK24
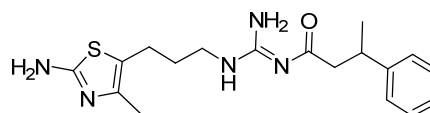
UR-PG276
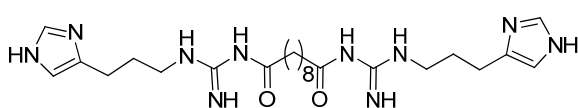
UR-AK480

Antagonists
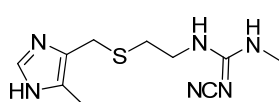
cimetidine
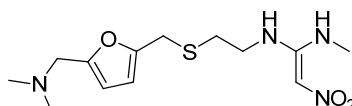
ranitidine
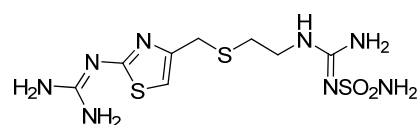
famotidine
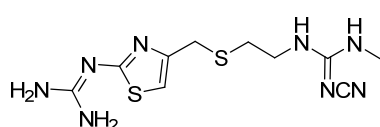
tiotidine
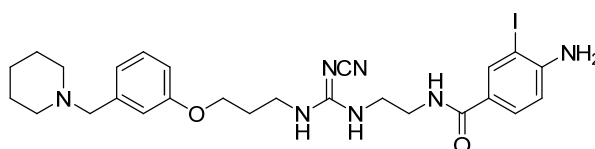
Iodoaminopotentidine

Figure 1.6: Selected H_2R ligands

1.2.4   The H_3-receptor

In 1983 Schwartz and coworkers[71] reported that histamine can inhibit its own synthesis and re-
lease in rat cerebral cortical slices, indicating the existence of a third histamine receptor (H_3).
Subsequently, the discovery of (*R*)-α-methylhistamine, acting as agonist and thioperamide, act-
ing as antagonist, confirmed this suggestion and defined the H_3-receptor[72]. In 1999 cloning of
the H_3R was reported[73]. The H_3R shares low sequence homology with the H_1 and H_2 receptor[30]. In
contrast to H_1R and H_2R-receptors, at least 20 isoforms of the H_3R exist[74], from which the best
characterized is the one described by Lovenberg et al., consisting of 445 amino acids[73]. The his-

tamine H_3-receptor is a presynaptic autoreceptor that can inhibit its own release and synthesis. Furthermore, it functions as a heteroreceptor on non-histaminergic neurons, regulating the release of several neurotransmitters, such as norepinephrine, acetylcholine, dopamine, serotonin and GABA[30, 40, 75]. Histaminergic neurons are present in the tuberomammilary nucleus of the hypothalamus projecting to different brain areas[76]. The majority of H_3Rs is expressed in the brain, for example in the cerebral cortex, hippocampus, amygdala, striatum, hypothalamus or the nucleus accumbens. It is supposed to be involved in sleep and wakefulness, energy homeostasis and cognitive processes. Therefore potential therapeutic applications are thought to be sleep and wake disorders[77] (e.g. narcolepsy), cognitive disorders[78] (e. g. Alzheimer's disease), schizophrenia[79], pain or obesity[80]. The H_3R couples to $G_{i/o}$ proteins. Thus, cAMP levels are lowered and downstream effects like modulation of gene transcription via the cAMP-response-element binding protein (CREB) are reduced. Additionally pathways, such as mitogen activated kinase (MAPK) and phosphatidylinositol 3-kinase pathways (PI3K) are influenced. Activation of phospholipase A_2 (PLA$_2$), which leads to arachidonic acid release, as well as inhibitory effects on the Na^+/H^+ exchanger and lowering of intracellular calcium levels can result from H_3R activation (Figure 1.4)[74, 76]. Activation of MAPK and PI3K leads to downstream effects associated with memory consolidation. Dysregulations in these downstream effects are associated, for example, with diabetes and Alzheimer's disease (for detailed review see [76]).
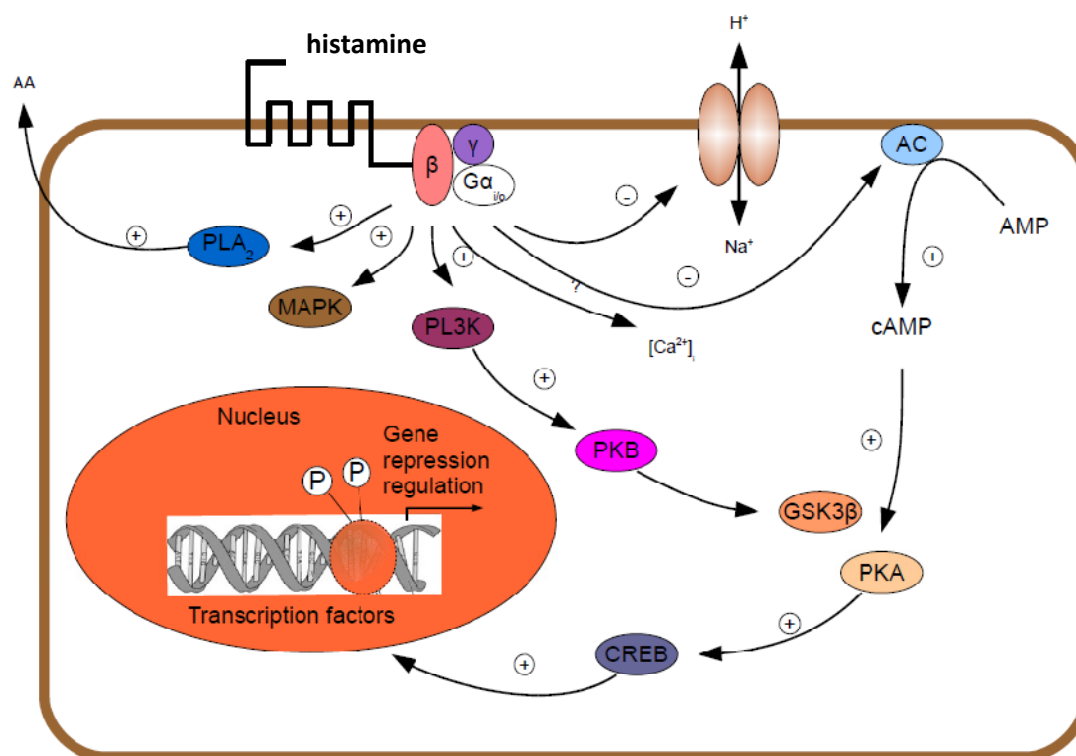
Figure 1.7: Assumed H$_3$R mediated signal transduction pathways, adapted from[76]

H$_3$R agonists are generally derivatives of histamine, such as N$^\alpha$-methylhistamine (in use as radio-ligand), (R)-α-methylhistamine, imetit, immepip and methimepip, which is a potent and selective agonist. Prominent partial agonists are proxyfan or cipralisant (GT-2331). Due to the high sequence homology of the receptors many H$_3$R ligands are also active at the H$_4$R. For example thioperamide, originally identified as selective H$_3$R antagonist has similar affinity for the H$_4$R. As the H$_3$R is constitutively active[76, 81], thioperamide and other H$_3$R ligands were reclassified as inverse agonists. In the last decade several HR subtype selective non–imidazole compounds (antagonists and inverse agonists) were developed, for instance, JNJ5207852[82], BF2.649, ABT-239[83-84], GSK-207040[85]. For recent advances in this field cf. ref[86-88]. Several H$_3$R ligands are currently under clinical investigations[78, 80, 89-90] with the aim to treat CNS diseases, but to date no proof-of-concept is available (detailed commentary see[91]). Hybrid molecules combining H$_3$R antagonism with inhibition of enzymes like acetylcholine esterase[92] or combination of inhibition of serotonin reuptake with H$_3$R antagonism provide promising therapeutic approaches[93]. Regarding ligand-receptor interactions different putative binding modes are suggested in literature. Yao et al.[94] and Rai et al.[95] agree in the interaction of the protonated imidazole group (e.g. in ciproxifan) with ASP114 of TM3. Interactions of the central phenyl ring and the lipophilic residue are dis-

cussed. Rai et al. assume the tail end of the molecule in a lipophilic region in the vicinity of Thr119 and aromatic residues surrounding the phenyl ring. According to their model the binding cavity is formed by TM3, 5 and 6. Other groups (Stark et al, Yao et al)[94, 96] propose different orientations of the tail and aromatic moiety of the molecules. In the following chapters, investigations on the H_3R were based on models describing the important structural features of H_3R ligands (see chapters 7 and 8).

Agonists

N$^\alpha$–methylhistamine   (R)-α–methylhistamine   methimmepip

Antagonists/ inverse agonists

JNJ5207852   cipralisant (BF2.649)

ABT-239   thioperamide   ciproxyfan
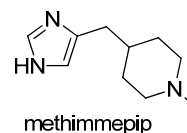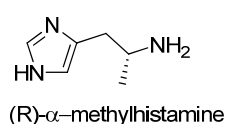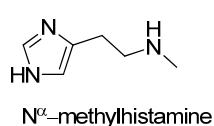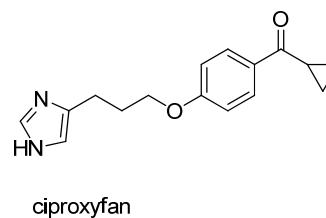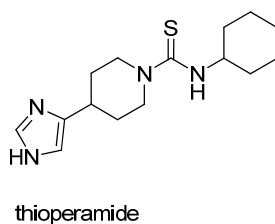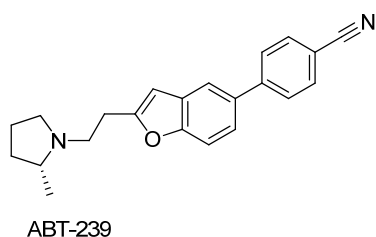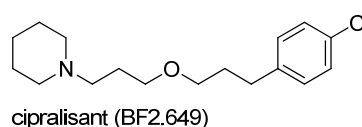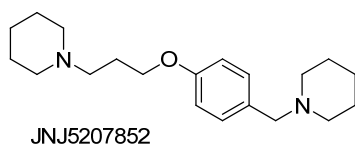
Figure 1.8: Selected H_3R-receptor ligands

1.2.5   The H_4-receptor

The H_4 receptor, which shares high homology with the H_3R, was cloned and functionally expressed, soon after the cloning of the human H_3-receptor (hH_3R), by several work groups in 2000 [97-101]. Overall sequence homology with the hH_3R is 37 – 43 %, reaching even 58 % in transmembrane domains, whereas the homology between the H_4R and the hH_1R and the hH_2R, respectively, is low. Since its discovery the H_4R has attracted attention as a potential drug target and numerous H_4R ligands have been developed[102-103]. H_4R receptors are mainly found in cells of the immune system[38], such as mast cells, dentritic cells, eosinophils, monocytes, basophils, T-cells[38,]

[102] and in the CNS[104-105]. The activation of the H_4R, which is a $G_{\alpha i/o}$ coupled pertussis toxin sensitive receptor, leads to inhibition of adenylyl cyclase activity resulting in a decrease in the cAMP level[38], PKA activity and CRE driven transcription. Additionally, activation of $G_{\beta\gamma}$ subunits leads to activation of the MAPK pathway, to Ca^{2+} release and probably to PLC_β-activation[106-107]. H_4R activation can induce several responses closely associated with immune cells, for example chemokine production, chemotaxis and Ca^{2+} mobilization in mast cells, monocytes and eosinophils[102].
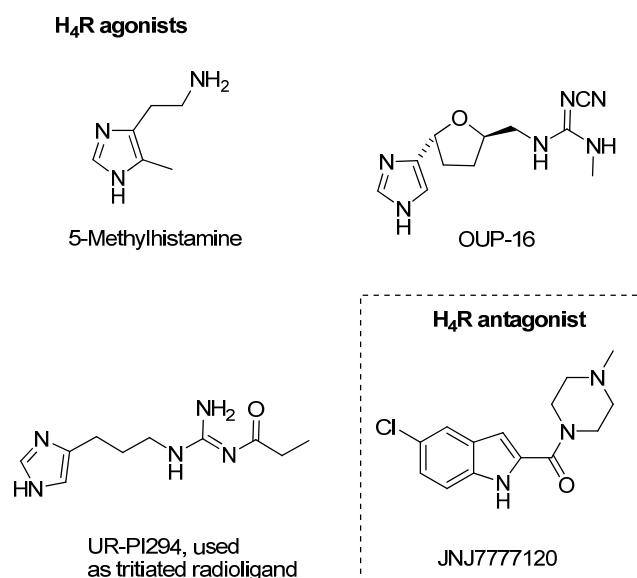
Figure 1.9: Selected H_4R agonists and antagonists

H_2R and H_3R agonists, especially those comprising imidazole rings, for instance clobenpropit, imetit, or compounds with isothiourea group (dimaprit) are known to be active at the H_4R, as well as the prominent inverse agonist thioperamide, which behaves as a potent inverse agonist at the H_4R. The first selective agonist was OUP-14[108], followed by 5-methylhistamine[109], which was originally reported as a selective H_2R agonist in the 1970s[50], but is considerably more potent at the H_4R[109]. Some selected substances like UR-PI294[110] are depicted in Figure 1.9. Currently drug research in the H_4R field is mainly focused on antagonists aiming at new pharmacotherapies for the treatment of inflammatory diseases. As first selective antagonist the indolylpiperazine JNJ7777120[111] was identified, which is in use in several animal models to study the biological function of the H_4R and the applicability of H_4R antagonists in vivo. These studies indicate that this receptor plays a crucial role in inflammatory and immunological processes, such as asthma, rheumatoid arthritis, puritus, pain, inflammatory bowel disease or even colorectal and breast cancer[103, 112]. The supposed role of the H_4R in immunological responses overlaps with H_1R function, which suggests that combined H_1- and H_4-receptor antagonism might be beneficial for the treatment of inflammatory diseases.

References

1.   Foord, S. M.; Bonner, T. I.; Neubig, R. R.; Rosser, E. M.; Pin, J. P.; Davenport, A. P.; Spedding, M.; Harmar, A. J. International Union of Pharmacology. XLVI. G protein-coupled receptor list. *Pharmacol. Rev.* **2005,** 57, 279-88.

2.   Jacoby, E.; Bouhelal, R.; Gerspacher, M.; Seuwen, K. The 7 TM G-protein-coupled receptor target family. *ChemMedChem* **2006,** 1, 761-82.

3.   Lagerstrom, M. C.; Schioth, H. B. Structural diversity of G protein-coupled receptors and significance for drug discovery. *Nat Rev Drug Discov* **2008,** 7, 339-357.

4.   Fredriksson, R.; Lagerström, M. C.; Lundin, L.-G.; Schiöth, H. B. The G-Protein-Coupled Receptors in the Human Genome Form Five Main Families. Phylogenetic Analysis, Paralogon Groups, and Fingerprints. *Mol. Pharmacol.* **2003,** 63, 1256-1272.

5.   Palczewski, K.; Kumasaka, T.; Hori, T.; Behnke, C. A.; Motoshima, H.; Fox, B. A.; Le Trong, I.; Teller, D. C.; Okada, T.; Stenkamp, R. E.; Yamamoto, M.; Miyano, M. Crystal structure of rhodopsin: A G protein-coupled receptor. *Science* **2000,** 289, 739-45.

6.   Rasmussen, S. G.; Choi, H. J.; Rosenbaum, D. M.; Kobilka, T. S.; Thian, F. S.; Edwards, P. C.; Burghammer, M.; Ratnala, V. R.; Sanishvili, R.; Fischetti, R. F.; Schertler, G. F.; Weis, W. I.; Kobilka, B. K. Crystal structure of the human beta2 adrenergic G-protein-coupled receptor. *Nature* **2007,** 450, 383-7.

7.   Cherezov, V.; Rosenbaum, D. M.; Hanson, M. A.; Rasmussen, S. G.; Thian, F. S.; Kobilka, T. S.; Choi, H. J.; Kuhn, P.; Weis, W. I.; Kobilka, B. K.; Stevens, R. C. High-resolution crystal structure of an engineered human beta2-adrenergic G protein-coupled receptor. *Science* **2007,** 318, 1258-65.

8.   Warne, T.; Serrano-Vega, M. J.; Baker, J. G.; Moukhametzianov, R.; Edwards, P. C.; Henderson, R.; Leslie, A. G.; Tate, C. G.; Schertler, G. F. Structure of a beta1-adrenergic G-protein-coupled receptor. *Nature* **2008,** 454, 486-91.

9.   Jaakola, V. P.; Griffith, M. T.; Hanson, M. A.; Cherezov, V.; Chien, E. Y.; Lane, J. R.; Ijzerman, A. P.; Stevens, R. C. The 2.6 angstrom crystal structure of a human A_2A adenosine receptor bound to an antagonist. *Science* **2008,** 322, 1211-7.

10.   Scheerer, P.; Park, J. H.; Hildebrand, P. W.; Kim, Y. J.; Krauss, N.; Choe, H. W.; Hofmann, K. P.; Ernst, O. P. Crystal structure of opsin in its G-protein-interacting conformation. *Nature* **2008,** 455, 497-502.

11.   Park, J. H.; Scheerer, P.; Hofmann, K. P.; Choe, H. W.; Ernst, O. P. Crystal structure of the ligand-free G-protein-coupled receptor opsin. *Nature* **2008,** 454, 183-7.

12.   Cabrera-Vera, T. M.; Vanhauwe, J.; Thomas, T. O.; Medkova, M.; Preininger, A.; Mazzoni, M. R.; Hamm, H. E. Insights into G protein structure, function, and regulation. *Endocr. Rev.* **2003,** 24, 765-81.

13.   Luttrell, L. M. Reviews in molecular biology and biotechnology: transmembrane signaling by G protein-coupled receptors. *Mol. Biotechnol.* **2008,** 39, 239-64.

14.   Ross, E. M.; Wilkie, T. M. GTPase-activating proteins for heterotrimeric G proteins: regulators of G protein signaling (RGS) and RGS-like proteins. *Annu. Rev. Biochem.* **2000,** 69, 795-827.

15.   Roland Seifert, T. W. *G Protein-Coupled Receptors as Drug Targets: Analysis of Activation and Constitutive Activity*. Wiley-VCH, Weinheim: **2005**.

16.   Thomsen, W.; Frazer, J.; Unett, D. Functional assays for screening GPCR targets. *Curr. Opin. Biotechnol.* **2005,** 16, 655-65.

17.   De Lean, A.; Stadel, J. M.; Lefkowitz, R. J. A ternary complex model explains the agonist-specific binding properties of the adenylate cyclase-coupled beta-adrenergic receptor. *J. Biol. Chem.* **1980,** 255, 7108-17.

18.   Samama, P.; Cotecchia, S.; Costa, T.; Lefkowitz, R. J. A mutation-induced activated state of the beta 2-adrenergic receptor. Extending the ternary complex model. *J. Biol. Chem.* **1993,** 268, 4625-36.

19.   Leff, P. The two-state model of receptor activation. *Trends Pharmacol. Sci.* **1995,** 16, 89-97.

20.   Weiss, J. M.; Morgan, P. H.; Lutz, M. W.; Kenakin, T. P. The Cubic Ternary Complex Receptor-Occupancy Model II. Understanding Apparent Affinity. *J. Theor. Biol.* **1996,** 178, 169-182.

21.   Weiss, J. M.; Morgan, P. H.; Lutz, M. W.; Kenakin, T. P. The Cubic Ternary Complex Receptor-Occupancy Model I. Model Description. *J. Theor. Biol.* **1996,** 178, 151-167.

22.   Kenakin, T. Principles: receptor theory in pharmacology. *Trends Pharmacol. Sci.* **2004,** 25, 186-92.

23.   Vauquelin, G.; Van Liefde, I.; Birzbier, B. B.; Vanderheyden, P. M. New insights in insurmountable antagonism. *Fundam. Clin. Pharmacol.* **2002,** 16, 263-72.

24.   Vauquelin, G.; Van Liefde, I.; Vanderheyden, P. Models and methods for studying insurmountable antagonism. *Trends Pharmacol. Sci.* **2002,** 23, 514-8.

25.   Prinster, S. C.; Hague, C.; Hall, R. A. Heterodimerization of g protein-coupled receptors: specificity and functional significance. *Pharmacol. Rev.* **2005,** 57, 289-98.

26.   Angers, S.; Salahpour, A.; Bouvier, M. Dimerization: an emerging concept for G protein-coupled receptor ontogeny and function. *Annu. Rev. Pharmacol. Toxicol.* **2002,** 42, 409-35.

27.   Gouldson, P. R.; Snell, C. R.; Bywater, R. P.; Higgs, C.; Reynolds, C. A. Domain swapping in G-protein coupled receptor dimers. *Protein Eng.* **1998,** 11, 1181-93.

28.   Bakker, R. A.; Lozada, A. F.; van Marle, A.; Shenton, F. C.; Drutel, G.; Karlstedt, K.; Hoffmann, M.; Lintunen, M.; Yamamoto, Y.; van Rijn, R. M.; Chazot, P. L.; Panula, P.; Leurs, R. Discovery of naturally occurring splice variants of the rat histamine H_3 receptor that act as dominant-negative isoforms. *Mol. Pharmacol.* **2006,** 69, 1194-206.

29.   Barger, G.; Dale, H. H. CCLXV.-4-[small beta]-Aminoethylglyoxaline ([small beta]-iminazolylethylamine) and the other active principles of ergot. *Journal of the Chemical Society, Transactions* **1910,** 97, 2592-2595.

30.   Parsons, M. E.; Ganellin, C. R. Histamine and its receptors. *Br. J. Pharmacol.* **2006,** 147 Suppl 1, S127-35.

31.   Ganellin, C. R.; Parsons, M. E. *Pharmacology of Histamine Receptors*. John Wright & sons Ltd.; Bristol: **1982**; p 10-15.

32.   Ganellin, C. R. The tautomer ratio of histamine. *J. Pharm. Pharmacol.* **1973,** 25, 787-92.

33.   Schayer, R. W. Origin and fate of histamine in the body. *Ciba Foundation Symposium, Histamine* **1956**, 183-188.

34.   Beaven, M. A. *Factors Regulating Availability of Histamine at Tissue Receptors In Pharmacology of Histamine Receptors*. Ganellin, C.R. Parsons, M.E: **1982**; p 102-145.

35.   Leurs, R.; Smit, M. J.; Timmerman, H. Molecular pharmacological aspects of histamine receptors. *Pharmacol. Ther.* **1995,** 66, 413-63.

36.   Hill, S. J.; Ganellin, C. R.; Timmerman, H.; Schwartz, J. C.; Shankley, N. P.; Young, J. M.; Schunack, W.; Levi, R.; Haas, H. L. International Union of Pharmacology. XIII. Classification of histamine receptors. *Pharmacol. Rev.* **1997,** 49, 253-78.

37.   Schwartz, J. C.; Pollard, H.; Quach, T. T. Histamine as a neurotransmitter in mammalian brain: neurochemical evidence. *J. Neurochem.* **1980,** 35, 26-33.

38.   Thurmond, R. L.; Gelfand, E. W.; Dunford, P. J. The role of histamine H_1 and H_4 receptors in allergic inflammation: the search for new antihistamines. *Nat Rev Drug Discov* **2008,** 7, 41-53.

39.   Mossner, J.; Caca, K. Developments in the inhibition of gastric acid secretion. *Eur. J. Clin. Invest.* **2005,** 35, 469-75.

40.   Haas, H.; Panula, P. The role of histamine and the tuberomamillary nucleus in the nervous system. *Nat Rev Neurosci* **2003,** 4, 121-30.

41.   Dy, M.; Schneider, E. Histamine-cytokine connection in immunity and hematopoiesis. *Cytokine Growth Factor Rev.* **2004,** 15, 393-410.

42.   Meyer, U. Die Geschichte der Antihistaminika: „Fast könnte man ein Indikations-ABC anlegen". *Pharm. Unserer Zeit* **2004,** 33, 86-91.

43.   Ash, A. S.; Schild, H. O. Receptors mediating some actions of histamine. *Br J Pharmacol Chemother* **1966,** 27, 427-39.

44.   De Backer, M. D.; Gommeren, W.; Moereels, H.; Nobels, G.; Van Gompel, P.; Leysen, J. E.; Luyten, W. H. Genomic cloning, heterologous expression and pharmacological characterization of a human histamine H1 receptor. *Biochem. Biophys. Res. Commun.* **1993,** 197, 1601-8.

45.   Hill, S. J. Distribution, properties, and functional characteristics of three classes of histamine receptor. *Pharmacol. Rev.* **1990,** 42, 45-83.

46.   Esbenshade, T. A.; Kang, C. H.; Krueger, K. M.; Miller, T. R.; Witte, D. G.; Roch, J. M.; Masters, J. N.; Hancock, A. A. Differential activation of dual signaling responses by human H_1 and H_2 histamine receptors. *J. Recept. Signal Transduct. Res.* **2003,** 23, 17-31.

47.   Barak, N. Betahistine: what's new on the agenda? *Expert Opin Investig Drugs* **2008,** 17, 795-804.

48.   Elz, S.; Kramer, K.; Pertz, H. H.; Detert, H.; ter Laak, A. M.; Kuhne, R.; Schunack, W. Histaprodifens: synthesis, pharmacological in vitro evaluation, and molecular modeling of a new class of highly active and selective histamine H($_1$)-receptor agonists. *J. Med. Chem.* **2000,** 43, 1071-84.

49.   Menghin, S.; Pertz, H. H.; Kramer, K.; Seifert, R.; Schunack, W.; Elz, S. N(alpha)-imidazolylalkyl and pyridylalkyl derivatives of histaprodifen: synthesis and in vitro evaluation of highly potent histamine H(1)-receptor agonists. *J. Med. Chem.* **2003,** 46, 5458-70.

50.   Black, J. W.; Duncan, W. A.; Durant, C. J.; Ganellin, C. R.; Parsons, E. M. Definition and antagonism of histamine H_2-receptors. *Nature* **1972,** 236, 385-90.

51.   Black, J. W.; Duncan, W. A.; Emmett, J. C.; Ganellin, C. R.; Hesselbo, T.; Parsons, M. E.; Wyllie, J. H. Metiamide--an orally active histamine H_2-receptor antagonist. *Agents Actions* **1973,** 3, 133-7.

52.   Gantz, I.; Munzert, G.; Tashiro, T.; Schaffer, M.; Wang, L.; DelValle, J.; Yamada, T. Molecular cloning of the human histamine H_2 receptor. *Biochem. Biophys. Res. Commun.* **1991,** 178, 1386-92.

53.   Del Valle, J.; Gantz, I. Novel insights into histamine H_2 receptor biology. *Am. J. Physiol.* **1997,** 273, G987-96.

54.   Kuhn, B.; Schmid, A.; Harteneck, C.; Gudermann, T.; Schultz, G. G proteins of the Gq family couple the H2 histamine receptor to phospholipase C. *Mol. Endocrinol.* **1996,** 10, 1697-707.

55.   Soll, A. H.; Wollin, A. Histamine and cyclic AMP in isolated canine parietal cells. *Am. J. Physiol.* **1979,** 237, E444-50.

56.   Johnson, C. L.; Weinstein, H.; Green, J. P. Studies on histamine H2 receptors coupled to cardiac adenylate cyclase. Blockade by H_2 and H_1 receptor antagonists. *Mol. Pharmacol.* **1979,** 16, 417-28.

57.   Verma, S. C.; McNeill, J. H. The effect of histamine, isoproterenol and tyramine on rat uterine cyclic AMP. *Res. Commun. Chem. Pathol. Pharmacol.* **1976,** 13, 55-64.

58.   Seifert, R.; Hoer, A.; Offermanns, S.; Buschauer, A.; Schunack, W. Histamine increases cytosolic Ca^{2+} in dibutyryl-cAMP-differentiated HL-60 cells via H_1 receptors and is an incomplete secretagogue. *Mol. Pharmacol.* **1992,** 42, 227-34.

59.   Preuss, H. Spezies- selective Interactions of histamine H_2 Receptors with Guanidine type Agonists: Molecular Modelling, Sit - directed -Mutagenisis and Pharmacological Analysis. doctoral thesis, **2007**.

60.   Baumann, G.; Permanetter, B.; Wirtzfeld, A. Possible value of H_2-receptor agonists for treatment of catecholamine-insensitive congestive heart failure. *Pharmacol. Ther.* **1984,** 24, 165-77.

61.   Mörsdorf, P.; Engler H.; Schickanender H.; Buschauer A.; Schunack, W.; Baumann, G. Cardiohistaminergics - new developments in histamine H_2-agonists. *Drugs of the Future* **1990**, 919-933.

62.   Nederkoorn, P. H.; van Gelder, E. M.; Donne-Op den Kelder, G. M.; Timmerman, H. The agonistic binding site at the histamine H_2 receptor. II. Theoretical investigations of histamine binding to receptor models of the seven alpha-helical transmembrane domain. *J. Comput.-Aided Mol. Des.* **1996,** 10, 479-89.

63.   Nederkoorn, P. H.; van Lenthe, J. H.; van der Goot, H.; Donne-Op den Kelder, G. M.; Timmerman, H. The agonistic binding site at the histamine H_2 receptor. I. Theoretical investigations of histamine binding to an oligopeptide mimicking a part of the fifth transmembrane alpha-helix. *J. Comput.-Aided Mol. Des.* **1996,** 10, 461-78.

64.   Gantz, I.; DelValle, J.; Wang, L. D.; Tashiro, T.; Munzert, G.; Guo, Y. J.; Konda, Y.; Yamada, T. Molecular basis for the interaction of histamine with the histamine H_2 receptor. *J. Biol. Chem.* **1992,** 267, 20840-3.

65.   Durant, G. J.; Ganellin, C. R.; Parsons, M. E. Dimaprit, (S-[3-(N,N-dimethylamino)propyl]isothiourea). A highly specific histamine H_2-receptor agonist. Part 2. Structure-activity considerations. *Agents Actions* **1977,** 7, 39-43.

66.   Parsons, M. E.; Owen, D. A.; Ganellin, C. R.; Durant, G. J. Dimaprit -(S-[3-(N,N-dimethylamino)prophyl]isothiourea) - a highly specific histamine H_2 -receptor agonist. Part 1. Pharmacology. *Agents Actions* **1977,** 7, 31-7.

67.   Buschauer, A. Synthesis and in vitro pharmacology of arpromidine and related phenyl(pyridylalkyl)guanidines, a potential new class of positive inotropic drugs. *J. Med. Chem.* **1989,** 32, 1963-70.

68.   Buschauer, A.; Friese-Kimmel, A.; Baumann, G.; Schunack, W. Synthesis and histamine H2 agonistic activity of arpromidine analogues: replacement of the pheniramine-like moiety by non-heterocyclic groups. *European Journal of Medicinal Chemistry* 27, 321-330.

69.   Ghorai, P.; Kraus, A.; Keller, M.; Gotte, C.; Igel, P.; Schneider, E.; Schnell, D.; Bernhardt, G.; Dove, S.; Zabel, M.; Elz, S.; Seifert, R.; Buschauer, A. Acylguanidines as bioisosteres of guanidines: NG-acylated imidazolylpropylguanidines, a new class of histamine H_2 receptor agonists. *J. Med. Chem.* **2008,** 51, 7193-204.

70.   Kraus, A.; Ghorai, P.; Birnkammer, T.; Schnell, D.; Elz, S.; Seifert, R.; Dove, S.; Bernhardt, G.; Buschauer, A. N$^{(G)}$-acylated aminothiazolylpropylguanidines as potent and selective histamine H($_2$) receptor agonists. *ChemMedChem* **2009,** 4, 232-40.

71.   Arrang, J. M.; Garbarg, M.; Schwartz, J. C. Auto-inhibition of brain histamine release mediated by a novel class (H_3) of histamine receptor. *Nature* **1983,** 302, 832-7.

72.   Arrang, J. M.; Garbarg, M.; Lancelot, J. C.; Lecomte, J. M.; Pollard, H.; Robba, M.; Schunack, W.; Schwartz, J. C. Highly potent and selective ligands for histamine H$_3$-receptors. *Nature* **1987,** 327, 117-23.

73.   Lovenberg, T. W.; Roland, B. L.; Wilson, S. J.; Jiang, X.; Pyati, J.; Huvar, A.; Jackson, M. R.; Erlander, M. G. Cloning and functional expression of the human histamine H$_3$ receptor. *Mol. Pharmacol.* **1999,** 55, 1101-7.

74.   Bongers, G.; Bakker, R. A.; Leurs, R. Molecular aspects of the histamine H$_3$ receptor. *Biochem. Pharmacol.* **2007,** 73, 1195-204.

75.   Haas, H. L.; Sergeeva, O. A.; Selbach, O. Histamine in the nervous system. *Physiol. Rev.* **2008,** 88, 1183-241.

76.   Leurs, R.; Bakker, R. A.; Timmerman, H.; de Esch, I. J. The histamine H$_3$ receptor: from gene cloning to H$_3$ receptor drugs. *Nat Rev Drug Discov* **2005,** 4, 107-20.

77.   Parmentier, R.; Anaclet, C.; Guhennec, C.; Brousseau, E.; Bricout, D.; Giboulot, T.; Bozyczko-Coyne, D.; Spiegel, K.; Ohtsu, H.; Williams, M.; Lin, J. S. The brain H$_3$-receptor as a novel therapeutic target for vigilance and sleep-wake disorders. *Biochem. Pharmacol.* **2007,** 73, 1157-71.

78.   Esbenshade, T. A.; Browman, K. E.; Bitner, R. S.; Strakhova, M.; Cowart, M. D.; Brioni, J. D. The histamine H$_3$ receptor: an attractive target for the treatment of cognitive disorders. *Br. J. Pharmacol.* **2008,** 154, 1166-81.

79.   Ligneau, X.; Landais, L.; Perrin, D.; Piriou, J.; Uguen, M.; Denis, E.; Robert, P.; Parmentier, R.; Anaclet, C.; Lin, J. S.; Burban, A.; Arrang, J. M.; Schwartz, J. C. Brain histamine and schizophrenia: potential therapeutic applications of H$_3$-receptor inverse agonists studied with BF2.649. *Biochem. Pharmacol.* **2007,** 73, 1215-24.

80.   Gemkow, M. J.; Davenport, A. J.; Harich, S.; Ellenbroek, B. A.; Cesura, A.; Hallett, D. The histamine H$_3$ receptor as a therapeutic drug target for CNS disorders. *Drug Discov Today* **2009,** 14, 509-15.

81.   Arrang, J. M.; Morisset, S.; Gbahou, F. Constitutive activity of the histamine H$_3$ receptor. *Trends Pharmacol. Sci.* **2007,** 28, 350-7.

82.   Barbier, A. J.; Berridge, C.; Dugovic, C.; Laposky, A. D.; Wilson, S. J.; Boggs, J.; Aluisio, L.; Lord, B.; Mazur, C.; Pudiak, C. M.; Langlois, X.; Xiao, W.; Apodaca, R.; Carruthers, N. I.; Lovenberg, T. W. Acute wake-promoting actions of JNJ-5207852, a novel, diamine-based H$_3$ antagonist. *Br. J. Pharmacol.* **2004,** 143, 649-61.

83.   Cowart, M.; Faghih, R.; Curtis, M. P.; Gfesser, G. A.; Bennani, Y. L.; Black, L. A.; Pan, L.; Marsh, K. C.; Sullivan, J. P.; Esbenshade, T. A.; Fox, G. B.; Hancock, A. A. 4-(2-[2-(2(R)-methylpyrrolidin-1-yl)ethyl]benzofuran-5-yl)benzonitrile and related 2-aminoethylbenzofuran H$_3$ receptor antagonists potently enhance cognition and attention. *J. Med. Chem.* **2005,** 48, 38-55.

84.   Esbenshade, T. A.; Fox, G. B.; Krueger, K. M.; Miller, T. R.; Kang, C. H.; Denny, L. I.; Witte, D. G.; Yao, B. B.; Pan, L.; Wetter, J.; Marsh, K.; Bennani, Y. L.; Cowart, M. D.; Sullivan, J. P.; Hancock, A. A. Pharmacological properties of ABT-239 [4-(2-{2-[(2R)-2-Methylpyrrolidinyl]ethyl}-benzofuran-5-yl)benzonitrile]: I. Potent and selective histamine H$_3$ receptor antagonist with drug-like properties. *J. Pharmacol. Exp. Ther.* **2005,** 313, 165-75.

85.   Medhurst, A. D.; Briggs, M. A.; Bruton, G.; Calver, A. R.; Chessell, I.; Crook, B.; Davis, J. B.; Davis, R. P.; Foley, A. G.; Heslop, T.; Hirst, W. D.; Medhurst, S. J.; Ociepka, S.; Ray, A.; Regan, C. M.; Sargent, B.; Schogger, J.; Stean, T. O.; Trail, B. K.; Upton, N.; White, T.; Orlek, B.; Wilson, D. M. Structurally novel histamine H$_3$ receptor antagonists GSK207040 and GSK334429 improve scopolamine-induced memory impairment and capsaicin-induced secondary allodynia in rats. *Biochem. Pharmacol.* **2007,** 73, 1182-94.

86.   Isensee, K.; Amon, M.; Garlapati, A.; Ligneau, X.; Camelin, J. C.; Capet, M.; Schwartz, J. C.; Stark, H. Fluorinated non-imidazole histamine H$_3$ receptor antagonists. *Bioorg. Med. Chem. Lett.* **2009,** 19, 2172-5.

87.   Ting, P. C.; Lee, J. F.; Albanese, M. M.; Wu, J.; Aslanian, R.; Favreau, L.; Nardo, C.; Korfmacher, W. A.; West, R. E.; Williams, S. M.; Anthes, J. C.; Rivelli, M. A.; Corboz, M. R.; Hey, J. A. The synthesis and structure-activity relationship of 4-benzimidazolyl-piperidinylcarbonyl-piperidine analogs as histamine H$_3$ antagonists. *Bioorg. Med. Chem. Lett.* **2010,** 20, 5004-8.

88.   Kuder, K. J.; Ligneau, X.; Camelin, J. C.; Lazewska, D.; Schwartz, J. C.; Schunack, W.; Stark, H.; Kiec-Kononowicz, K. Diether (substituted) piperidine derivatives as novel, histamine H$_3$ receptor ligands. *Inflammation Res.* **2009,** 58 Suppl 1, 47-8.

89.   Celanire, S.; Wijtmans, M.; Talaga, P.; Leurs, R.; de Esch, I. J. Keynote review: histamine H$_3$ receptor antagonists reach out for the clinic. *Drug Discov Today* **2005,** 10, 1613-27.

90.   Sander, K.; Kottke, T.; Stark, H. Histamine H$_3$ receptor antagonists go to clinics. *Biol. Pharm. Bull.* **2008,** 31, 2163-81.

91.   Hancock, A. A. The challenge of drug discovery of a GPCR target: analysis of preclinical pharmacology of histamine H$_3$ antagonists/inverse agonists. *Biochem. Pharmacol.* **2006,** 71, 1103-13.

92.   Bembenek, S. D.; Keith, J. M.; Letavic, M. A.; Apodaca, R.; Barbier, A. J.; Dvorak, L.; Aluisio, L.; Miller, K. L.; Lovenberg, T. W.; Carruthers, N. I. Lead identification of acetylcholinesterase inhibitors-histamine H$_3$ receptor antagonists from molecular modeling. *Bioorg. Med. Chem.* **2008,** 16, 2968-73.

93.   Barbier, A. J.; Aluisio, L.; Lord, B.; Qu, Y.; Wilson, S. J.; Boggs, J. D.; Bonaventure, P.; Miller, K.; Fraser, I.; Dvorak, L.; Pudiak, C.; Dugovic, C.; Shelton, J.; Mazur, C.; Letavic, M. A.; Carruthers, N. I.; Lovenberg, T. W. Pharmacological characterization of JNJ-28583867, a histamine H($_3$) receptor antagonist and serotonin reuptake inhibitor. *Eur. J. Pharmacol.* **2007,** 576, 43-54.

94.   Yao, B. B.; Hutchins, C. W.; Carr, T. L.; Cassar, S.; Masters, J. N.; Bennani, Y. L.; Esbenshade, T. A.; Hancock, A. A. Molecular modeling and pharmacological analysis of species-related histamine H(3) receptor heterogeneity. *Neuropharmacology* **2003,** 44, 773-86.

95.   Rai, B. K.; Tawa, G. J.; Katz, A. H.; Humblet, C. Modeling G protein-coupled receptors for structure-based drug discovery using low-frequency normal modes for refinement of homology models: Application to H$_3$ antagonists. *Proteins: Structure, Function, and Bioinformatics* **2010,** 78, 457-473.

96.   Stark, H.; Sippl, W.; Ligneau, X.; Arrang, J. M.; Ganellin, C. R.; Schwartz, J. C.; Schunack, W. Different antagonist binding properties of human and rat histamine H3 receptors. *Bioorg. Med. Chem. Lett.* **2001,** 11, 951-4.

97.   Oda, T.; Morikawa, N.; Saito, Y.; Masuho, Y.; Matsumoto, S. Molecular cloning and characterization of a novel type of histamine receptor preferentially expressed in leukocytes. *J. Biol. Chem.* **2000,** 275, 36781-6.

98.   Liu, C.; Wilson, S. J.; Kuei, C.; Lovenberg, T. W. Comparison of human, mouse, rat, and guinea pig histamine H_4 receptors reveals substantial pharmacological species variation. *J. Pharmacol. Exp. Ther.* **2001,** 299, 121-30.

99.   Morse, K. L.; Behan, J.; Laz, T. M.; West, R. E., Jr.; Greenfeder, S. A.; Anthes, J. C.; Umland, S.; Wan, Y.; Hipkin, R. W.; Gonsiorek, W.; Shin, N.; Gustafson, E. L.; Qiao, X.; Wang, S.; Hedrick, J. A.; Greene, J.; Bayne, M.; Monsma, F. J., Jr. Cloning and characterization of a novel human histamine receptor. *J. Pharmacol. Exp. Ther.* **2001,** 296, 1058-66.

100.   Nguyen, T.; Shapiro, D. A.; George, S. R.; Setola, V.; Lee, D. K.; Cheng, R.; Rauser, L.; Lee, S. P.; Lynch, K. R.; Roth, B. L.; O'Dowd, B. F. Discovery of a novel member of the histamine receptor family. *Mol. Pharmacol.* **2001,** 59, 427-33.

101.   Zhu, Y.; Michalovich, D.; Wu, H.; Tan, K. B.; Dytko, G. M.; Mannan, I. J.; Boyce, R.; Alston, J.; Tierney, L. A.; Li, X.; Herrity, N. C.; Vawter, L.; Sarau, H. M.; Ames, R. S.; Davenport, C. M.; Hieble, J. P.; Wilson, S.; Bergsma, D. J.; Fitzgerald, L. R. Cloning, expression, and pharmacological characterization of a novel human histamine receptor. *Mol. Pharmacol.* **2001,** 59, 434-41.

102.   Igel, P.; Dove, S.; Buschauer, A. Histamine H(4) receptor agonists. *Bioorg. Med. Chem. Lett.* **2010,** 20, 7191-9.

103.   Smits, R. A.; Leurs, R.; de Esch, I. J. Major advances in the development of histamine H_4 receptor ligands. *Drug Discov Today* **2009,** 14, 745-53.

104.   Connelly, W. M.; Shenton, F. C.; Lethbridge, N.; Leurs, R.; Waldvogel, H. J.; Faull, R. L.; Lees, G.; Chazot, P. L. The histamine H_4receptor is functionally expressed on neurons in the mammalian CNS. *Br. J. Pharmacol.* **2009,** 157, 55-63.

105.   Strakhova, M. I.; Nikkel, A. L.; Manelli, A. M.; Hsieh, G. C.; Esbenshade, T. A.; Brioni, J. D.; Bitner, R. S. Localization of histamine H_4 receptors in the central nervous system of human and rat. *Brain Res.* **2009,** 1250, 41-8.

106.   Lim, H. D.; Smits, R. A.; Leurs, R.; De Esch, I. J. The emerging role of the histamine H_4 receptor in anti-inflammatory therapy. *Curr Top Med Chem* **2006,** 6, 1365-73.

107.   de Esch, I. J.; Thurmond, R. L.; Jongejan, A.; Leurs, R. The histamine H_4 receptor as a new therapeutic target for inflammation. *Trends Pharmacol. Sci.* **2005,** 26, 462-9.

108.   Hashimoto, T.; Harusawa, S.; Araki, L.; Zuiderveld, O. P.; Smit, M. J.; Imazu, T.; Takashima, S.; Yamamoto, Y.; Sakamoto, Y.; Kurihara, T.; Leurs, R.; Bakker, R. A.; Yamatodani, A. A selective human H(4)-receptor agonist: (-)-2-cyano-1-methyl-3-[(2R,5R)-5- [1H-imidazol-4(5)-yl]tetrahydrofuran-2-y] methylguanidine. *J. Med. Chem.* **2003,** 46, 3162-5.

109.   Lim, H. D.; van Rijn, R. M.; Ling, P.; Bakker, R. A.; Thurmond, R. L.; Leurs, R. Evaluation of histamine H_1-, H_2-, and H_3-receptor ligands at the human histamine H4 receptor: identification of

4-methylhistamine as the first potent and selective H$_4$ receptor agonist. *J. Pharmacol. Exp. Ther.* **2005,** 314, 1310-21.

110.   Igel, P.; Schnell, D.; Bernhardt, G.; Seifert, R.; Buschauer, A. Tritium-labeled N(1)-[3-(1H-imidazol-4-yl)propyl]-N(2)-propionylguanidine ([(^{3})H]UR-PI294), a high-affinity histamine H($_3$) and H($_4$) receptor radioligand. *ChemMedChem* **2009,** 4, 225-31.

111.   Jablonowski, J. A.; Grice, C. A.; Chai, W.; Dvorak, C. A.; Venable, J. D.; Kwok, A. K.; Ly, K. S.; Wei, J.; Baker, S. M.; Desai, P. J.; Jiang, W.; Wilson, S. J.; Thurmond, R. L.; Karlsson, L.; Edwards, J. P.; Lovenberg, T. W.; Carruthers, N. I. The first potent and selective non-imidazole human histamine H$_4$ receptor antagonists. *J. Med. Chem.* **2003,** 46, 3957-60.

112.   Maslinska, D.; Laure-Kamionowska, M.; Maslinski, K. T.; Deregowski, K.; Szewczyk, G.; Maslinski, S. Histamine H($_4$) receptors on mammary epithelial cells of the human breast with different types of carcinoma. *Inflammation Res.* **2006,** 55 Suppl 1, S77-8.

Chapter 2

Scope and Objectives

2 Scope and Objectives

The development of new fluorescence based methods for the determination of ligand receptor interactions on G-protein coupled receptors (GPCRs) is part of an extensive research project in our department, focusing on histamine and neuropeptide Y (NPY) receptors as models of aminergic and peptidergic GPCRs, respectively. Compared to small molecules such as histamine receptor ligands, the affinity of peptides is much less affected by space-filling fluorophores. For instance, fluorescence labelled NPY and pancreatic polypeptide ([K^4]hPP) proved to be very useful tools in flow cytometry to determine binding affinities of new ligands at NPY receptors[1-4]. Flow cytometric and fluorescence-based assays in the microplate format are valuable procedures for the determination of affinities and functional activities of compound libraries, for high throughput screenings in industrial drug research as well as for detailed pharmacological investigations. Moreover, fluorescence ligands are applicable in confocal microscopy and open attractive alternatives to conventional methods such as radioligand binding studies. Therefore, the feasibility of this approach to aminergic GPCRs such as histamine receptors has been explored. Previous investigations with fluorescent human (h) histamine H$_1$ (hH$_1$R) and H$_2$ receptor (hH$_2$R) antagonists revealed that, depending on the chemical nature, bulky fluorophores are tolerated[5-6]. Although these compounds achieve antagonistic activities in the range of commercially available H$_1$R and H$_2$R antagonists, their suitability for cell-based assays turned out to be limited due to unfavourable spectral properties (maximum emission around 500 nm), interference with cellular autofluorescence and high unspecific binding. As demonstrated for NPY receptor ligands, one of the major problems is autofluorescence. However, this can be overcome by using fluorophores emitting light at wavelengths above 630 nm.

This work is aiming at the synthesis and pharmacological characterization of novel histamine H$_2$ and H$_3$ receptor antagonists and the application of the fluorescent ligand approach to aminergic GPCRs. In addition, the preparation of "bivalent antagonists" and radioligands is taken into account.

Fluorescent H$_2$R antagonists: For the synthesis of H$_2$R antagonists, potentidine and related core structures (e.g. cyanoguanidines[7-8], squaramides[9]) were considered most promising, as such piperidinomethylphenoxyalkylamine derivates are known to tolerate a broad variety of modifications.[6, 8, 10] In addition to cyanoguanidines, squaramides were selected as so-called "urea equivalents" due to high H$_2$R antagonistic activities reported for N-mono-substituted 2,3-diaminobutene-1,2-diones.[9] With respect to labelling, spacers of various lengths, bearing termi-

nal amino groups, had to be introduced and modified in the "eastern part" of the molecule
Scheme 2.1).
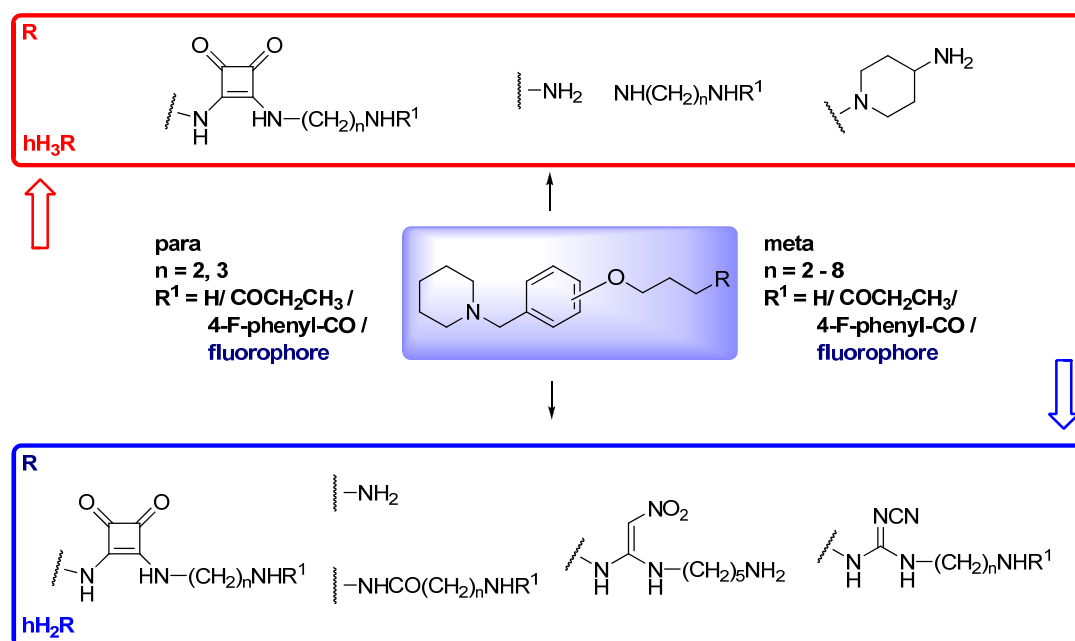
Scheme 2.1: Overview of planned variations of H_2R and H_3R antagonists bearing a piperidinylmethyl-phenoxy moiety

Taking possible differences in histamine receptor selectivity of different types of H_2R antagonists into account, in addition to the aforementioned compounds, the suitability of imidazoles (e.g. cimetidine) and guanidinothiazoles were explored. Ideal fluorophores should emit light at wavelengths above 630 nm and confer additional receptor affinity/activity (Scheme 2.2).
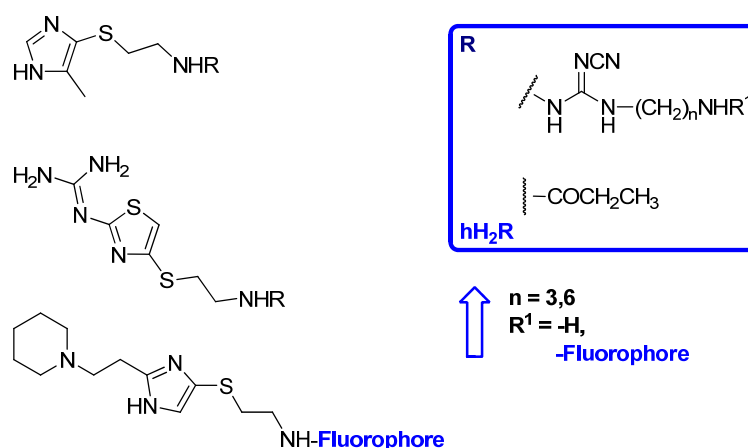
Scheme 2.2: Overview of planned variations of H_2R antagonists bearing an imidazolyl, cimetidine or guanidinothiazole moiety

Fluorescent H₃R antagonists: Currently, great efforts are made in the human H_3 receptor (hH_3R) field aiming at drugs for the treatment of diseases of the central nervous system (e.g. Alzheimer's disease, sleep and wake disorders, narcolepsy, attention disorders)[11-13]. A high affinity fluorescent ligand will be a useful standard ligand for the screening of compound libraries and a versatile tool for detailed pharmacological studies and the detection of H_3R on cells and in tissues. For this purpose the above described approach was extended to the H_3R field using 3-[4-(piperidin-1-ylmethyl)phenoxy]propan-1-aminederivatives[14] related to JNJ 5207852 as a core structure (Scheme 2.1).

Bivalent ligands: By analogy with the application of the bivalent ligand approach to other GPCR agonists/antagonists[15-16], a small series of bivalent compounds was prepared and investigated pharmacologically.

(Potential) radioligands: Propionylated H_2R and H_3R antagonists were synthesized in an attempt to develop new tritiated radioligands. In the case of the H_2R such a radioactive tracer should be superior to known radioligands, especially in terms of specific binding.[17-19]

Pharmacological characterisation and application of the synthesized compounds: For detailed functional analysis of the compounds a steady state GTPase assay using the four human histamine receptor subtypes hH_1R, hH_2R, hH_3R, hH_4R expressed in Sf9 insect cells was considered the method of choise. In parallel, selected H_2R antagonists were investigated at the guinea pig H_2R (isolated guinea pig right atrium). Additionally, the H_2R and H_3R affinity of selected substances had to be determined in radioligand binding studies. The most potent fluorescent substances were investigated in fluorescence based competition binding assays (e.g. by flow cytometry) to explore their suitability for the characterization of new histamine receptor ligands. The applicability of the fluorescence- and radio-labelled ligands to confocal microscopy and binding studies, respectively, was investigated.

References

1.   Ziemek, R.; Brennauer, A.; Schneider, E.; Cabrele, C.; Beck-Sickinger, A. G.; Bernhardt, G.; Buschauer, A. Fluorescence- and luminescence-based methods for the determination of affinity and activity of neuropeptide Y_2 receptor ligands. *Eur. J. Pharmacol.* **2006,** 551, 10-8.

2.   Ziemek, R.; Schneider, E.; Kraus, A.; Cabrele, C.; Beck-Sickinger, A. G.; Bernhardt, G.; Buschauer, A. Determination of affinity and activity of ligands at the human neuropeptide Y Y_4 receptor by flow cytometry and aequorin luminescence. *J. Recept. Signal Transduct. Res.* **2007,** 27, 217-33.

3.   Schneider, E.; Keller, M.; Brennauer, A.; Hoefelschweiger, B. K.; Gross, D.; Wolfbeis, O. S.; Bernhardt, G.; Buschauer, A. Synthesis and characterization of the first fluorescent nonpeptide NPY Y$_1$ receptor antagonist. *ChemBioChem* **2007,** 8, 1981-8.

4.   Schneider, E.; Mayer, M.; Ziemek, R.; Li, L.; Hutzler, C.; Bernhardt, G.; Buschauer, A. A simple and powerful flow cytometric method for the simultaneous determination of multiple parameters at G protein-coupled receptor subtypes. *ChemBioChem* **2006,** 7, 1400-9.

5.   Li, L.; Kracht, J.; Peng, S.; Bernhardt, G.; Buschauer, A. Synthesis and pharmacological activity of fluorescent histamine H$_1$ receptor antagonists related to mepyramine. *Bioorg. Med. Chem. Lett.* **2003,** 13, 1245-8.

6.   Li, L.; Kracht, J.; Peng, S.; Bernhardt, G.; Elz, S.; Buschauer, A. Synthesis and pharmacological activity of fluorescent histamine H$_2$ receptor antagonists related to potentidine. *Bioorg. Med. Chem. Lett.* **2003,** 13, 1717-20.

7.   Buschauer, A.; Postius, S.; Szelenyi, I.; Schunack, W. [Isohistamine and homologs as components of H$_2$-antagonists. 22. H$_2$-antihistaminics]. *Arzneimittelforschung.* **1985,** 35, 1025-9.

8.   Hirschfeld, J.; Buschauer, A.; Elz, S.; Schunack, W.; Ruat, M.; Traiffort, E.; Schwartz, J. C. Iodoaminopotentidine and related compounds: a new class of ligands with high affinity and selectivity for the histamine H$_2$ receptor. *J. Med. Chem.* **1992,** 35, 2231-8.

9.   Buyniski J.P., R. L. C., R.L., Pircio, A.W. Algieri A.A., Crenshaw R.R. . Highlights in Receptor Chemistry. *Melchiorre, C, Gianella, M, eds. Structure- activity relationships among newer histamine H$_2$-receptor antagonists, Amsterdam: Elsevier Sciences,* **1984**, 195-215.

10.   Ruat, M.; Traiffort, E.; Bouthenet, M. L.; Schwartz, J. C.; Hirschfeld, J.; Buschauer, A.; Schunack, W. Reversible and irreversible labeling and autoradiographic localization of the cerebral histamine H$_2$ receptor using [^{125}I]iodinated probes. *Proc. Natl. Acad. Sci. U. S. A.* **1990,** 87, 1658-62.

11.   Celanire, S.; Wijtmans, M.; Talaga, P.; Leurs, R.; de Esch, I. J. Keynote review: histamine H3 receptor antagonists reach out for the clinic. *Drug Discov Today* **2005,** 10, 1613-27.

12.   Leurs, R.; Bakker, R. A.; Timmerman, H.; de Esch, I. J. The histamine H$_3$ receptor: from gene cloning to H$_3$ receptor drugs. *Nat Rev Drug Discov* **2005,** 4, 107-20.

13.   Esbenshade, T. A.; Browman, K. E.; Bitner, R. S.; Strakhova, M.; Cowart, M. D.; Brioni, J. D. The histamine H$_3$ receptor: an attractive target for the treatment of cognitive disorders. *Br. J. Pharmacol.* **2008,** 154, 1166-81.

14.   Apodaca, R.; Dvorak, C. A.; Xiao, W.; Barbier, A. J.; Boggs, J. D.; Wilson, S. J.; Lovenberg, T. W.; Carruthers, N. I. A new class of diamine-based human histamine H$_3$ receptor antagonists: 4-(aminoalkoxy)benzylamines. *J. Med. Chem.* **2003,** 46, 3938-44.

15.   Halazy, S. G-protein coupled receptors bivalent ligands and drug design. *Exp. Opin. Ther. Patents* **1999,** 9, 431-446.

16.   Portoghese, P. S. From models to molecules: opioid receptor dimers, bivalent ligands, and selective opioid receptor probes. *J. Med. Chem.* **2001,** 44, 2259-69.

17.   Kelley, M. T.; Burckstummer, T.; Wenzel-Seifert, K.; Dove, S.; Buschauer, A.; Seifert, R. Distinct interaction of human and guinea pig histamine H_2-receptor with guanidine-type agonists. *Mol. Pharmacol.* **2001,** 60, 1210-25.

18.   Wenzel-Seifert, K.; Kelley, M. T.; Buschauer, A.; Seifert, R. Similar apparent constitutive activity of human histamine $H_{(2)}$-receptor fused to long and short splice variants of $G_{(salpha)}$. *J. Pharmacol. Exp. Ther.* **2001,** 299, 1013-20.

19.   Gajtkowski, G. A.; Norris, D. B.; Rising, T. J.; Wood, T. P. Specific binding of ^{3}H-tiotidine to histamine H_2 receptors in guinea pig cerebral cortex. *Nature* **1983,** 304, 65-7.

Chapter 3

Piperidinomethylphenoxyal-kylamines as potent H_2-receptor antagonists

3   Piperidinomethylphenoxyalkylamines as potent H₂-receptor antagonists

3.1   Introduction

The H₂-receptor (H₂R) is known as the target of drugs such as cimetidine, famotidine, ranitidine, nizatidine or roxatidine, which are used as antisecretory agents for the treatment of gastroduodenal ulcer and gastroesophageal diseases[1-2]. In addition to the marketed drugs numerous structurally diverse highly active H₂R antagonists are known, e. g. iodoaminopotentidine[3], BMY25368[4], lamtidine[5] and tiotidine[6], and several of these compounds are used as pharmacological tools, for instance, to characterize H₂Rs and their ligands in functional studies, and, using the corresponding radiolabelled forms, to detect H₂Rs on cells and in tissues and to perform competition binding studies[7-9]. Nevertheless, the reported labelled H₂R ligands are far from being ideal, in particular with respect to selective binding and availability. Moreover, high affinity fluorescent H₂R ligands suitable for cellular investigations or in vivo imaging are not described so far.

Aiming at new high affinity/activity H₂R ligands, piperidinomethylphenoxyalkylamines were considered promising core structure suitable for coupling to fluorophores or radiolabels or appropriate as building blocks for the synthesis of bivalent ligands. Previous work from our group suggested that bulky residues are tolerated without loss of H₂R activity. For this purpose the new ligands should comprise alkanediyl spacers with a terminal amino group to enable coupling procedures under mild experimental conditions. According to the pharmacophore model for potentidine and related substances[3] (e.g aminopotentidine, see Figure 3.1 and Figure 3.2) the "western part" of the molecule, including a piperidinomethylphenoxy moiety connected via an alkyl spacer to a "urea equivalent", is important for receptor binding. Obviously, additional polar groups and aromatic residues, connected via alkyl chains (B/C), are tolerated in the "eastern part" and can confer additional H₂R binding (Figure 3.1)[3]. In addition to different aromatic residues in this part of the molecule small fluorophores turned out to be tolerated[10]. This prompted us to use the potentidine pattern as initial point for the design of new H₂R ligands with special properties and to optimize the structures stepwise, starting from the H₂R antagonist skeleton via pharmacophoric groups, linkers and fluorophores.
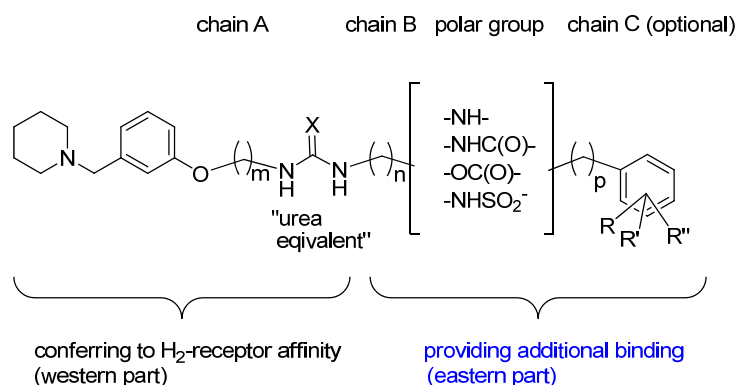
Figure 3.1: Structural features of potentidine-like H_2-receptor ligands, derived from ref.[3]

In this chapter the optimisation of the "urea equivalent" is described, starting from potentidine-like substances containing a cyanoguanidine group, which was replaced by nitroethenediamine, amide or squaric amide moieties. Squaric amide derivatives such as BMY 25368 are known to exert high activity at the H_2R, as well as the hydroxyacetamide roxatidine, which is marketed as the prodrug roxatidine acetate. With respect to structural modifications including labelling, the new compounds should bear an alkyl spacer with a terminal amino group in the eastern part of the molecule. In order to gain new insights into structure-activity and structure-selectivity relationships, modifications of the western part of the molecule were performed by introduction of a cimetidine-like moiety (cf. Figure 3.2).
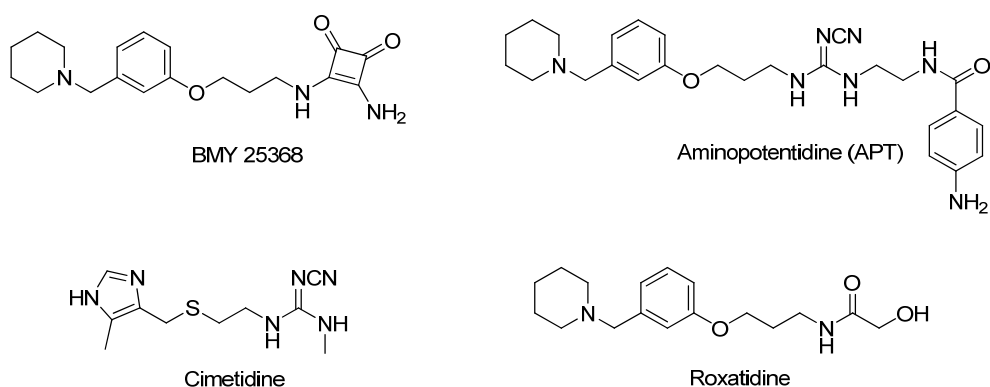
Figure 3.2: Selected prominent H_2R antagonists

3.2 Chemistry

Synthesis of piperidinomethylphenoxypropane derivatives

3-(3-(Piperidin-1-ylmethyl)phenoxy)propan-1-amine (**3.4**) was prepared in a 3 step synthesis as described in literature[11] starting with 3-hydroxybenzaldehyde (Scheme 3.1). For the synthesis of compound **3.2** the Leuckart-Wallach reaction was used, followed by cyanethylation of **3.2** with an excess of acrylonitrile in the presence of catalytic amounts of Triton B (Benzyltrimethylammonium hydroxide) leading to the nitrile **3.3**. The nitrile was dissolved in diethyl ether and was precipitated as hydrochloride with 5N-6N HCl in isopropanol. Reduction of the nitrile was accomplished with lithium aluminium hydride in diethyl ether. Compound **3.4** served as key intermediate for the preparation of ω-aminoalkyl-substituted potentidine like structures in analogy to previously described methods.[11]
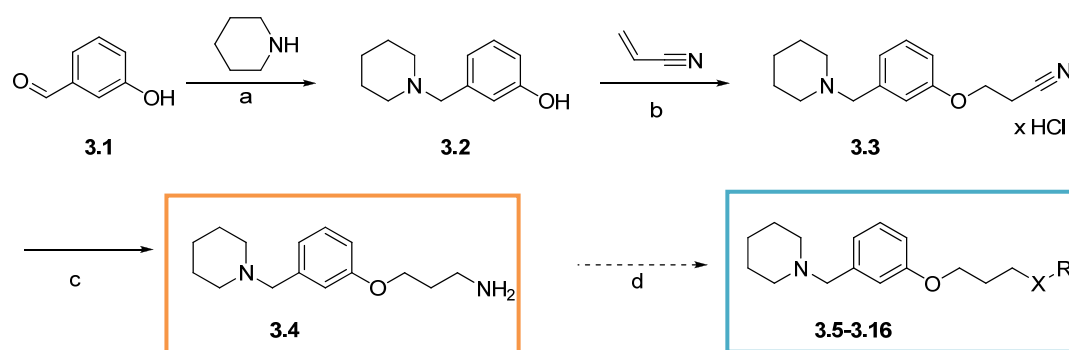
Compd.	3.5, 3.6	3.7, 3.8	3.9-3.15	3.16
X				
R	$-(CH_2)_nNH_2$			

Scheme 3.1: Synthesis of 3-(3-(piperidin-1-ylmethyl)phenoxy)propan-1-amine derivatives. Reagents and conditions: (a) HCOOH, 2 h reflux; (b) acrylonitrile, Triton B, 26 h, 80 °C; converted to hydrochloride (c) diethyl ether, LAlH₄, rt 3-4 h; (d) see next schemes

Preparation of potentidine-like cyanoguanidines and roxatidine-like amides

For the synthesis of roxatidine like structures phthalic anhydride was used as protecting group for the amino group of ω-aminoalkanoic acids as described previously[12]. The ω-phthalimidoalkanoic acids were obtained from the ω-aminoalkanoic acids (**3.17** or **3.18**) and phthalic ahydride at 135-140 °C under stirring without the use of solvent in 56-86 % yields (Scheme 3.2).
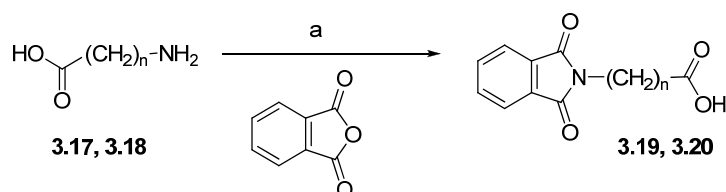
Scheme 3.2: Synthesis of ω-aminoalkanoic acids; Reagents and conditions: (a) Phthalic anhydride, 135-140 °C, 30 min

Compound **3.4** was converted into the amides **3.21** and **3.22** by acylation with **3.19**, **3.20** using carbonyldiimidazole (CDI) as coupling reagent. Amines **3.7** and **3.8** were obtained after cleavage of the phthaloyl protecting group with aqueous hydrazine solution and purification by flash chromatography on silica gel (Scheme 3.3). Starting point for the synthesis of cyanoguanidines was the amine **3.4**, which was treated with diphenyl cyanocarbonimidate by analogy with published protocols[3, 11] to give the intermediate **3.23**. Aminolysis, performed with an excess of ethane-1,2-diamine or hexane-1,6-diamine, at rt in methanol yielded the cyanoguanidines **3.5** and **3.6** as sticky yellow oils (Scheme 3.3), which could be used without purification.

Scheme 3.3: Synthesis of cyanoguanidines and amides; Reagents and conditions: (a1) methanol, rt 5 h; (a2) rt overnight; (b) CDI + **3.19/3.20**: 30 min-1 h in anhydrous THF, rt; +**3.4**: rt overnight; (c) 1.hydrazine hydrate, 1 h, reflux, 2. 2N HCl, 30 min reflux
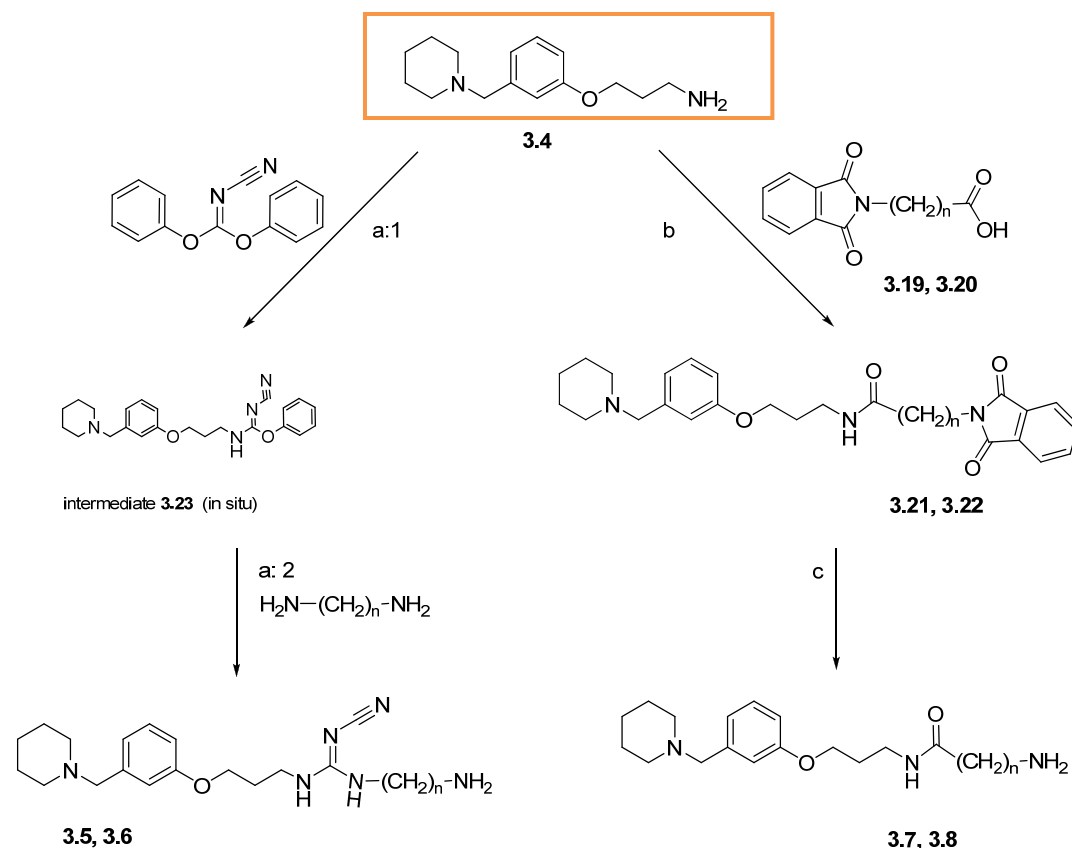
Compd	3.5	3.6	3.7	3.8	3.21	3.22
n	2	6	1	5	1	5

Preparation of squaric acid derivatives

The synthesis of the ether derivative **3.24** was adapted from described procedures[13-15]. The precursor **3.4** and 3,4-diethoxycyclobut-3-ene-1,2-dione were stirred in ethanol at rt for 3-5 h. Attempts to perform the subsequent reaction in one pot without isolation of **3.24** were unsuccessful. Therefore, the solvent of the reaction mixture, containing the squaric monoester **3.24**, was evaporated. A subsequent washing step yielded the product **3.24** as sticky yellow to orange oil in 50 to 90 % yields (Scheme 3.4). The following reaction, leading to the amines **3.9-3.15**, was done in ethanol at rt using an 5- to 20-fold excess of the reactive alkanediamine to avoid the formation of symmetric by-products. After evaporation of the solvent, dissolving the residue in a small amount of methanol or ethanol and addition of diethyl ether, the compounds precipitated as white to yellow solids. If necessary, the amines were purified by preparative HPLC. An alterna-

tive, but more expensive, synthetic route comprises the use of mono-boc protected alkanedia-mines, which can be used in equimolar amounts in ethanol as solvent at rt to form the boc - protected squaramide derivative **3.25**. Cleavage of the protection group with 10 % TFA led to the corresponding squaramide **3.9** (Scheme 3.4).

Compd.	n
3.25	2
3.9	2
3.10	3
3.11	4
3.12	5
3.13	6
3.14	7
3.15	8
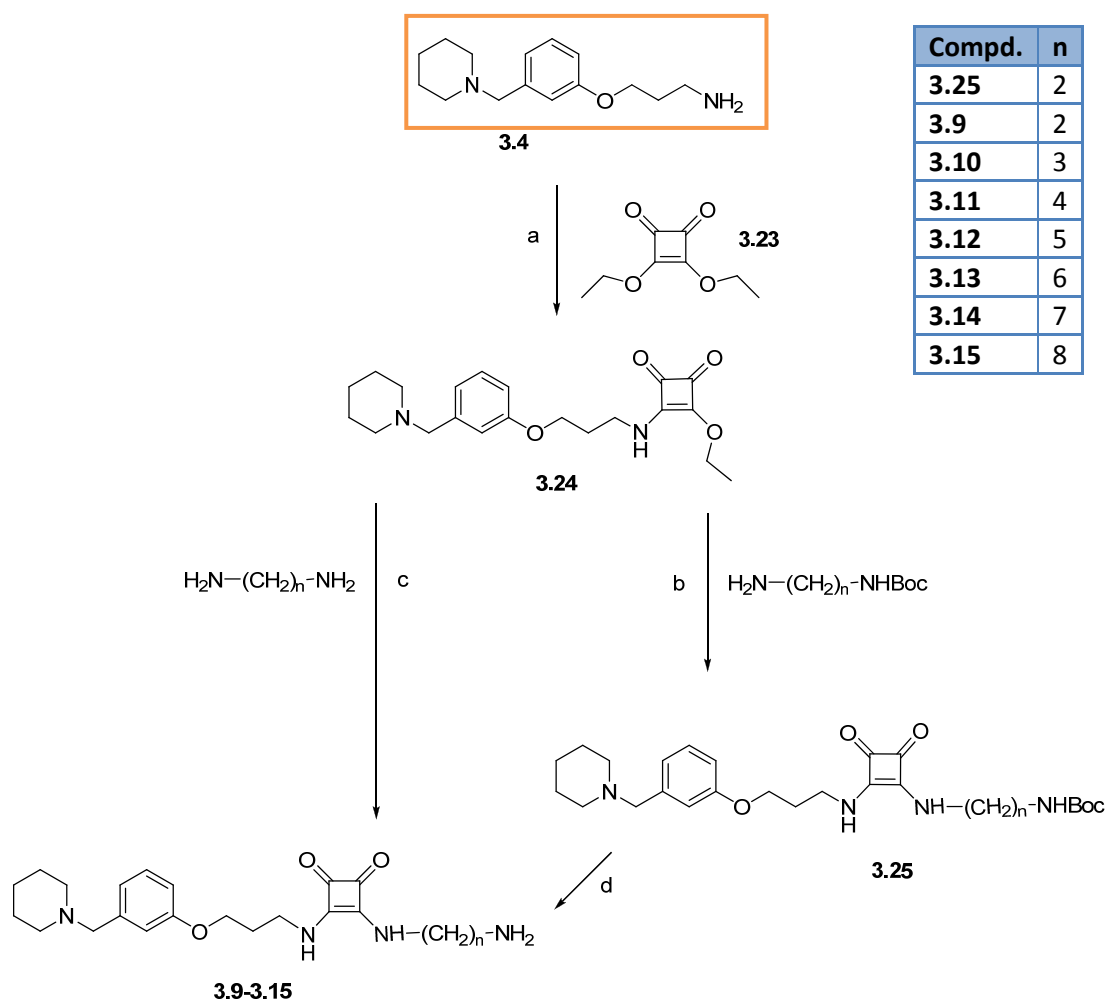
Scheme 3.4: Synthesis of squaramides; Reagents and conditions: (a) ethanol, rt 3 h; (b) ethanol, rt, overnight; (c) ethanol, rt 5-18 h; (d) CH$_2$Cl$_2$, TFA, rt overnight

Squaramides are vinylogous amides, which show high hydrogen bonding capability[16]. This is fa-cilitated by delocalisation of the nitrogen lone pair through the partially aromatic cyclobu-tenedione system. These zwitterionic structures are often regarded as a mimic of an α-ammoniumcarboxylate motif[17]. Restricted rotation about the C-N bond, comparable to simple amides, is possible, which results in different Z/E-configurations[16, 18]. As an example the ^{1}H-NMR spectrum of compound **3.24** (Scheme 3.5) is depicted in Figure 3.3. The signals of the methylene

group adjacent to the squaramide moiety at 3.68 and 3.88 ppm corresponding to a ratio of about 7 : 3 in favour of the (*E*)-configured stereoisomer of **3.24** under these conditions.
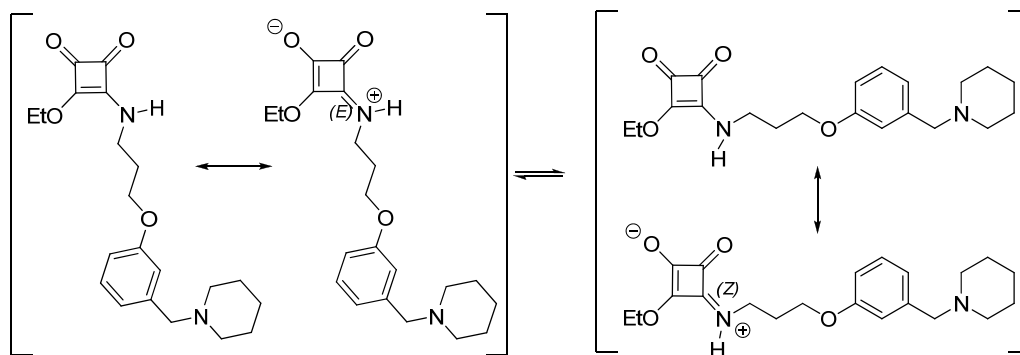
Scheme 3.5: E and Z configurations of **3.24**

Signal splitting of amide substituents in ^{1}H-NMR spectra was also observed for N,N'-disubstituted squaramides, for instance for ligand **3.14** at higher concentrations using DMSO-d_6 as solvent (see experimental data).
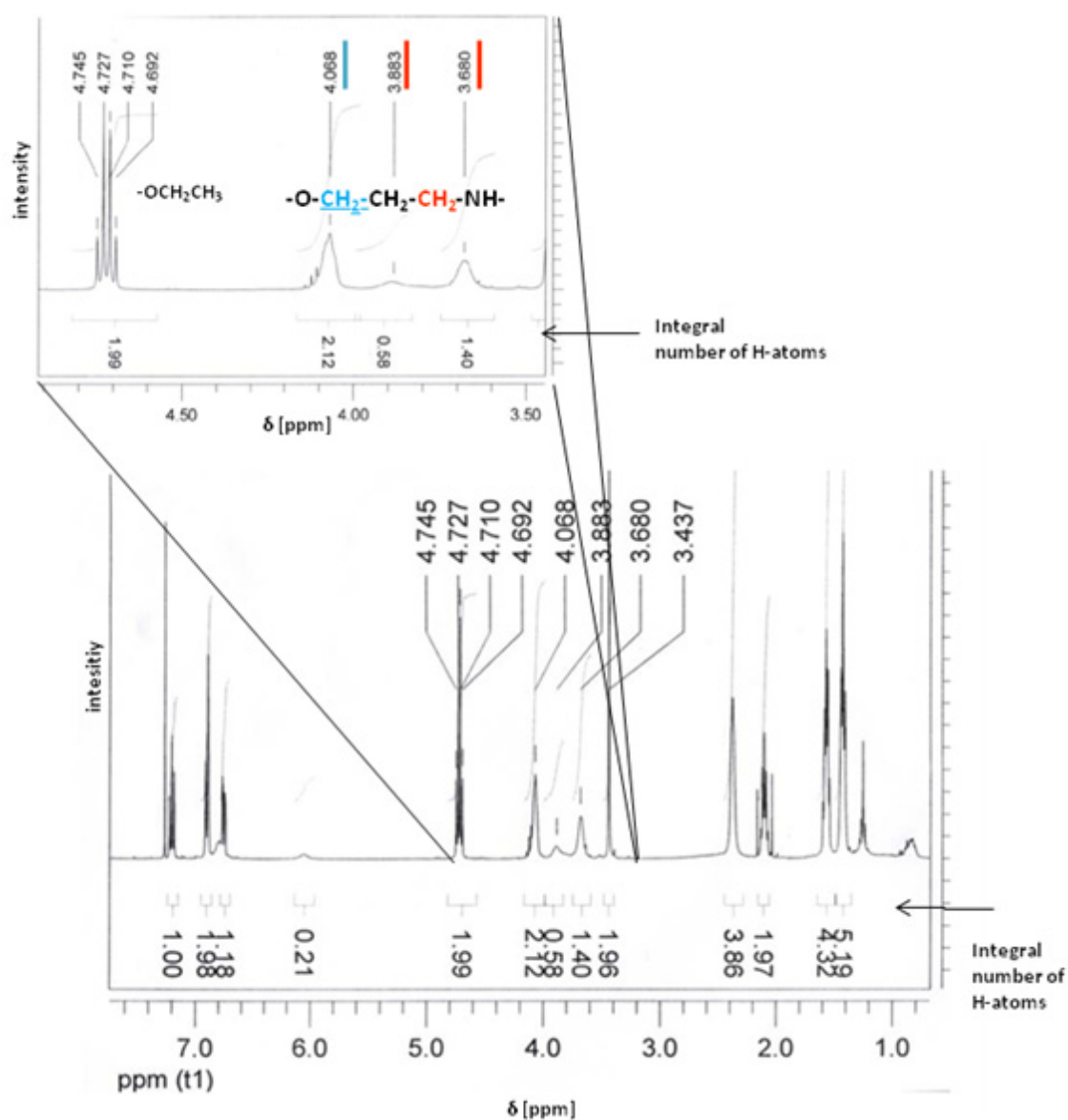
Figure 3.3: ^{1}H-NMR spectra of **3.24** in CDCl$_3$, showing the splitting of signals, corresponding to amide Z/E-isomers, in the zoomed section

Structural variations: nitroethenediamines and cimetidine-like cyanoguanidines

Compound **3.32** was prepared from compound **3.26**, which was available in our workgroup and hexane-1,6-diamine in methanol according to the procedure described for cyanoguanidines **3.5** and **3.6.** For pharmacological investigations a small amount of the product was purified by preparative HPLC, affording the product as yellow oil. The building blocks **3.26** and **3.27**, required for the synthesis of **3.28** and **3.16**, were also available in our workgroup. The preparation

of the cyanoguanidines and nitroethenediamines, respectively, was performed by analogy with procedures described in literature[19], using an excess of the respective diamine in methanol. The products were purified by flash chromatograpy on silica gel or preparative HPLC to yield the amines as semi solids or as oil (Scheme 3.6).
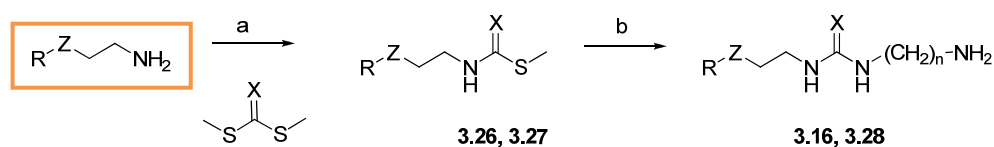
Compd.	3.26	3.28	3.27	3.16
Z	-CH$_2$-S-		CH$_2$	
X	NCN		CNO$_2$	
R				
n	-	3	-	5

Scheme 3.6: Synthesis of **3.16**,and **3.28**; Reagents and conditions: (a) EtOH, rt, 3 h (b) NH$_2$(CH$_2$)$_n$NH$_2$, methanol rt, overnight.

3.3   Pharmacological results

3.3.1   H$_2$-receptor antagonism

GTPase assay at the guinea pig and human histamine H$_2$-receptor

H$_2$-receptor antagonism and inverse agonistic effects were investigated in a steady state GTPase assay on Sf9 cell membranes expressing gpH$_2$R-G$_{s\alpha S}$ and hH$_2$R-G$_{s\alpha S}$ fusion proteins.[9] All compounds exerted moderate to negligible inverse agonism (E$_{max}$= -0.2 to -0.03, see Table 3.1) and inhibited the histamine stimulated GTP hydrolysis (antagonist mode) at low nanomolar to micromolar concentrations. The potentidine like compound **3.5**, already known from former investigations[3, 10] at the guinea pig atrium, exhibited activities (K$_{b'}$ = 979 nM) comparable to data from the guinea pig right atrium (pA$_2$ values around 6.0, see Table 3.2). Ligand **3.6**, with an enlarged alkanediyl spacer, possessed slightly higher H$_2$R antagonistic activity compared to **3.5** (K$_{b'}$ about 500 nM). The cimetidine-like cyanoguanidine **3.28** showed lower activity at the H$_2$R than **3.5** and **3.6**. Attachment of an alkanediyl spacer in the eastern part of the molecule resulted in a 5-fold decrease in activity for **3.28** compared to the parent compound cimetidine (Table 3.1). Modifying the "urea equivalent" while keeping the piperidinylmethylphenoxy moiety constant resulted in compounds **3.7/3.8** (with an amide group), structurally derived from roxatidine (roxatidinacetate pA$_2$ = 7.0), and compound **3.16** with a nitroethenediamine moiety. These ligands had only moderate to low antagonistic activity at the H$_2$R (1500 - 5000 nM, Table 3.1). By contrast, combination of the piperidinylmethylphenoxy moiety with a squaramide moiety and additional modifications at the eastern part of the molecule (**3.9** - **3.15**) resulted in a tremendous increase in H$_2$R activity compared to the above mentioned ligands. The activities of these H$_2$R antagonists were in the same range as that of the structurally related N-monosubstituted squaramide BMY25363[4] (K$_b$ gp atrium: 13 nM). The K$_b$-values (1 to 200 nM) increased with the chain length of the attached alkanediyl spacer. This structural class of H$_2$R antagonists showed species-dependent differences in activity at the receptor, comparing gpH$_2$R and hH$_2$R. The preference for the gpH$_2$R increased with the length of the spacers from 2 fold to 5-8 fold.

Table 3.1: : H$_2$R antagonistic activities and efficacies of H$_2$R ligands in GTPase assays [a]

Compd.	gpH$_2$R-G$_{s\alpha s}$	hH$_2$R-G$_{s\alpha s}$	
	K$_{b'}$ [nM]	K$_{b'}$ [nM]	E$_{max}$
Histamine	EC$_{50}$ 850 ±340[b]	EC$_{50}$ 990 ± 92[b]	1.00
Cimetidine	1300 ± 270 [b]	1700 ±430 [b]	-0.03 ± 0.02 [b]
Famotidine	38 ± 3 [b]	48 ± 10[b]	-0.09 ±0.08 [b]
Aminopotentidine	260 ± 43 [b]	180 ±12[b]	-0.27 ±0.06 [b]
Iodoaminopotentidine	26 ± 4 [b]	35 ±7 [b]	-0.1 ±0.01 [b]
Tiotidine	50 (30-90) [c]	60 (30-130)[c]	-0.04 ±0.09 [c]
3.5	n.d.	979 ±285	-0.16 ±0.17
3.6	n.d.	592 ±63	-0-06 ±0.00
3.7	n.d.	1567 ±284	-0.14 ± 0.00
3.8	3858	5157 ±30	-0.12 ±0.12
3.9	87 ±16.6	211 ±11	0.18±0.07
3.10	21 ±3.41	75 ±9.5	-0.17 ±0.07
3.11	8.6	39 ±18.5	-0.2 ±0.03
3.12	0.36	13 ±9.4	-0.2 ±0.06
3.13	3.3 ±1.0	18 ±2.2.	-0.19 ±0.08
3.14	0.2 ±0.1	1.3 ±0.1	-0.21 ± 0.03
3.15	0.78 ± 0.3	4.5 ±0.8	-0.19 ± 0.00
3.16	n.d.	>1000	-0.11 ± 0.02
3.24	n.d.	605 ±48	-0.09
3.28	n.d.	8733 ±552	-0.10 ± 0.00

[a] Steady state GTPase assay on Sf9 cell membranes; ligands were used at concentrations from 1 nM to 100 μM; typical GTPase activities (stimulation with 1 μM histamine (gpH$_2$R, hH$_2$R): 3.0-7 pmol x mg^{-1} x min^{-1}; E$_{max}$= intrinsic activity, relative to histamine (HIS), E$_{max}$ HIS = 1 (ligands at a concentration of 10 μM, HIS: 100 μM); mean values ± S.E.M. (n = 1-4), performed in duplicate; n.d.: not determined; [b]see[20], [c] numbers in parentheses represent the 95 % confidence intervals

Antagonism at the guinea pig atrium

Two selected squaramides (**3.9**, **3.13**) were tested at the spontaneously beating guinea pig right atrium. Cumulative concentration-response curves of histamine in the presence and absence of antagonist were recorded and pA$_2$-values were calculated from the EC$_{50}$ shifts of the curves. The cyanoguanidine **3.5** is known from literature to have comparable activities at the guinea pig atrium[3, 10] and in GTPase assays with an average pA$_2$ value 6. Compound **3.9** behaved as H$_2$R antagonist at the guinea pig atrium with a pA$_2$ value of 7.4 (K$_b$: 42 nM, Table 3.2) corresponding to GTPase data. For ligand **3.13** K$_{b'}$-values in the low nanomolar range were determined in the GTPase assay, whereas the H$_2$R antagonistic activity was about 10-fold lower at the guinea pig right atrium (Table 3.2). Both squaramides (**3.9**, **3.13**) caused a slight depression of the maxi-

mum response (E_{max} HIS: 64-94 %) of histamine. The same phenomenon was already reported for BMY25363[4] which may be considered the parent compound of **3.9** and **3.13**.

Table 3.2: H_2R antagonism of selected compounds at the isolated guinea pig right atrium (gpH_2R)

Compd.	gpH₂R			
	c [nM]	pA$_2$[b]	K$_B$[nM]	n[a]
3.9	1000	7.4	42	4
3.13	100/300/1000	7.4 ±0.1	39	9
BMY25363			13[c]	
3.5		5.96[d]		

[a] number of experiments, SEM calculated from 4-9 experiments, [b] calculated from pEC$_{50}$ shifts, for details see experimental procedures; [c] see ref [4], [d] see ref [10]

3.3.2 Receptor selectivity

H_1-receptor antagonism on U373-MG cells and activities on human H_1-, H_3- and H_4-receptors in GTPase assays

Determination of H_1-receptor (H_1R) selectivity was performed according to a reported protocol[21] on U373-MG cells using a spectrofluorimetric Ca^{2+} assay. All compounds had only weak H_1R antagonistic effects ($K_{b'}$-values 30 - 100 μM, see appendix) on the intracellular Ca^{2+} mobilisation. Additionally, the compounds were investigated in a steady state GTPase assay on Sf9 cell membranes expressing hH_1R + RGS4, thereby focussing on efficacies. There were no noteworthy agonistic or inverse agonistic effects (efficacies between -0.12 and 0.04, see appendix). The investigation at the H_4 receptor in the GTPase assay (Sf9 cell membranes expressing hH_4R-RGS19 + $G_{i\alpha2}$+$G_{\beta1\gamma2}$) revealed no remarkable effects on intrinsic activity (-0.28 to 0.2, see appendix). Selected substances (**3.5, 3.6, 3.13, 3.16** and **3.28**) were investigated in the antagonist mode and showed no activity or only low activities ($K_{b'}$-value) above 1 μM (**3.6**, **3.6**, **3.16**) in the antagonist mode (hH_4R, see appendix). In contrast to the high preference for H_2R compared to H_1R and H_4R, the selectivity for the H_2R over the H_3R was remarkably lower.

High intrinsic activities in the range of the prominent inverse agonist thioperamide (E_{max} = -0.66) were detected in steady state GTPase assays on Sf9 cell membranes bearing hH_3R+ $G_{i\alpha2}$ +$\beta_{1\gamma2}$ + RGS4. Therefore GTPase assays in the antagonist mode were performed to determine the $K_{b'}$-values of the substances from their IC_{50} values (Table 3.3). The $K_{b'}$-values of the cimetidine-like compound **3.28** and the amides **3.7** and **3.8** were above 1 μM. Taken the high $K_{b'}$-values at the

hH$_2$R into account (Table 3.1) the histamine receptor subtype selectivity of these compounds was low. Only **3.28** with K$_{b'}$ > 10 µM showed a slight preference for the H$_2$R over the H$_3$R. Experimental data for the cyanoguanidines (**3.5** and **3.6**) and for compound **3.16** unexpectedly revealed higher activities at the H$_3$-receptor than at the H$_2$-receptor. In the squaramide series H$_2$R selectivity could not be achieved at all. All compounds of this series inhibited H$_3$R-stimulated GTP hydrolysis in the nanomolar range (120-1000 nM). Increasing the chain length of the alkanediyl spacer resulted in a preference for H$_2$R over the H$_3$R (Table 3.3). From 2 to 8 methylene groups an increase in selectivity (H$_2$R versus the H$_3$R) from non-selective (K$_{b'}$=160 nM, **3.10**) to 20- and 300-fold, respectively (H$_3$R, K$_{b'}$-values: **3.13**: 590 nM, **3.15**: 970 nM,) was determined (Table 3.1 and Table 3.3).

H$_3$-receptor binding affinities

The results from GTPase assays were confirmed in radioligand binding studies performed with selected compounds on HEK-293-FLAG-hH$_3$R-His$_6$ cells expressing the human H$_3$R. [^{3}H]N$^\alpha$-Methylhistamine ([^{3}H]NAMH) was used as radioligand at a concentration of 1 nM (K$_D$ = 5.1 nM). The new compounds displaced the radioactive tracer [^{3}H] NAMH in a concentration-dependent manner. The calculated K$_i$-values are in the same range as data (K$_{b'}$) from functional experiments (see Table 3.3).

Table 3.3: H$_3$R antagonism and binding data of selected compounds on Sf9 cell membranes (GTPase^a) and on HEK-293-FLAG-hH3R-His6cells^b

Compd.	GTPase assay hH$_3$R+ G$_{i\alpha2}$ +β$_1$γ$_2$ + RGS4^a		Binding data HEK-293-FLAG-hH$_3$R-His$_6$ cells^b
	K$_{b'}$ (EC$_{50}$) [nM]	E$_{max}$	K$_i$ (K$_D$) [nM]
[^{3}H]NAMH	-	-	(5.1)^d
Histamine	(25 ± 3)^c	1.00	n.d
Thioperamide	97 ± 18	-0.66 ± 0.1	n.d
JNJ5207852	4.3 ± 0.6	-0.88 ±0.12	n.d.
3.5	273 ± 129	-0-81 ±0..0	217 ±21
3.6	263.9 ±34	-0.81 ±0.01	n.d
3.7	n.d.	n.d.	n.d
3.8	1179 ±786	-0.85 ±0.05	n.d
3.9	300 ±187	-0.82 ±0.07	n.d
3.10	159 ±31	-0.72 ±0.06	n.d
3.11	214 ±44	-0.73 ±0.09	886 ±204
3.12	122±10	-0.61 ±0.05	811 ±264
3.13	590 ±407	-0.61 ± 0.05	665 ±155
3.14	> 500	-0.56	n.d
3.15	972 ±295	-0.52	n.d
3.16	434 ±92	n.d.	n.d
3.24	>1000	-0.85±0.08	n.d
3.28	>10000	0.09	>4000

^{a} steady state GTPase assay on Sf9 cell membranes; c. ligands: 1 nM - 100 µM; typical GTPase activities (stimulation with 100 nM histamine (hH$_3$R): 2.5-6.0 pmol x mg^{-1} x min^{-1}; E$_{max}$ = efficacy relative to histamine (HIS) = 1, E$_{max}$ HIS = 1 (c Ligands and HIS: 10 µM), Mean values ± S.E.M. (n = 1-3) performed in duplicate; ^{b}c. ligands: 1 nM- 100 µM, c. [^{3}H]NAMH: 1 nM, 2-5 million cells /well; Mean values ± S.E.M. (n= 1-2), performed in duplicate; n.d.: not determined; ^{c} see[22], ^{d}see[23];

3.4 Discussion

The investigated compounds revealed high selectivity for the H_2R compared to hH_1R and hH_4R, whereas selectivity over the hH_3R was low to moderate depending on the structural characteristics of the ligand.

Compounds with cyanoguanidine moiety

The introduction of alkanediyl spacers of different chain length is tolerated in compounds derived from potentidine such as the known compounds **3.5** and **3.6**, but selectivity for the H_2R over the hH_3R was relatively low. Functional activities at the H_3R were in the same range as at the H_2R. In case of compound **3.6** even higher antagonistic activity at the H_3R compared to the H_2R was detected. H_3R antagonistic activity was also determined for iodoaminopotentidine, when the compound was investigated on the electrically stimulated guinea pig ileum[24]. Variation in the pharmacophoric groups, resulting in cimetidine like compound **3.28**, were not tolerated and led to a decrease in activity at the H_2R compared to the parent compound. Although **3.28** exerted no remarkable activity at the hH_3R ($K_{b'}$= 4-10 µM), the use as a building block for coupling to fluorophores or synthesizing new bivalent ligands is inadvisable due to low H_2R activity ($K_{b'}$ > 5 µM).

Potentidine-related structures: amides and compound 3.16

Substitution of the cyanoguanidine group in potentidine like structures by a nitroethenediamine moiety (**3.16**) or by an amide group (**3.7**, **3.8**) resulted in ligands with higher antagonistic activity at the H_2R compared to **3.28** (except **3.8**). The activity at the H_2R was slightly lower (for **3.8**) or in the same range as for the cyanoguanidines **3.5** and **3.6** with a comparable selectivity profile.

Potentidine-related structures: squaramides

In the squaramide series considerable improvement in H_2R activity ($K_{b'}$ = 1 - 200 nM) was achieved. Increasing the chain length of the alkanediyl spacer resulted in a 40 to 130 fold increase in antagonistic activity at hH_2R and gpH_2R, accompanied by a preference for the H_2R over the H_3R with increasing spacer length. Elongation of the spacer from two to six, seven or eight methylene groups led to an increase in selectivity for the H_2R over the H_3R from 1.5 fold to 33 or 250 fold. Regarding species-dependent selectivity the comparison of $K_{b'}$-values from the hH_2R with $K_{b'}$-values from the gpH_2R (both from GTPase assays) revealed a two to eight fold increase in activity at the gpH_2R compared to the human H_2R ortholog, with increasing preference for the

gpH$_2$R depending on elongation of the spacer. Recently, species selective interactions of guanidine type agonists at the hH$_2$R and the gpH$_2$R were reported, supporting the concept of ligand specific conformations in H$_2$R species (hH$_2$R, gpH$_2$R and rH$_2$R) for this type of agonists[20]. It may be speculated that species selectivity of squaramidetype H$_2$R antagonists are due to ligand specific conformations of orthologous receptors, too, however there is no proof so far. The compounds **3.9** and **3.13** showed H$_2$R antagonistic activity in the low nanomolar range at the guinea pig atrium, a standard model for the investigation of H$_2$R, which proved to be predictive with respect to the development of H$_2$R antagonists such as cimetidine or ranitidine as antiulcer drugs. For compound **3.9** both test systems, GTPase assay and guinea pig right atrium, revealed comparable results, whereas for compound **3.13** a 13 fold lower activity compared to the functional data from the GTPase assays on recombinant hH$_2$Rs was observed. It should be noted that this discrepancies might be due to the different pharmacological systems, in particular the different receptor systems (H$_2$R-G$_{s\alpha S}$ fusion proteins versus native receptors), or due to different access to the receptors in both systems. Impaired diffusion in isolated organs is conceivable. For compound **3.13,** which is of low solubility in physiological buffers, partial precipitation during the assay cannot be ruled out. As the experiments had to be conducted with a minimum incubation time of 60 min to get rightward shifts of the histamine curve and to create reliable results, another possible explanation could be a slow association kinetic of the compounds. Thus, it is possible that equilibrium was not fully reached leading (apparently) to higher K$_b$-values. The maximum increase in heart rate induced by histamine was depressed in the presence of **3.9** and **3.13** (amounting 65-95 %). This phenomenon – often referred to as unsurmountable antagonism[4, 25-26] - might be caused by slow kinetics or interaction with additional (allosteric) binding sites at the receptor. The phenomenon of unsurmountable antagonism will be discussed in more detail in chapter 5.

As the major difference between the potentidine related substances is the chemical nature of the urea equivalent, the high activity of the squaramides had to be attributed to a high extent to the squaric acid moiety and to the length of the spacer. The squaric acid motif is a priviledged structure, which is regarded as a sort of a bioisoster of an α-amino carboxylic functionality and can serve as both proton donor and acceptor, enabling multiple interaction modes with putative additional binding sites at the receptor.

3.5 Summary and conclusion

From a structural point of view, only variations in the eastern part of H_2R ligands derived from piperidinomethylphenoxyalkylamines were succesful, providing potent antagonists. $K_{b'}$-values between one and 1000 nM and high selectivity versus the H_1R and H_4R were achieved. H_2R antagonistic activity and selectivity over the H_3R could be improved for squaramide ligands by increasing the spacer length. The H_2R antagonists with high activity at the H_2R (preferably K_b'-values below 1000 nM) are promising building blocks for the preparation of fluorescence- and radio and bivalent ligands. This will be discussed in the following chapters.

3.6 Experimental section

3.6.1 Chemistry

General conditions

Chemicals and solvents were purchased from commercial suppliers Merck KGaA (Darmstadt, Germany), Acros Organics (Geel, Belgium) and Sigma Aldrich GmbH (Munich, Germany) and used without further purification unless otherwise stated. DMF was stored over 3 Å molecular sieves.

Flash chromatography was performed on silica gel (Merck silica gel 60, 40 - 63 µM). Thin layer chromatography (TLC) was done on aluminum plates coated with silica gel (Merck silica gel 60 F254, thickness 0.2 mm) and the compounds were detected by UV light (254 nm). All melting points were determined with a Büchi 530 melting point apparatus and are uncorrected.

NMR spectra were measured on an Avance 300 (^{1}H: 300 MHz, ^{13}C: 75.5 MHz), an Avance 600 Kryo (^{1}H: 600 MHz, ^{13}C: 150.9 MHz) and an Avance 400 (^{1}H: 400 MHz, ^{13}C: 100.6 MHz, Bruker, Karlsruhe, Germany) with tetramethylsilan (TMS) as external standard. Chemical shifts are given in δ (ppm) relative to external standards. The multiplicity of carbon atoms (^{13}C-NMR) was determined by DEPT 135 and DEPT 65 (distortionless enhancement by polarization transfer). For selected substances 2D-NMR techniques (COSY, HSQC, HMBC, NOESY) were used to assign ^{1}H and ^{13}C chemical shifts.

Mass spectrometry (MS) was performed on a Finnigan ThermoQuest TSQ 7000 (ES-MS), a Finnigan SSQ710A (EI-MS 70 eV, CI-MS) and Finnigan MAT 95 (LSIMS, HRMS). Lyophilization of the products was done with a Christ alpha 2-4 LD, equipped with a vacuubrand RZ 6 rotary vane vacuum pump.

For preparative HPLC a system from Knauer (Berlin, Germany), consisting of two K-1800 pumps and a K-2001 detector was used. Mixtures of acetonitrile (A) and 0.05- 0.1 % aq TFA (B) served as mobile phase and were degassed with Helium prior to HPLC analysis. Unless otherwise noted the concentration of TFA aq. for B was 0.1 % and as water millipore water was used. All compounds were filtered through PTFE-filters (25 mm, 0.2 μm, Phenomenex Ltd., Aschaffenburg, Germany) prior to preparative HPLC. The conditions used for the purification of the compounds are listed below (Table 3.4):

Table 3.4: Instrument settings in preparative HPLC analysis:

	Flow [ml/min]	Wavelength λ [nm]	Temperature [°C]	Column (RP)
System 1	38	220 /254	rt	**Eurospher**-100 C18, 250 × 32 mm, 5μm (Knauer, Berlin, Germany)
System 2	18-20	220/ 254	rt	**Nucleodur** 100-5 C18 ec (250 × 4 mm, 5 μ (Macherey-Nagel, Germany)
System 2-1	18-20	220/ 254	30	**Nucleodu**r 100-5 C18 ec (250 × 4 mm, 5 μ (Macherey-Nagel, Germany)

Analytical HPLC analysis was performed on a system from Merck, composed of an L-5000 controller, a 655A-12 pump, a 655A-40 auto sampler and an L-4250 UV-VIS detector. Mixtures of 0.025 % TFA in acetonitrile (A) and 0.025 % aq. TFA (B) were used as mobile phase. A part of the spectra was recorded with methanol (C) and 0.1 % aq TFA (D) as eluent. Helium degassing prior to HPLC analysis was necessary. Important instrument settings are listed in Table 3.5.

Table 3.5: Instrument settings applied for analytical HPLC analysis:

	Flow [ml/min]	Wavelength λ [nm]	Temperature [°C]	Column (RP)
	0.7	210/220 /254	30	**Eurospher**-100 C18, 250 × 4.0 mm, 5 μm; Knauer, Berlin, Germany
	Applied gradients			**Dead time** t_0 **[min]**
Gradient 1	00 to 20 min: A/B: 20 to 30 min: A/B:	15/85 to 90/10 90/10		**2.54**
Gradient 2	00 to 20 min: C/D 20 to 30 min: C/D	15/85 to 90/10 90/10		**2.54**

Infrared spectra (IR) were determined on a Bruker Tensor 27 spectrometer equipped with an ATR (attenuated total reflexion) unit from Harrick Scientific Products Inc. (Ossining/NY, US).

UV- and VIS spectra were recorded on a Cary 100 UV/VIS photometer (Varian Inc., Mulgrave, Victoria, Australia).

Preparation of 3-[3-(piperidin-1-ylmethyl)phenoxy]propan-1-amine derivatives

3-(Piperidin-1-ylmethyl)phenol (3.2)

Fresh piperidine (8.4 g, 97.6 mmol, 2 eq) and formic acid (5.0 ml, p.A.) were slowly added under cooling (ice) and stirring to 3-hydroxybenzaldehyde (6.1 g, 50 mmol, 1 eq). The reaction mixture was stirred for 2 h at 90 -110 °C. After cooling to room temperature (rt.) the solution was added to 30 ml water and 20 ml of ammonia solution (25 %) were added. The precipitated product (sticky solid) was filtered off and dissolved in 70 ml ethyl acetate. After extraction of the residual product from the water containing phase with 25 ml ethyl acetate (3 times), the ethyl acetate phases were combined, washed with 25 ml water (4 times) and dried over sodium sulphate. The organic solvent was evaporated under reduced pressure and dried in vacuo. Subsequently, the product was suspended in ethanol to dissolve impurities. Brown crystals were isolated after storage of the suspension at 4 °C for 12 h and the isolated compound was dried in vacuo (6.8 g, 72 %). Mp: 133 °C (ref: 136-137 °C[11]);

^{1}H-NMR (300 MHz, DMSO-d_6): δ (ppm) 1.37-1.39 (m, 2H, **C4-H** Pip.), 1.46 (qui, 4H, **C3,5-H** Pip), 2.41 (s, 4H, **C2,6-H** Pip), 3.31 (s, 2H, Pip-**CH₂**) 6.62 (dd, 1H, **C6-H** Phenoxy), 6.67 (s, 1-H, **C2-H** Phenoxy), 6.7 (m, 1-H, **C4-H** Phenoxy), 7.07 (t, 1-H, **C5-H** Phenoxy), 9.25 (s, 1-H, **OH**); ^{1}H-NMR (300 MHz, MeOH-d4): δ (ppm) 1.44-1.48 (m, 2H, **C4-H** Pip), 1.55-1.62 (m, 4H, **C3,5-H** Pip), 2.41 (m, 4H, 4H, **C2,6-H** Pip), 3.41 (s, 2H, Pip-**CH₂**), 6.68 (dd, 2-H, ^{4}J = 2.9 Hz, ^{3}J = 8.0 Hz **C6-H** phenoxy), 6.75-6.77 (m, 2H, **C2, 4-H** phenoxy), 7.11 (t, 1H, ^{3}J = 8.0 Hz, **C5-H** phenoxy); ^{13}C-NMR (75.5 MHz, methanol-d_4): δ (ppm) 25.21 (C4-Pip) , 26.47 (2C, C3,5-Pip), 55.37 (2C, C2,6-Pip), 64.80 (Pip-**CH₂**), 115.34 (**C6** phenoxy), 117.81 (**C2** phenoxy), 122.12 (**C4** phenoxy), 130.22 (**C5** phenoxy), 139.64 (q, **C3** phenoxy), 158.56 (q, **C1** phenoxy); CIMS: (NH$_3$) 192.1 (MH^{+}, 100 %); C$_{12}$H$_{17}$NO (191.3)

3-[3-(Piperidin-1-ylmethyl)phenoxy]propanenitrile (3.3)

A catalytic amount of 40 % benzyltrimethylammonium hydroxide in methanol (0.6 ml) was slowly added under cooling to 3-(piperidin-1-ylmethyl)phenol (12.1 g, 63 mmol, 1 eq) and acrylonitrile (33.4 g, 624 mmol, 10 eq) under stirring. Cooling with ice was necessary to avoid local overheating. Afterwards the reaction mixture was stirred for 24 h at 85 °C. After cooling to room temperature (rt.) the organic solvent was removed under reduced pressure. The oil was dissolved in diethyl ether (150 ml), washed with 40 ml of a 5 % sodium hydroxide solution (3 times) and subsequently with 40 ml water (3 times). The organic phase was dried over sodium sulphate before the product was precipitated as HCl salt with 5 - 6 M HCl in 2-propanol. The resulting white crystals were dried over phosphorus pentoxide in vacuo (13.4 g, 75 %). Mp: 157 °C; (ref:,161-162 °C[11])

^{1}H-NMR (300 MHz, DMSO-d_6): δ (ppm) 1.27-1.40 (m, 1H, **C4-H** Pip), 1.66-1.88 (m, 5H, **C3,4,5-H** Pip), 2.75-2.9 (m, 2H, OCH$_2$**CH$_2$**CN), 3.06 (t, 2H, ^3J = 6 Hz **C2/C6-H** Pip), 3.22-3.26 (m, 2H, **C2/C6-H** Pip), 3.77 (s, 1H, NH), 4.21-4.25 (m, 4H, Pip**CH$_2$**, O**CH$_2$**CH$_2$CN), 7.02-7.06 (dd, 1H, ^4J = 1.9 Hz, ^3J = 9.6 Hz **C6-H** phenoxy), 7.20 (d, 1-H, ^3J = 7.5 Hz Aromat **C4-H** phenoxy), 7.37 (t, 1H, ^3J = 8.0 Hz, **C5-H** phenoxy) 7.41 (s, 1H, **C2-H** phenoxy), 11.03 (s, 1H, NH); ^{13}C-NMR (75.5 MHz, DMSO-d_6): δ (ppm) 17.8 (-OCH$_2$**CH$_2$**CN), 21.36 (**C4**-Pip), 21.89 (2C, **C3,5** Pip), 51.42 (2C, **C2,6** Pip), 58.52 (Pip-**CH$_2$**), 62.69 (-O**CH$_2$**CH$_2$CN), 115.54 (**C6** phenoxy), 117.2 (**C2** phenoxy), 118.79 (q), 124.01 (**C4** phenoxy), 129.77 (**C5** phenoxy), 131.34 (q, **C3** Phenoxy), 157.61 (q, **C1** Phenoxy); CIMS: (C_4H_{10}) 245.0 (MH$^+$, 100 %); $C_{15}H_{20}N_2O$ x HCl (280.79)

3-[3-(Piperidin-1-ylmethyl)phenoxy]propan-1-amine (3.4)

1-[3-(2-Cyanoethoxy)benzyl]piperidinium chloride (10.65 g, 38 mmol, 1 eq) was slowly added to a suspension of 2.2 g (56 mmol, 1.5 eq) lithium aluminium hydride (LiAlH$_4$), in anhydrous diethyl ether under cooling. After 3.5 h the remaining LiAlH$_4$ was hydrolysed with 25 ml of 5 % sodium hydroxide solution. Insoluble material was filtered off, diethyl ether was added to obtain a volume of 100 ml, and the solution was washed with 40 ml water (3 times). The diethyl ether phase was dried over sodium sulphate the solvent was evaporated under reduced pressure and dried in vacuo to obtain the desired product as yellow oil (6.55 g, 70 %).

^{1}H-NMR (300 MHz, CDCl$_3$): δ (ppm) 1.41-1.43 (m, 2H, **C4-H** Pip), 1.53-1.60 (m, 4H, **C3,5-H** Pip), 1.92 (qui, 2H, ^3J= 6.4 Hz, -OCH$_2$**CH$_2$**CH$_2$NH$_2$), 2.36 (m, 4H, **C2,6-H** Pip), 2.91 (t, 2H, ^3J= 6.8 Hz, -

OCH$_2$CH$_2$**CH$_2$**NH$_2$), 3.43 (s, 2H, Pip**CH$_2$**), 4.04 (t, 2H, ^{3}J= 6.1, Hz -O**CH$_2$**CH$_2$CH$_2$NH$_2$), 6.77 (dd, 1H, ^{4}J = 1.9 Hz, ^{3}J = 7.6 Hz, **C6-H** phenoxy), 6.86-6.89 (m, 2H, **C2, 4-H** phenoxy), 7.19 (t, 1H, ^{3}J = 8.1 Hz, **C5-H** phenoxy); ^{13}C-NMR (75.5 MHz, CDCl$_3$): δ (ppm) 24.39 (**C4** Pip), 25.99 (2C, **C3,5**-Pip), 33.14 (C, -O**CH$_2$**CH$_2$CH$_2$NH$_2$), 39.35 (C, -OCH$_2$CH$_2$**CH$_2$**NH$_2$), 54.53 (2C, **C2/6** Pip), 63.85 (Pip-**CH$_2$**), 65.82 (C, -O**CH$_2$**CH$_2$CH$_2$NH$_2$), 112.84 (C6 phenoxy) , 115.21 (**C2** phenoxy), 121.57 (**C4** phenoxy), 129.01 (**C5** phenoxy), 140.34 (q, **C3** phenoxy), 158.94 (q, **C1** phenoxy) CIMS: m/z (NH$_3$) 249.2 (MH$^+$), 100 %; C$_{15}$H$_{24}$N$_2$O (248.4)

Preparation of cyanoguanidines 3.5 and 3.6- General procedure 1

3-[3-(Piperidin-1-ylmethyl)phenoxy]propan-1-amine, **3.4** (1 eq) and diphenyl cyanocarbonimidate (1 eq) were dissolved in methanol (40 -50 ml) and stirred at rt for 5 h to prepare the intermediate phenyl N'-cyano-N-{3-[3-(piperidin-1-ylmethyl)phenoxy]propyl} carbamimidate. The respective diamine, dissolved in 10- 15 ml methanol, was added and the solution was stirred overnight at rt. The organic solvent was evaporated under reduced pressure and the residue was dissolved in CH$_2$Cl$_2$ (60- 80 ml). The solution was washed with water (2 times, 20 ml) and subsequently two times with 20 ml sodium hydroxide solution (10 % m/v). The organic phase was dried over sodium sulphate, filtered, and the organic solvent was removed under reduced pressure. Yellow oil, dried over phosphorus pentoxide in vacuo was obtained.

1-(2-Aminoethyl)-2-cyano-3-{3-[3-(piperidin-1-ylmethyl)phenoxy]propyl}guanidine (3.5)

Compound **3.5** was synthesized from **3.4** (819 mg, 3.3 mmol, 1 eq), diphenyl cyanocarbonimidate (0.82 mg, 3.4 mmol, 1.1 eq) and ethane-1,2-diamine (3.9 g, 64 mmol, 20 eq) according to procedure 1 in 50 ml methanol. After work-up 900 mg (76 %) of the product were obtained as yellow oil.

RP-HPLC (220 nm, MeOH gradient 2): 98 % (t$_R$=13.1 min, k=4.2); ^{1}H-NMR (300 MHz, methanol -d$_4$): δ (ppm) 1.45-1.46 (m, 2H, **C4-H** Pip), 1.55-1.62 (m, 4H, **C3,5-H** Pip), 2.00-2.08 (qui, 2H, -OCH$_2$**CH$_2$**CH$_2$NH-), 2.41 (m, 4H, **C2,6-H** Pip), 2.74 (t, 2H, ^{3}J= 6.3 Hz, CH$_2$), 3.24 (t, 2H, ^{3}J= 6.3 Hz, CH$_2$), 3.42 (t, 2H, ^{3}J=6.7 Hz, - CH$_2$), 3.45 (s, 2H, Pip**CH$_2$**), 4.05 (t, 2H, ^{3}J=5.9 Hz, -O**CH$_2$**CH$_2$CH$_2$NH-), 6.85-6.90 (m, 2H, **C6-H** phenoxy), 6.94-6.95 (m, 1H, **C2, 4-H** phenoxy,), 7.21 (t, 1H, ^{3}J=7.8 Hz, **C5-H** phenoxy); ^{13}C-NMR (75.5 MHz, methanol-d$_4$): δ (ppm) 25.23 (**C4** Pip), 26.52 (2C, **C3,5** Pip), 30.13, 40.34, 41.94, 45.18, 55.41 (2C, **C2,6** Pip), 64.78 (Pip-**CH$_2$**) 66.67 (C, -O**CH$_2$**CH$_2$CH2NH-),

114.65 (**C6** phenoxy), 116.94 (**C2** phenoxy), 120.05 (q, -**CN**) 123.49 (**C4** phenoxy), 130.3 (**C5** phenoxy), 139.96 (q, **C3** phenoxy), 160.3 (q, **C1** phenoxy), 161.67 (q); IR: 3265, 2931, 2163 (CN), 1580, 1441, 1343, 1258; <u>HRMS</u>: (EI) m/z calcd. for $C_{19}H_{30}N_6O$ 358.2481 [M$^+$], found: 358.2474; $C_{19}H_{30}N_6O$ (358.48)

1-(6-Aminohexyl)-2-cyano-3-{3-[3-(piperidin-1-ylmethyl)phenoxy]propyl}guanidine (3.6)

Compound **3.4** (500 mg, 2 mmol, 1 eq), diphenyl cyanocarbonimidate (500 mg, 2 mmol, 1 eq) and hexane-1,6-diamine (4.7 g, 40 mmol, 20 eq) reacted in 60 ml methanol as described in procedure 1. After work-up according to procedure 1 we got 690 mg (84 %) of the product as oil.

<u>RP-HPLC</u> (220 nm, MeOH gradient 2): 96 % (t_R=15.1 min, k=4.9); <u>^{1}H-NMR</u> (600 MHz, DMSO-d$_4$): δ (ppm) 1.22 (m, 4H), 1.31-1.43 (m, 6H), 1.45-1.48 (m, 5H), 1.87-1.92 (m, 2H, -OCH$_2$**CH$_2$**CH$_2$NH-), 2.28 (m, 4H, **C2,6**-H Pip), 2.5 (-NH-CH$_2$(CH$_2$)$_4$**CH$_2$**NH$_2$), 3.06-3.07 (m, 2H, -NH-**CH$_2$**(CH$_2$)$_4$CH$_2$NH$_2$), 3.25-3.26 (m, 2H, -OCH$_2$CH$_2$**CH$_2$**NH-), 3.36 (s, 2H, **PipCH$_2$**), 3.95 (t, 2H, ^{3}J=6.1 Hz -O**CH$_2$**CH$_2$CH$_2$NH-), 6.24 (s, 1H, NH), 6.77-6.78 (m, 1H, **C6 –H** phenoxy), 6.84 (s, 1H, **C2 –H** phenoxy), 6.94-6.99 (m, 1H **C4-H** phenoxy), 7.19 (t, 1H, ^{3}J=8 Hz, **C5-H** phenoxy); <u>^{13}C-NMR</u> (150.95 MHz, DMSO-d$_4$): δ (ppm) 24.00 (**C4** Pip), 25.59 (2C, **C3,5** Pip), 26.07 (**C** hexyl), 28.73 (-OCH$_2$**CH$_2$**CH$_2$NH-), 28.97 (**C** hexyl), 32.79 (**C** hexyl), 38.29 (-OCH$_2$CH$_2$**CH$_2$**NH-), 40.04 (**C** hexyl), 41.03 (**C** hexyl), 41.34 (**C** hexyl), 53.89 (2C, **C2,6** Pip), 62.79 (Pip-**CH$_2$)**, 65.00 (C, -O**CH$_2$**CH$_2$CH$_2$NH-), 112.65 (**C6** phenoxy), 114.60 (**C2** phenoxy), 118.17 (q, CN), 120.91 (**C4** phenoxy), 129.04 (**C5** phenoxy), 140.29 (q, **C3** phenoxy), 158.45 (q, **C1** phenoxy), 159.28 (q,); IR: 3265, 2930, 2162 (CN), 1580, 1443, 1341, 1259, 1039; <u>HRMS</u>: (EI) m/z calcd. for $C_{23}H_{38}N_6O$ 414.3107 [M$^+$], found: 414.3098; $C_{23}H_{38}N_6O$ (414)

Preparation of amides 3.7 and 3.8

2-Amino-N-{3-[3-(piperidin-1-ylmethyl)phenoxy]propyl}acetamide (3.7)

To a solution of **3.21** (0.23 g, 0.53 mmol, 1 eq) in 15 ml methanol hydrazine hydrate (0.09 ml, 1.8 mmol, 3.3 eq) was added and heated to reflux for 1 h. After addition of 1.5 ml of 2N HCl the solution was heated to reflux for another 30 min. The insoluble material was filtered off and washed with water. The filtrate was concentrated, adjusted to a pH between 9 and 10 and ex-

tracted with CHCl$_3$. The organic layers were combined, dried over magnesium sulphate and the solvent evaporated to give sticky yellow oil 108 mg (68 %)

<u>^{1}H-NMR (300 MHz, CDCl$_3$):</u> δ (ppm) 1.42-1.60 (m, 6 H, **C3,4,5-H** Pip), 2.02 (qui, 2H, ^{3}J=6.1 Hz, -OCH$_2$**CH$_2$**CH$_2$NH-), 2.37 (m, 4H, **C2,C6**-H Pip), 3.35 + 3.43 both (s, 2H, Pip**CH$_2$,** CO**CH$_2$**), 3.47-3.51 (qua, 2H, ^{3}J=6.2 Hz, OCH$_2$CH$_2$**CH$_2$**NH-), 4.05 (t, 2H, ^{3}J=5.9 Hz, -O**CH$_2$**CH$_2$CH$_2$NH-), 6.75-6.80 (m, 1H, **C6 –H** phenoxy), 6.88-6.91 (m, 2H, **C2,4 –H** phenoxy), 7.17-7.23 8 (m, 1H, **C5-H** phenoxy), 7.62 8s, 1H, NH); <u>^{13}C-NMR (75.5 MHz, CDCl$_3$):</u> δ (ppm) 24.36 (**C4** Pip), 25.97 (2C, **C3/5**-Pip), 29.08 (-OCH$_2$**C**H$_2$CH$_2$NH-), 36.92, 44.92, 44.82, 54.53 (2C, **C2,6**-Pip), 63.78 (Pip-**C**H$_2$), 66.22 (-O**C**H$_2$CH$_2$CH$_2$NH-), 112.83, (**C6** phenoxy), 115.12 (**C2** phenoxy), 121.77 (**C4** phenoxy), 129.07 (**C5** phenoxy), 140.39 (q, **C3** phenoxy), 158.68 (q, **C1** phenoxy), 172.84 (q, CO); <u>CIMS</u> (NH$_3$) 306.3 (MH$^+$), 100 %; C$_{17}$H$_{27}$N$_3$O$_2$ (305.4)

6-Amino-N-{3-[3-(piperidin-1-ylmethyl)phenoxy]propyl}hexanamide (3.8)

To a solution of **3.22** (0.73 g, 1.48 mmol, 1 eq) in 20 ml methanol hydrazine hydrate (0.24 ml, 4.9 mmol, 3 eq) was added and heated to the boiling point for 1 h. After addition of 2 ml of 2N HCl the solution was heated to reflux for another 30 min. The insoluble material was filtered off and washed with water. The filtrate was concentrated, adjusted to a pH between 8 and 9 and extracted with CHCl$_3$. The organic layers were combined, dried over magnesium sulphate and the solvent was evaporated to give 108 mg (68 %) of sticky yellow oil. The product was purified by column chromatography on silica gel (elution with methanol containing 1 % NH$_3$) yielding 250 mg of the compound as sticky yellow oil (47 %).

<u>^{1}H-NMR (300 MHz, CDCl$_3$):</u> δ (ppm) 1.25-1.60 (m, 12 H, **C3,4,5-H** Pip), 2.02 (m, 2H, **CH$_2$),** 2.17 (m, 2H, **CH$_2$**), 2.42 (m, 4H, **C2,C6**-H Pip), 2.75-2.80 (m, 2H, **CH$_2$**), 3.37-3.46 (m, 2H, **CH$_2$**-), 3.49 (s, 2H, Pip**CH$_2$),** 4.00-4.04 (m, 2H, -O**CH$_2$**CH$_2$CH$_2$NH-), 6.74-6.78 (m, 1H, **C6 –H** phenoxy), 6.87-6.93 (m, 2H, **C2,4 –H** phenoxy), 7.17-7.22 (m, 1H, **C5-H** phenoxy), 7.62 (s, 1H, NH); <u>^{13}C-NMR (75.5 MHz, CDCl$_3$):</u> δ (ppm) 24.2, 25.2, 25.6 (2C, **C3/5**-Pip), 26.1, 27.9, 29.2, 36.0, 36.8, 39.9, 54.3 (2C, **C2,6**-Pip), 63.5 (Pip-**C**H$_2$), 65.8 (-O**C**H$_2$CH$_2$CH$_2$NH-), 113.1, (**C6** phenoxy), 115.3 (**C2** phenoxy), 121.8 (**C4** phenoxy), 129.1 (**C5** phenoxy), 139.5 (q, **C3** phenoxy), 158.8 (q, **C1** phenoxy), 173.8 (q, CO); <u>CIMS</u> (NH$_3$) 306.3 (MH$^+$), 100 %; C$_{17}$H$_{27}$N$_3$O$_2$ (305.4); <u>CI-MS</u> (NH$_3$) 362.2 (MH$^+$), 100 %; C$_{21}$H$_{35}$N$_3$O$_2$ (361.52)

Preparation of squaramides 3.9-3.15, 3.24 and 3.25

3-Ethoxy-4-{3-[3-(piperidin-1-ylmethyl)phenoxy]propylamino}cyclobut-3-ene-1,2-dione (3.24)

3,4-Diethoxycyclobut-3-ene-1,2-dione (0.29 g, 1.7 mmol, 1.1 eq), dissolved in 10 ml ethanol, was slowly added to a solution of 3-[3-(piperidin-1-ylmethyl)phenoxy]propan-1-amine (0,38 g, 1.5 mmol, 1 eq) in 10 ml ethanol. The yellow solution was stirred for 3 h at rt. before the solvent was evaporated under reduced pressure. The residue was dissolved in 30 ml ethyl acetate and washed 3 times with 20 ml water. After drying over sodium sulphate the ethyl acetate phase was evaporated and the product dried in vacuo to give 570 mg (99.8 %) of sticky yellow oil with sufficient purity.

^{1}H-NMR: (400 MHz, CDCl$_3$): δ (ppm) 1.43 (m, 5H, -OCH$_2$**CH$_3$**, **C4**-H Pip), 1.57 (m, 4H, **C3,5-H** Pip), 2.07-2.13 (m, 2H, -OCH$_2$**CH$_2$**CH$_2$NH-), 2.37 (m,4H, **C2/4-H** Pip), 3.43 (s, 2H, Pip**CH$_2$**), 3.68 (m,1.4 H, -OCH$_2$CH$_2$**CH$_2$**NH-), 3.88 (0.7 H, -OCH$_2$CH$_2$**CH$_2$**NH-), 4.07 (m, 2H, -O**CH$_2$**CH$_2$CH$_2$NH-), 4.71 (qua,2H, ^{3}J = 7.1 Hz, -O**CH$_2$**CH$_3$), 6.05 (bs, 0.2 H, **NH**), 6.74-6.77 (m, 1H, C6-H phenoxy), 6.79 (bs, 0.7 H, **NH**), 6.89-6.91 (m, 2H, **C2,4-H** phenoxy), 7.2 (t, 1H, ^{3}J = 7.8 Hz, **C5-H** phenoxy); ^{13}C-NMR (100.6 MHz, CDCl$_3$): δ (ppm) 15.77 (-OCH$_2$**CH$_3$)**, 24.29 (**C4-Pip)**, 25.87 (2C, **C3/5**-Pip), 30.00 (-OCH$_2$**CH$_2$**CH$_2$NH-), 42.43 (OCH$_2$CH$_2$**CH$_2$**NH-), 54.49 (2C, **C2/6**-Pip), 63.66 (Pip-**CH$_2$**), 64.93 (-O**CH$_2$**CH$_2$CH$_2$NH-), 69.64 (-O**CH$_2$**CH$_3$), 112.92 (**C6**-phenoxy) , 114.94 (**C2**-phenoxy), 122.04 (**C4**-phenoxy), 129.12 (**C5**-phenoxy), 140.41 (q, **C3**-phenoxy), 158.42 (q, **C1**-phenoxy), 177.47; ESMS (CH$_2$Cl$_2$/ MeOH+ 10 mmol/l NH$_4$Ac): m/z 373.2, [MH$^+$]; 395.1 [MNa$^+$]; C$_{21}$H$_{28}$N$_2$O$_4$ (372,5)

Preparation of squaramides with alkylamine spacers - General procedure 2

3-Ethoxy-4-{3-[3-(piperidin-1-ylmethyl)phenoxy]propylamino}cyclobut-3-ene-1,2-dione (**3.24**) (1 eq) was dissolved in 15-30 ml ethanol. After addition of the respective diamine (18-20 eq), dissolved in 5-15 ml ethanol, the solution was stirred at rt. The reaction is completed within 1-5 h (partial precipitation of the product). To ensure a quantitative reaction the mixture was stirred over night before evaporating the solvent. The residue was dissolved in a small amount of ethanol or methanol (1-3 ml), before diethyl ether was added to precipitate the product. The suspension was stored for 2 h to 1 d at 4-6 °C. Afterwards the white or yellow crystals were filtered through glass filter crucibles and dried in vacuo. Products were obtained with purities of 85- 98 %. Compounds with purity below 96 % were purified by preparative HPLC (system 2-1).

**tert-Butyl 2-(3,4-dioxo-2-{3-[3-(piperidin-1-ylmethyl)phenoxy]propylamino}cyclobut-1-
enylamino)ethylcarbamate (3.25)**

Compound **3.24** (230 mg, 618 μmol, 1 eq) and *tert*-butyl 2-aminoethylcarbamate (120 mg, 732
μmol, 1.1 eq) were dissolved in 30 ml ethanol and stirred overnight at rt. After evaporation of
the solvent the product crystallised from ethyl acetate/hexane (8/2, v/v), leading to 201 mg of a
yellow solid (67 %). Mp: 110 °C;

RP-HPLC (220 nm, gradient 1): 97 % (t_R = 15.2 min, k= 4.98); ^{1}H-NMR: (400 MHz, CDCl$_3$): δ (ppm)
1.40-1.44 (m, 11H, **C4**-H Pip, **tertbutoxy**), 1.5-1.6 (m, 4H, **C3,4,5-H** Pip), 1.95 (bs, 1H, -NH-), 2.12
(qui, 2H, ^{3}J= 6.0 Hz, -NHCH$_2$**CH$_2$**CH$_2$NH-); 2.38 (m, 4H, **C2,6-H** Pip), 3.27 (m, 2H, CH$_2$) 3.42 (s, 2H,
Pip**CH$_2$**), 3.57 (m, 2 H, CH$_2$), 3.84 (m, 2 H, CH$_2$), 4.06 (m, 2H, ^{3}J= 5.8 Hz, -O**CH$_2$**CH$_2$CH$_2$NH-),5.58
(bs, 0.5 H, NH), 6.75 (dd, ^{4}J= 2 Hz, ^{3}J= 8.2 Hz, **C6-H** phenoxy), 6.86-6.91 (m, 2H, **C2,4-H** phenoxy),
,7.19 (t, ^{3}J=7.8 Hz, **C5-H** phenoxy); ^{13}C-NMR (75.5 MHz, CDCl$_3$): δ (ppm) 24.30 (**C4** Pip), 25.86 (2C,
C3,5-Pip), 28.36 (3C, **tertbutoxy**), 30.71 (2C weak signal), 41.66 (broad; weak signal) 54.52 (2C,
C2,6-Pip), 63.8 (Pip-**CH$_2$**), 64.86 (-O**CH$_2$**CH$_2$CH$_2$NH-), 112.81 (**C6** phenoxy) , 115.42 (**C2** phenoxy),
121.91 (**C4** phenoxy), 129.06 (**C5** phenoxy), 140.10 (q, **C3** phenoxy), 158.66 (q, **C1** phenoxy),
167.86 (q, cyclobutenedione) 2q C not detected; ESMS (CH$_2$Cl$_2$, MeOH + 10 mmol/l sodium ace-
tate): *m/z* 487.3 [MH$^+$]; C$_{26}$H$_{38}$N$_4$O$_5$ (486.28)

**3-(2-Aminoethylamino)-4-{3-[3-(piperidin-1-ylmethyl)phenoxy]propylamino}cyclobut-3-ene-
1,2-dione (3.9)**

Compound **3.25** (100 mg, 206 μmol) was dissolved in CH$_2$Cl$_2$ and TFA in CH$_2$Cl$_2$ (10 %) was added.
The solution was stirred overnight at rt. The solvent was evaporated and a mixture of etha-
nol/diethyl ether (1/10, v/v) was added and stored 16 h at 4- 6 °C. The resulting yellow crystals
were filtered off and dried in vacuo to give a yellow semi solid. RP-HPLC (210 nm, gradient 1): 96
%. A sample of 26.4 mg was purified by preparative HPLC (system 2-1, 220 nm). Acetonitrile was
removed under reduced pressure. After lyophilisation 3.25 mg were obtained as yellow oil.

RP-HPLC (220 nm, gradient 1): 99 % (t_R = 9.5 min, k= 2.7); (measured as amine) ^{1}H-NMR (300
MHz, methanol-d$_4$): δ (ppm) 1.46-1.48 (m, 2 H, **C4-H** Pip), 1.56-1.64 (m, 4H, **C3,5-H** Pip), 2.1 (qui,
2H, ^{3}J= 6.3 Hz, -OCH$_2$**CH$_2$**CH$_2$NH-), 2.43 (m, 4H, **C2, 6**-H Pip), 2.8 (t, 2H, ^{3}J= 6.1 Hz, -NH-CH$_2$**CH$_2$**NH),
3.48 (s, 2H, Pip**CH$_2$**), 3.63-3.65 (m, 2H, -NH-**CH$_2$**CH$_2$NH-), 3.82 (m, 2H, -OCH$_2$CH$_2$**CH$_2$**NH-), 4.09 (t,
2H, ^{3}J= 6.0 Hz, -O**CH$_2$**CH$_2$CH$_2$NH-), 6.84 (dd, 1H, ^{4}J= 2.1 Hz, ^{3}J= 7.9 Hz, **C6 –H** phenoxy), 6.89 (d,

1H, ^{3}J=7.6 Hz, **C4 –H** phenoxy), 6.92 (s, 1H, **C2-H** phenoxy), 7.21 (t, 1H, ^{3}J= 7.8 Hz, **C5-H** phenoxy); ^{13}C (150.95 MHz, methanol-$\underline{d_4}$): δ (ppm) 25.09 (**C4** Pip), 26.38 (2C, **C3,5**-Pip), 31.84 (C -OCH$_2$**C**H$_2$CH$_2$NH-), 42.49 (C -OCH$_2$CH$_2$**C**H$_2$NH-), 43.36 (C -NH**C**H$_2$CH$_2$NH$_2$) 47.36 (C -NHCH$_2$**C**H$_2$NH$_2$) 55.33 (2C, **C2,6**-Pip), 64.65 (Pip-**C**H$_2$), 66.56 (C -O**C**H$_2$CH$_2$CH$_2$NH-), 114.67, (**C6** phenoxy), 116.91 (**C2** phenoxy), 123.45 (**C4** phenoxy), 130.26 (**C5** phenoxy), 139.67 (q, **C3** phenoxy), 160.29 (q, **C1** phenoxy), 169.79 (q, cyclobutenedione), 183.78 (q, **CO** cyclobutenedione), 183.83 (q, **CO** cyclo-butenedione); HRMS: (EI) m/z calcd. for C$_{21}$H$_{30}$N$_4$O$_3$ 386.2318 [M$^+$], found: 386.2315; C$_{21}$H$_{30}$N$_4$O$_3$ x C$_4$H$_2$F$_6$O$_4$ (614.6)

3-(3-Aminopropylamino)-4-{3-[3-(piperidin-1-ylmethyl)phenoxy]propylamino}cyclobut-3-ene-1,2-dione (3.10)

Compound **3.24** (140 mg, 376 µmol, 1 eq) and propane-1,3-diamine (0.64 ml, 7.56 mmol, 20 eq) were used according to procedure 2 (10 ml ethanol), affording the product as yellow crystals (100 mg, 66 %). Mp: 115 °C (decomp). 40 mg were purified by preparative HPLC (220 nm, system 2-1). Acetonitrile was removed under reduced pressure. Lyophilisation gave 32.2 mg of yellowish oil.

RP-HPLC (220 nm, gradient 1): 99.9 % (t$_R$= 9.1 min, k= 2.6); ^{1}H-NMR (300 MHz, methanol-$\underline{d_4}$): δ (ppm) 1.46-2.01 (m, 8H, **C3,4,5-H** Pip, -NHCH$_2$**CH$_2$**CH$_2$NH$_2$), 2.1 (qui, 2H, ^{3}J=6.3 Hz, -OCH$_2$**CH$_2$**CH$_2$NH-), 2.9-3.03 (m, 4H, **C2/C6**-H Pip, **CH$_2$**), 3.46 (m, 2H, **C2/C6**-H Pip), 3.68 (t, 2H, ^{3}J=6.6 Hz, **CH$_2$**), 3.84 (m, 2H, -OCH$_2$CH$_2$**CH$_2$**NH-), 4.12 (t, 2H, ^{3}J=5.9 Hz, -O**CH$_2$**CH$_2$CH$_2$NH-), 4.23 (s, 2H, Pip**CH$_2$**), 7.02-7.06 (m, 3H, **C2,4,6 –H** phenoxy), 7.37 (t, 1H, ^{3}J=7.8 Hz, **C5-H** phenoxy); ^{13}C-NMR (75.5 MHz, methanol-$\underline{d_4}$): δ (ppm) 22.76 (**C4** Pip), 24.14 (2C, **C3,5** Pip), 30.41 (C CH$_2$), 31.65 (C, CH$_2$), 37.9 (C, CH$_2$), 41.89 (C CH$_2$), 42.5 (C CH$_2$), 54.09 (2C, **C2,6**-Pip), 61.73 (Pip-**C**H$_2$), 66.21 (C -O**C**H$_2$CH$_2$CH$_2$NH-), 117.19, (**C6** phenoxy), 118.4 (**C2** phenoxy), 124.49 (**C4** phenoxy), 131.45 +131.75 (**C5** phenoxy+ q, **C3** phenoxy), 160.79 (q, **C1** phenoxy), 183.76 (q, **CO** cyclobutenyl), 2q C cyclobutenyl not seen; HRMS (FAB$^+$, Glycerine): m/z calcd. for C$_{22}$H$_{33}$N$_4$O$_3$ 401.2553 [MH$^+$], found: 401.2551; C$_{22}$H$_{32}$N$_4$O$_3$ x C$_4$H$_2$F$_6$O$_4$ (628.6)

3-(4-Aminobutylamino)-4-{3-[3-(piperidin-1-ylmethyl)phenoxy]propylamino}cyclobut-3-ene-1,2-dione (3.11)

Ligand **3.11** was synthesised in 30 ml ethanol from **3.24** (140 mg, 376 µmol, 1 eq) and butane-1,4-diamine (480 mg, 6.4 mmol, 14.5 eq) as described in procedure 2 yielding 140 mg (89 %) of a white solid. RP-HPLC (210 nm, gradient 1): 94 %. Mp: 138 °C (decomp.). A sample (13 mg) was purified by preparative HPLC (220nm, system 2-1). Acetonitrile was removed under reduced pressure. Lyophilisation gave 8.47 mg of the product as white semi solid.

RP-HPLC (220 nm, gradient 1): 99.8 %. (t_R= 9.7 min, k= 2.8); ^{1}H-NMR (300 MHz, methanol-$\underline{d_4}$): δ (ppm) 1.5-1.52 (1H, **C-H** Pip), 1.7-1.76 (m, 7 H, 3H **C3,4,5-H** Pip, NH-CH$_2$(**CH$_2$)$_2$**CH$_2$NH$_2$), 1.92-1.95 (m, 2H, **C3/5-H** Pip), 2.1 (qui, 2H, ^{3}J=6.4 Hz, -OCH$_2$**CH$_2$**CH$_2$NH-), 2.92-2.97 (m, 4H, **C2/C6**-H Pip, NH-CH$_2$(CH$_2$)$_2$**CH$_2$**NH$_2$), 3.42-3.44 (m, 2H, **C2/C6**-H Pip), 3.60 (m, 2H, NH-**CH$_2$**(CH$_2$)$_2$CH$_2$NH$_2$), 3.83 (m, 2H, OCH$_2$CH$_2$**CH$_2$**NH-), 4.12 (t, 2H, ^{3}J=5.9 Hz, O**CH$_2$**CH$_2$CH$_2$NH-), 4.23 (s, 2H, PipCH$_2$), 7.02-7.04 (m, 2H, **4,6 –H** phenoxy), 7.06 (s, 1H, **C2-H** phenoxy), 7.37 (t, 1H, ^{3}J=7.9 Hz, C5 –H phenoxy); ^{13}C-NMR (150.95 MHz, methanol-$\underline{d_4}$): δ (ppm) 22.72 (**C4** Pip), 24.11 (2C, **C3,5** Pip), 25.34, (**C**-butyl), 29.17 , (**C**-butyl), 31.68 (-OCH$_2$**CH$_2$**CH$_2$NH-), 40.16, (**C**-butyl), 42.47 (-OCH$_2$CH$_2$**CH$_2$**NH-), 44.29 (-NH-**CH$_2$**(CH$_2$)$_2$CH$_2$NH$_2$), 54.09 (2C, **C2,6**-Pip), 61.72 (Pip-**CH$_2$**), 66.24 (-O**CH$_2$**CH$_2$CH$_2$NH-), 117.15, (**C6** phenoxy), 118.45 (**C2** Phenoxy), 124.46 (**C4** phenoxy), 131.42 + 131.70 (**C5** phenoxy, q, **C3** phenoxy), 160.77 (q, **C1** Phenoxy), 183.63 (q, **CO** cyclobutenedione), not detected: q, **2C**, cyclobutenedione; HRMS: (EI) m/z calcd. for C$_{23}$H$_{34}$N$_4$O$_3$ 414.2631 [M$^+$], found: 414.2636; C$_{23}$H$_{34}$N$_4$O$_3$ x C$_4$H$_2$F$_6$O$_4$ (642.6)

3-(5-Aminopentylamino)-4-{3-[3-(piperidin-1-ylmethyl)phenoxy]propylamino}cyclobut-3-ene-1,2-dione (3.12)

Compound **3.12** was synthesized from **3.24** (130 mg, 349 µmol, 1 eq) and pentane-1,5-diamine (0.7 mg, 6.6 mmol, 19.6 eq) according to procedure 2 in 15 ml ethanol yielding 80 mg (53.5 %) of compound 142 as white solid. Mp: > 130°C (decomp.); RP-HPLC (220 nm, gradient 1): 94 %; 55 mg were purified by preparative HPLC (220 nm, system 2-1). The organic solvent was removed under reduced pressure. After lyophilisation 11.87 mg of the product were obtained as yellow oil.

RP-HPLC (220 nm, gradient 1): 99.4 % (t_R= 9.3 min, k= 2.7); ^{1}H-NMR (300 MHz, methanol-d_4): δ (ppm) 1.44-1.52 (3H, **C-H** Pip, **CH$_2$** pentyl), 1.66-1.81 (m, 7 H, 2x CH$_2$ pentyl +**C-H** Pip), 1.74-1.81 (m, 2H, **C-H** Pip), 2.1 (qui, 2H, ^{3}J=6.3 Hz, -OCH$_2$**CH$_2$**CH$_2$NH-), 2.9-2.96 (m, 4H, **C2/C6**-H Pip, **CH$_2$** pentyl), 3.42-3.44 (m, 2H, **C2/C6**-H Pip), 3.60 (m, 2H, **CH$_2$** pentyl), 3.83 (m, 2H, -OCH$_2$CH$_2$**CH$_2$**NH-), 4.12 (t, 2H, ^{3}J=5.9 Hz, O**CH$_2$**CH$_2$CH$_2$NH-), 4.23 (s, 2H, Pip**CH$_2$**), 7.02-7.06 (m, 3H, **2,4,6 –H** phenoxy), 7.36 (t, 1H, ^{3}J=7.9 Hz, **C5 –H** phenoxy); ^{13}C-NMR (150.95 MHz, methanol-d_4): δ (ppm) 22.72 (**C4** Pip), 24.1+ 24.16 (2C, **C3,5**-Pip, **C** pentyl), 28.042 (**C** pentyl), 31.65 +31.71 (C, -OCH$_2$**CH$_2$**CH$_2$NH-, **C** pentyl), 40.52 (**C** pentyl), 42.46 (C, -OCH$_2$CH$_2$**CH$_2$**NH-), 44.78 (**C** pentyl), 54.09 (2C, **C2, 6**-Pip), 61.71 (Pip-**C**H$_2$), 66.25 (C, -O**C**H$_2$CH$_2$CH$_2$NH-), 117.17, (**C6** phenoxy), 118.41 (**C2** phenoxy), 124.46 (**C4** phenoxy), 131.4 + 131.70 (**C5** phenoxy, q, **C3** phenoxy), 160.76 (q, **C1** phenoxy), 169.51 (q, cyclobutenedione), 183.56 (q, **CO** cyclobutenedione); HRMS: (EI) m/z calcd. for C$_{24}$H$_{36}$N$_4$O$_3$ 428.2787 [M$^+$], found: 428.2783; C$_{24}$H$_{36}$N$_4$O$_3$ x C$_4$H$_2$F$_6$O$_4$ (656.6)

3-(6-Aminohexylamino)-4-{3-[3-(piperidin-1-ylmethyl)phenoxy]propylamino}cyclobut-3-ene-1,2-dione (3.13)

Synthesis of **3.13** according to procedure 2 from **3.24** (220 mg, 591 µmol, 1 eq) and hexane-1,6-diamine (1.3 mg, 11 mmol, 18 eq) in 30 ml ethanol afforded 190 mg of the product (beige solid, 73 %). Mp: > 130 °C (decomp.).

RP-HPLC (210 nm, gradient 1): 98 % (t_R=9.9 min, k=2.9); ^{1}H-NMR (300 MHz, DMSO-d_6): δ (ppm) 1.28-1.48 (m, 14 H, **C3,4,5-H** Pip, **4x CH$_2$**-Hexyl), 1.93-1.99 (m, 2H, -OCH$_2$**CH$_2$**CH$_2$NH-), 2.29 (m, 4H, **C2/C6**-H Pip), 2.55-2.59 (m, 1H, -NH-CH$_2$(CH$_2$)$_4$**CH$_2$**NH$_2$), 2.89 (m, 1H, -NH-CH$_2$(CH$_2$)$_4$**CH$_2$**NH$_2$), 3.36 (s, 2H, Pip**CH$_2$**), 3.47 (m, 2H, -NH**CH$_2$**(CH$_2$)$_4$CH$_2$NH-), 3.65 (m, 2H, -OCH$_2$CH$_2$**CH$_2$**NH-), 4.00 (t, 2H, ^{3}J=6.1 Hz -O**CH$_2$**CH$_2$CH$_2$NH-), 6.2 (s, 0.5 H, NH/NH$_2$), 6.78-6.85 (m, 3H, **2,4,6 –H** phenoxy), 7.2 (t, 1H, ^{3}J=8.0 Hz, **C5 –H** phenoxy), 7.93 (s, 2H, NH/NH$_2$); ^{13}C-NMR (150.95 MHz, DMSO-d_6): δ (ppm) 24.0 (**C4** Pip), 25.55 (2C, **C3,5**-Pip, **C**-Hexyl), 25.81 (**C** Hexyl), 29.86 (**C** Hexyl), 30.43 (C, -OCH$_2$**CH$_2$**CH$_2$NH-), 30.72 (**C** Hexyl), 31.59 (**C** Hexyl), 40.2 +40.8 (**C** Hexyl, -OCH$_2$CH$_2$**CH$_2$**NH-), 41.2 (C, -NH-CH$_2$(CH$_2$)$_4$**CH$_2$**NH$_2$-)"), 43.13 (C, -NH-**CH$_2$**(CH$_2$)$_4$CH$_2$NH$_2$), 53.89 (2C, **C2,6**-Pip), 62.77 (Pip-**C**H$_2$), 64.52 (C, -O**C**H$_2$CH$_2$CH$_2$NH-), 112.62, (**C6** phenoxy), 114.67 (**C2** phenoxy), 120.94 (**C4** phenoxy), 129.04 (**C5** phenoxy), 140.34 (q, **C3** phenoxy), 158.41 (q, **C1** phenoxy), 167.9 (q, cyclobutenedione), 182.26 + 182.4 (q, **CO** cyclobutenedione),; HRMS: (EI) m/z calcd. for C$_{25}$H$_{38}$N$_4$O$_3$ 442.2944 [M$^+$], found: 442.2954; C$_{25}$H$_{38}$N$_4$O$_3$ (442.6)

3-(7-Aminoheptylamino)-4-{3-[3-(piperidin-1-ylmethyl)phenoxy]propylamino}cyclobut-3-ene-1,2-dione (3.14)

Compound **3.24** (280 mg, 753 µmol, 1 eq) and heptane-1,7-diamine (1.7 g, 14.9 mmol, 19.8 eq) were used as described in procedure 2 (40 ml ethanol) leading to 50 mg (15 %) of the product as yellow solid. Mp: > 130 °C (decomp.). Compound **3.14** (50 mg) was purified by preparative HPLC (220 nm, system 2-1). After evaporation of acetonitrile and lyophilisation the product was obtained as yellow oil (11 mg, 22 % from crude product).

RP-HPLC (220 nm, gradient 1): 97 % (t_R=10.4 min, k=3.1); ^{1}H-NMR (300 MHz, methanol-d_4): δ (ppm) 1.4-1.93 (m, 16H, **5x CH$_2$** heptyl), **C3,4,5-H** Pip), 2.06-2.14 (qui, 2H, ^{3}J=6.3 Hz, -OCH$_2$**CH$_2$**CH$_2$NH-), 2.88-2.98 (m, 4H, **C2/6**-H Pip, **CH$_2$** heptyl), 3.42-3.46 (m, 2H, **C2/C6**-H Pip), 3.58 (m, 2H, **CH$_2$** heptyl), 3.83 (m 2H, OCH$_2$CH$_2$**CH$_2$**NH-), 4.13 (t, 2H, ^{3}J=5.7 Hz, -O**CH$_2$**CH$_2$CH$_2$NH-), 4.23 (s, 2H, Pip**CH$_2$**), 7.02-7.05 (m, 3H, **2,4,6 –H** phenoxy), 7.37 (t, 1H, ^{3}J=7.8 Hz, **C5 –H** phenoxy), ^{13}C-NMR (75.5 MHz, methanol-d_4): δ (ppm) 22.78 (**C4** Pip), 24.15 (2C, **C3,5** Pip), 27.1 (**C**, heptyl), 27.29 (**C**, heptyl), 28.52 (**C**, heptyl), 29.7 (**C**, heptyl), 31.5 (-OCH$_2$**CH$_2$**CH$_2$NH-), 32.19 (**C**, heptyl), 40.71 (**C**, heptyl), 42.5 (-OCH$_2$CH$_2$**CH$_2$**NH-), 45.12 (**C**, heptyl), 54.12 (2C, **C2,6**-Pip), 61.75 (Pip-**CH$_2$**), 65.52 (-O**CH$_2$**CH$_2$CH$_2$NH-), 118.77 (**C6** phenoxy), 120.56 (**C2** phenoxy), 124.5 (**C4** phenoxy), 130.92+ 131.45 (**C5** phenoxy, q, **C3** phenoxy), q, **C1** phenoxy, q, **4C**, cyclobutenyl, not seen; HRMS: (EI) m/z calcd. for C$_{26}$H$_{40}$N$_4$O$_3$ 456.3100 [M$^+$], found: 456.3090; C$_{25}$H$_{38}$N$_4$O$_3$ x C$_4$H$_2$F$_6$O$_4$ (684.7)

3-(8-Aminooctylamino)-4-{3-[3-(piperidin-1-ylmethyl)phenoxy]propylamino}cyclobut-3-ene-1,2-dione (3.15)

Compound **3.15** was synthesized according to procedure 2 from **3.24** (250 mg, 672 µmol, 1 eq) and octane-1,8-diamine (1.9 g, 14.8 mmol, 22 eq) in 20 ml ethanol. 233 mg (74 %) of the crude product were obtained. Mp: > 130 °C (decomp.). Compound **3.15** (47 mg) was purified by preparative HPLC (220 nm, system 2-1). After evaporation of acetonitrile and lyophilisation the product was obtained as yellow oil (19.9 mg, 42 % from crude product).

RP-HPLC (220 nm, gradient 1): 99.9 % (t_R=11.4 min, k=3.49); ^{1}H-NMR (300 MHz, methanol-d_4): δ (ppm) 1.37 (m, 8H, **CH$_2$** octyl), 1.59-1.96 (m, 10H, **C3,4,5-H** Pip, **2x CH$_2$**-octyl), 2.1 (qui, 2H, ^{3}J=6.3 Hz, -OCH$_2$**CH$_2$**CH$_2$NH-), 2.87-2.98 (m, 4H, **C2,C6**-H Pip, **CH$_2$** octyl), 3.42-3.46 (m, 2H, **C2,C6**-H Pip), 3.56-3.58 (m, 2H, **CH$_2$** octyl), 3.83 (m 2H, OCH$_2$CH$_2$**CH$_2$**NH-), 4.12 (t, 2H, ^{3}J=5.9 Hz, -O**CH$_2$**CH$_2$CH$_2$NH-), 4.23 (s, 2H, Pip**CH$_2$**), 7.02-7.05 (m, 3H, **2,4,6 –H** phenoxy), 7.36 (t, 1H, ^{3}J=7.9

Hz, **C5 –H** phenoxy), ^{13}C-NMR (75.5 MHz, methanolD-d$_4$): δ (ppm) 22.77 (**C4** Pip), 24.14 (2C, **C3,5**-Pip), 27.23, (**C**, octyl), 27.34 (**C**, octyl), 28.54 (**C**, octyl), 29.9 (C, octyl), 30.02 (**C,** octyl), 31.68 (C, -OCH$_2$**C**H$_2$CH$_2$NH-), 32.19 (**C**, octyl), 40.74 (**C**-octyl), 42.5 (-OCH$_2$CH$_2$**C**H$_2$NH-) 45.2 (**C**, octyl), 54.11 (2C, **C2,6**-Pip), 61.74 (Pip-**C**H$_2$), 66.31 (C, -O**C**H$_2$CH$_2$CH$_2$NH-), 117.22, (**C6** phenoxy), 118.38 (**C2** phenoxy), 124.5 (**C4** phenoxy), 131.43+ 131.76 (**C5** phenoxy, q, **C3** phenoxy), 160.8 (q, **C1** phenoxy), 169.56 (q, cyclobutenyl), 183.56+183.42 (q, **CO** cyclobutenedione), HRMS: (EI) m/z calcd. for C$_{27}$H$_{42}$N$_4$O$_3$ 470.3257 [M$^+$], found: 470.3263; C$_{27}$H$_{42}$N$_4$O$_3$ x C$_4$H$_2$F$_6$O$_4$ (698.7)

Preparation of the nitroethenediamine 3.16

N^1-(2-Nitro-1-{3-[3-(piperidin-1-ylmethyl)phenoxy]propylamino}ethenyl)pentane-1,5-diamine (3.16)

N-[1-(Methylthio)-2-nitroethenyl]-3-[3-(piperidin-1-ylmethyl)phenoxy]propan-1-amine (50 mg, 137 µmol, 1 eq,) was dissolved in 10 ml methanol, 70 mg (685 µmol, 5 eq) of pentane-1,5-diamine were added and the solution was stirred at rt for 12 h. The solvent was evaporated and the residue purified by preparative HPLC (220 nm, system 2-1). Acetonitrile was removed under reduced pressure. Lyophilisation gave 42 mg (47 %) of the product as brown oil.

RP- HPLC: (220 nm gradient 1): 99.8 %; (t$_R$=8.6 min, k=2.4); ^{1}H-NMR (600 MHz, methanol-d$_4$): δ (ppm) 1.29-1.35 (m, 4H, 2x CH$_2$ pentyl), 1.47-1.81 (m, 8 H, 3x CH$_2$ Pip, 1x CH$_2$ pentyl), 1.93-2.03 (s, 2H, -OCH$_2$**CH$_2$**CH$_2$NH-), 2.75-2.76 (m, 2H, CH$_2$ pentyl), 2.84 (m, 2H, **C2/6-H** Pip), 3.08-3.09 (m, 2H, CH$_2$ pentyl) 3.16 (s, 1H), 3.29 (m, 4H, -OCH$_2$CH$_2$**CH$_2$**NH-, **C2/6-H** Pip),4.01- 4.06 (m, 2H, -O**CH$_2$**CH$_2$CH$_2$NH-), 4.22 (s, Pip**CH$_2$**), 7.03-7.09 (m, 3H, **C2,4,6-H** phenoxy), 7.37 (t, 1H, ^{3}J=7.9 Hz, C5-H phenoxy), 7.63 (3H, NH$_2$/NH); ^{13}C–NMR (150.95 MHz, methanol-d$_4$): δ (ppm) 21.29 (C Pip, C pentyl), 22.31 +22.91 (3C, C Pip, C pentyl), 26.63 (C pentyl), 38.64 + 40.04 (C, pentyl, -OCH$_2$CH$_2$CH$_2$NH-) 45.71 (C pentyl), 48.67, 51.83 (2C, **C2,6** Pip), 58.9 (Pip-**C**H$_2$), 117.14 (**C6** phenoxy), 119.7 (**C2** phenoxy), 123.44 (**C4** phenoxy), 128.0+ 130.05 (**C5** phenoxy, q C), 138.03 (q), 155.58 (q), 158.51 (q); 2C -OCH$_2$CH$_2$CH$_2$NH not seen in ^{13}C, only in HSQC (broad signals), LSIMS: (FAB, Glycerine) m/z calcd. for C$_{22}$H$_{38}$N$_5$O$_3$ 420.2975 [MH$^+$], found 420.2980; C$_{22}$H$_{37}$N$_5$O$_3$ x C$_4$H$_2$F$_6$O$_4$ (647.6)

Preparation of ω-phthalimidoalkanoic acids – 3.19 and 3.20-General procedure 3

Phthalic anhydride (1 eq) and 1 eq of the respective ω-aminoalkanoic acid were melted and stirred at 135-150 °C for 30 min. The mixture was cooled to rt, dissolved in 30 ml of hot methanol, and subsequently 30 ml of cold water were added. The precipitate was filtered off, washed with 100 ml water and dried in vacuo. Recrystallization from a mixture of acetic acid/H_2O = 1/1 gave the desired products as colourless to white powders in yields of 56-86 % and a purity of 95-99 %. The products were used without further purification.

2-(1,3-Dioxoisoindolin-2-yl)acetic acid (3.19)

Phthalic anhydride (2.96 g, 19.98 mmol, 1 eq) and 2-aminoacetic acid (1.53 g, 20.37 mmol, 1 eq) reacted according to procedure 3 to give 2.3 g (56 %) of **3.19**. Mp. 185 °C (ref. 199-200 °C)[27].

^{1}H-NMR (300 MHz, CDCl$_3$): δ (ppm) 4.49 (s, 2H, CH$_2$), 7.74-7.78 (m, 2H, phthalimido), 7.87-7.91 (m, 2H, phthalimido); ^{13}C-NMR (75.5 MHz, CDCl$_3$) : δ (ppm) 38.48 (C, CH$_2$), 123.75 (C, phthalimido), 131.9 (q), 134.36 (C, phthalimido), 167.35 (q), 171.95 (q); EIMS: m/z 205.0 [M$^+$] 2.45 % ; 160.1 (100.0 %); C$_{10}$H$_7$NO$_4$ (205.2)

6-(1,3-Dioxoisoindolin-2-yl)hexanoic acid (3.20)

Phthalic anhydride (85.9 g, 39.8 mmol, 1 eq) and 6-aminohexanoic acid (5.3 g, 40.4 mmol, 1 eq) reacted according to procedure 3 to give 8.9 g (86 %) of **3.20**. Mp.105 °C (ref. 104-105 °C)[27].

^{1}H-NMR (300 MHz, CDCl$_3$): δ (ppm) 1.63-1.75 (m, 4H, N-CH$_2$(**CH$_2$**)$_3$CH$_2$COOH), 1.35-1.45 (m, 2H, N-CH$_2$(**CH$_2$**)$_3$CH$_2$COOH), 2.35 (,t, 2H, ^{3}J=7.4 Hz, -CH$_2$(CH$_2$)$_3$**CH$_2$**COOH), 3.68 (t, 2H, ^{3}J=7.2 Hz, N-**CH$_2$**(CH$_2$)$_3$CH$_2$COOH), 7.68-7.74 (m, 2H, phthalimido), 7.81-7.87 (m, 2H, phthalimido), ^{13}C-NMR (75.5 MHz, CDCl$_3$) : δ (ppm) 24.17 (C, hexanoic acid) , 26.27 (C, hexanoic acid), 28.26 (C, hexanoic acid), 33.73 (C, hexanoic acid), 37.74 (C, hexanoic acid), 123.23 (C, phthalimido), 132.11 (q), 133.92 (C, phthalimido), 168.47 (q), 179.05 (q); EIMS: m/z 261.1 [M$^+$] 4.6 %, 160.1 (100 %); C$_{14}$H$_{15}$NO$_4$ (261.3)

Preparation of phthalimides 3.21 and 3.22

2-(1,3-Dioxoisoindolin-2-yl)-N-{3-[3-(piperidin-1-ylmethyl)phenoxy]propyl}acetamide (3.21)

Carbonyldiimidazole (0.4 g, 2.47 mmol, 1 eq) and **3.19** (0.51 g, 2.48 mmol, 1 eq) were dissolved in anhydrous THF (15 ml) and stirred at rt until the formation of carbon dioxide ceased. Compound **3.4** (0.6 g, 2.4 mmol, 1 eq), dissolved in 5 ml THF was added, and the solution was stirred overnight at rt. The solvent was evaporated affording yellow sticky oil. Water (20 ml) was added and the suspension was triturated for 1 h, before the water was decanted and the residue dissolved in ethyl acetate. The solution was dried over sodium sulphate and the solvent was evaporated. After purification by flash chromatography (silica gel, Toluol/THF =1/1) and evaporation of the solvent the compound was dried in vacuo affording 430 mg of a white solid (40 %). Mp. 98-100 °C.

<u>^{1}H-NMR (300 MHz, CDCl$_3$):</u> δ (ppm) 1.54-1.62 (m, 6H, **C3,4,5-H** Pip), 1.97-2.05 (m, 2H, -OCH$_2$**CH$_2$**CH$_2$NH-), 2.38 (m, 4H, **C2,6**-H Pip), 3.44 (s, 2H, -NHCOCH$_2$-), 3.5 (qua, 2H, ^{3}J=6.2 Hz, -OCH$_2$CH$_2$**CH$_2$**NH-), 4.04 (t, 2H, ^{3}J=5.8 Hz, -O**CH$_2$**CH$_2$CH$_2$NH-), 4.34 (s, 2H, PipCH$_2$), 6.23 (s, 1H, NH), 6.70-6.73 (m, 1H, **C6–H** phenoxy), 6.88-6.90 (m, 2H, **C2,4–H** phenoxy), 7.17 (t, 1H, ^{3}J=8.0 Hz, **C5-H** phenoxy), 7.72-7.75 (m, 2H, phthal.), 7.85-7.88 (m, 2H, phthal.); <u>^{13}C-NMR (75.5 MHz, CDCl$_3$):</u> δ (ppm) 24.28 (**C4** Pip), 25.82 (2C, **C3,5**-Pip), 28.7 (-OCH$_2$**CH$_2$**CH$_2$NH-), 37.79, 40.86, 54.46 (2C, **C2/6**-Pip), 63.68 (Pip-**CH$_2$**), 66.24 (-O**CH$_2$**CH$_2$CH$_2$NH-), 113.19, (**C6** phenoxy), 115.17 (**C2** phenoxy), 121.99 (**C4** phenoxy), 123.64 (phthal.), 125.54 (q), 129.1 (**C5** phenoxy), 132.01 (q, **C3** phenoxy), 134.24 (phthal.), 158.57 (q, **C1** phenoxy), 166.12 (q, CO), 167.80 (q); <u>CIMS</u> (NH$_3$) 436.1 (MH$^+$), 100 %; C$_{25}$H$_{29}$N$_3$O$_4$ (435.52)

6-(1,3-Dioxoisoindolin-2-yl)-N-{3-[3-(piperidin-1-ylmethyl)phenoxy]propyl}hexanamide (3.22)

Compound **3.20** (1.3 g, 4.98 mmol, 1 eq) and CDI (0.81 g, 5.0 mmol, 1 eq) were dissolved in anhydrous THF (15 ml) and stirred at rt until the formation of carbon dioxide ceased. **3.4** (1.23 g, 4.95 mmol, 1 eq) in 5 ml THF was added and the solution was stirred overnight at rt. The solvent was evaporated leading to yellow sticky oil. 20 ml water was added and the suspension was triturated for 1 h, before the water was decanted and the residue dissolved in ethyl acetate. The solution was dried over sodium sulphate and the solvent was evaporated. The yellow oil was

dried in vacuo to give 2.19 g of a yellow to orange semi solid (90 %). The substance was used without further purification.

<u>^{1}H-NMR (300 MHz, CDCl$_3$):</u> δ (ppm) 1.31-1.73 (m, 12H, **C3,4,5-H** Pip, -NHCOCH$_2$(**CH$_2$**)$_3$CH$_2$-), 1.93-2.02 (m, 2H, -OCH$_2$**CH$_2$**CH$_2$NH-), 2.17 (t, 2H, ^{3}J= 7.4 Hz, CH$_2$), 2.39 (m, 4H, **C2,6**-H Pip), 3.41-3.45 (m, 2H, CH$_2$) 3.46 (s, 2H, PipCH$_2$), 3.66 (t, 2H, ^{3}J=7.2 Hz, CH$_2$), 4.02 (t, 2H, ^{3}J=5.8 Hz, O**CH$_2$**CH$_2$CH$_2$NH-), 6.0-6.03 (m, 1H, NH), 6.75-6.78 (m, 1H, **C6–H** phenoxy), 6.87-6.9 (m, 2H, **C2, 4 –H** phenoxy), 7.2 (t, 1H, ^{3}J=8.0 Hz, **C5-H** phenoxy), 7.68-7.72 (m, 2H, phthal.), 7.80-7.83 (m, 2H, phthal.); <u>^{13}C-NMR (75.5 MHz, CDCl$_3$):</u> δ (ppm) 24.23, 25.18, 25.74 (2C, **C3,5**-Pip), 26.44, 28.31, 28.97, 36.56, 37.38, 37.73, 54.38 (2C, **C2/6**-Pip), 63.57 (Pip-**CH$_2$**), 66.21 (-O**CH$_2$**CH$_2$CH$_2$NH-), 113.07, (**C6** phenoxy), 115.18 (**C2** phenoxy), 121.96 (**C4** phenoxy), 123.19 (phthal.), 129.16 (**C5** phenoxy), 132.11 (q, **C3** phenoxy), 133.92 (phthal.), 135.2 (q), 139.94 (q), 158.64 (q, **C1** phenoxy), 168.45 (q, CO), 172.85 (q, CO,); <u>CIMS</u> m/z (NH$_3$) 492.2 [MH$^+$] 100 %; C$_{29}$H$_{37}$N$_3$O$_4$ (491.62)

Preparation of 3.28- 1-(3-Aminopropyl)-2-cyano-3-{2-[(5-methyl-1*H*-imidazol-4-yl)methylthio]ethyl}guanidine (3.28)

Phenyl N'-cyano-N-{2-[(5-methyl-1*H*-imidazol-4-yl)methylthio]ethyl}carbamimidate (250 mg, 793 µmol, 1 eq,) and propane-1,3-diamine (0.33 ml, 3.9 mmol, 5 eq) were dissolved in 25 ml methanol and stirred overnight at rt. Evaporation of the solvent afforded the product as yellow oil, which was purified by flash chromatography (silica gel) with 1.5 % Et$_3$N in methanol. 175 mg (75 %) of the desired compound were isolated as pale yellow oil.

<u>RP-HPLC</u> (220 nm gradient 1): 99.2 % (t$_R$=4.4 min, k=0.7), <u>^{1}H-NMR</u> (300 MHz, methanol-d$_4$): δ (ppm) 1.7 (qui, 2H, ^{3}J=6.9 Hz, -NHCH$_2$**CH$_2$**CH$_2$NH$_2$), 2.21 (s, 2H, **5-methyl**-1H-imidazol), 2.62 (t, 2H, ^{3}J=7 Hz, **CH$_2$**), 2.7 (t, 2H, ^{3}J=6.9 Hz, **CH$_2$**), 3.24-3.29 (m, 2H, -**CH$_2$**), 3.33-3.38 (m, 2H, **CH$_2$**), 3.70 (2H, **CH$_2$**S), 7.48 (s, 1H, **C2-H** 5-methyl-1H-imidazol); <u>^{13}C-NMR</u> (75.5 MHz, methanol -d$_4$): δ (ppm) 10.09 (**5-methyl**-1H-imidazol), 27.34 (**C**, CH$_2$S), 31.65 (**C**, CH$_2$), 32.88 (**C**, CH$_2$), 39.4 (**C** CH$_2$), 40.18 (**C** CH$_2$), 42.12 (**C** CH$_2$), 119.95 (q, **C**N), 134.7 (**C2** 5-methyl-1H-imidazol), 161.3 (q) 2q c not detected; IR: 2930, 2162 (CN), 1580, 1443, 1341, 1259, 1039; <u>HRMS:</u> (EI) m/z calcd. for C$_{12}$H$_{21}$N$_7$S 295.1579 [M$^+$], found 295.1579; C$_{12}$H$_{21}$N$_7$S (295.4)

3.6.2 Pharmacological methods

3.6.2.1 Steady state GTPase assay

General

Chemicals, reagents, standard ligands and buffer components are listed below including their source: Tris HCl (USB GmbH, Staufen, Germany); NaCl, Na_2HPO_4, $MgCl_2$, EDTA, activated charcoal (Merck KGaA, Darmstadt, Germany); adenosine triphosphate (ATP), guanosine triphosphate (GTP), adenylyl imidophosphate (AppNHp), creatine kinase (CK), creatine phosphate (CP) (Roche, Mannheim, Germany), bovine serum albumin (BSA, VWR International GmbH, Darmstadt, Germany), famotidine, ranitidine (Sigma Aldrich GmbH, Munich, Germany), thioperamide (Tocris Cookson, Ballwin, USA), scintillation cocktail Optiphase Supermix (Perkin Elmer, Rodgau, Germany). The radionuclides $[\gamma\text{-}^{32}P]GTP$ and $[\gamma\text{-}^{33}P]GTP$ were synthesized according to a previously described method[28]. $[^{32}P]P_i$ (8,500 – 9,100 Ci/mmol orthophosphoric acid) was from PerkinElmer Life Sciences (Boston, MA) and $[\gamma\text{-}^{33}P]P_i$ from Hartmann Analytik GmbH (Braunschweig, Germany). $[\gamma\text{-}^{32}P]GTP$ or either $[\gamma\text{-}^{33}P]GTP$ can be used equally in GTPase assays. In case of $[\gamma\text{-}^{32}P]GTP$ a final concentration of 0.1 µCi/tube was used and Cherenkov radiation was measured in water, whereas $[\gamma\text{-}^{33}P]GTP$ was used in a final assay concentration of 0.05 µCi/tube and radioactivity was determined in a scintillation cocktail (Optiphase Supermix). Scintillation counting was done with the Tri-carb 2800 TR Liquid scintillation analyzer (Perkin Elmer, Rodgau, Germany).

Steady state GTPase assay

GTPase assays were performed as previously described using membranes of Sf9 cells expressing H_1R[29], H_2R[9], H_3R and H_4R[30] (Table 3.6).

Table 3.6: Used membranes of histamine receptor expressing Sf9 cells

Receptor	Used membranes	
H_1R	H_1R + RGS4	coexpression
H_2R	$hH_2R\text{-}G_{s\alpha S}$	fusion protein
H_3R	H_3R + mammalian $G_{i\alpha2}$, $G_{\beta1\gamma2}$ and RGS4	coexpression
H_4R	$hH_4R\text{-}RGS19$+ $G_{i\alpha2}$ and $G_{\beta1\gamma2}$	fusion protein + coexpression

All used membranes were thawed (on ice, 4 °C) and sedimented by a 10 min centrifugation at 4 °C and 13,000 rpm. Subsequently, the membranes were resuspended in 10 mM Tris/HCl at a pH

of 7.4. Assay tubes consisted of 10 µl of the ligand of interest in various concentrations (1 nM -
100 µM, final concentration), the Sf9 cell membranes (20 µl) expressing the respective histamine
receptor (10-20 µg protein/tube) and 50 µl of the reaction mixture (see Table 3.7). The tubes (80
µL) were preincubated for 2 min at 25 °C before 20 µl of [γ-^{32}P]GTP (dissolved in the reaction
mixture) or [γ-^{33}P]GTP (dissolved in the reaction mixture) were added. After incubation for 20
min at 25 °C the reaction was stopped by addition of 900 µL slurry, consisting of 5 % (w/v) acti-
vated charcoal and 50 mM NaH$_2$PO$_4$ (pH 2.0). Nucleotides are absorbed by the latter, whereas P$_i$
remains free. Afterwards the charcoal-quenched reaction mixtures were centrifuged (7 min) at
13,000 rpm. 600 µL of the supernatant were pipetted and ^{32}P$_i$ (or ^{33}P$_i$) was measured by liquid
scintillation counting in 3 ml of H$_2$0 or in 3 ml scintillation cocktail. To take the spontaneous deg-
radation of [γ-^{32}P]GTP (or [γ-^{33}P]GTP) into account, samples with an excess of GTP (1 mM), in-
stead of ligand, were determined (blank). Due to competition of GTP with [γ-^{32}P]GTP (or [γ-
^{33}P]GTP) the enzymatic degradation is prevented and does not exceed 1-2 % of the total amount
of radioactivity added. Under the described experimental conditions not more than 10 % of the
total amount of the added [γ-^{32}P]GTP (or [γ-^{33}P]GTP) were hydrolyzed to ^{32}Pi (or ^{33}P$_i$).

Table 3.7: Reaction mixtures used in GTPase assays

	Reaction mixture (Rea mix)	
	100 µM EDTA, 100 µM ATP, 100 nM GTP, 100 µM AppNHp, 5 mM CP, 40 µg CK and 0.2 % (w/v) BSA in 50 mM Tris/HCl, pH 7.4	
additional components for hH$_x$R	**hH$_1$R /hH$_2$R** : MgCl$_2$ 1 mM	**hH$_3$R/ hH$_4$R**: MgCl$_2$ 5 mM and **hH$_4$R**: NaCl 100 mM
additional components for antagonist mode:	**hH$_1$R**: 200 nM HIS **hH$_2$R**: 1 µM HIS	**hH$_3$R /hH$_4$R**: 100 nM HIS

The GTPase activity (given as pmol P$_i$ per mg of protein per minute) was calculated according to
the following **equation:**

$$GTPase\ activity = \frac{(cpm_{total} - cpm_{blank}) \times pmol\ GTP/tube}{cpm_{total\ added} \times mg\ protein \times t\ (\mathrm{min})} \times \frac{1\ ml}{0.6\ ml}$$

Given in $\lfloor pmol \times mg^{-1} \times min^{-1} \rfloor$

cpm$_{total}$:   radioactivity counted for the investigated ligands
cpm$_{blank}$:   radioactivity counted for the blank
pmol GTP/ tube: amount of unlabelled GTP in each tube: 10 pmol
cpm$_{total\ added}$: counts representing total added [γ^{32}P]-GTP or [γ^{33}P]-GTP to each tube
      (without charcoal addition)
mg protein: amount of protein/tube (10-15 µg)

t (min): incubation period (20 min)

Sigmoidal dose response curves were created to determine the IC_{50}- values of the compounds, from which $K_{b'}$-values were calculated according to the Cheng Prussoff equation[31].

Cheng Prussoff equation:

$$K_{b'} = \frac{IC_{50}}{(1 + \frac{[L]}{EC_{50}})}$$

given in [nM]

$IC_{50:}$ antagonist concentration causing 50 % inhibition
K_i: dissociation constant of the investigated ligand (inhibitor)
[L]:   concentration of the used standard ligand (e.g. HIS)
EC_{50}:   agonist concentration causing the half maximal effect (e.g. 50 % activation, for HIS)

The E_{max}-values were determined with only one concentration of the respective ligands (10 µM, final concentration) without histamine addition to the reaction mixture ("agonist mode"). The effect of histamine was determined in the same way as for the ligands at one concentration (10 µM for hH_3R/hH_4R; 100 µM for hH_1R/hH_2R; final c.). Basal activity was the GTPase activity measured with the solvent of the ligands (10 % DMSO). The inverse agonistic effect (E_{max}) of the used ligands on basal activity was referred to histamine (E_{max} of histamine was set 1.0).

3.6.2.2 *Histamine H₂R assay at the guinea pig atrium*

Hearts were rapidly removed from guinea pigs as described in literature[32]. The right atrium was quickly dissected and set up isometrically in Krebs-Henseleit solution under a diastolic resting force of 5 mN in a jacketed 20 ml organ bath of 32.5 °C as previously described. The bath fluid (comp position [mM]: NaCl 118.1, KCl 4.7, CaCl 21.8, MgSO 41.64, KH₂PO 41.2, NaHCO₃ 325.0, glucose 5.0, sodium pyruvate 2.0) was gassed with 95 % O_2 – 5 % CO_2 and additionally contained (RS)-propranolol (0.3 µM) and mepyramine (1 µM). Experiments were started after 30 min of continuous washing and an additional equilibration period of 15 min. Antagonists: two successive concentration-frequency curves to histamine (0.1 – 30 µM) were established, the first in the absence and the second in the presence of the compound under study (incubation time 60 min).

pEC_{50} differences were corrected since two successive curves for histamine showed a significant desensitization of 0.13 ± 0.02 (n=16). The investigated antagonists were used at concentrations of 100-1000 nM and the affinities were given as apparent pA_2 or full pA_2 value. The apparent pA_2 value was calculated from:

$$pA_2= -log\ c(B) +log\ (r-1)$$

where   c (B) is the concentration of antagonist
             r the ratio of agonist EC_{50} (HIS) in the absence and presence of antagonist[33]

3.6.2.3   *Fluorimetric Ca²⁺ assay (fura-2 assay) on U-373 MG cells*

General

Fura-2/AM (Fura-2) and Leibovitz (L15) were from Invitrogen (Invitrogen GmbH, Darmstadt, Germany), FBS from Biochrom AG (Berlin, Germany), HEPES and BSA from Serva GmbH (Heidelberg, Germany), Pluronic® F-127 from molecular probes – now Invitrogen GmbH (Darmstadt, Germany). Used chemicals and solvents were purchased from commercial suppliers (Sigma Aldrich GmbH, Munich, Germany, Merck KGaA, Darmstadt, Germany) unless otherwise noted.

- Loading buffer: NaCl 120 mM; KCl 5 mM; $MgCl_2$ 2 mM; $CaCl_2$ 1.5 mM; HEPES 25 mM; glucose 10 mM in Millipore water, pH 7.4
- Loading suspension: 20 mg of BSA, 5 µL of 20 % Pluronic® F-127 / DMSO solution and 4 µL of Fura-2/AM (1 mM stock solution in DMSO) in 1 ml of loading buffer
- Histamine: 200-fold feed solution in Millipore water (3 mM)
- Antagonists: 200-fold feed solutions, prepared from 1 mM, 10 mM or 20 mM stock solutions (stock solutions in DMSO)
-

Fluorimetric Ca²⁺ assay on U-373 MG cells

The spectrofluorimetric calcium assay was performed with the ratiometric Ca²⁺ indicator Fura-2. Cell culture, preparation of U-373 MG cells, loading cells with Fura-2 and investigations of the ligands of interest at the hH_1R in a spectrofluorimetric Ca²⁺ assay were done according to a standard procedure described in literature[21]. Loading of the cells and measurement at the fluorimeter, in brief: On the day of the investigation cells were trypsinized and detached with EMEM 5 % FBS. Cells were centrifuged at 300 g (Minifuge 2, Heraeus, Christ Osterode, Germany) for 5 min and resuspended in loading buffer. After adjusting of the cells to a density of 1.3×10^6 cells/ml, a defined volume of the cell suspension was added to a defined volume of the loading suspension.

This procedure leads to final concentrations of 1 x 10^6 cells /ml, 1 µM Fura-2, 0.2 % DMSO and 0.025 % Pluronic® F-127. Cells were incubated for 30 min at rt under light protection, centrifuged at 300 g for 5 min and resuspended in the same volume of loading buffer. Another incubation was performed for 30 min at room temperature in the dark. Afterwards the cells were washed, resuspended in loading buffer and adjusted to a density of 1 x 10^6 cells/ml. Measurements were performed in a Perkin Elmer LS 50 B spectrofluorimeter (Perkin Elmer, Überlingen, Germany) at 25 °C under continuous stirring (low). For measurements, 1 ml of the cell suspension was transferred into disposable cuvettes containing 1 ml of loading buffer under continuous stirring. Baseline recordation was done for 30 s before agonist (HIS, final c: 30 µM) was added. Antagonists (10 µl) in the desired concentration were incubated with the cells 15 min prior to measurement. Kinetics was measured at an excitation wavelength of 340 nm and 380 nm before and after eliciting of calcium transients with 10 µl of histamine. Emission was measured at 510 nm. Data analysis was done according to the procedure described previously[21]. The calcium concentration was calculated according to the Grynkiewicz equation[34].

3.6.2.4 Radioligand binding assay at HEK293-FLAG-hH$_3$R-His$_6$ cells

General

Used chemicals and solvents were from commercial suppliers (Sigma Aldrich GmbH, Munich, Germany; Merck KGaA, Darmstadt, Germany) unless otherwise stated. [^{3}H]N$^\alpha$-Methylhistamine ([^{3}H]NAMH) was purchased from PerkinElmer Life Sciences (Boston, MA), Leibovitz without phenol red (L15) from Invitrogen GmbH (Darmstadt, Germany), GF/C filters from Skatron Instruments AS (Lier, Norway), fetal bovine serum (FBS) from Biochrom AG (Berlin, Germany) and Rotiszint®eco plus from Carl Roth GmbH (Karslruhe, Germany). Separation of bound radioactivity from free radioactive tracer was done with a Brandel Harvester (M-48, Robotic Cell Harvester, Gaithersburg, MD, US) and radioactivity could be measured by scintillation counting on a Beckmann LS-6500 device.

Radioligand binding assay

HEK293-FLAG-hH$_3$R-His$_6$ cells were essentially cultured and used as described by J. Mosandl (materials and methods, Chapter 4.2.3.19)[35] with minor modifications[22]: Cells were cultured in DMEM with 10 % FBS and selection antibiotics (600 µg/ml of G418) in a water saturated atmos-

phere containing 5 % CO_2 at 37 °C. Cells were seeded into 175 cm^2 culture flasks (Nunc GmbH & Co. KG, Langenselbold, Germany) and grown within 5 days to approximately 100 % confluence. On the day of the investigation the cells were detached with trypsin and suspended in L15 containing 1 % FBS (instead of DMEM with 10 % FBS). Centrifugation and adjustment of cell density was done as described previously. Competition binding experiments were performed in analogy to described methods[35] with minor modifications[22]. In brief: 160 µl of the suspended cells (2-4 x 10^6 cells/ml in L15) were used per well (96 well plate). The cells were incubated in the presence of 5 nM [^{3}H] NAMH (final c. in water, K_D: 5.1 nM) with the ligand of interest at various concentrations (1 nM - 100 µM, final c.) to measure total binding. Unspecific binding was the value determined at the highest concentration of the ligand of interest (10-100 µM, final c.) in the presence of 5 nM [^{3}H]NAMH (final c.). This concentration was sufficient to prevent specific binding of the radioactive tracer. The well plate was shaken (rt, light protection) for 65 min at 100 - 150 rpm before cell bound radioactivity was transferred to glass fibre filters, pretreated with 0.3 % PEI, by the Combi Cell Harvester. Filters were washed 10 s before transfer to vials with 3 ml scintillation cocktail. Samples were measured under light protection after 12 h by liquid scintillation counting. Estimation of IC_{50} – and K_i-values was performed with Graph Pad Prism 5 (GraphPad Software, Inc., La Jolla, USA) using the "One site- Fit K_i"-option.

References

1.   Hill, S. J.; Ganellin, C. R.; Timmerman, H.; Schwartz, J. C.; Shankley, N. P.; Young, J. M.; Schunack, W.; Levi, R.; Haas, H. L. International Union of Pharmacology. XIII. Classification of histamine receptors. *Pharmacol. Rev.* **1997,** 49, 253-78.

2.   Parsons, M. E.; Ganellin, C. R. Histamine and its receptors. *Br. J. Pharmacol.* **2006,** 147 Suppl 1, S127-35.

3.   Hirschfeld, J.; Buschauer, A.; Elz, S.; Schunack, W.; Ruat, M.; Traiffort, E.; Schwartz, J. C. Iodoaminopotentidine and related compounds: a new class of ligands with high affinity and selectivity for the histamine H_2 receptor. *J. Med. Chem.* **1992,** 35, 2231-8.

4.   Buyniski J.P., R. L. C., R.L., Pircio, A.W. Algieri A.A., Crenshaw R.R. . Highlights in Receptor Chemistry. *Melchiorre, C, Gianella, M, eds. Structure- activity relationships among newer histamine H_2-receptor antagonists, Amsterdam: Elsevier Sciences,* **1984**, 195-215.

5.   Stables, R.; Daly, M. J.; Humphray, J. M. Comparison of antisecretory potency and duration of action of the H_2-receptor antagonists AH 22216, cimetidine, ranitidine and SK & F 93479 in the dog. *Agents Actions* **1983,** 13, 166-9.

6.   Yellin, T. O.; Buck, S. H.; Gilman, D. J.; Jones, D. F.; Wardleworth, J. M. ICI 125,211: a new gastric antisecretory agent acting on histamine H_2-receptors. *Life Sci.* **1979,** 25, 2001-9.

7.   Ruat, M.; Traiffort, E.; Bouthenet, M. L.; Schwartz, J. C.; Hirschfeld, J.; Buschauer, A.; Schunack, W. Reversible and irreversible labeling and autoradiographic localization of the cerebral histamine H_2 receptor using [^{125}I]iodinated probes. *Proc. Natl. Acad. Sci. U. S. A.* **1990,** 87, 1658-62.

8.   Leurs, R.; Smit, M. J.; Menge, W. M.; Timmerman, H. Pharmacological characterization of the human histamine H_2 receptor stably expressed in Chinese hamster ovary cells. *Br. J. Pharmacol.* **1994,** 112, 847-54.

9.   Kelley, M. T.; Burckstummer, T.; Wenzel-Seifert, K.; Dove, S.; Buschauer, A.; Seifert, R. Distinct interaction of human and guinea pig histamine H_2-receptor with guanidine-type agonists. *Mol. Pharmacol.* **2001,** 60, 1210-25.

10.   Li, L.; Kracht, J.; Peng, S.; Bernhardt, G.; Elz, S.; Buschauer, A. Synthesis and pharmacological activity of fluorescent histamine H_2 receptor antagonists related to potentidine. *Bioorg. Med. Chem. Lett.* **2003,** 13, 1717-20.

11.   Buschauer, A.; Postius, S.; Szelenyi, I.; Schunack, W. [Isohistamine and homologs as components of H_2-antagonists. 22. H_2-antihistaminics]. *Arzneimittelforschung.* **1985,** 35, 1025-9.

12.   Li, L.; Kracht, J.; Peng, S.; Bernhardt, G.; Buschauer, A. Synthesis and pharmacological activity of fluorescent histamine H_1 receptor antagonists related to mepyramine. *Bioorg. Med. Chem. Lett.* **2003,** 13, 1245-8.

13.   Schmidt, A. H. Reaktionen von Quadratsäure und Quadratsäure-Derivaten. *Synthesis* **1980,** 1980, 961 - 994.

14.   Schmidt, A. H.; Ried, W. Die präparative Chemie der Cyclobutendione; III. Synthese von Quadratsäure, Benzocyclobutendion und deren Derivaten. *Synthesis* **1978,** 1978, 869,880.

15.   Gilbert, A. M.; Antane, M. M.; Argentieri, T. M.; Butera, J. A.; Francisco, G. D.; Freeden, C.; Gundersen, E. G.; Graceffa, R. F.; Herbst, D.; Hirth, B. H.; Lennox, J. R.; McFarlane, G.; Norton, N. W.; Quagliato, D.; Sheldon, J. H.; Warga, D.; Wojdan, A.; Woods, M. Design and SAR of novel potassium channel openers targeted for urge urinary incontinence. 2. Selective and potent benzylamino cyclobutenediones. *J. Med. Chem.* **2000,** 43, 1203-14.

16.   Rotger, M. C.; Piña, M. N.; Frontera, A.; Martorell, G.; Ballester, P.; Deyà, P. M.; Costa, A. Conformational Preferences and Self-Template Macrocyclization of Squaramide-Based Foldable Modules. *The Journal of Organic Chemistry* **2004,** 69, 2302-2308.

17.   Kinney, W. A.; Lee, N. E.; Garrison, D. T.; Podlesny, E. J., Jr.; Simmonds, J. T.; Bramlett, D.; Notvest, R. R.; Kowal, D. M.; Tasse, R. P. Bioisosteric replacement of the alpha-amino carboxylic acid functionality in 2-amino-5-phosphonopentanoic acid yields unique 3,4-diamino-3-cyclobutene-1,2-dione containing NMDA antagonists. *J. Med. Chem.* **1992,** 35, 4720-6.

18.   Tietze, L. F.; Arlt, M.; Beller, M.; Gl üsenkamp, K.-H.; Jähde, E.; Rajewsky, M. F. Anticancer Agents, 15. Squaric Acid Diethyl Ester: A New Coupling Reagent for the Formation of Drug Biopolymer Conjugates. Synthesis of Squaric Acid Ester Amides and Diamides. *Chem. Ber.* **1991,** 124, 1215-1221.

19.   Buschauer, A.; Wegener, K.; Schunack, W. H2-Antihistaminika XIV. Basisch substituierte Cimetidine-Analoge. *Eur. J. Med.Chem.* **1982,** 17, 505-508.

20.   Preuss, H.; Ghorai, P.; Kraus, A.; Dove, S.; Buschauer, A.; Seifert, R. Constitutive activity and ligand selectivity of human, guinea pig, rat, and canine histamine H_2 receptors. *J. Pharmacol. Exp. Ther.* **2007,** 321, 983-95.

21.   Kracht, J. Bestimmung der Affinität und Aktivität subtypselektiver Histamin- und Neuropeptid Y-Rezeptorliganden an konventionellen und neuen pharmakologischen In-vitro-Modellen. *Doctoral thesis*, University of Regensburg, **2001**.

22.   Nordemann, U. *Personal communication*. In Department of Pharmaceutical and Medicinal Chemistry II, University of Regensburg (Germany), **2009**.

23.   Schnell, D. *Personal communication*. In Department of Pharmacology and Toxicology, University of Regensburg (Germany), **2008**.

24.   Hemedah, M.; Mitchelson, F. J.; Coupar, I. M. Evidence of H_3 receptor inhibition by iodoaminopotentidine in the guinea pig ileum. *Life Sci.* **1998,** 63, 1371-6.

25.   Vauquelin, G.; Van Liefde, I.; Birzbier, B. B.; Vanderheyden, P. M. New insights in insurmountable antagonism. *Fundam. Clin. Pharmacol.* **2002,** 16, 263-72.

26.   Vauquelin, G.; Van Liefde, I.; Vanderheyden, P. Models and methods for studying insurmountable antagonism. *Trends Pharmacol. Sci.* **2002,** 23, 514-8.

27.   Li, L. Synthesis and Pharmacological Activity of Fluorescent Ligands for Neuropeptide Y, Histamine H_1 and H_2 Receptors. Doctoral thesis, University of Peking / University of Regensburg, **2001**.

28.   Walseth, T. F.; Johnson, R. A. The enzymatic preparation of [alpha-(^{32})P]nucleoside triphosphates, cyclic [^{32}P] AMP, and cyclic [^{32}P] GMP. *Biochim. Biophys. Acta* **1979,** 562, 11-31.

29.   Seifert, R.; Wenzel-Seifert, K.; Burckstummer, T.; Pertz, H. H.; Schunack, W.; Dove, S.; Buschauer, A.; Elz, S. Multiple differences in agonist and antagonist pharmacology between human and guinea pig histamine H_1-receptor. *J. Pharmacol. Exp. Ther.* **2003,** 305, 1104-15.

30.   Ghorai, P.; Kraus, A.; Keller, M.; Gotte, C.; Igel, P.; Schneider, E.; Schnell, D.; Bernhardt, G.; Dove, S.; Zabel, M.; Elz, S.; Seifert, R.; Buschauer, A. Acylguanidines as bioisosteres of guanidines: NG-acylated imidazolylpropylguanidines, a new class of histamine H_2 receptor agonists. *J. Med. Chem.* **2008,** 51, 7193-204.

31.   Cheng, Y.; Prusoff, W. H. Relationship between the inhibition constant (K1) and the concentration of inhibitor which causes 50 per cent inhibition (I50) of an enzymatic reaction. *Biochem. Pharmacol.* **1973,** 22, 3099-108.

32.   Black, J. W.; Duncan, W. A.; Durant, C. J.; Ganellin, C. R.; Parsons, E. M. Definition and antagonism of histamine H_2 -receptors. *Nature* **1972,** 236, 385-90.

33.   Furchgott, R. F. *In Catecholamines, Handbook of Experimental Pharmacology; Blaschko, H., Muscholl, E*. Springer-Verlag: Berlin: 1972; Vol. 33, p 283-335.

34.   Grynkiewicz, G.; Poenie, M.; Tsien, R. Y. A new generation of Ca^{2+} indicators with greatly improved fluorescence properties. *J. Biol. Chem.* **1985,** 260, 3440-50.

35.   Mosandl, J. Radiochemical and luminescence-based binding and functional assays for human histamine receptors using genetically engineered cells. *Doctoral thesis*, University of Regensburg, Germany, http://epub.uni-regensburg.de/12335/, **2009**.

Chapter 4

Bivalent H$_2$-receptor antagonists

4 Bivalent H$_2$-receptor antagonists

4.1 Introduction

General aspects

As outlined in Chapter 1, there is evidence that GPCRs do not only exist as monomeric entities but form homooligomeric and/or heterooligomeric quaternary structures[1-4]. Histamine receptors, for instance, were reported to form oligomers[5-8]. Different experimental techniques were applied to substantiate dimerized GPCRs (e.g. β$_2$-adrenergic[9], δ-opioid receptors[10], thyrotropin-releasing hormone receptors[11], serotonin 5-HT$_4$-receptor[2]). Among them are BRET[2, 9] (bioluminescence resonance energy transfer), photobleaching[4] and FRET[12] (time resolved fluorescence energy transfer). Further confirmations of GPCR oligomerization were achieved by immunoprecipitation[5-6] and functional complementation[13].

Receptor dimers and oligomers are supposed to be involved in physiological responses via activation and inhibition of receptor mediated signal transduction[14]. In addition to the mentioned techniques bivalent ligands are used to investigate the phenomenon of dimerization and/or oligomerization of receptors[15]. The term bivalent ligand (twin compounds) is widely used and refers to molecules containing two pharmacophoric moieties linked through a spacer of appropriate length. The two pharmacophoric moieties can be identical to form a homobivalent ligand or in case of heterobivalent compounds consist of different pharmacophores[2]. According to the concept, bivalent ligands should "bridge" receptor dimers and bind to the two binding pockets of a putative receptor dimer, thus exhibiting higher affinity/potency at the receptor compared to their monomeric counterparts. Therefore, on one hand, the binding to receptor oligomers/dimers might contribute to the elucidation of the function and biological role of dimeric/oligomeric receptors. On the other hand, the bivalent ligand approach could be useful to improve selectivity and potency of the respective ligands[10, 16-17].

A requirement to bridge two receptors via bivalent ligands is the appropriate nature (peptidic, methylenic, PEGylated...), length and flexibility (avoidance of steric hindrance) of the spacer[2, 17-18]. For example in the opioid receptor field, based on molecular modelling, a distance of 27 to 32 Å was suggested as a requirement for the bridging of the distance between two binding sites of 7 TM receptor dimers[10]. Successful application of bivalent compounds, which show improved potency and/or selectivity, was for example achieved in the opioid receptor (δ and κ receptors)[19-20] and serotonin receptor (5HT$_4$ receptor)[2] field.

Assumed binding mode of bivalent ligands

Different modes of binding are imaginable for bivalent ligands as depicted in a simplified scheme adapted from Portoghese et al [10, 21](Scheme 4.1). Twin compounds with spacers of appropriate length may bridge two neighbouring receptors, and each pharmacophoric group can interact with the binding pocket (orthosteric binding site) of one receptor (see Scheme 4.1, B, 7). Binding of bivalent entities to one receptor (see Scheme 4.1 A, 2/3), where one pharmacophoric moiety occupies the orthosteric binding site and the other one an acessory binding site at this receptor, probably due to allosteric interactions, is also possible. In both cases, the ligand binds univalently (Scheme 4.1, 2/3), followed by binding of the second pharmacophoric unit to the binding pocket on the neighbouring receptor (e.g. 7). The proximity of the second pharmacophoric unit favours binding of this moiety over binding of a second ligand. Occupation of receptor dimers by two ligands, with only one pharmacophore per ligand fitting into the binding pocket, is also imaginable (Scheme 4.1, B, 6). Additionally, after binding of one pharmacophore to a receptor dimer (5) allosteric effects might change the affinity of the second binding site in the receptor dimer, leading to either enhanced binding of the second unit (of the bivalent ligand) or hindrance of binding (for details see Portoghese et al.[10, 21]).
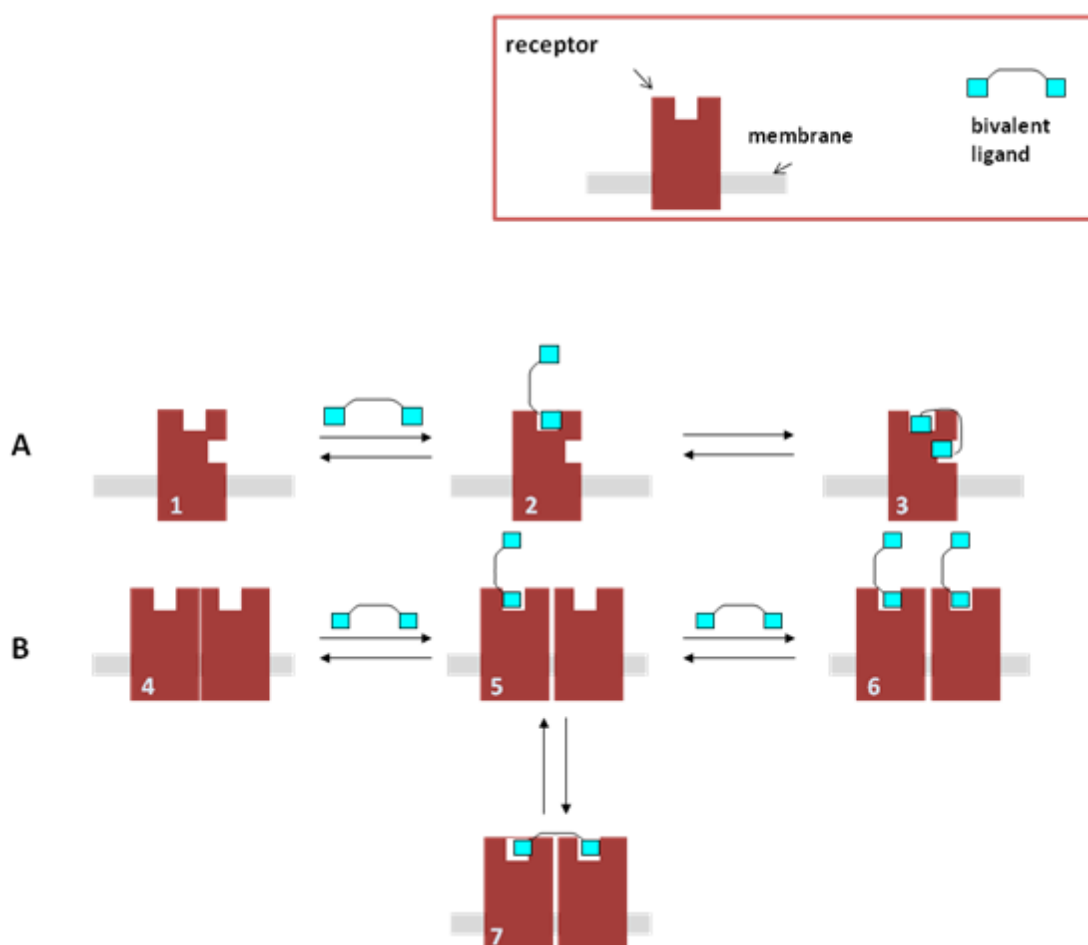
Scheme 4.1: Bivalent ligand binding to one receptor (A) or to receptor dimers (B), adapted from Portoghese et al., 2001

Taking oligomerization of GPCRs into account, recently, the bivalent ligand concept was applied to histamine H_2 receptor agonists. N^G-Acylated hetarylpropylguanidines were used as starting pharmacophoric residue and bridged via alkanedioic acid linkers of 6 to 22 methylene groups (Figure 4.1)[22], representing distances between 6 and 27 Å. According to theory, ligands with linkers containing 20 to 21 carbon atoms should have the highest affinity/potency. In recent studies, performed in our workgroup on acylated guanidines[22], pharmacophores connected via hexamethylene and octamethylene spacers (9-11Å) had the highest H_2R agonistic potencies with pEC_{50}-values between 8 and 9.
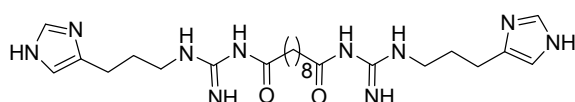
Figure 4.1: Representative bivalent H_2-receptor agonist (UR AK480)

As these linkers are presumably too short to bridge two receptors, these findings do not support the simultaneous occupation of both binding pockets of a putative H_2R dimer by bivalent compounds. It is assumed that the higher affinity for the H_2R, compared to monovalent ligands, must be attributed to additional binding at one receptor molecule to regions different from the orthosteric binding site.

In this work the bivalent ligand approach was extended to H_2R antagonists (Figure 4.2) using compounds bearing spacers between 2 and 10 methylene groups. Comparison of antagonistic twin compounds to agonistic compounds will possibly enlarge our level of knowledge about the binding properties of these kinds of ligands to orthosteric or allosteric binding sites. The prepared H_2-receptor antagonists were investigated in terms of their antagonistic activities and selectivity profiles.
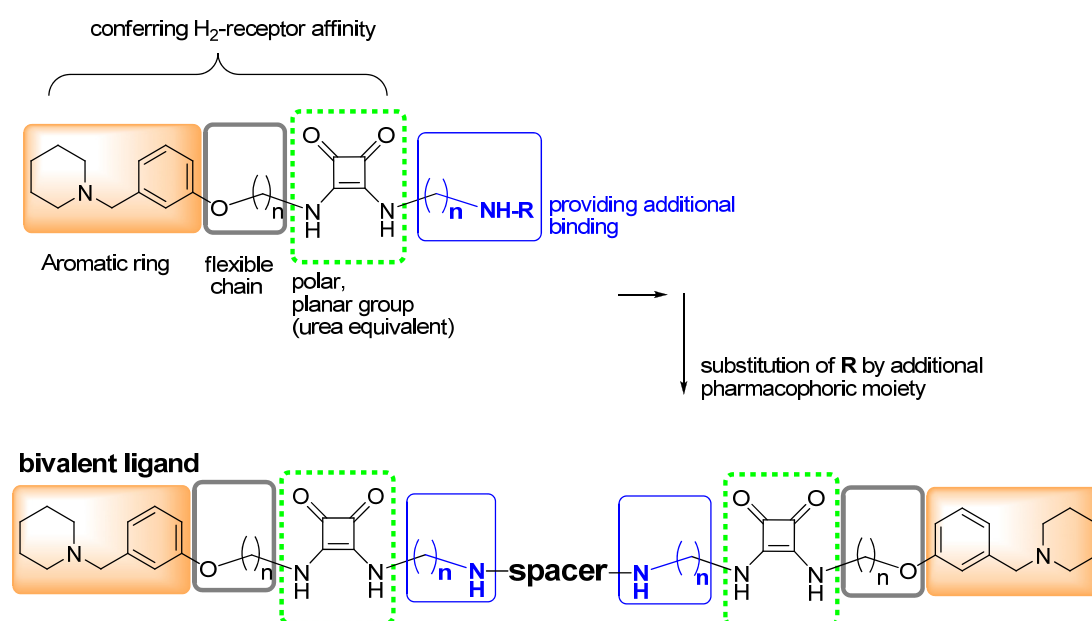
Figure 4.2: Structural design of bivalent H_2-receptor ligands. Squaramides are shown as an example; structures are derived and modified from the pharmacophore model for H_2R antagonists described in chapter 3

4.2 Chemistry

Bivalent ligands with a simple alkanediyl spacer can be synthesized by analogy with the proce-dure for squaramide preparation described in chapter 3. The ratio of the respective monoethyl squarate to the pertinent alkanediamine was modified using a 2 fold excess of the squaric acid ester (cf. Scheme 4.2 and Scheme 4.3). The reaction was carried out for 12 h to 5 days at rt or for 3 hours under reflux in ethanol with stirring giving the products in 28-60 % yield.
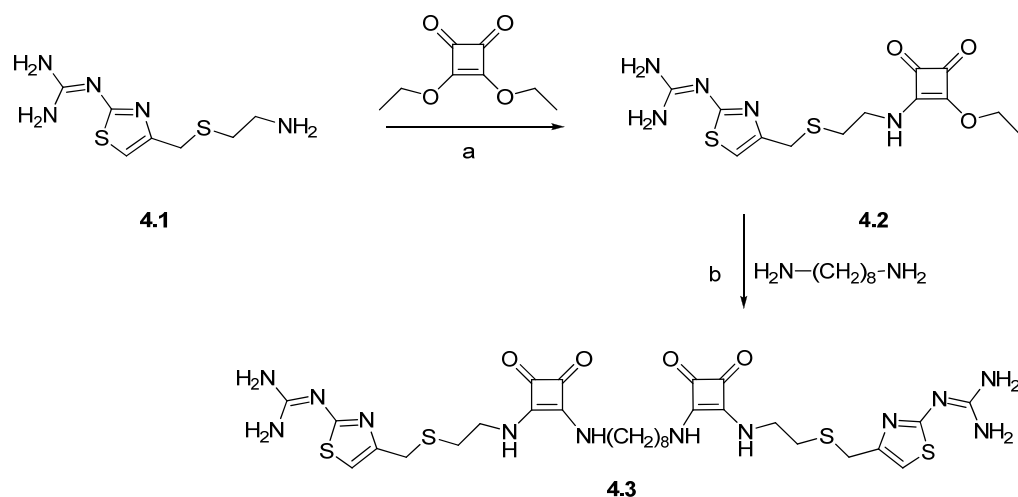
Scheme 4.2: Synthesis of bivalent ligand **4.3**; Reagents and conditions: (a) EtOH, rt, reflux 8 h (b) MeOH, 80 °C, 3 h

A purification step, including suspension of the compounds in a mixture of ethanol/water and heating to reflux (to solve impurities), gave the products as yellow solids with a purity above 95 %. If necessary, compounds were subsequently purified by preparative HPLC.
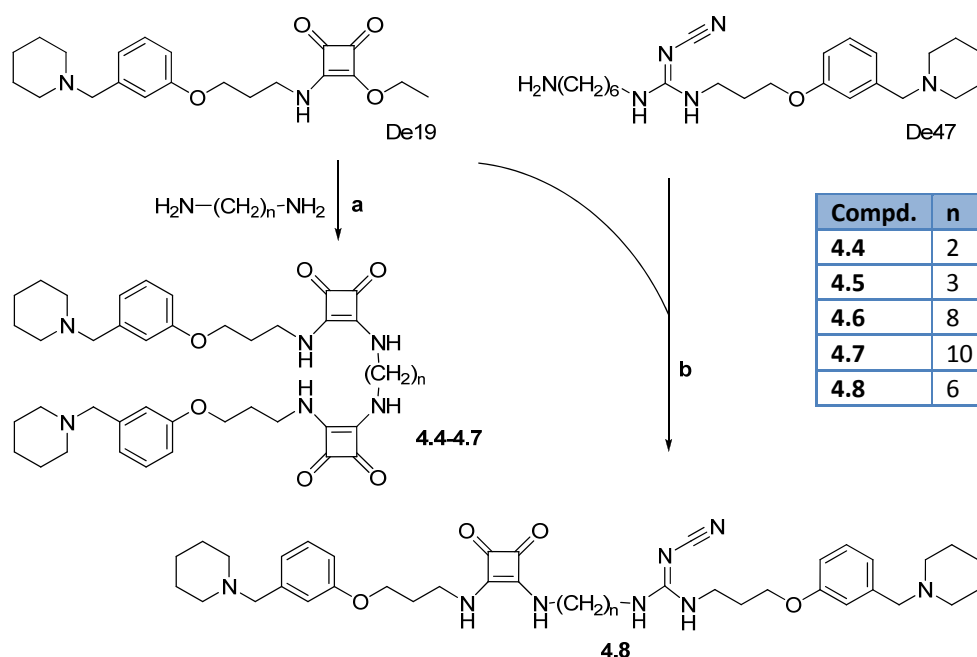
Scheme 4.3 Synthesis of squaramide-derived bivalent ligands; Reagents and conditions: (a) EtOH, rt 12 h - 5 d or 3 - 48 h reflux (b) EtOH, 48 h reflux

4.3 Pharmacological results

4.3.1 H$_2$-receptor antagonism

GTPase assay at the guinea pig and human histamine H$_2$ receptor

The bivalent ligands were investigated for H$_2$R antagonism versus histamine in a steady state GTPase assay using Sf9 cell membranes expressing gpH$_2$R-G$_{s\alpha s}$ or hH$_2$R-G$_{s\alpha s}$ fusion proteins[23]. Histamine- stimulated GTP hydrolysis (antagonist mode) was inhibited by all test compounds in the low nanomolar range (K$_{b'}$: 1.6 - 65 nM). The investigation of two selected compounds (**4.4** and **4.5**) at the gpH$_2$R receptor gave comparable results as at the hH$_2$R (Table 4.1). Compounds **4.6** and **4.7** proved to be the most potent ligands in this series, with K$_{b'}$ values between 6 and 7 nM. None of these compounds exerted noteworthy inverse agonistic effects (E$_{max}$= -0.13 to - 0.07).

Table 4.1: H$_2$R antagonistic activities and efficacies of bivalent ligands in GTPase assays [a]

Compd.	gpH$_2$R-G$_{s\alpha s}$	hH$_2$R-G$_{s\alpha s}$	
	K$_{b'}$ (EC$_{50}$) [nM]	K$_{b'}$ (EC$_{50}$) [nM]	E$_{max}$
Histamine	(850 ± 340)[b]	(990 ± 92)[b]	1.00
Cimetidine	1300 ± 270 [b]	1700 ±430[b]	-0.03 ± 0.02
Famotidine	38 ±3 [b]	48 ± 10 [b]	-0.09 ± 0.08
4.3	n.d.	64.8 ± 37	-0.17 ± 0.01
4.4	22.7 ±4	26.7 ±3	-0.06 ± 0.02
4.5	21.1 ± 3	16.1 ± 3	-0.13± 0.05
4.6	5.5 ± 1.2	7.3 ± 0.4	-0.07 ± 0.05
4.7	6.1 ±4.5	6.1 ± 3	-0.11 ± 0.05
4.8	n.d.	64.5 ± 50	0.07 ± 0.00

[a] Steady state GTPase assay on Sf9 cell membranes; ligands were used at concentrations from 1 nM to 100 µM; typical GTPase activities (stimulation with 1 µM histamine (gpH$_2$R, hH$_2$R): 3.5-7 pmol x mg^{-1} x min^{-1}; E$_{max}$= intrinsic activity, relative to histamine, E$_{max}$ HIS = 1 (at a concentration of 10 µM); mean values ± S.E.M. (n = 2-4), performed in duplicate; n.d.: not determined, [b]see[24]

H$_2$R antagonism of selected substances at the guinea pig right atrium

The ligands **4.6** and **4.7** behaved as H$_2$R antagonists at the isolated guinea pig right atrium with pA$_2$ values of about 6.5 (K$_B$ values in the range of 300-400 nM Table 4.2) corresponding to a 40-fold decrease in H$_2$R antagonistic activity compared to the data from the GTPase assay at the hH$_2$R. The maximum response to histamine in the presence of **4.6** at a concentration of 300 nM was slightly decreased. Increasing the antagonist concentration to 1 µM (**4.6** and **4.7**) led to a depression of the concentration-response curve, the maximum response (E$_{max}$) to histamine amounting only to 58 % and 87 %, respectively.

Table 4.2: H$_2$R antagonism of compounds **4.6** and **4.7** at the isolated guinea pig right atrium (gpH$_2$R)

Compd.	gpH$_2$R			
	c [nM]	pA$_2$[b]	K$_B$[nM]	n[a]
4.6	300/1000	6.5 ± 0.1	302	7
4.7	1000	6.4 ± 0.2	372	5

[a]number of experiments, S.E.M calculated from n = 5-7 experiments, [b]calculated from pEC$_{50}$ shifts, for details see experimental procedures.

4.3.2   Receptor selectivity

H$_1$-receptor antagonism on U-373 MG cells and activity on human H$_1$-, H$_3$- and H$_4$-receptors in GTPase assays

Spectrofluorimetric Ca^{2+} assays on U-373 MG cells[25], human cells expressing the H$_1$ receptor, revealed very weak antagonistic effects (IC$_{50}$ values between 5 and 100 µM) for the investigated ligands. In GTPase assays on recombinant hH$_1$R (hH$_1$R and RGS4 co-expressed in Sf9 cells) the test compounds were devoid of agonistic and considerable inverse agonistic activity (data cf. appendix; the E$_{max}$ values ranged from -3 to 3% relative to histamine). Investigations at the hH$_4$R (Sf9 cells expressing hH$_4$R-RGS19+ Gi$_{\alpha2}$+G$_{\beta1\gamma2}$; GTPase assays) revealed similar results for the respective ligands with very low inverse agonistic activities (E$_{max}$ values -0.25 to -0.1; cf. appendix).

By contrast, assays at the human H$_3$ receptor revealed E$_{max}$ values between -0.5 and -0.9, i. e. in the same range as for the reference compound, the inverse H$_3$R agonist thioperamide (E$_{max}$= -0.5 to -0.8, Lit.: -0.71 ± 0.06[26]). Therefore, assays were performed in the antagonist mode to determine the antagonistic activity of the compounds at the hH$_3$R (see Table 4.3). All bivalent ligands had the ability to inhibit GTPase hydrolysis in the nanomolar to micromolar range, depending on the spacer length between the pharmacophoric moieties. In the series of squaramides extended alkanediyl spacers resulted in higher selectivity for the H$_2$R over the hH$_3$R. Compound **4.6** and **4.7**, which have 8- and 10-membered spacers, are 50-200 fold more active at the hH$_2$R relative to the hH$_3$R, whereas the ligands **4.4** and **4.5** possess only 7-8 fold selectivity, as well as **4.8** the compound combining a cyanoguanidine and a squaramide moiety (Table 4.3). The guanidino-thiazole **4.3** was acting preferably at the hH$_2$R with a 30-fold selectivity compared to the hH$_3$R, but with lower activity than **4.6** and **4.7** (Table 4.3). The functional activities of **4.3** and **4.6** were compared to binding affinities from radioligand binding experiments.

Affinities at the human H$_3$ receptor in radioligand binding experiments

Competition binding assays were performed with [^{3}H]N$^\alpha$-methylhistamine ([^{3}H]NAMH) as radioactive tracer (K$_D$: 5.1 nM[27]) on HEK-293 FLAG hH$_3$R His$_6$ cells. As representative ligands **4.3** and **4.6** were tested for their ability to inhibit binding of [^{3}H]NAMH to the receptor (Table 4.3). Both compounds bound with low to moderate affinity to the human histamine H$_3$R and substantiated the data from the GTPase assays. Thus, the selectivity for H$_2$R versus H$_3$R was improved with spacers consisting of 8 methylene groups (Table 4.3).

Table 4.3: hH$_3$R antagonism of bivalent ligands in the GTPase assay[a] and radioligand binding data[b]

Compd.	GTPase assay hH$_3$R+ G$_{i\alpha2}$ +$\beta_1\gamma_2$ + RGS4[a]		Binding data HEK-293-FLAG hH$_3$R His$_6$ cells[b]
	K$_{b'}$ (EC$_{50}$) [nM]	E$_{max}$	K$_i$ (K$_D$) [nM]
Histamine	(25 ± 3)[b]	1.0	39.8[b]
Thioperamide	97 ± 18 [b]	-0.86 ± 0.08	316.2 [b]
JNJ5207852	4.3 ± 0.6	-0.88 ± 0.12	12.6 [b]
NAMH	-	-	(5.1)[b]
4.3	> 2000	n.d.	> 1000
4.4.	21.2± 0.6	-0.64± 0.25	n.d.
4.5	165.7 ±62	-0.83 ± 0.13	n.d.
4.6	413.3 ±40	-0.48 ± 0.1	346 ± 136
4.7	>1000	n.d.	n.d.
4.8	185 ± 243	-0.50 ± 0.04	n.d.

[a] steady state GTPase assay on Sf9 cell membranes; c. ligands: 1 nM- 100 µM; typical GTPase activities (stimulation with 100 nM Histamine (HIS) (hH$_3$R): 2.5-6.0 pmol x mg^{-1} x min^{-1}; E $_{max}$= efficacy relative to histamine =1, E$_{max}$ HIS=1 (c. ligands: 10 µM), Mean values ± S.E.M. (n = 1-3) performed in duplicate;

[b] c. ligands: 1 nM-100 µM, c. [^{3}H]NAMH: 1 nM, 2-5 million cells/well; Mean values ± S.E.M. (n = 1-2) performed in duplicate; n.d.: not determined, [a] see also[28], [b] see also[27]

4.4 Discussion

All new H$_2$-receptor ligands proved to have high antagonistic activity (K$_{b'}$< 100nM) in functional assays at the hH$_2$R, depending on the spacer length. The activity of compounds **4.6** and **4.7** at the guinea pig atrium was also in the nanomolar range, but 40-fold lower compared to the functional data from GTPase assays on recombinant hH$_2$Rs. It should be stressed that significant species-dependent differences are not obvious for this series of compounds, when data from functional assays at hH$_2$R and gpH$_2$R are compared. Therefore, the discrepancies between data from GTPase assay and guinea pig right atrium may result from different conditions of the experimental setup, and, using membrane preparations or isolated organs, respectively. One possible explanation could be impaired diffusion and/or slow association kinetics of the compounds at the isolated guinea pig right atrium. Experiments had to be conducted with a minimum incubation period of 60 min to get reliable data from rightward shifts of the histamine curve. Despite that long incubation period it is conceivable that equilibrium was not fully reached, resulting in higher K$_b$ values. Additionally, limited solubility (or fractional precipitation) of the substances in physiological buffers cannot be ruled out. In the presence of **4.6** and **4.7** the maximum increase in heart rate induced by histamine was depressed, amounting to 58 and 87 %, respectively, of the control experiments. The shape of the concentration-response curves of histamine in the presence of these H$_2$R antagonists (at higher concentrations) suggests unsurmountable antago-

nism. This phenomenon is not fully understood. It may be speculated that additional binding sites (allosteric?) at the receptor, slow kinetics (dissociation from the receptor) and/or ligand-specific conformations of the receptor protein are involved[29-31].

All investigated bivalent compounds revealed high selectivity for the H_2R compared to hH_1R and hH_4R, whereas, depending on the individual ligand, the selectivity over the hH_3R was only low to moderate.

To estimate the contribution of the second set of H_2R antagonist pharmacophoric groups the activities of the bivalent compounds should be compared to an appropriate monomeric H_2R antagonist. For this purpose, the monomers bearing an alkanediyl spacer with a terminal primary amino group were used. It has to be noted that these entities can only be considered an approximation to a "monomeric" analogue as the alkyl chain with the amino group, which is converted to an amide group in the twin compounds, may also confer to H_2R antagonisic activity. Compound **4.4** and **4.5** with short spacers (ethylene and trimethylene) were about 10 fold more potent at the H_2R than the corresponding monomers from chapter 3 ($K_{b'}$ values of **3.9** and **3.10** about 200 nM), but selectivity versus the hH_3R was low and could not be considerably improved compared to the monomers (**3.9**, **3.10**). The homobivalent ligands **4.6** and **4.7,** bearing hexamethylene and octymethylene spacers proved to be the most potent H_2R antagonists of this series with activities below 10 nM. Compared to the monomer UR-De183 ($K_{b'}$ 4.5 nM) the bivalent antagonist **4.6** was slightly (1.6 fold) less active. However, the selectivity of the twin compound **4.6** and **4.7** for H_2R over H_3R was improved (50-200 fold selectivity versus the hH_3R), indicating that elongation of the spacer favours preferential binding to the hH_2R in the squaramide series.

The bivalent antagonist **4.3**, consisting of two guanidinothiazole moieties connected with squaramide groups and the heterodimeric ligand **4.8** combining squaramide and cyanoguanidine moiety, showed moderate $K_{b'}$ values around 65 nM in the GTPase assay. Compound **4.8** may be considered a combination of the monovalent antagonists **3.6** and **3.13** which differ markedly in H_2R antagonistic activities ($K_{b'}$ values, **3.6** 592 nM, **3.13** 18 nM). The measured activity of **4.8** (65 nM) was between the $K_{b'}$ values of the monomers. The combination of two different pharmacophoric moieties in a heterobivalent ligand did not result in improved selectivity for the H_2R versus the H_3R (selectivity only 2 fold over the H_3R). Selectivity was even lower than for the homobivalent squaramides. Compound **4.3** behaved similar at the hH_2R but showed higher selectivity versus the hH_3R (15-30-fold) compared to **4.8.**

4.5 Summary

In this study all bivalent ligands exerted high activity at the hH$_2$R, slightly lowering (**4.6**), maintaining (**4.4** and **4.5**) or increasing activity (**4.3** and **4.8**) for H$_2$R. It is unlikely that the twin compounds bound to a receptor dimer, due to insufficient spacer length of the ligands. The maintained or increased potency of the new ligands might be rather attributed to interactions with the binding pocket of a single receptor and an additional binding site at the same receptor molecule. Interactions of the second pharmacophore on extracellular loop regions of the respective receptor are also imaginable. Taken together, results concerning bivalent ligands are in agreement with former investigations in the H$_2$R agonist field[22], that these H$_2$-receptor ligands supposedly bind to only one receptor and cannot bridge neighbouring receptors. Among the synthesized bivalent ligands the compounds with octamethylene and decamethylene spacers, connecting squaramide-type H$_2$R antagonist monomeric entities, turned out to be potent and selective and possessed an improved selectivity profile versus the H$_3$R.

4.6 Experimental section

4.6.1 Chemistry

4.6.1.1 General conditions

See chapter 3

4.6.1.2 Preparation of bivalent ligands

2-(4-{[2-(2-Ethoxy-3,4-dioxocyclobut-1-enylamino)ethylthio]methyl}thiazol-2-yl)guanidine (4.2)

Compound **4.1** x 2HCl (533 mg, 1.7 mmol, 1 eq) was suspended in 20 ml ethanol and 290 mg (3.4 mmol, 2 eq) of Et$_3$N were added to release the free amine of **4.1**. 3,4-Diethoxycyclobut-3-ene-1,2-dione (300 mg, 1.7 mmol, 1 eq), dissolved in 20 ml ethanol and 0.18 ml Et$_3$N, were added and the solution was stirred under reflux for 8 h. The solvent was evaporated and methanol/ethyl acetate (1/10) was added to the residue. After storage at 4-6 °C, the precipitate was filtered off and dried in vacuo yielding 408 mg of the product as yellow crystals (68 %). Mp. >135 °C (decomp.)

^{1}H-NMR (600 MHz, DMSO-d$_6$): δ (ppm) 1.33-1.37 (m, 3H, -OCH$_2$**CH$_3$**), 2.64-2.68 (m, 2H, -SCH$_2$CH$_2$NH-), 3.44-3.45 (m, 1H, -SCH$_2$CH$_2$NH-), 3.64-3.65 (m, 1H, -SCH$_2$CH$_2$NH-), 3.75 (s, 2H, -CH$_2$-

S-), 4.4 (qua, 2H, ^{3}J=7.0 Hz, -O**CH$_2$**CH$_3$), 7.10 (s, 1H, **C5-H** Thiazolyl), 8.22 (bs, 4H, NH$_2$), 8.68-8.84 (2x s, 1H), 12.45 (bs, 1H); $\underline{^{13}\text{C-NMR (150.95 MHz, DMSO-d}_6)}$: δ (ppm) 15.59 (-OCH$_2$**C**H$_3$), 30.05 - **C**H$_2$-S), 31.35 (31.74) (-S**C**H$_2$CH$_2$NH), 42.65 (42.65) (-SCH$_2$**C**H$_2$NH-) 68.81 (-O**C**H$_2$CH$_3$-), 109.43 (**C5** thiazolyl), 148.41 (q), 154.19 (q), 172.24 (172.65) (q), 176.65 (176.60) (q), 181.92 (182.15) (q), 189.0 (189.37) (q); numbers in parentheses from isomer; ESMS: m/z 355.9 [MH$^+$]; C$_{14}$H$_{18}$N$_4$O$_3$S$_2$ (355.44)

2,2'-[4,4'-(2,2'-{2,2'-[Octane-1,8-diylbis(azanediyl)]bis(3,4-dioxocyclobut-1-ene-2,1-diyl)}bis(azanediyl)bis(ethane-2,1-diyl))bis(sulfanediyl)bis(methylene)bis(thiazole-4,2-diyl)]diguanidine (4.3)

Compound **4.2** (106 mg, 300 mmol, 2 eq) was dissolved in 15 ml methanol. After addition of octane-1,8 diamine (22 mg, 150 μmol, 1 eq), dissolved in 5 ml MeOH, the solution was heated to 65-70 °C (reflux) for 3 h. The product precipitated. After evaporation of the solvent the solid was suspended in ethyl acetate to dissolve impurities and filtered off. Drying in vacuo gave 95 mg (44 %) of a yellow solid. Mp: > 135 °C (decomp.). The compound was purified by preparative HPLC. Compound **4.3** (52 mg) was dissolved in DMF/acetonitrile/1 % TFA (aq) (1/1/1, v/v/v) to a total volume of 7 ml using an ultrasonic bath. Afterwards during filtration through PTFE-filters the compound partly precipitated, resulting in a solution containing less of the designated product, which was used for preparative HPLC (system 2, 220 nm). After purification acetonitrile was evaporated and the remaining water was removed by lyophilisation. The product was obtained as a white semi solid (19.2 mg).

RP-HPLC (220 nm, gradient 1): 98 % (t$_R$ =12.2 min, k=3.8); $\underline{^1\text{H-NMR (600 MHz, DMSO-d}_6)}$: δ (ppm) 1.27 (m, 8H, 4x -NH-CH$_2$(**CH$_2$**)$_6$CH$_2$NH-), 11.48-1.49 (m, 4H, -NH-CH$_2$(**CH$_2$**)$_6$CH$_2$NH-), 2.66 (t, 4H, ^{3}J=6.7 Hz, 2x -S**CH$_2$**CH$_2$NH-), 3.38-3.48 (m, 10H, 4H-NH-**CH$_2$**(CH$_2$)$_6$**CH$_2$**NH-,+ water residue), 3.69 (m, 4H, 2x -SCH$_2$**CH$_2$**NH-), 3.78 (s, 4H, 2x **–CH$_2$**-S-), 7.12 (s, 2H, 2x **C5-H** thiazolyl), 7.51 (bs, 3H, NH cyclobutenyl), 8.29 (bs, 6H, NH$_2$), 12.2 (bs, 1H); $\underline{^{13}\text{C-NMR (150.95 MHz, DMSO-d}_6)}$: δ (ppm) 25.78 (2C, -NH-CH$_2$(**CH$_2$**)$_6$CH$_2$NH-), 28.52 (2C, -NH-CH$_2$(**CH$_2$**)$_6$CH$_2$NH-), 29.96 (2C, **–C**H$_2$-S-), 30.68 (2C, -NH-CH$_2$(**CH$_2$**)$_6$CH$_2$NH-), 32.19 (2C, -S**C**H$_2$CH$_2$NH-), 42.47 (2C, -SCH$_2$**C**H$_2$NH-), 43.23 (2C, -NH-**C**H$_2$(CH$_2$)$_6$CH$_2$NH-), 110.12 (2C **C5 t**hiazolyl), 182.3 (q, 2C,**C**O cyclobutenyl), not all q C detected; HRMS: (NI-LSI, FAB$^+$, DCM/MeOH/glycerol): *m/z* found: 763.2 [MH$^+$]; C$_{30}$H$_{42}$N$_{12}$O$_4$S$_4$ x C$_4$H$_2$F$_6$O$_4$ (991.0)

4,4'-[Ethane-1,2-diylbis(azanediyl)]bis(3-{3-[3-(piperidin-1-ylmethyl)phenoxy]propyl-amino}cyclobut-3-ene-1,2-dione) (4.4)

Compound **3.24** (199 mg, 268 μmol, 1.8 eq) and ethane-1,2-diamine (9 mg, 150 μmol, 1 eq), were dissolved in 15 ml ethanol and heated to reflux for 2 h. After evaporation of the solvent ethanol/diethyl ether (1/10, v/v) was added and the formed crystals were filtered off. The crude product was suspended in H_2O/ethanol (3/2, v/v) and heated to the boiling point for 3 h to solve impurities. Filtration through a sintered glass crucible and drying in vacuo yielded yellow crystals (56 mg, 44 %) with a purity of 86 % (RP-HPLC, 210 nm, gradient 1). Mp. > 135 °C(decomp.). 36 mg, dissolved in a mixture of 1.5 ml DMSO, 4.5 ml acetonitrile/ H_2O (80/20) and 2-3 drops of TFA, were purified by preparative HPLC (system 2-1, 220 nm). Evaporation of acetonitrile and lyophili-sation resulted in yellow oil (25 mg).

RP-HPLC (220 nm, gradient 1): 99 % (t_R=11.5 min, k= 3.5); ^{1}H-NMR (600 MHz, methanol-d_4): δ (ppm) 1.48-1.50 (m, 2H, **C-H** Pip), 1.72-1.82 (m, 6H, **C3-H** Pip), 1.90-1.93 (m, 4H, **C-H** Pip), 2.05-2.07 (m, 4H, 2x -OCH$_2$**CH$_2$**CH$_2$NH-), 2.93-2.97 (m, 4H, **C2/C6**-H Pip), 3.43-3.45 (m, 4H, **C2/C6**-H Pip), 3.78 (m, 6H, 2x -NH-CH$_2$**CH$_2$**NH-, 1x -OCH$_2$CH$_2$**CH$_2$**NH-), 4.07 (t, 4H, ^{3}J=5.6 Hz, 2x -O**CH$_2$**CH$_2$CH$_2$NH-), 4.25 (s, 4H, 2x Pip**CH$_2$**), 7.02-7.05 (m, 4H, 2x **C4,6 –H** phenoxy), 7.13 (s, 2H, 2x **C2 –H** phenoxy), 7.36 (t, 2H, ^{3}J=7.9 Hz, 2x **C5-H** phenoxy); ^{13}C-NMR (150.95 MHz, methanol-d_4): δ (ppm) 22.74 (2**C, C4** Pip), 24.09 (4C, **C3,5** Pip), 31.62 (2C, -OCH$_2$**CH$_2$**CH$_2$NH-), 42.22 (2C, -OCH$_2$CH$_2$**CH$_2$**NH-), 46.2 (2C, NHCH$_2$**CH$_2$**NH-) 54.12 (4C, **C2,6** Pip), 61.76 (2C, Pip-**CH$_2$**), 66.99 (2C, -O**CH$_2$**CH$_2$CH$_2$NH-), 117.66 + 117.91 (4C, **C6** Ph, **C2** phenoxy), 124.49 (2C, **C4** phenoxy), 131.36 (C2**, C5** phenoxy), 131.78 (q, 2x **C3** phenoxy), 160.84 (q, 2x **C1** phenoxy), 169.67 +169.89 (q, 2x cyclobutenyl), 183.46 +183.85 (q, 2x **CO** cyclobutenyl); HRMS: (FAB, MeOH/glycerol): *m/z* calcd. for C$_{40}$H$_{53}$N$_6$O$_6$ 713.4027 [MH$^+$], found: 713.4023; C$_{40}$H$_{52}$N$_6$O$_6$ x C$_4$H$_2$F$_6$O$_4$ (941.4)

4,4'-[Propane-1,3-diylbis(azanediyl)]bis(3-{3-[3-(piperidin-1-ylmethyl)phenoxy]propyl-amino}cyclobut-3-ene-1,2-dione) (4.5)

Compound **3.24** (250 mg, 671 μmol, 2 eq) and propane-1,3-diamine (25 mg, 337 μmol, 1 eq) were dissolved in 15 ml ethanol and 5 ml DMSO, and the mixture was heated to reflux for 3 h. The solvent (ethanol) was evaporated. Addition of diethyl ether to the remaining solution in DMSO gave a yellow semi solid. Suspension of the residue in a mixture of H_2O/ ethanol (3/2, v/v) and refluxing for 3 h to dissolve impurities gave the product (82 mg, 36 %) with a purity of 90 % (RP-HPLC, 210 nm, gradient 1). Mp > 135 °C (decomp). 44 mg, dissolved in a mixture of 1 ml

DMSO, 5 ml acetonitrile/H$_2$0 (80/20) and 2-3 drops TFA, were purified by preparative HPLC (system 2-1, 220 nm). Evaporation of acetonitrile and lyophilisation afforded the product as yellow oil (29.84 mg).

RP-HPLC (220 nm, gradient 1): 99.8 % (t$_R$=11.8 min, k=3.7); ^{1}H-NMR (300 MHz, DMSO-d$_6$): δ (ppm) 1.37-1.48 (m, 12H, 2x **C3,4,5-H** Pip), 1.77-1.81 (m, 2H, -NH-CH$_2$**CH$_2$**CH$_2$NH-), 1.99-2.01 (m, 4H, 2x -OCH$_2$**CH$_2$**CH$_2$NH-), 2.31 (m, 8H, 2x **C2,6-H** Pip), 3.34-3.37 (s, 4H, 2x Pip**CH$_2$**), 3.53-3.65 (m, 8H, 2x -NH-CH$_2$CH$_2$CH$_2$NH-, 2x-OCH$_2$CH$_2$CH$_2$NH-), 4.01 (t, 4H, ^{3}J=6.0 Hz, 2x -O**CH$_2$**CH$_2$CH$_2$NH-), 6.78-7.86 (m, 6H, 2x **C2,4,6 –H** phenoxy), 7.20 (m, 2H, ^{3}J=8.0 Hz, 2x **C5-H** phenoxy); 7.49 (bs, 2H, 2x NH); ^{13}C-NMR (75.5 MHz, DMSO-d$_6$): δ (ppm) 23.87 (2**C 2x C4** Pip), 25.42 (4C, 2x **C3,5** Pip), 30.32 (2C, 2x -OCH$_2$**CH$_2$**CH$_2$NH-), 32.2, 40.3 (2C), 40.52 (2C) 53.77 (4C, 2x **C2,6**-Pip), 62.63 (2C, 2x Pip-**C**H$_2$), 64.32 (2C, 2x -O**C**H$_2$CH$_2$CH$_2$NH-), 112.55, (2C, 2x **C6** phenoxy), 114.56 (2C, 2x **C2** Ph), 120.89 (2C, 2x **C4** phenoxy), 128.98 (C2, 2x **C5** phenoxy), 158.31 (q, 2x **C1** phenoxy), 167.22 (q, 2x cyclobutenyl), 182.37 (q, 2x **CO** cyclobutenyl); 2q C: signals not visible; HRMS: (FAB$^+$, MeOH/glycerol): *m/z* calcd. for C$_{41}$H$_{55}$N$_6$O$_6$ [MH$^+$] 727.4183, found: 721.4198; C$_{41}$H$_{54}$N$_6$O$_6$ x C$_4$H$_2$F$_6$O$_4$ (950.5)

4,4'-[Octane-1,8-diylbis(azanediyl)]bis(3-{3-[3-(piperidin-1-ylmethyl)phenoxy]propyl-amino}cyclobut-3-ene-1,2-dione) (4.6)

A solution of compound **3.24** (274 mg, 736 μmol, 1.6 eq) and octane-1,8 diamine (53 mg, 464 μmol, 1 eq) in ethanol (60 ml) was stirred at rt for 24 h. The solvent was evaporated from the turbid solution, the residue suspended in a mixture of H$_2$0/ethanol (3/2, v/v) and heated to reflux for 3 h. Filtration of the compound and subsequent washing with H$_2$0/ethanol (3/2, v/v) afforded the product as a white solid, which was dried in vacuo (176 mg, 60 %). Mp. > 135 °C (decomp).

RP-HPLC (210 nm, gradient 1): 97 % (t$_R$=14.3 min, k=4.6); ^{1}H-NMR (600 MHz, DMSO-d$_6$): δ (ppm) 1.25 (m, 8H, 4x -NH-CH$_2$(**CH$_2$**)$_6$CH$_2$NH), 1.36 (m, 4H, 2x **C-H** Pip), 1.45-1.48 (m, 12H, 2x **C-H** Pip, 2x -NH-CH$_2$(**CH$_2$**)$_6$CH$_2$NH-), 1.94-1.98 (m, 4H, 2x -OCH$_2$**CH$_2$**CH$_2$NH-), 2.28 (m, 8H, 2x **C2,6-H** Pip), 3.35 (s, 4H, 2x Pip**CH$_2$**), 3.40-3.46 (m, 4H, -NH-**CH$_2$**(CH$_2$)$_6$**CH$_2$**NH-), 3.65 (m, 4H, 2x -OCH$_2$CH$_2$**CH$_2$**NH-), 3.99 (t, 4H, ^{3}J=6.2 Hz, 2x -O**CH$_2$**CH$_2$CH$_2$NH-), 6.77-6.78 (m, 2H, 2x **C6 –H** phenoxy), 6.82-6.84 (m, 4H, 2x **C2, 4-H** phenoxy), 7.18 (m, 2H, ^{3}J=7.9 Hz, 2x **C5-H** phenoxy); 7.40 (bs, 2H, 2x NH); ^{13}C-NMR (150.95 MHz, DMSO-d$_6$) : δ (ppm) 23.99 (2**C 2x C4** Pip), 25.54 (4C, 2x **C3,5** Pip), 25.76 (2C, -NH-

CH$_2$(**CH$_2$**)$_6$CH$_2$NH-) 28.53 (2C, -NH-CH$_2$(**CH$_2$**)$_6$CH$_2$NH-) 30.41 + 30.72 (4C, 2x -OCH$_2$**CH$_2$**CH$_2$NH-,2x -NH-CH$_2$(**CH$_2$**)$_6$CH$_2$NH-), 40.38 (2C, 2x -OCH$_2$CH$_2$**CH$_2$**NH-), 43.22 (2C, -NH-**C**H$_2$(CH$_2$)$_6$CH$_2$NH-) 53.88 (4C, 2x **C2,6**-Pip), 62.76 (2C, 2x Pip-**C**H$_2$), 64.48 (2C, 2x -O**C**H$_2$CH$_2$CH$_2$NH-), 112.63, (2C, 2x **C6** phenoxy), 114.64 (2C, 2x **C2** Ph), 120.96 (2C, 2x **C4** phenoxy), 129.04 (C2**, 2x C5** phenoxy), 140.34 (q, 2C, **C3** phenoxy), 158.4 (q, 2C, 2x **C1** phenoxy), 167.75 (q, 2x cyclobutenyl), 182.27 + 182.43(q, 2x **CO** cyclobutenyl); HRMS: (EI) m/z calcd. C$_{46}$H$_{64}$N$_6$O$_6$ [M$^+$] 796.4887, found: 796.4882; C$_{46}$H$_{64}$N$_6$O$_6$ x C$_4$H$_2$F$_6$O$_4$ (1025.1)

4,4'-[Decane-1,10-diylbis(azanediyl)]bis(3-{3-[3-(piperidin-1-ylmethyl)phenoxy]propylamino}-cyclobut-3-ene-1,2-dione) (4.7)

A solution of **3.24** (294 mg, 790 µmol, 12.3 eq) and decane-1,10-diamine (60 mg, 330 µmol, 1 eq) both dissolved in ethanol (15 ml), was stirred at rt for 5 days. The precipitate was filtered and then suspended in a small amount of ethanol. Addition of diethyl ether (final ratio ethanol/diethyl ether 1/10, v/v) and storage for 1 day at 4-6 °C afforded yellow crystals, which were washed with the respective mixture of solvents and dried in vacuo (148 mg, 51 %). Mp > 135 °C (decomp).

RP-HPLC (210 nm, gradient 1): 97 % (t$_R$=15 min, k=4.91); ^{1}H-NMR (600 MHz, DMSO-d$_6$): δ (ppm) 1.22-1.24 (m, 12H, 6x NH-CH$_2$(**CH$_2$**)$_8$CH$_2$NH), 1.37 (m, 4H, 2x **C4-H** Pip), 1.47-1.48 (m, 12H, 2x **C3,5-H** Pip, 2xCH$_2$ -NH-CH$_2$(**CH$_2$**)$_8$CH$_2$NH-), 1.95-1.97 (m, 4H, 2x -OCH$_2$**CH$_2$**CH$_2$NH-), 2.32 (m, 8H, 2x **C2,6-H** Pip), 3.3-3.46 (m, 8H, 2x Pip**CH$_2$,** -NH-**CH$_2$**(CH$_2$)$_8$**CH$_2$**NH), 3.65 (m, 4H, 2x -OCH$_2$CH$_2$**CH$_2$**NH-), 3.99 (t, 4H, ^{3}J = 6.1 Hz, 2x -O**CH$_2$**CH$_2$CH$_2$NH-), 6.78-6.79 (m, 2H, 2x **C6 –H** phenoxy), 6.84-6.85 (m, 4H, 2x **C2,4-H** phenoxy), 7.19 (m, 2H, ^{3}J=7.9 Hz, 2x **C5-H** phenoxy); 7.40 (bs, 2H, 2x NH); ^{13}C-NMR (150.95 MHz, DMSO-d$_6$) : δ (ppm) 23.84 (2**C 2x C** Pip), 25.37 +25.78 (6C, 4x **C** Pip, 2x C -NH-CH$_2$(**CH$_2$**)$_8$CH$_2$NH-), 28.55 (2C, -NH-CH$_2$(**CH$_2$**)$_8$CH$_2$NH-), 28.85 (2C, -NH-CH$_2$(**C**H$_2$)$_8$CH$_2$NH-), 30.40 (2C, 2x -OCH$_2$**CH$_2$**CH$_2$NH-), 30.72 (2C, -NH-CH$_2$(**CH$_2$**)$_8$CH$_2$NH-) 40.37 (2C, 2x -OCH$_2$CH$_2$**C**H$_2$NH-), 43.23 (2C, -NH-**CH$_2$**(CH$_2$)$_8$**C**H$_2$NH-) 53.77 (4C, 2x **C2,6**-Pip), 62.58 (2C, 2x Pip-**C**H$_2$), 64.50 (2C, 2x -O**C**H$_2$CH$_2$CH$_2$NH-), 112.81 (2C, 2x **C6** phenoxy), 114.75 (2C, 2x **C2** Ph), 121.10 (2C, 2x **C4** phenoxy), 129.08 (C2**, 2x C5** phenoxy), 158.41 (q, 2C, 2x **C1** phenoxy), 167.87 (q, 2x cyclobutenyl), 182.27 + 182.442(q, 2x **CO** cyclobutenyl); 2qC: signals not visible; HRMS: (EI) m/z calcd. C$_{48}$H$_{69}$N$_6$O$_6$ [M$^+$] 824.9200, found: 824.5217; C$_{48}$H$_{68}$N$_6$O$_6$ (852.6)

2-Cyano-1-[6-(3,4-dioxo-2-{3-[3-(piperidin-1-ylmethyl)phenoxy]propylamino}cyclobut-1-enylamino)hexyl]-3-{3-[3-(piperidin-1-ylmethyl)phenoxy]propyl}guanidine (4.8)

Compounds **3.6** (100 mg, 250 µmol, 1 eq) and **3.24** (91 mg, 240 µmol, 0.96 eq) were dissolved in 30 ml ethanol and heated to reflux for 48 h. The solvent was evaporated and the residue dissolved in chloroform. The organic phase was washed 3 times with H_2O, dried, and the solvent was evaporated. After addition of ethanol/diethyl ether (1/10, v/v) the precipitate was filtered of and washed with ethanol/diethyl ether (1/10, v/v). Drying of the compound in vacuo gave yellow crystals (50 mg, 28 %) with a purity of 88 % (RP-HPLC, 210 nm, gradient 1). For pharmacological investigations **4.8** was purified by preparative HPLC (system 2, 220 nm). Evaporation of acetonitrile and lyophilisation afforded the product as yellow oil (25.51 mg).

RP-HPLC (220 nm, gradient 1): 99.6 % (t_R=13.8 min, 4.4); ^{1}H-NMR (600 MHz, methanol-d_4): δ (ppm) 1.34-1.61 (m, 10H, 4x NH-CH$_2$(**CH$_2$**)$_4$CH$_2$NH-, 1x **C-H** Pip), 1.74-1.94 (m, 10H, **C-H** Pip), 2.03-2.15 (m, 4H, 2x -OCH$_2$**CH$_2$**CH$_2$NH-), 2.94 (m, 4H, 2x **C2/6-H** Pip), 3.16-3.22 (m, 2H, -CH$_2$), 3.-42-3.44 (m, 6H, 2x **C2/6-H** Pip, 1x –CH$_2$), 3.57 (m, 2H, CH$_2$), 3.83 (m, 2H, -OCH$_2$CH$_2$**CH$_2$**NH-), 4.09-4.13 (m, 4H, 2x -O**CH$_2$**CH$_2$CH$_2$NH-), 4.22 (s, 2H, Pip**CH$_2$**), 4.24 (s, 2H, Pip**CH$_2$**), 7.02-7.13 (m, 6H, 2x **C2,4,6 –H** phenoxy), 7.35-7.39 (m, 2H, 2x **C5-H** phenoxy); ^{13}C-NMR (150.95 MHz, methanol-d_4) : δ (ppm) 22.78 (2C 2x **C4** Pip), 24.09 (4C, 2x **C3,5** Pip), 26.99+27.21 (2C, -NH-CH$_2$(**C**H$_2$)$_6$CH$_2$NH-), 29.92 + 30.27 (2C, -NH-CH$_2$(CH$_2$)$_8$CH$_2$NH-, -OCH$_2$CH$_2$CH$_2$NH-), 31.61 + 31.99 (2C, -OCH$_2$CH$_2$CH$_2$NH-, -NH-CH$_2$(CH$_2$)$_8$CH$_2$NH-), 40.44 (1C, -NH-CH$_2$(CH$_2$)$_8$CH$_2$NH-) 42.49+42.62 (2C, -OCH$_2$CH$_2$CH$_2$NH-, -NH-CH$_2$(CH$_2$)$_6$CH$_2$NH-) 44.96 (1C, -OCH$_2$CH$_2$**C**H$_2$NH-), 54.07 (4C, 2x **C2,6**-Pip), 66.71 (2C, 2x Pip-**C**H$_2$), 66.31 +67.22 (2C, 2x -O**C**H$_2$CH$_2$CH$_2$NH-), 116.95 + 117.18 (2C, 2x **C6** phenoxy), 118.33+ 118.38 (2C, 2x **C2** Ph), 124.48 +124.66 (2C, 2x **C4** phenoxy), 131.41 + 131.7 (2C, C2, **2x C5** phenoxy+ 1q), 160.76 (q), 161.95 (q), 162.74 (q) 169.55 (q, 2C, cyclobutenyl), 183.52 (q, 2C, 2x cyclobutenyl); LSIMS (FAB$^+$, Methanol/glycerol) m/z calcd. $C_{42}H_{61}N_8O_4$ [MH$^+$] 741.4816, found: 741.4798; $C_{42}H_{60}N_8O_4$ x $C_4H_2F_6O_4$ (1052.6)

4.6.2   Pharmacological methods

4.6.2.1   Steady state GTPase assay

See chapter 3

4.6.2.2   Histamine H$_2$R assay at the guinea pig atrium

See chapter 3

4.6.2.3   Fluorimetric Ca^{2+} assay on U-373MG cells

See chapter 3

4.6.2.4   Radioligand binding assay on HEK293-FLAG-hH$_3$R-His$_6$ cells

See chapter 3

References

1.   Prinster, S. C.; Hague, C.; Hall, R. A. Heterodimerization of g protein-coupled receptors: specificity and functional significance. *Pharmacol. Rev.* **2005,** 57, 289-98.

2.   Lezoualc'h, F.; Jockers, R.; Berque-Bestel, I. Multivalent-based drug design applied to serotonin 5-HT($_4$) receptor oligomers. *Curr. Pharm. Des.* **2009,** 15, 719-29.

3.   Waldhoer, M.; Fong, J.; Jones, R. M.; Lunzer, M. M.; Sharma, S. K.; Kostenis, E.; Portoghese, P. S.; Whistler, J. L. A heterodimer-selective agonist shows in vivo relevance of G protein-coupled receptor dimers. *Proc. Natl. Acad. Sci. U. S. A.* **2005,** 102, 9050-5.

4.   Rocheville, M.; Lange, D. C.; Kumar, U.; Sasi, R.; Patel, R. C.; Patel, Y. C. Subtypes of the somatostatin receptor assemble as functional homo- and heterodimers. *J. Biol. Chem.* **2000,** 275, 7862-9.

5.   Fukushima, Y.; Asano, T.; Saitoh, T.; Anai, M.; Funaki, M.; Ogihara, T.; Katagiri, H.; Matsuhashi, N.; Yazaki, Y.; Sugano, K. Oligomer formation of histamine H$_2$ receptors expressed in Sf9 and COS7 cells. *FEBS Lett.* **1997,** 409, 283-6.

6.   Bakker, R. A.; Dees, G.; Carrillo, J. J.; Booth, R. G.; Lopez-Gimenez, J. F.; Milligan, G.; Strange, P. G.; Leurs, R. Domain swapping in the human histamine H$_1$ receptor. *J. Pharmacol. Exp. Ther.* **2004,** 311, 131-8.

7.   Shenton, F. C.; Hann, V.; Chazot, P. L. Evidence for native and cloned H$_3$ histamine receptor higher oligomers. *Inflammation Res.* **2005,** 54 Suppl 1, S48-9.

8.   van Rijn, R. M.; Chazot, P. L.; Shenton, F. C.; Sansuk, K.; Bakker, R. A.; Leurs, R. Oligomerization of recombinant and endogenously expressed human histamine H($_4$) receptors. *Mol. Pharmacol.* **2006,** 70, 604-15.

9.   Angers, S.; Salahpour, A.; Joly, E.; Hilairet, S.; Chelsky, D.; Dennis, M.; Bouvier, M. Detection of beta 2-adrenergic receptor dimerization in living cells using bioluminescence resonance energy transfer (BRET). *Proc. Natl. Acad. Sci. U. S. A.* **2000,** 97, 3684-9.

10.   Portoghese, P. S. From models to molecules: opioid receptor dimers, bivalent ligands, and selective opioid receptor probes. *J. Med. Chem.* **2001,** 44, 2259-69.

11.   Kroeger, K. M.; Hanyaloglu, A. C.; Seeber, R. M.; Miles, L. E.; Eidne, K. A. Constitutive and agonist-dependent homo-oligomerization of the thyrotropin-releasing hormone receptor. Detection in living cells using bioluminescence resonance energy transfer. *J. Biol. Chem.* **2001,** 276, 12736-43.

12.   Dinger, M. C.; Bader, J. E.; Kobor, A. D.; Kretzschmar, A. K.; Beck-Sickinger, A. G. Homodimerization of neuropeptide y receptors investigated by fluorescence resonance energy transfer in living cells. *J. Biol. Chem.* **2003,** 278, 10562-71.

13.   Milligan, G.; Bouvier, M. Methods to monitor the quaternary structure of G protein-coupled receptors. *FEBS J* **2005,** 272, 2914-25.

14.   Angers, S.; Salahpour, A.; Bouvier, M. Dimerization: an emerging concept for G protein-coupled receptor ontogeny and function. *Annu. Rev. Pharmacol. Toxicol.* **2002,** 42, 409-35.

15.   Halazy, S. G-protein coupled receptors bivalent ligands and drug design. *Exp. Opin. Ther. Patents* **1999,** 9, 431-446.

16.   Bhushan, R. G.; Sharma, S. K.; Xie, Z.; Daniels, D. J.; Portoghese, P. S. A bivalent ligand (KDN-21) reveals spinal delta and kappa opioid receptors are organized as heterodimers that give rise to delta(1) and kappa(2) phenotypes. Selective targeting of delta-kappa heterodimers. *J. Med. Chem.* **2004,** 47, 2969-72.

17.   Portoghese, P. S.; Larson, D. L.; Sayre, L. M.; Yim, C. B.; Ronsisvalle, G.; Tam, S. W.; Takemori, A. E. Opioid agonist and antagonist bivalent ligands. The relationship between spacer length and selectivity at multiple opioid receptors. *J. Med. Chem.* **1986,** 29, 1855-61.

18.   Portoghese, P. S.; Ronsisvalle, G.; Larson, D. L.; Takemori, A. E. Synthesis and opioid antagonist potencies of naltrexamine bivalent ligands with conformationally restricted spacers. *J. Med. Chem.* **1986,** 29, 1650-3.

19.   Daniels, D. J.; Kulkarni, A.; Xie, Z.; Bhushan, R. G.; Portoghese, P. S. A bivalent ligand (KDAN-18) containing delta-antagonist and kappa-agonist pharmacophores bridges delta$_2$ and kappa$_1$ opioid receptor phenotypes. *J. Med. Chem.* **2005,** 48, 1713-6.

20.   Daniels, D. J.; Lenard, N. R.; Etienne, C. L.; Law, P. Y.; Roerig, S. C.; Portoghese, P. S. Opioid-induced tolerance and dependence in mice is modulated by the distance between pharmacophores in a bivalent ligand series. *Proc. Natl. Acad. Sci. U. S. A.* **2005,** 102, 19208-13.

21.   Portoghese, P. S. Bivalent ligands and the message-address concept in the design of selective opioid receptor antagonists. *Trends Pharmacol. Sci.* **1989,** 10, 230-5.

22.   Kraus, A. Highly potent, selective acylguanidine-type H2 receptor agonists: Synthesis and structure activity relationships. *Doctoral thesis*, University of Regensburg,Germany, http://epub.uni-regensburg.de/10699/, **2007**.

23.   Kelley, M. T.; Burckstummer, T.; Wenzel-Seifert, K.; Dove, S.; Buschauer, A.; Seifert, R. Distinct interaction of human and guinea pig histamine H_2-receptor with guanidine-type agonists. *Mol. Pharmacol.* **2001,** 60, 1210-25.

24.   Preuss, H.; Ghorai, P.; Kraus, A.; Dove, S.; Buschauer, A.; Seifert, R. Constitutive activity and ligand selectivity of human, guinea pig, rat, and canine histamine H_2 receptors. *J. Pharmacol. Exp. Ther.* **2007,** 321, 983-95.

25.   Kracht, J. Bestimmung der Affinität und Aktivität subtypselektiver Histamin- und Neuropeptid Y-Rezeptorliganden an konventionellen und neuen pharmakologischen In-vitro-Modellen. *Doctoral thesis*, University of Regensburg, **2001**.

26.   Schnell, D. *Personal communication*. In Department of Pharmacology and Toxicology, University of Regensburg (Germany), **2008**.

27.   Nordemann, U. *Personal communication*. In Department of Pharmaceutical and Medicinal Chemistry II, University of Regensburg (Germany), **2009**.

28.   Ghorai, P.; Kraus, A.; Keller, M.; Gotte, C.; Igel, P.; Schneider, E.; Schnell, D.; Bernhardt, G.; Dove, S.; Zabel, M.; Elz, S.; Seifert, R.; Buschauer, A. Acylguanidines as bioisosteres of guanidines: NG-acylated imidazolylpropylguanidines, a new class of histamine H_2 receptor agonists. *J. Med. Chem.* **2008,** 51, 7193-204.

29.   Vauquelin, G.; Van Liefde, I.; Birzbier, B. B.; Vanderheyden, P. M. New insights in insurmountable antagonism. *Fundam. Clin. Pharmacol.* **2002,** 16, 263-72.

30.   Vauquelin, G.; Van Liefde, I.; Vanderheyden, P. Models and methods for studying insurmountable antagonism. *Trends Pharmacol. Sci.* **2002,** 23, 514-8.

31.   Kenakin, T.; Jenkinson, S.; Watson, C. Determining the potency and molecular mechanism of action of insurmountable antagonists. *J. Pharmacol. Exp. Ther.* **2006,** 319, 710-23.

Chapter 5

Towards H$_2$-receptor antagonists as new radioligands

5 Towards H₂-receptor antagonists as new radioligands

5.1 Introduction

Usually radioligands are used as pharmacological tools to characterize new compounds with respect to their binding properties and their pharmacological profile. Requirements for an ideal radioligand are: high purity (>90 %), sufficient stability, high specific activity (> 10 Ci/mmol) for traceability and defined interactions with the receptor (antagonist if possible)[1]. According to these requirements, former standard ligands like [³H]metiamide, [³H]histamine, [³H]cimetidine[2-3] and [³H]ranitidine are not considered suitable for labelling the H_2-receptor[4], e.g. the commercially available radioligand [³H] histamine has low affinity to the H_2R (> 200 nM) and low specific activity (about 14 Ci/mmol), whereas [³H]tiotidine, used for competition binding studies at the H_2R[5-6], shows high unspecific binding and is expensive. [¹²⁵I]-APT was used in radioligand binding studies at guinea pig cerebral membranes[7] and for binding studies on CHO cell membranes[8], but radioligands bearing [¹²⁵I] possess the disadvantage of difficult handling due to safety precautions. The use of

	R
Iodoaminopotentidine (I-APT)	NH₂
Iodoazidopotentidine (I-AZP)	N₃
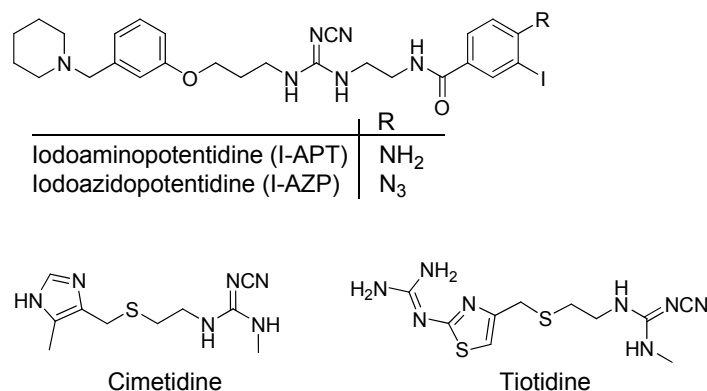
Scheme 5.1: Representative compounds, which can be used as radioligands

tritium herein is beneficial, as the introduction of the small tritium atom generally does not affect the physicochemical properties of the ligand. Furthermore the half-life ($T_{1/2}$) of 12.4 years is beneficial in laboratory practice. For ligands bearing [¹²⁵I], with a short half-life of 59.4 days, repeated synthesis is required. But the high costs, difficult accessibility and high unspecific binding (e.g. for tiotidine[6]) limit the use of tritiated ligands. Propionic acid is commercially available in its tritiated form and allows a convenient preparation of radioligands under standard laboratory conditions, The fact that several H₂-receptor antagonists described in chapter 3 have high activities at the human histamine H₂-receptor in the range of aminopotentidine ($K_{b'}$ = 180 nM) and iodaminopotentidine ($K_{b'}$ = 35 nM, Scheme 5.1)[9,] encouraged us to synthesize propionylated H₂-receptor antagonists in order to obtain a new radioligand with beneficial properties compared to tiotidine.

Squaramides, which showed the highest antagonistic activity ($K_{b'}$ = 2-200 nM) at the H$_2$ receptor were considered most promising for modifications in the eastern part of the molecule (Scheme 5.2**)**. However, cyanoguanidines as moderate H$_2$R antagonists were also included, due to the structural similarities with iodaminopotentidine (Scheme 5.1).
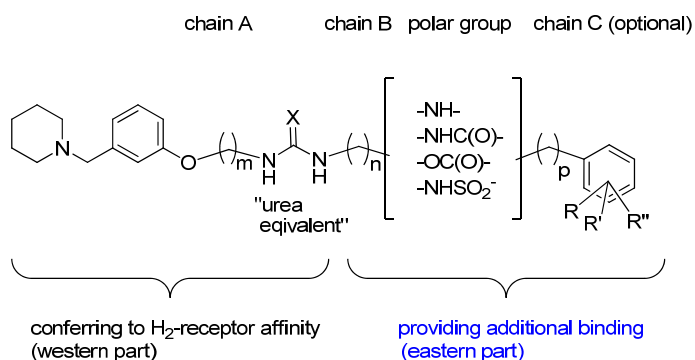
Scheme 5.2: Structural features of potentidine-like H$_2$-receptor ligands, derived from ref [10]

Additionally, a different pharmacophore, namely guanidinothiazole, related to tiotidine[11], was used to investigate, whether this part of the molecule (Scheme 5.2) confers to improved histamine H$_2$-receptor selectivity. In general, the "urea equivalent" of H$_2$R ligands confers to receptor affinity[10] (see chapter 3). The fluorescent ligands **6.8** and **8.7** described in chapter 6 and 8, comprising only one amino group instead of the "urea equivalent" without any additional alkyl spacers proved to maintain antagonistic activity at the H$_2$R (**6.8**) and the H$_3$R (**8.7**), despite the lack of an additional pharmacophoric moiety. Therefore, this approach was also applied to the guanidinothiazole in an attempt to find a new low molecular weight H$_2$R ligand.

The primary amino group present in squaramide-, cyanoguanidine- and guanidinothiazole-type building blocks were coupled to propionic and 4-F-benzoic acid. Such labelled acids are already in use to prepare potent [^{3}H] and [^{18}F] bearing radioligands. [^{3}H]UR-PI294, a combined H$_3$/H$_4$ -receptor agonist[12], and the highly potent and selective neuropeptide YY$_1$ receptor antagonist [^{3}H]UR-MK114[13] are examples for the successful application of such strategies. In the following sections the steps towards the new potent H$_2$-receptor radioligand **5.10a** ([^{3}H]UR-DE257) will be described, including the synthesis and pharmacological investigations.

5.2 Chemistry

Synthesis of amides from primary amines and carboxylic acids can be accomplished with differ-
ent coupling reagents, for example with EDAC and CDI, which form an active ester in situ, or
directly with chlorides or anhydrides. Another approach is the direct use of active esters, often
employed in peptide chemistry, to achieve amides. With respect to radiolabelling, complete
conversion to the radiotracer in a one pot reaction without side products and only one purifica-
tion step (preparative HPLC) are desired. The "cold forms" of potential radioligands were syn-
thesized to investigate the structure-activity relationships and to optimize the reaction condi-
tions. By analogy with a procedure, which was previously developed in our laboratory[14], we used
active esters of propionic- and 4-F-benzoic acid for the derivatisation of the respective amine
precursors. The dissolved amines (in acetonitrile or methanol) were treated with Et_3N to prevent
protonation of the primary amino group (pH 8-9). Due to poor solubility the squaric acid deriva-
tives were dissolved in DMSO alone, or in combination with methanol.
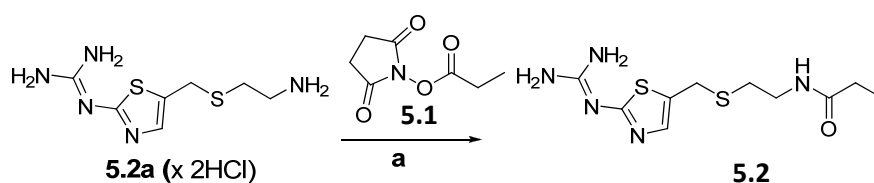
Scheme 5.3: Synthesis of **5.2**; Reagents and conditions: (a) MeOH, Et_3N, rt, 18 h

After addition of active ester (**5.1** or **5.3**) the reaction generally is completed within 30 min to 3 h
at rt. To ensure complete conversion to the product, in case of the radioligand an excess of the
amine was used and the solution was stirred at rt overnight, before the reaction mixture was
purified by preparative HPLC on a RP column (Scheme 5.3, Scheme 5.4). Radioligand **5.10a** was
obtained after purification by preparative HPLC with a specific activity of 69.3 Ci/mmol and a
radiochemical purity of 92 %.
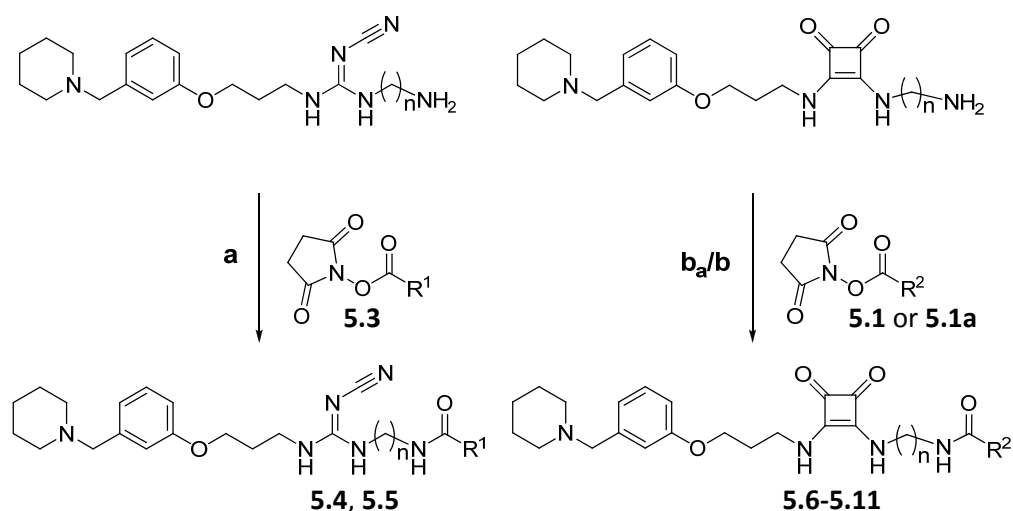
Compd.	n	R^1/R^2	Compd.	n	R^1/R^2
5.4	2	4-F-phenyl	**5.9**	5	CH_2-CH_3
5.5	6	4-F-phenyl	**5.10**	6	CH_2-CH_3
5.6	2	CH_2-CH_3	**5.11**	4	4-F-phenyl
5.7	3	CH_2-CH_3	**[³H]UR-De257, 5.10a**		
5.8	4	CH_2-CH_3			

Scheme 5.4: Synthesis of **5.4 – 5.11**; Reagents and conditions: (a) MeCN, Et$_3$N, rt 30 min – 18 h (b$_a$) MeCN/DMSO (3/2), 18 h, rt; (b) MeCN or DMSO or methanol/DMSO (1/1), Et$_3$N, rt, 30 min - 18 h

To confirm the identity of the radioligand the chromatograms of unlabelled and labelled ligands were compared regarding their retention times (Scheme 5.5). The small differences in the retention times were due to the setup of UV- and radiodetector.

Scheme 5.5: Purity control of **5.10a** by HPLC

A: Radiochromatogramm of **5.10a** c: 0.06 µM; **B**: unlabelled **5.10** , c= 5 µM; UV (290 nm)

A+B: Conditions: injection volume: 200 µl; gradient: 0.05 % TFA in acetonitrile/0.05 % TFA in H_2O: 0 min: 20/80 (v/v), 37 min: 30/70 (v/v), 3 8 min 90/10 (v/v), 48 min 90/10 (v/v), flow: 0.8 ml/min
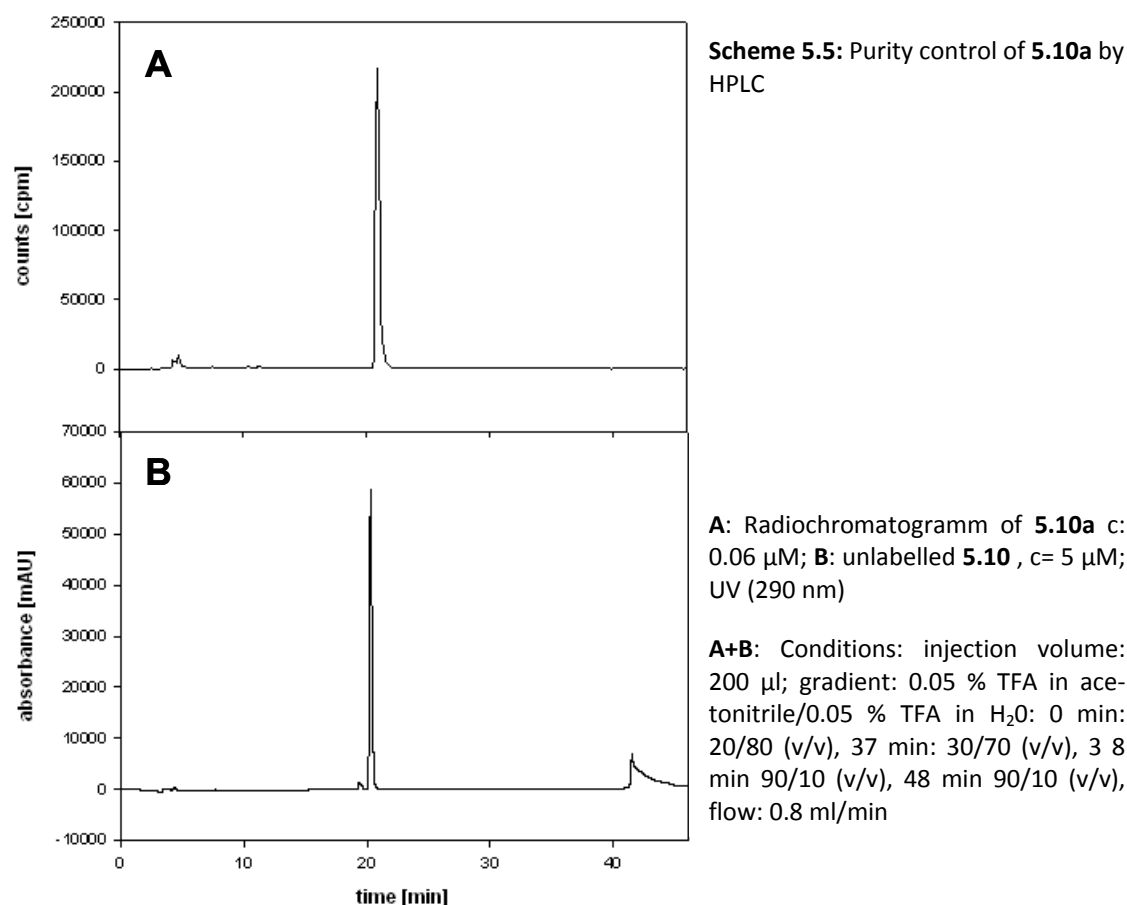
5.3   Pharmacological results

5.3.1 H_2-receptor antagonism

GTPase assay at the guinea pig and human histamine H_2-receptor

The compounds **5.4-5.11** were investigated for H_2R antagonism in the GTPase assay using membrane preparations of Sf9 cells expressing the hH_2R-$G_{s\alpha S}$ or the gpH_2R-$G_{s\alpha S}$ fusion protein[5]. Compounds **5.2** and **5.5** displayed only weak activity at the hH_2R in the micromolar range (Table 5.1). Thus these compounds were not considered for further investigations at the gpH_2R. On the contrary the squaric acid derivatives **5.6-5.11** and **5.4** proved to be potent gpH_2R and hH_2R antagonists in the low nanomolar range and showed only very weak inverse agonistic effects with intrinsic activities (E_{max}) of -0.03 to -0.2. In this series, compound **5.10** with the longest alkyl chain (hexamethylene spacer), had the highest antagonistic activity with $K_{b'}$ values of 38 nM and 28 nM at the hH_2R and the gpH_2R, respectively (see Table 5.1). The activities of the propionylated ligands were slightly higher at the gpH_2R compared to the human receptor.

Table 5.1: H$_2$R antagonism in GTPase assays determined on membranes of Sf9 cells expressing the hH$_2$R-G$_{s\alpha S}$ or gpH$_2$R-G$_{s\alpha S}$ fusion protein[a]

Compd.	gpH$_2$R-G$_{s\alpha s}$	hH$_2$R-G$_{s\alpha s}$	
	K$_{b'}$ (EC$_{50}$) [nM]	K$_{b'}$ (EC$_{50}$) [nM]	E$_{max}$
Histamine	(850 ±340)[b]	(990 ± 92)[b]	1.00
5.2	n.d	>5000	n.d.
5.4	n.d	50.61	n.d.
5.5	n.d	>1000	n.d.
5.6	95 ± 47	114 ± 15	0.11 ± 0.04
5.7	n.d.	59 ± 13	-0.33 ± 0.18
5.8	138 ± 61	195 ± 48	-0.23 ± 0.05
5.9	64 ± 22	69 ± 7	n.d.
5.10	28 ± 12	38± 8	0.08 ± 0.01
5.11	97 ± 28	53 ± 10	0.03 ±0.01

[a] Steady state GTPase assay on Sf9 cell membranes; c. ligands: 1 nM- 100 µM; typical GTPase activities (stimulation with 1 µM histamine (gpH$_2$R/hH$_2$R): 3.5-7 pmol x mg^{-1} x min^{-1}; E$_{max}$= efficacy relative to histamine, E$_{max}$ HIS=1 (c. Ligands for efficacy: 10 µM), Mean values ± S.E.M. (n = 2-4), performed in duplicate; n.d.: not determined; [b] see ref. [9]

H$_2$R Antagonism of 5.6 and 5.7 at the guinea pig atrium

The squaramides **5.6** and **5.7** were tested for inhibition of the histamine stimulated positive chronotropic response at the isolated spontaneously beating guinea pig right atrium. Cumulative concentration-response curves of histamine in the absence and presence of antagonist (**5.6**, **5.7**) were recorded and pA$_2$-values were calculated from the increase in the EC$_{50}$ values of the agonist. Compounds **5.6** and **5.7** proved to have pA$_2$ values in the low nanomolar

Table 5.2: H$_2$R antagonism of **5.6** and **5.7** at the isolated spontaneously beating guinea pig right atrium (gpH$_2$R).

Compd.	gpH$_2$R			
	c [nM]	pA$_2$	K$_B$[nM]	n[a]
5.6	300/1000	7.36 ±0.14	44	6
5.7	100	7.22 ±0.08	60	4

[a]Number of experiments, SEM calculated from n experiments,

range (Table 5.2) corresponding to data from GTPase assays. Both compounds caused a decrease of the maximum response of histamine (E$_{max}$ HIS 77 %, c **5.6**: 300 nM). The depression of the concentration-response curve was enhanced with increasing antagonist concentrations (at 1000 nM antagonist: E$_{max}$ HIS: 54 % (**5.6**) and 77 % (**5.7**), respectively.

5.3.2   Receptor selectivity

H_1 - eceptor antagonism on U373 MG cells and activity on human H_1-, H_3- and H_4- receptors in GTPase assays

The compounds were investigated for antagonism at the H_1-receptor in a Ca^{2+} assay on U373 MG cells[15]. None of the substances had remarkable effect on the histamine-induced Ca^{2+} signal. Calculated IC_{50} values ranged from 30 - 100 µM, indicating no relevant H_1-receptor antagonism (see appendix). Determination of the E_{max} values in GTPase assays revealed no inverse agonistic effects (E_{max}= -0.05 - 0.0) at the hH_1R[16]. The same holds for the results from Sf9 cell membranes expressing hH_4R-RGS19+ $G_{i\alpha2}$+$G_{\beta1\gamma2}$[17]. Neither agonism nor inverse agonism detected (E_{max} values (-0.16 - 0.12). The investigation of two compounds (**5.2** and **5.10**) in the antagonist mode at the H_4R (GTPase assay) revealed activity over 5000 nM . Thus, these two compounds possess more than 100-fold selectivity for the H_2R over the H_4R (see appendix).

Regarding the H_3-receptor (Sf9 cell membranes expressing hH_3R+ $G_{i\alpha2}$ +$\beta_1\gamma_2$ + RGS4[17]) the E_{max} values of all investigated squaramide derivatives were in the range of –0.45 to -0.6. This means that the compounds reduced the basal activity of the GTPase by 45 % to 60 %, comparable to the known inverse agonist thioperamide. Therefore, $K_{b'}$ values of selected compounds (antagonist mode) were determined in order to estimate the selectivity ratio for H_2R versus H_3R. As depicted in Table 5.4 the inhibition of GTP hydrolysis at the hH_3R was in the nanomolar range ($K_{b'}$= 200-800 nM), corresponding to a 2 - 20 fold selectivity over the hH_3R. The antagonistic activities of the respective ligands were compared to affinities determined in radioligand binding assays on cells.

Affinities at the human H_3-receptor in radioligand binding experiments

Radioligand binding assays were performed with [3H]NAMH (N^α-methylhistamine) as radioactive tracer (K_D: 5.1 nM) on HEK-293-FLAG hH_3R-His_6 cells. One to two representative ligands out of each series of compounds were investigated for displacement of [3H]NAMH from the H_3R (Table 5.3)[18]. This competition binding experiments revealed moderate to high affinity to the human histamine H_3R and confirmed the order of potency determined in the GTPase assays. Regardless of the combined H_2/H_3-receptor activity the most potent of these compounds (**5.10**) was chosen for the preparation of a radioactive tracer for further analysis of the histamine H_2-receptor, as in

laboratory praxis often recombinant systems, expressing only one receptor subtype, are used. In this case a moderate selectivity profile will play a minor role

Table 5.3: Activitiy and Affinity of selected compounds on hH_3R expressing Sf9 cell membranes (GTPase[a]) and on HEK-293-FLAG-hH_3R-His_6cells[b]

	GTPase assay hH_3R+ $G_{i\alpha2}$ +$\beta_1\gamma_2$ + RGS4[a]		Binding data HEK-293 FLAG hH_3R His_6 cells[b]
Compd.	$K_{b'}$ (EC_{50}) [nM]	E_{max}	K_i (K_D) [nM]
[^{3}H]NAMH	-	-	(5.1)[d]
histamine	$(25 \pm 3)^c$	1.00	n.d.
thioperamide	97 ± 18	-0.66 ± 0.09	n.d.
5.2	no activity	n.d.	>10000
5.4	> 1000	-0.16 ± 0.04	n.d.
5.5	> 1000	n.d	>2000
5.6	>500	-0.46 ± 0.1	n.d
5.7	234 ± 173	n.d.	$234.2 \pm$
5.8	385	-0.48 ± 0.1	n.d.
5.9	963	-0.6 ± 0.01	n.d.
5.10	848 ± 390	-0.46 ± 0.3	>1000
5.11	n.d.	-0.41 ± 0.25	200 ± 75
5.2	no activity	n.d.	>10000

[a] Steady state GTPase assay on Sf9 cell membranes; c. ligands: 1 nM - 100 μM; typical GTPase activities (stimulation with 100 nM HIS (hH_3R): 2.5-6.0 pmol x mg^{-1} x min^{-1}; E_{max}= efficacy relative to histamine= 1, E_{max} HIS= 1 (c. ligands: 10 μM), Mean values ± S.E.M. from 1-3 experiments performed in duplicate;

[b] c. ligands: 1 nM-100 μM, c. [^{3}H]NAMH: 1 nM, 2-5 million cells/well; Mean values ± S.E.M. (n = 1-2) performed in duplicate; n.d.: not determined; [b] and [d] ref.[18], [c] ref.[19];

Affinity and functional activity of 5.10 on Hek293-hH_2R-qs5-HA cells

The affinity of compound **5.10** was investigated in a competition binding assay at the flow cytometer[20] using **6.23** (final c: 200 nM,) as the fluorescence ligand (see chapter 6). Functional activity was measured in a fluorescence based Ca-assay[20] using Fura-2 as a calcium-sensitive dye.

Table 5.4: Activity[a] and affinity[b] of **5.10** on HEK293-hH2R-qs5-HA cells

Compd.	HEK293-H$_2$-cells (flow cytometer)	HEK293-H$_2$-cells (Ca-assay)
	K$_i$	K$_{b'}$
HIS		1400 (EC$_{50}$)[c]
5.10	237 ±41	130 ± 34

c ligand: 1 nM-10 µM ; [a] determined in the Ca-assay described in 5.6.2.6, , c. HIS: 10 µM;
[b] determined as described in chapter 3, c: **6.23**: 200 nM (K$_D$: 180 nM); Mean values ± S.E.M. (n = 3), performed in duplicate;
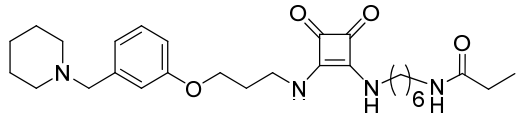
Compound **5.10** inhibited binding of **6.23** in a concentration-dependent manner, revealing a K$_i$ value of 237 nM, and inhibited the histamine-stimulated Ca^{2+} mobilisation in HEK293-hH$_2$R-qs5-HA cells (K$_{b'}$= 130 nM). H$_2$-receptor binding and functional data on whole cells resulted in 2-6 fold lower affinities/activities compared to the experiments performed on Sf9 cell membranes.

5.3.3   Pharmacological characterization of the radioligand 5.10a ([³H]UR-De257)

General

The designated radioligand **5.10** had sufficient affinity on Sf9 cell membranes consisting, of hH$_2$R-G$_{s\alpha s}$ fusion proteins, and acted as antagonist at the H$_2$-receptor (K$_{b'}$ = 38 nM). **5.10** possessed a 20-fold selectivity for the hH$_2$R relative to the hH$_3$R and showed no significant activity at the hH$_4$R and the hH$_1$R (summarized in Figure 5.1).

	K$_{b'}$ [nM]	E$_{max}$
hH$_1$R	n.d.	- 0.03 ± 0.03
hH$_2$R	38 ± 8	0.08 ± 0.01
hH$_3$R	848 ± 390	- 0.46 ± 0.3
hH$_4$R	> 5000	0.04 ± 0.05

Figure 5.1: Squaramide **5.10**: Structure and selectivity profile at histamine receptors, from [a] steady state GTPase assay on Sf9 cell membranes; c. ligands: 1 nM - 100 µM; typical GTPase activities (stimulation with 1 µM HIS (hH$_2$R): 3.5-7 pmol x mg^{-1} x min^{-1}; E$_{max}$= efficacy relative to histamine, E$_{max}$ HIS=1 (c. ligands: 10 µM), Mean values ± S.E.M. from 2-4 experiments performed in duplicate; n.d.: not determined

For the H$_2$R antagonist [^{125}I]I-APT[7] and its "cold form", I-APT[10], discrepancies between binding and functional data were reported. Regardless of a K$_{b'}$-value of "only" 35 nM[9] (I-APT), [^{125}I]I-APT turned out to be a valuable radioligand due to a K$_i$ value of 0.71 nM[10]. The reason for this discrepancy has not been reported, however it is conceivable that the lower activity at the guinea pig atrium results from the different time windows of the assays (see discussion). As the K$_{b'}$ value of **5.10** is in the same range

Table 5.5: Saturation binding of 5.10a at the hH$_2$R-G$_{s\alpha s}$,[a]

	K$_D$ [nM]	B$_{max}$[pmol/mg protein]
hH$_2$R	26.8 ± 3.8	0.70 ±0.1

[a] Mean values ± S.E.M. of 4 independent experiments, performed in duplicate

as the K$_{b'}$ value of the reference compound I-APT, we synthesized **5.10** in its tritiated form, **5.10a** and performed saturation studies and kinetic experiments at the hH$_2$R.

5.3.3.1 Saturation binding of [^{3}H]UR-De257 (5.10a) at the hH$_2$R-G$_{s\alpha s}$

The hH$_2$R-G$_{s\alpha s}$ fusion protein expressed in Sf9 insect cell membranes, bound **5.10a** in a saturable manner (Scheme 5.6). Total and specific binding versus radioligand concentrations were best fitted by nonlinear regression to a one-site binding model, nonspecific binding to a standard linear curve. Famotidine was used at a final concentration of 100 µM for the evaluation of unspecific binding. Saturation binding experiments revealed high specific binding (Scheme 5.6) in a concentration range from 2 to 50 nM, whereas, in the range of the K$_D$, nonspecific binding was low, reaching 10 to 20 % of total binding. The analysis afforded a K$_D$- value of 26.8 nM and a B$_{max}$ value of 0.72 pmol per mg of membrane protein (Table 5.5). Scatchard analysis showed a straight line (Scheme 5.7), indicating that the radioligand binds to a single binding site, following the law of mass action.[21]
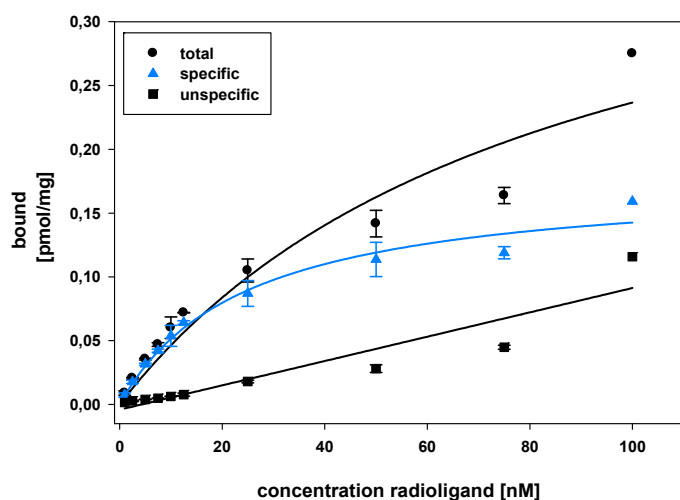
Scheme 5.6: Representative saturation binding curve of **5.10a** at the hH_2R-$G_{s\alpha s}$

Each data point was performed in duplicate. Membranes were incubated with increasing concentrations of **5.10a** as described in the experimental section
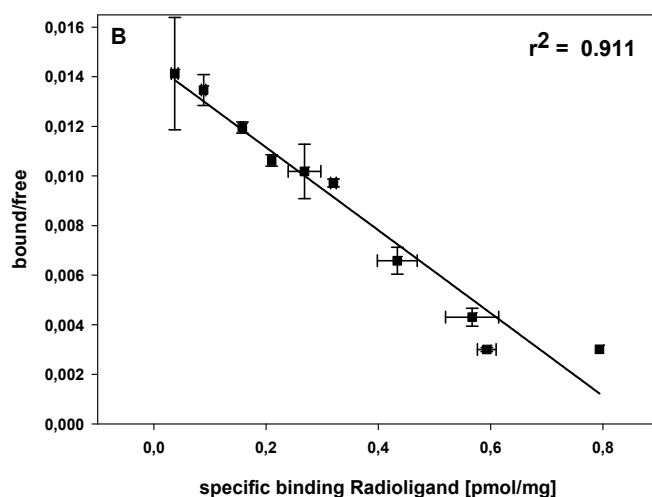
Scheme 5.7: Representative scatchard plot of saturation binding of **5.10a** at the hH_2R-$G_{s\alpha s}$; best fitted by linear regression

The B_{max} value is in agreement with data from radioligand binding studies performed with [³H]tiotidine[6] at the hH_2R-$G_{s\alpha s}$, and the K_D value (26.8 nM) for **5.10a** is in good agreement with the $K_{b'}$ value determined in the GTPase assay ($K_{b'}$ =38 nM, Table 5.5).

5.3.3.2   Association and dissociation kinetics

To measure the rate of dissociation/association[21] of the radioligand, experiments were carried out on Sf9-cell membranes (hH$_2$R-G$_{s\alpha s}$) using [^{3}H]UR-DE257 (**5.10a**) at a concentration of 25 nM at 22 °C. Association and dissociation kinetics (K$_{obs}$ = 0.011 min^{-1}, K$_{off}$ = 0.0004 min^{-1}) were slow, with an association half-life (T$_{1/2}$) of 64.26 min, reaching equilibrium after aproximately 150-200 min (Table 5.6). For the displacement of **5.10a** a dissociation half-life (T$_{1/2}$) of 121.58 min was measured (Table 5.6).

Table 5.6: Kinetic analysis of **5.10a** binding to hH$_2$R-G$_{s\alpha s}$ (Sf9 cell membranes)

K$_{obs}$	T$_{1/2}$	K$_{on}$^{b}	K$_{off}$	T$_{1/2}$	K$_{off}$/k$_{on}$^{a}	K$_D$(sat)
0.011 ± 0.001	64.3 ± 1.2	0.0002 ± 0.00001	0.0004 ± 0.0004	121.6 ± 8	29.9 ± 1.2	26.8 ± 3.8

Mean values ± S.E.M. (n =2), experiments performed in duplicate, ^{a} K$_{off}$/K$_{on}$ = K$_{D,}$, ^{b}K$_{on}$ = (K$_{obs}$-K$_{off}$)/c [**5.10a**]); K$_{obs}$: observed association rate, K$_{on}$: association rate constant, K$_{off}$: dissociation rate constant, K$_D$: equilibrium dissociation constant
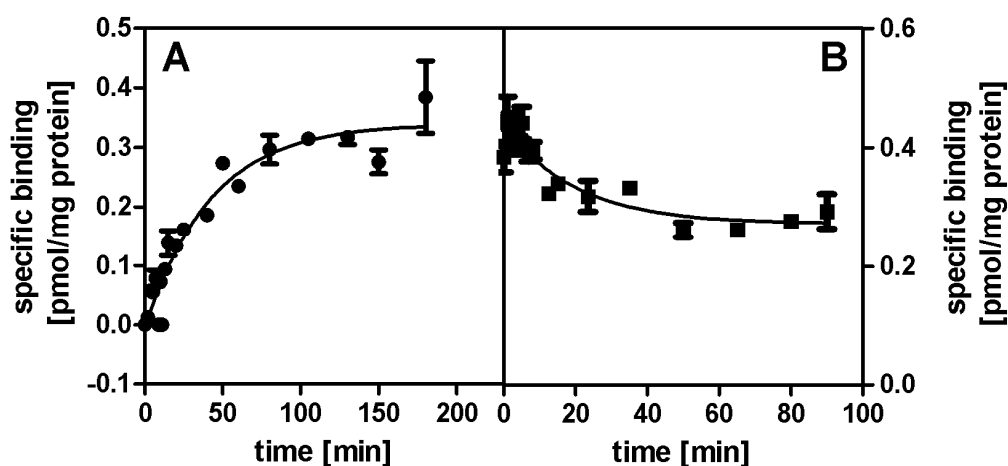
Scheme 5.8: Association and dissociation kinetics of **5.10a** to Sf9 membranes expressing hH$_2$R-G$_{s\alpha s.}$ at 22 °C**; A, B:** radioligand (c = 25 nM), specific binding is the difference between total and unspecific binding. **A**: association as a function of time, fitted to a one-phase exponential association model. **B**: dissociation as a function of time, displacement induced by famotidine (100 µM,see 6.4.2.3) fitted to a one-phase exponential decay model

Despite this slow kinetics the equilibrium dissociation constant (K_d), calculated from the ratio of k_{off} and k_{on} ($K_{off}/k_{on} = K_d = 29.9$ nM), is consistent with the K_d-value ($K_D = 26.8$ nM) determined in saturation binding experiments. This is a hint that the binding of the radioligand follows the law of mass action[21]. Taking the incomplete displacement of [^{3}H]UR-DE257 (30 %) into account, the calculated values can only be considered as an approximation of the actual half-lifes and off/on rates[22].

5.3.3.3   Competition binding experiments at the hH$_2$R-G$_{s\alpha S}$

Reference compounds and H$_2$R ligands synthesized in our workgroup were tested in competition binding assays on Sf9 insect cell membranes expressing the hH$_2$R-G$_{s\alpha S}$ fusion protein. All investigated ligands inhibited specific binding of **5.10a**. The determined K_i-values were compared to data from the literature (GTPase assays) and to binding studies using [^{3}H]tiotidine as radioligand on membranes expressing hH$_2$R-G$_{s\alpha S}$ (Table 5.7, Scheme 5.9).

The K_i-values determined for the reference antagonists (famotidine, cimetidine) and agonists like histamine or arpromidine are in the same range as those reported in the literature[5, 9]. In theory the dissociation constant of the unlabelled **5.10** (competition binding experiments) and the K_D-value of the corresponding radioligand **5.10a** (saturation analysis) have to be identical. As required, the determined values are close to each other, 26.8 nM for **5.10a** and 29.5 nM for **5.10**.

Comp.	R¹	R²	Comp.	R³	R⁴
Arpromidine	4-fluorophenyl	2-pyridyl	**UR-AK480**	imidazolyl	imidazolyl
BU-E43	phenyl	2-pyridyl	**UR-Bit82**	imidazolyl	2-amino-4-methylthiazolyl
BU-E96	4-fluorophenyl	2-methylthiazolyl			
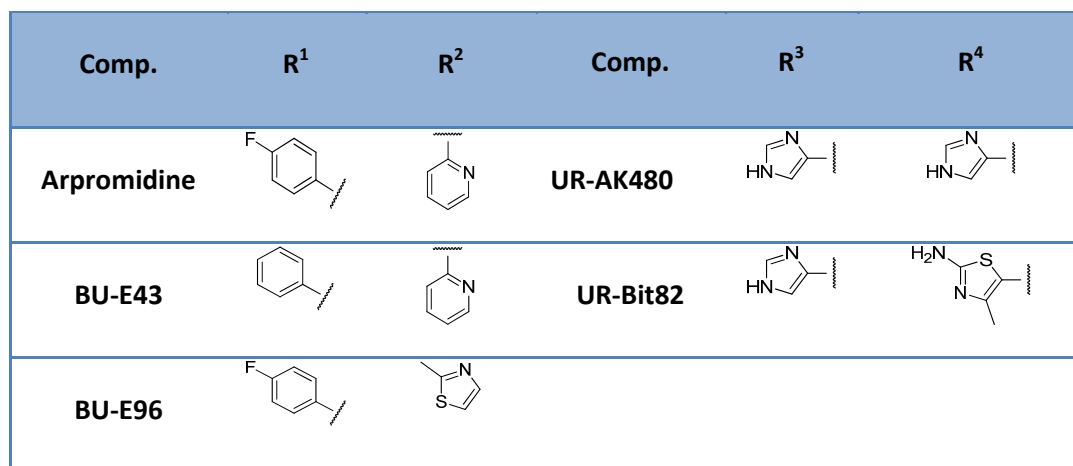
Scheme 5.9: H_2-receptor agonists and antagonists investigated in competition binding experiments

Table 5.7: K_i- values of reference H_2-agonists from competition binding experiments using **5.10a** as radioligand compared to reported data

Compound	K_i [nM][a]	K_i [nM][b]	EC_{50}[nM][c, d]
histamine	157.2 ± 32.1	264 ±96	990 ± 92 [d]
arpromidine	137.85 ± 51.25		72 ± 9 [c]
UR-Bit24	27.04 ± 3.94	39 ± 5	23.7 ± 8.0 [d]
BU-E43	374.93 ± 34.2		130 ± 13 [c]
BU-E96	78.1 ±10.89		310 ± 0.14 [c]
UR-AK480	6.49 ± 0.42	12 ± 3	6.3 ± 0.9 [d]
UR-Bit82	20.58 ±1.82	19 ± 8	7.4 ± 0.6 [d]

[a] Mean values ± S.E.M. of 2-3 independent experiments, performed in duplicate; [b] ref[23], [c] ref[9], [d] ref[24]

To explore the suitability of the radioactive tracer **5.10a** as a tool to characterize new histamine H_2-receptor ligands, known bivalent and monovalent agonists as well as fluorescent H₂R antagonists were investigated in binding assays. The determined K_i-values are comparable to binding and functional data from the literature[23] (see Table 5.7 and Table 5.8). Incubation periods of 3 h or 90 min gave K_i-values in the same range (Table 5.7). As shorter incubation periods are more convenient in laboratory praxis, 90 min were regarded sufficient to get reliable results. Determination of unspecific binding by addition of famotidine (50 µM) or ranitidine (50 µM) led to comparable results.
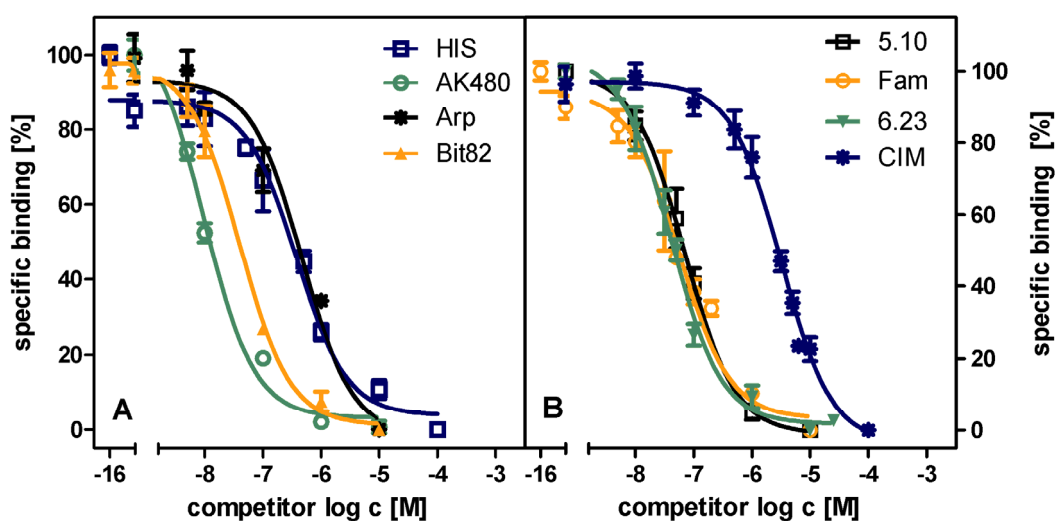
Scheme 5.10: Competition binding experiments with representative H$_2$R ligands (abbreviations: HIS: histamine, Arp: Arpromidine, Fam: famotidine, CIM: cimetidine), radioligand **5.10a**, c = 25 nM, analyzed by nonlinear regression and best fitted to a one-site competition model, 2-3 independent experiments performed in duplicate. **A**: agonists, **B**: antagonists

Table 5.8: K$_i$-values of H$_2$R antagonists from competition binding experiments using 5.10a as radioligand, compared to reported data[b,c] and GTPase data

	K$_i$ [nM][a] 1.5 h	K$_i$ [nM][a] 3 h	K$_i$ [nM] Lit. [b]	K$_{b'}$ [nM] [a] (GTPase)
5.10	29.5 ± 2.7		13.5 ± 1.2	37.7 ± 7.6
cimetidine	1551.2 ± 350.2	1376 ± 41		1700 ± 430[c]
famotidine	29.1 ± 0.5	36.49 ± 2.2	63 ± 5	48 ± 10 [c]
3.13	59.8 ± 0.5			14.5 ± 7.6
3.23	23.6 ± 2.3	22.8 ± 2.3		22.1 ± 1.8
6.2	1071.2± 383.9			1053.7 ± 228.6
6.11	152.7± 72.7			141.5 ± 58.9
6.13	329.3 ± 191.1			94.1 ±18.3
6.17	107.9± 37.4			183.4 ± 84.6

[a] Mean values ± S.E.M. of 2-3 independent experiments, performed in duplicate ; [b] ref[23], [c] ref[9]

5.4 Discussion

All potentidine-like ligands elicited high to moderate activity in the nanomolar range at the H_2R, no activity at the hH_1R and hH_4R, but moderate activity at the hH_3R. High H_3R affinity is known from structurally related ligands bearing a para-(piperidinylmethyl)phenoxy[25] moiety. Therefore, the low to moderate selectivity of the compounds described in this chapter for H_2R over H_3R (2-25-fold) is most probably inevitable due to the close structural similarities with the pharmacophore of the respective H_3R antagonists.

The propionylation of the primary amine related to guanidinothiazole-type H_2R antagonists such as tiotidine and famotidine resulted in substance **5.2**, which has only low affinity for the H_2R ($K_{b'}$> 5 µM) and no remarkable activity at the H_1, H_3 and H_4 receptor at concentrations below 10 µM. Regarding the presented guanidinothiazole the concept to use a "shortened" pharmacophoric moiety to create potent H_2R antagonists was unsuccessful. By acylation of the amino group in the piperidinomethylphenoxycyanoguanidine series with a fluorobenzoyl residue as in **5.4** and **5.5** the H_2R antagonistic activity was only retained in **5.4**. The $K_{b'}$-value was in the same low nanomolar range ($K_{b'}$ = 51 nM) as for APT ($K_{b'}$ = 180 nM)[9] and selectivity versus the H_3R was 10 to 20-fold. This may be interpreted as a hint that further substitutions at this position of the molecule is possible without a complete loss of activity. However, extending the spacer in the eastern part of the molecule from an ethylene to a hexamethylene group resulted in a drop of activity. This should be taken into account for further structural modifications. 4-Fluorobenzoylated ligands might be useful in creating new PET ligands, bearing [^{18}F] for imaging processes. For this purpose higher affinities are required, i. e. $K_{b'}$-values in the one-digit nanomolar range.

The squaramide-type compounds turned out to give the most potent propionylated H_2R antagonists with $K_{b'}$-values in the low nanomolar range (30 - 200 nM) depending on the spacer length and the investigated species (hH_2R/gpH_2R). Highest H_2R antagonistic activity resides in derivative **5.10** with a hexamethylene spacer. This compound was successfully synthesized as a tritiated radioligand (**5.10a**). Saturation binding analysis of the new radioactive tracer **5.10a** revealed high affinity and low unspecific binding to the human H_2R in a saturable manner. The corresponding scatchard plot indicated a single binding site. Binding constants of reference ligands determined by competition binding using **5.10a** were in good agreement with data from the literature. The analysis of the binding kinetics of **5.10a** showed slow association and dissociation. A similar behaviour has been discussed for several classes of H_2R antagonists, for instance, piperidinylmethylphenoxyalkyl substituted squaramides, thiadiazolamines or aminotriazoles [26-30].

Ligands bearing the piperidinomethylphenoxyalkyl moiety coupled to diaminocyclobutenedione such as BMY 25368[26] (Figure 5.2) are described as "insurmountable" (also named "unsurmountable") antagonists as the maximal response to the agonist is depressed in the presence of the antagonist. In this context the term "insurmountable antagonist" refers to experiments, for instance, on isolated organs, in which the receptor is preincubated with the antagonist before addition of agonist and measurement of a response. Ligands such as BMY 25368 show tight binding to the H_2R in the guinea pig right atrium (K_b = 13 nM), and are very difficult to remove from the active site by washing. They have a delayed onset of action, accompanied by a prolonged gastric acid antisecretory activity in the Heidenhain pouch dog (e.g. BMY25368) compared to standard ligands like famotidine. In the guinea pig atrium the basal rate is not affected and BMY 25368 binds to the same receptor population as ranitidine[26-27]. Therefore it was concluded that BMY 25368 does not produce true insurmountable antagonism[26]. This is confirmed by findings that BMY 25368 acts as competitive antagonist in the Heidenhain pouch dog. For BMY 25368 a slow dissociation was proposed as possible explanation for

Figure 5.2: Structure of BMY 25368

the apparent insurmountable antagonism[27]. Such particular binding properties at the guinea pig atria could also be confirmed (Prof. Dr. S. Elz, personal communication) for **5.6** and **5.7** substances structurally related to **5.10**, but bearing linkers consisting of only 2 or 3 instead of 6 methylene groups.

The phenomenon of insurmountable antagonism was subject of more detailed investigations[31], and a model was suggested to explain the mode of action of such ligands[32]. Surmountable antagonists produce a rightward shift of agonist concentration–response curves, whereas insurmountable antagonists additionally depress the maximal response. Surmountable antagonists have a competitive mode of action, combined with fast dissociation kinetics (Figure 5.3, adapted from[32]). Insurmountable antagonism can result from different mechanisms. Non-competitive binding via functional antagonism or an interaction with an allosteric binding site, distinct from the agonist binding site, is possible. Allosteric binding induces conformational changes and, therefore, the agonist does not bind any more or signal transduction is compromised. In case of long lasting competitive binding irreversible binding with a decline of the measured response is noted. Additionally, competitive binding can be mistaken as insurmountable due to a slow dissociation of the ligand from the receptor. Thus antagonist-receptor interactions are not in equilibrium when the response is measured (apparent insurmountability). The third approach uses the

"two inactive state competitive models", see chapter 1), proposing 2 inactive states of the receptor: **R** and **R'**. **R** binds the agonist with high affinity, **R'** has low affinity to the agonist, but high affinity to the respective antagonist. Here the slow conversion of R' to R, or the slow dissociation of antagonist receptor complex (BR'), are possible reasons for the observation of insurmountable antagonism.
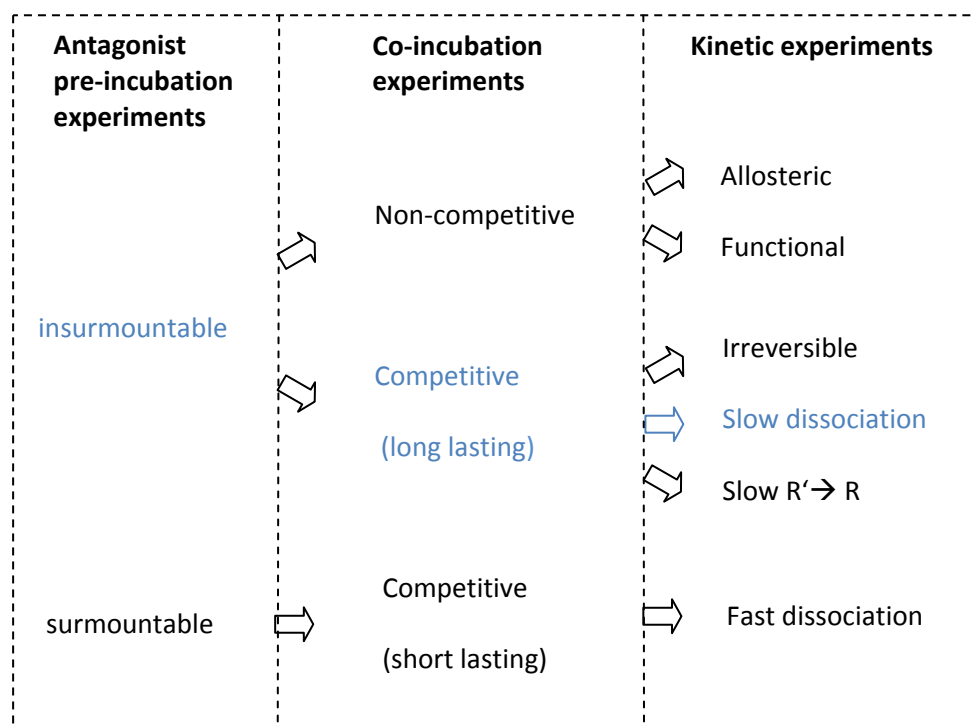
Figure 5.3: Schematic array of possible mechanisms responsible for insurmountable antagonism, adapted from Vauquelin et al., 2002[32]

The new radioligand **5.10a** is structurally related to the squareamide BMY 25368 and is also a slowly dissociating compound. Therefore we assume a similar binding mode for both substances at the receptor. An appropriate description for the binding behaviour might be "apparent insurmountable antagonism". This is compatible with the conception of slow dissociation responsible for insurmountable antagonism as depicted in Figure 5.3 (in blue). This kinetics may explain the discrepancies between data due to the different time windows of different assays, for instance, the lower activity of **5.10** in the functional Ca-assay (HEK cells) and the lower affinity determined by flow cytometry (HEK cells) compared to radioligand binding, respectively.

In general, competition binding assays should be performed at equilibrium. Incubation periods of at least 5 dissociation half-lives should be maintained[21]. In the case of radioligand **5.10a** incubation periods up to 5 or 10 hours (5x $T_{1/2}$) were considered inappropriate due to experimental practicability and the risk of instability of the receptor in the membrane preparations during

incubation. Regarding the association of **5.10** a time period of 90 min was sufficient to reach equilibrium (association) and to generate reliable data.

5.5 Summary

Potent and selective propionylated H_2R antagonists were obtained by derivatization of the amino groups of potentidine- and guanidinothiazole-like structures. The synthesized compounds possessed low to high activity at the histamine H_2-receptor, depending on their structural features. Neither activity at the hH_1R nor at the hH_4R was detected. The investigated cyanoguanidine **5.4** showed activities below 100 nM (GTPase assay) at the H_2R, i.e. in the range of APT and I-APT. Further variations in the eastern part of this molecule might lead to high affinity ligands suitable for PET imaging.

The aim to get a new radioligand, which can be used under standard laboratory conditions without special safety precautions, was achieved. Compound **5.10** is a potent H_2-receptor antagonist (hH_2R: $K_{b'}$ =38nM, GTPase assay) with 22-fold selectivity over the hH_3R. The determined K_D-value (29.94 nM) from kinetic experiments fitted well the dissociation equilibrium constant (26.82 nM) from saturation analysis. As the binding constants measured for reference ligands were in good agreement with data from literature, **5.10a** can be used as valuable tool to determine binding affinities of unlabelled ligands in competition binding experiments. The low costs, a facile preparation strategy and a high specific activity of 69 Ci/mmol present **5.10a** as an attractive alternative to the expensive [³H] tiotidine. Acting as a competitive, slowly dissociating H_2-antagonist **5.10a** might be a valuable tool supplementing and enlarging the knowledge achieved with the inverse agonist [³H] tiotidine[23, 33].

5.6   Experimental section

5.6.1   Chemistry

5.6.1.1   General conditions

See chapter 3

5.6.1.2   Amidation of primary amines with 4-fluorobenzoic acid and propionic acid derivatives

General procedure 1

The respective amine (1 eq) was dissolved in 2-3 ml of acetonitrile, methanol or methanol/DMSO (1/1) in a small flask. 2-3 drops Et_3N were added to avoid protonation of the amino group. 2,5-Dioxopyrrolidin-1-yl propionate (succinimidyl propionate, 0.7 -2 eq), dissolved in acetonitrile or methanol, was added and the solution stirred for 30 min to 18 h at rt. Subsequently, the reaction mixture was filtered through 0.2 µm filters, adjusted with MeCN/0.1 % TFA to a volume of 2-5 ml and purified by preparative HPLC (system 1). Acetonitrile was evaporated, and the products were lyophilised. The compounds were obtained as semi solid or as yellow oil and stored at -20 °C.

N-(2-{[2-(Diaminomethyleneamino)thiazol-4-yl]methylthio}ethyl)propionamide (5.2)

2-(5-((2-aminoethylthio)methyl)thiazol-2-yl)guanidine x 2HCl (**5.2a**) (47 mg, 154 mmol, 1.1 eq) and succinimidyl propionate (25 mg, 146 mmol, 1 eq) were dissolved in methanol under addition of Et_3N (31 mg, 308 µmol, 2 eq) to trap HCl and to prevent reprotonation of the amino group. The reaction mixture was used according to general procedure 1. Reaction time: 12 h. preparative HPLC (system 2-1, 220 nm). Lyophilisation afforded a semi white solid (11 mg, 17 %).

RP-HPLC (220 nm, gradient 1): 98 % (t_R=9.5 min, k=2.7); ^{1}H-NMR (600 MHz, methanol-d_4): δ (ppm) 1.11 (t, 3H, ^{3}J=7.6 Hz, -COCH$_2$**CH$_3$**), 2.18 (qua, 2H, ^{3}J=7.6 Hz, CO**CH$_2$**CH$_3$), 2.6 (m 2H, Hz, -SCH$_2$**CH$_2$**-NH-), 3.33 (m, 2H, -S**CH$_2$**CH$_2$-NH-), 3.78 (s, 2H, -**CH$_2$**S-), 7.05 (s, 1H, **C5-H**-thiazol); ^{13}C-NMR (150.95 MHz, methanol-d_4): δ (ppm) 10.45 (CO CH$_2$**CH$_3$**), 30.16 (CO**CH$_2$**CH$_3$), 31.66 (2C, -**C**H$_2$S**C**H$_2$CH$_2$-NH-), 39.77 (-CH$_2$S**CH$_2$**CH$_2$-NH-), 110.91 (**C5**-thiazol), 156.21 (q), 161.63 (q), 163.34

(q), 177.12 (-NH**C**OCH$_2$CH$_3$); <u>HRMS:</u> (FAB$^+$, glycerol): *m/z* calcd. for C$_{10}$H$_{18}$N$_5$OS$_2$ 288.0953 [MH$^+$], found: 288.0956; C$_{10}$H$_{17}$N$_5$OS$_2$ x C$_2$HF$_3$O$_2$ (401.4)

N-[2-(2-Cyano-3-{3-[3-(piperidin-1-ylmethyl)phenoxy]propyl}guanidino)ethyl]-4-fluorobenzamide (5.4)

Compound **3.5** (58.5 mg, 163 mmol, 1.9 eq) and 2,5-dioxopyrrolidin-1-yl 4-fluorobenzoate (20 mg, 84.4 µmol, 1 eq) were used as described in procedure 1 with acetonitrile as solvent. The solution was purified by preparative HPLC (system 2, 220 nm). After evaporation of acetonitrile and lyophilisation the product was obtained as white solid (13.25 mg, 27 %). <u>Mp:</u> 115 °C;

<u>RP-HPLC</u> (220 nm, gradient 1): 95.5 % (t$_R$=15.8 min, k=5.2). ¹H-NMR (600 MHz, methanol-d$_4$): δ (ppm) 1.64-1.82 (m, 6H, C**3,4,5-H** Pip), 2.05 (qui, 2H, ^{3}J=6.1 Hz, -OCH$_2$**CH$_2$**CH$_2$NH-), 2.9-3.2 (m, 4H, C2,6-H Pip), 3.42 (t, 4H, ^{3}J=5.9 Hz, CH$_2$ ethyl, -OCH$_2$CH$_2$**CH$_2$**NH-), 3.5 (t, 2H, ^{3}J=6.0 Hz, CH$_2$ ethyl), 4.09 (t, 2H, ^{3}J=5.8 Hz, -O**CH$_2$**CH$_2$CH$_2$NH-), 4.22 (s, 2H, Pip**CH$_2$**), 7.03-7.05 (m, 2H, C**4,6-H** phenoxy), 7.12 (s, 1H, **C2-H** phenoxy), 7.15 (t, 2H, ^{3}J=8.7 Hz, 4F-benz.), 7.36 (t, 1H, ^{3}J=7.9 Hz, **C5-H** phenoxy), 7.85 (m, 2H, 4 F-benz.) C2/6-H Pip not seen; ¹³C-NMR (150.95 MHz, methanol-d$_4$): δ (ppm) 22.74 (**C** Pip), 24.04 (2C, **C** Pip), about 30 (not detected in ¹³C-NMR, only in HSQC,-OCH$_2$CH$_2$CH$_2$NH-), 40.66 (2**C, C ethyl, C** OCH$_2$CH$_2$CH$_2$NH-), 42.36 (**C**-ethyl), 54.02 (2C, **C2,6**-Pip), 61.66 (Pip-**C**H$_2$), about 66 (not detected in ¹³C-NMR, only in HSQC,-O**CH$_2$**CH$_2$CH$_2$NH-), 116.33 (**C** F-benz.), 116.48 (**C** F-benz.), 117.28 (**C6** phenoxy), 118.54 (**C2** phenoxy), 119.22 (q), 121.16 (q), 124.48 (**C4** phenoxy), 130.92 (**C** F-benz.), 130.98 (**C** F-benz.), 131.41 (**C5** phenoxy), 131.81 (q), 160.74 (q) , 163.42 (q); <u>HRMS:</u> (EI) m/z calcd. for C$_{26}$H$_{33}$FN$_6$O$_2$ 480.2649 [M$^+$], found: 480.2635; C$_{26}$H$_{33}$FN$_6$O$_2$ x C$_2$HF$_3$O$_3$ (594.5)

N-[6-(2-Cyano-3-{3-[3-(piperidin-1-ylmethyl)phenoxy]propyl}guanidino)hexyl]-4-fluorobenzamide (5.5)

Compound **3.6** (62.6 mg, 151 mmol, 1.8 eq) and 2,5-dioxopyrrolidin-1-yl 4-fluorobenzoate (20 mg, 84.4 µmol, 1 eq) were used as described in procedure 1 with acetonitrile as solvent. The solution was purified by preparative HPLC (system 2, 220 nm). After evaporation of acetonitrile and lyophilisation the product was obtained as semi white solid (13.25 mg, 27 %). <u>Mp:</u> 117 °C;

RP-HPLC (220 nm, gradient 1): 99.5 % (t_R = 16.9 min, k=5.7); ^{1}H-NMR (600 MHz, methanol-d$_4$): δ (ppm) 1.37-1.83 (m, 12H, 2x CH$_2$ Pip, 4x CH$_2$ hexyl), 2.01-2.05 (m, 2H, -OCH$_2$**CH$_2$**CH$_2$NH-), 2.9-3.2 (m, 4H, C2,6-H Pip), 3.17-3.19 (4H, CH$_2$ –NH**CH$_2$**(CH$_2$)$_4$CH$_2$NHCO-, -OCH$_2$CH$_2$**CH$_2$**NH-), 3.33- 3.37 (m, 2H, –NH**CH$_2$**(CH$_2$)$_4$**CH$_2$**NHCO-,), 3.41 (t, 2H, ^{3}J= 6.5 Hz, -OCH$_2$CH$_2$**CH$_2$**NH-), 4.09 (t, 2H, ^{3}J=5.7 Hz, -O**CH$_2$**CH$_2$CH$_2$NH-), 4.22 (s, 2H, Pip**CH$_2$**), 7.03- 7.06 (m, 2H, **C4,6-H** phenoxy), 7.13 (s, 1H, **C2-H** phenoxy), 7.16 (t, 2H, ^{3}J=8.7 Hz, 4F-benz.), 7.36 (t, 1H, ^{3}J=7.9 Hz, **C5-H** Ph), 7.85 (m, 2H, 4 F-benz.), C2/6-H Pip not seen; ^{13}C-NMR (150.95 MHz, methanol-d$_4$): δ (ppm) 22.74 (**C** Pip), 24.05 (2C, **C** Pip), 27.41 (**C** hexyl), 27.68 (**C** hexyl), 30.39 (-OCH$_2$CH$_2$CH$_2$NH-, **2C** hexyl, low signal), about 40 (not detected in ^{13}C-NMR, only in HSQC, -OCH$_2$**CH$_2$**CH$_2$NH-), 44.83 (**C** hexyl), 45.45 (**C** hexyl), 54.02 (2C, **C2,6**-Pip), 61.67 (Pip-**CH$_2$**), about 66 (not detected in ^{13}C-NMR, only in HSQC,- O**CH$_2$**CH$_2$CH$_2$NH-), 116.28 (**1C** F-benz.), 116.43 (**1C** F-benz.), 117.28 (**C6** phenoxy), 119.22 (**C2** Ph), 121.16 (q), 124.50 (**C4** Ph), 130.78 (**C** F-benz.), 130.84 (**C** F-benz.), 131.43 (**C5** Ph), 131.83 (q), 160.74, 163.43 (q, C1 Ph) not all q C detected; HRMS: (EI) m/z calcd. for C$_{30}$H$_{41}$FN$_6$O$_2$ 536.3275 [M$^+$], found: 536.3265; C$_{30}$H$_{41}$FN$_6$O$_2$x C$_2$HF$_3$O$_3$ (650.7)

N-[2-(3,4-Dioxo-2-{3-[3-(piperidin-1-ylmethyl)phenoxy]propylamino}cyclobut-1-enylamino)ethyl]propionamide (5.6)

Compound **3.9** (33.2 mg, 86 μmol, 1 eq) and succinimidyl propionate (16 mg, 94 μmol, 1.1 eq), in acetonitrile, were prepared according to general procedure 1. Reaction time: 30 min; Prepara-tive HPLC (system 1, 220 nm). Acetonitrile was removed under reduced pressure. Lyophilisation afforded 11.87 mg of yellow oil (25 %).

RP-HPLC (210 nm, gradient 1): 98 % (t_R=10.9 min, k= 3.3); ^{1}H-NMR (600 MHz, methanol-d$_4$): δ (ppm) 1.07 (t, 3H, ^{3}J=7.6 Hz, -COCH$_2$**CH$_3$**), 1.78-1.93 (m, 6H, **C3/5-H** Pip), 2.09-2.11 (m, 2H, -OCH$_2$**CH$_2$**CH$_2$NH-), 2.17 (m, 2H,-CO**CH$_2$**CH$_3$), 2.94 (m, 2H, **C2/6-H** Pip), 3.36 (m, 2H, -NH**CH$_2$**CH$_2$NHCO-), 3.42 (m, 2H, **C2/6-H** Pip), 3.64 (m, 2H, -NH**CH$_2$**CH$_2$NHCO-), 3.82 (m, 2H, -OCH$_2$CH$_2$**CH$_2$**NH-), 4.14 (t, 2H, ^{3}J=5.8 Hz, -O**CH$_2$**CH$_2$CH$_2$NH-), 4.22 (s, 2H, Pip**CH$_2$**) 7.01-7.06 (m, 3H, **C2,3,4-H** phenoxy), 7.36 (t, 1H, ^{3}J=7.9 Hz, **C5-H** phenoxy); ^{13}C-NMR (150.95 MHz, methanol-d$_4$): δ (ppm) 10.33 (-COCH$_2$**CH$_3$**), 22.74 (**C** Pip), 24.11 (2C, **C** Pip), 30.16 (-CO**C**H$_2$CH$_3$), 31.61 (-OCH$_2$**C**H$_2$CH$_2$NH-), 41.46 (-NH**C**H$_2$CH$_2$NH-), 42.5 (-OCH$_2$CH$_2$**C**H$_2$NH-), 49.58 (-NHCH$_2$**C**H$_2$NH-), 54.11 (2C, **C2,6**-Pip), 61.11 (Pip-**CH$_2$**), 66.36 (-O**C**H$_2$CH$_2$CH$_2$NH-), 117.09 (**C6** phenoxy), 118.50 (**C2** phenoxy), 124.45 (**C4** phenoxy), 131.41 (**C5** phenoxy), 131.73 (q), 160.77 (q, **C1** phenoxy), 5q C

not detected; <u>HRMS:</u> (EI) m/z calcd. for $C_{24}H_{35}N_4O_4$ 442.2580 [MH$^+$], found: 442.25843; $C_{24}H_{34}N_4O_4$ x $C_2HF_3O_2$ (556.3)

N-[3-(3,4-Dioxo-2-{3-[3-(piperidin-1-ylmethyl)phenoxy]propylamino}cyclobut-1-enylamino)propyl]propionamide (5.7)

Compound **5.3** was prepared from **3.10** (35 mg, 87 µmol, 1 eq) and succinimidyl propionate (12 mg, 70 µmol, 0.8 eq) in DMSO (general procedure 1). The solution was stirred for 45 min at rt and stopped by addition of 250 µl 10 % TFA in acetonitrile. Purification was done by preparative HPLC (system 1, 220 nm). Acetonitrile was removed under reduced pressure and the product was freeze dried resulting in 22 mg of the product (yellow oil 55 %).

<u>RP-HPLC</u> (210 nm, gradient 1): 99 % (t$_R$=11.6 min, k=3.6); <u>^{1}H-NMR (300 MHz, methanol-d$_4$):</u> δ (ppm) 1.12 (t, 3H, ^{3}J=7.6 Hz, -COCH$_2$**CH$_3$**)**,** 1.49-1.97 (m, 8H, C**3,4,5-H** Pip/**CH$_2$** propyl), 2.1 (qui, 2H, ^{3}J=6.2 Hz -OCH$_2$**CH$_2$**CH$_2$NH-), 2.12 (qua, 2H, ^{3}J=7.6 Hz,-CO**CH$_2$**CH$_3$), 2.89-2.94 (m, 2H, C2/6-H Pip), 3.23 (t, 2H, ^{3}J=7.6 Hz, propyl), 3.42-3.46 (m, 2H, C2/6-H Pip), 3.58-3.61 (m, 2H, propyl), 3.82-3.85 (m, 2H, -OCH$_2$CH$_2$**CH$_2$**NH-), 4.14 (t, 2H, ^{3}J=5.8 Hz, -O**CH$_2$**CH$_2$CH$_2$NH-), 4.23 (s, 2H, Pip**CH$_2$**), 7.02-7.04 (m, 3H**, C2,4,6-H** phenoxy), 7.36 (m, 1H, **C5-H** phenoxy); <u>^{13}C-NMR (150.95 MHz, methanol-d$_4$):</u> δ (ppm) 10.52 (-COCH$_2$**CH$_3$**)**,** 22.76 (**C** Pip), 24.15 (2C, **C** Pip), 30.26 (-CO**CH$_2$**CH$_3$), 31.60 (-OCH$_2$**CH$_2$**CH$_2$NH-), 32.05 (C propyl), 37.07 (C propyl), 42.56 (-OCH$_2$CH$_2$**CH$_2$**NH-) (C propyl, not seen (solvent), 54.14 (2C, **C2,6**-Pip), 61.75 (Pip-**C**H$_2$), 66.34 (-O**CH$_2$**CH$_2$CH$_2$NH-), 117.11 (**C6** phenoxy), 118.49 (**C2** phenoxy), 120.94 (**C4** phenoxy), 124.50, 131.46 (**C5** phenoxy), 131.73 (q), 160.77 (q, **C1** phenoxy), 177.30 (**CO**CH$_2$CH$_3$), 4q C cyclobutenyl not visible in the spectrum; <u>HRMS:</u> (EI) m/z calcd. for $C_{25}H_{37}N_4O_4$ 456.2737 [MH$^+$], found: 456.2749; $C_{25}H_{36}N_4O_4$ x $C_2HF_3O_2$ (570.3)

N-[4-(3,4-Dioxo-2-{3-[3-(piperidin-1-ylmethyl)phenoxy]propylamino}cyclobut-1-enylamino]butyl)propionamide (5.8)

Compound **3.11** (29.7 mg, 72 µmol, 1 eq) and succinimidyl propionate (20 mg, 116 µmol, 1.6 eq) in DMSO were prepared according to general procedure 1. The solution was stirred for 45 min at rt. and stopped by addition of 250 µl 10 % TFA in acetonitrile. Preparative HPLC: system 1, 220 nm. Acetonitrile was removed under reduced pressure. After lyophilisation the product was obtained as yellow oil (28 mg, 69 %).

RP-HPLC (210 nm, gradient 1): 99.1 % (t_R=11.5 min, k=3.5); ^{1}H-NMR (600 MHz, methanol-d$_4$): δ (ppm) 1.1 (t, 3H, ^{3}J=7.7 Hz, -COCH$_2$**CH$_3$**); 1.52-1.61 (m, 4H, 2x **CH$_2$** butyl); 1.71-1.95(m, 6H, **C3,4,5**-H Pip), 2.07-2.11 (m, 2H, -OCH$_2$**CH$_2$**CH$_2$NH-), 2.17 (q, 2H, ^{3}J=7.7 Hz, -CO**CH$_2$**CH$_3$), 2.94 (m,2H, C2/6-H Pip), 3.18 (t, 2H, ^{3}J=6.8 Hz, -NHCH$_2$(CH$_2$)$_2$**CH$_2$**NHCO-), 3.43-3.45 (m, 2H, **C2/6-H** Pip), 3.6-3.61 (m, 2H, -NH**CH$_2$**(CH$_2$)$_2$CH$_2$NHCO-), 3.83 (m, 2H, -OCH$_2$**CH$_2$**NH-), 4.13 (t, 2H, ^{3}J=5.8 Hz, -O**CH$_2$**CH$_2$CH$_2$NH-), 4.22 (s, 2H, Pip**CH$_2$**) 7.02- 7.03 (m, 3H, **C4,2,6-H** phenoxy), 7.36 (t, 1H, ^{3}J=8.0 Hz, **C5-H** phenoxy); ^{13}C-NMR (150.95 MHz, methanol-d$_4$): δ (ppm) 10.57 (-COCH$_2$CH$_3$), 22.73 (**C** Pip), 24.13 (2C, **C** Pip), 27.36 (**C** butyl), 29.63 + 30.24 (**C** butyl, -COCH$_2$CH$_3$), 31.58 (-OCH$_2$CH$_2$CH$_2$NH-), 39.78 (**C** butyl), 42.55 (-OCH$_2$CH$_2$CH$_2$NH-), 44.89 (**C** butyl), 54.14 (2C, **C2/6**-Pip), 61.74 (Pip-**C**H$_2$), 66.34 (-O**C**H$_2$CH$_2$CH$_2$NH-), 117.07 (**C6** phenoxy), 118.5 (**C2** phenoxy), ,124.48 (q, **C4** phenoxy), 131.45 (**C5** phenoxy), 131.69 (q), 160.74 (q, **C1** phenoxy), 169.55 (q, cyclobutenyl), 177.10 (q, **C**OCH$_2$CH$_3$), 183.57 (q, **C**O cyclobutenyl); HRMS: (EI) m/z calcd. for C$_{26}$H$_{39}$N$_4$O$_4$ 470.2893 [MH$^+$], found: 470.2891; C$_{26}$H$_{38}$N$_4$O$_4$ x C$_2$HF$_3$O$_2$ (584.6)

N-[5-(3,4-Dioxo-2-{3-[3-(piperidin-1-ylmethyl)phenoxy]propylamino}cyclobut-1-enylamino)pentyl]propionamide (5.9)

Compound **3.12** (33 mg, 77 µmol, 1 eq) and succinimidyl propionate (9.7 mg, 57 µmol, 0.7 eq), in MeOH/DMSO (1/1) were prepared according to general procedure 1. The solution was stirred for 30 min at rt. and stopped by addition of 250 µl 10 % TFA in acetonitrile. Preparative HPLC gradient: system 1, 220 nm. Acetonitrile was evaporated under reduced pressure. Lyophilisation afforded the product as yellow oil (20.67 mg, 61 %).

RP-HPLC (210 nm, gradient 1): 99.5 % (t_R=12.0 min, k=3.7); ^{1}H-NMR (600 MHz, methanol-d$_4$): δ (ppm) 1.1 (t, 3H, ^{3}J=7.6 Hz, -COCH$_2$**CH$_3$**), 1.34-1.39 (m, 2H, **CH$_2$**-pentyl), 1.49-1.60 (m, 4H, **CH$_2$**-pentyl); 1.72-1.95 (m, 6H, **C3,4,5-H** Pip), 2.07-2.11 (m, 2H, -OCH$_2$**CH$_2$**CH$_2$NH-), 2.17 (q, 2H, ^{3}J=7.6 Hz, -CO**CH$_2$**CH$_3$), 2.94 (m, 2H, **C2/6-H** Pip), 3.15 (t, 2H, ^{3}J=7.1 Hz, -NHCH$_2$(CH$_2$)$_3$**CH$_2$**NHCO-), 3.43-3.45 (m, 2H, **C2/6-H** Pip), 3.57 (m, 2H, NH**CH$_2$**(CH$_2$)$_3$CH$_2$NHCO-), 3.83 (m, 2H, -OCH$_2$**CH$_2$**NH-), 4.13 (t, 2H, ^{3}J=5.8 Hz, -O**CH$_2$**CH$_2$CH$_2$NH-), 4.22 (s, 2H, Pip**CH$_2$**) 7.02- 7.03 (m, 3H, **C2,4,6-H** phenoxy), 7.40 (t, 1H, ^{3}J=7.6 Hz, **C5-H** phenoxy); ^{13}C-NMR (150.95 MHz, methanol-d$_4$): δ (ppm) 10.60 (-COCH$_2$**C**H$_3$), 22.72 (**C** Pip), 24.13 (2C, **C** Pip), 24.64 (**C** pentyl), 29.99 + 30.24 (**C** pentyl, -COCH$_2$CH$_3$), 31.57 +31.85 (-OCH$_2$CH$_2$CH$_2$NH-, **C** Pentyl), 40.09 (**C** pentyl), 42.54 (-OHCH$_2$CH$_2$CH$_2$NH-), 45.14 (**C** pentyl), 54.14 (2C, **C2,6**-Pip), 61.74 (Pip-**C**H$_2$), 66.34 (-O-

O$CH_2CH_2CH_2NH$-), 117.05 (**C6** phenoxy), 118.53, (**C2** phenoxy), 124.48 (**C4** phenoxy), 131.45 (**C5** phenoxy), 131.68 (q), 160.73 (q, **C1** phenoxy), 169.73 (q), 177.05 (q, **C**OCH_2CH_3), 183.55 (q, **C**O cyclobutenyl); <u>HRMS:</u> (EI) m/z calcd. for $C_{27}H_{40}N_4O_4$ 484.3050 [M$^+$], found: 484.305; $C_{27}H_{40}N_4O_4$ x $C_2HF_3O_2$ (598.3)

N-[6-(3,4-Dioxo-2-{3-[3-(piperidin-1-ylmethyl)phenoxy]propylamino}cyclobut-1-enylamino)hexyl]propionamide (5.10)

Compound **3.13** (19.5 mg, 44 µmol, 1 eq) and succinimidyl propionate (13 mg, 94 µmol, 1.7 eq) in MeOH/DMSO (1/1) were prepared according to general procedure 1. Reaction time: 3 h, preparative HPLC (system 1, 220 nm). Lyophilisation afforded 14.69 mg of yellow oil (54 %).

<u>RP-HPLC</u> (210 nm, gradient 1): 98 % (t_R=13.1 min, k=4.2); <u>^{1}H-NMR (600 MHz, methanol-d$_4$):</u> δ (ppm) 1.0 (t, 3H, ^{3}J=7.7 Hz, -COCH_2**CH$_3$**); 1.33-1.38 (m, 4H, **CH$_2$** hexyl), 1.47-1.51 (m, 2H, **CH$_2$** hexyl); 1.58-1.60 (m, 2H, **CH$_2$** hexyl), 1.75-1.93 (m, 6H, **C3,4,5-H** Pip), 2.09 (qui, 2H, ^{3}J=6.2 Hz, -OCH_2**CH$_2$**CH_2NH-), 2.17 (qua, 2H, ^{3}J=7.6 Hz, -CO**CH$_2$**CH_3), 2.89-2.94 (m, 2H, **C2/6-H** Pip), 3.14 (t, 2H, ^{3}J=7.1 Hz, -NHCH_2(CH$_2$)$_4$**CH$_2$**NHCO-), 3.43-3.44 (m, 2H, **C2/6-H** Pip), 3.56-3.61 (m, 2H, -NH**CH$_2$**(CH$_2$)$_4$CH$_2$NHCO-), 3.83 (m, 2H, -OCH_2CH_2**CH$_2$**NH-), 4.2 (t, 2H, ^{3}J=5.8 Hz, -O**CH$_2$**CH_2CH_2NH-), 4.20 (s, 2H, Pip**CH$_2$**) 7.02- 7.04 (m, 3H, **C2,4,6-H** phenoxy), 7.36 (t, 1H, ^{3}J=7.69 Hz, **C5-H** phenoxy); <u>^{13}C-NMR (150.95 MHz, methanol-d$_4$):</u> δ (ppm) 10.61 (-COCH_2**CH$_3$**), 22.73 (**C** Pip), 24.12 (2C, **C** Pip), 26.94 (C hexyl), 27.39 (C hexyl), 30.24+30.29 (C hexyl, -COCH_2CH_3), 31.57 (-O$CH_2CH_2CH_2NH$-), 32.12 (C hexyl), 40.15 (C hexyl), 42.52 (-O$CH_2CH_2CH_2NH$-), 45.11 (C hexyl), 54.13 (2C, **C2,6**-Pip), 61.74 (Pip-**C**H$_2$), 66.33 (-O$CH_2CH_2CH_2NH$-), 117.08 (**C6** phenoxy), 118.51, (**C2** phenoxy), 124.47 (**C4** phenoxy), 131.50 (**C5** phenoxy), 131.68 (q), 160.74 (q, **C1** phenoxy), 169.59 (q, C cyclobutenyl), 177.04 (q, -**C**OCH_2CH_3), 183.53 (**C**O cyclobutenyl), <u>HRMS:</u> (EI) m/z calcd. for $C_{28}H_{43}N_4O_4$ 498.3206 [MH$^+$], found: 498.3204; $C_{28}H_{42}N_4O_4$ x $C_2HF_3O_2$ (612.7)

N-[4-(3,4-dioxo-2-{3-[3-(piperidin-1-ylmethyl)phenoxy]propylamino}cyclobut-1-enylamino)butyl]-4-fluorobenzamide (5.11)

Compound **3.11** (14.17 mg, 34 µmol, 0.9 eq), in 2 ml DMF, and 2,5-dioxopyrrolidin-1-yl-4-fluorobenzoate (9 mg, 38 µmol, 1.7 eq), in 1 ml acetonitrile, were stirred at rt for 1 h. The solvent was evaporated and the residue was dissolved in MeCN/0.1 % TFA = 30/70. This solution was purified by preparative HPLC (system 1, 220 nm). The organic solvent (A) was evaporated at reduced pressure. Lyophilisation gave 14.69 mg of the product as yellow oil (54 %).

RP-HPLC (210 nm, gradient 1): 99 % (t_R=14.1 min, k=4.6); ^{1}H-NMR (600 MHz, methanol-d$_4$): δ (ppm) 1.5-1.51 (m, 1H, C-H Pip), 1.67 (m, 4H, -NHCH$_2$**(CH$_2$)$_2$**CH$_2$NHCO-), 1.73-1.95 (m, 5H, **C3,4,5-H** Pip), 2.08 (qui, 2H, ^{3}J=6.2 Hz, -OCH$_2$**CH$_2$**CH$_2$NH-), 2.93 (m, 2H, **C2/6-H** Pip), 3.39-3.944 (m, 4H, **C2/6-H** Pip, -NHCH$_2$(CH$_2$)$_2$**CH$_2$**NHCO-), 3.61 (m, 2H, NH**CH$_2$**(CH$_2$)$_2$CH$_2$NHCO-), 3.82 (m, 2H, -OCH$_2$CH$_2$**CH$_2$**NH-), 4.12 (t, 2H, ^{3}J=5.8 Hz, -O**CH$_2$**CH$_2$CH$_2$NH-), 4.21 (s, 2H, Pip**CH$_2$**), 7.00-7.03 (m, 3H, **C2,4,6-H** phenoxy), 7.16 (t, 2H, ^{3}J=8.8 Hz, **C-H** F-benz.), 7.35 (t, 1H, ^{3}J=8.1 Hz, **C5-H** phenoxy), 7.85 (m, 2H, **C-H** F-benz.); ^{13}C-NMR (150.95 MHz, methanol-d$_4$): δ (ppm) 22.71 (**C** Pip), 24.12 (2C, **C** Pip), 27.40 (**C-**butyl), 29.71 (**C-**butyl), 31.56 (-OCH$_2$**CH$_2$**CH$_2$NH-), 40.43 (**C-**butyl), 42.56 (-OCH$_2$CH$_2$**CH$_2$**NH-), 44.91 (**C-**butyl), 54.14 (2C, **C2,6**-Pip), 61.74 (Pip-**CH$_2$**), 66.36 (-O**CH$_2$**CH$_2$CH$_2$NH-), 115.79 + 116.3 (**C** F-benz.), 116.45 (**C6** phenoxy), 118.52 (**C2** phenoxy), 124.46 (**C4** phenoxy), 130.76 + 130.85 (**C** F-benz.), 131.44 (**C5** phenoxy), 131.67 (q), 160.73 (q, **C1** phenoxy), 169.09 (q, **C**-cyclobutenyl), 183.56 (q, **CO**-cyclobutenyl), 2q C not detected; HRMS: (EI) m/z calcd. for $C_{28}H_{42}N_4O_4$ 536.2799 [MH$^+$], found: 536.2782 $C_{30}H_{37}FN_4O_4$ x $C_2HF_3O_2$ (650.7)

5.6.1.3   *Preparation of the radioligand 5.10a ([^{3}H]UR-De257)*

General conditions

Chemicals and solvents were purchased from Merck KGaA (Darmstadt, Germany) and Sigma Aldrich GmbH (Munich, Germany) and used without further purification unless otherwise stated. The N-succinimidyl [2, 3-^{3}H$_2$] propionate solution in ethyl acetate/ hexane (9/1, v/v., 83 Ci/mmol, 2 mCi/ml) was from Hartmann Analytik GmbH (Braunschweig, Germany) and the Scintillation cocktail from Carl Roth GmbH (Rotiscint eco plus, Karlsruhe, Germany). The tritiated compound was analyzed and purified with a RP column (Synergi Hydro-RP 250 xl 4.6mm, 4µm, Phenomenex, Aschaffenburg, Germany, flow rate 0.8ml/min) on a HPLC System from Waters (Waters GmbH, Eschborn, Germany). It was equipped with a Waters pump control module (Waters 510 HPLC pump), Waters 486 UV/VIS detector and a Packard radiomatic Flo-one beta series A500 radiodetector (liquid scintillator: Rotiscint eco plus, flow rate: 4 ml/min). For analytical analysis and purification MeCN/TFA 0.05 % (v/v) and H$_2$O/ TFA 0.5% (v/v) was used as mobile phase. The substances were detected at 290 nm or radioactivity was measured by scintillation counting with the radiomatic.

5.6.1.4 Preparation of 5.10a ([^{3}H]UR-De257)

A solution of N-succinimidyl [2, 3-^{3}H$_2$] propionate in ethyl acetate/ hexane (9/1, v/v, 750 µl, 18.05 nmol, 1 eq, 3.09µg, 1.5mCi) was added to a solution of **3.13** (0.722 µmol, 20 eq, 320 µg) in 40µl DMSO/ MeCN = 1/1 (v/v) and the solvent was evaporated by a rotary evaporator. This procedure was repeated. The residue was taken up in 40 µl acetonitrile and the solution was stirred overnight (18 h) at rt. To the reaction mixture MeCN and 0.05 % TFA were added to give 760 µl of a solution containing 5.26 % DMSO and 20 % MeCN in 0.05 % TFA. Aliquots (4x 190 µl) were purified by HPLC collecting the radioligand at approximately 20-21 min (gradient: 0.05 % TFA in MeCN/ 0.05 % TFA in H$_2$0: 0 min: 20/80 (v/v), 37 min: 30/70 (v/v), 38 min 90/10 (v/v), 48 min 90/10 (v/v)). λ=290 nm, 0.8 ml/min. The solvent of the combined fractions was evaporated under reduced pressure, the product dissolved in 500 µl Ethanol and transferred to an Amersham glass vial.

A seven point calibration curve (c: 0.1, 0.3, 0.5, 1.0, 2.5, 5.0 10.0 µM; inj. Vol.: 200 µl) with the unlabelled ligand 8.10 was recorded at λ=290 nm (eluent: 0.05 % TFA in MeCN/ 0.05 % TFA in H$_2$0: 0 min: 20/80 (v/v), 3 7min: 30/70 (v/v), 38 min 90/10 (v/v), 48min 90/10 (v/v)). The standard solutions were freshly prepared from a 1 mM solution of 8.10 in MeCN/ 0.05 % TFA: 20/80 (v/v), containing 20 % DMSO for solubility, or from a 100 µM dilution (solvent: MeCN/ 0.05 % TFA: 20/80 (v/v). 2.5 µl of the radioligand were added to 297.5 µl MeCN/ 0.05 % TFA: 20/80 (v/v) and 200 µl of this solution were analyzed by HPLC. Subsequent the concentration of the radioligand (6.6) was calculated from the peak area (24.47 µM, 11.92 nmol, yield: 33 %). A HPLC purity control (gradient see calibration curve) showed a radiochemical purity of 92.3 %. For the determination of specific activity 1.5 µl of the stock solution were added to 448.5 µl of MeCN/TFA 0.05 % 20/80 (v/v). 9 µl of this dilution (two times in duplicate) were counted in 3 ml of a scintillation cocktail. In a third measurement 2.5 µl of the stock solution were diluted in 297.5 µl MeCN/TFA 0.05 % 20/80 (v/v). Finally 4.5 µl of this dilution were counted (in duplicate) in 3 ml scintillation cocktail. These three measurements resulted in a specific activity of 69.33 Ci/mmol (2.5676T Bq/mmol). The activity concentration of the stock solution was adjusted to 1mCi/ml (62.83 MBq/ml) by addition of 338.95 µl ethanol (14.4 3µM).The radioligand was stored at -20 °C.

5.6.2   Pharmacological methods

General

Chemicals and solvents (analytical grade) were from commercial suppliers unless otherwise noted (Merck KGaA (Darmstadt, Germany), Sigma Aldrich GmbH (Munich, Germany). The used histamine dihydrochloride was from Alfa Aesar GmbH & Co. KG (Karlsruhe, Germany), cimetidine, ranitidine and famotidine from Sigma Aldrich GmbH, GF/C filters were purchased from Whatman (Maidstone, UK). The tested substances AK 480, Bit28 and Bit82 were provided by Dr. A. Kraus and T. Birnkammer. Arpromidin, BUE43 and BUE96 were available in our laboratories. Radioactivity was measured by scintillation counting on a Beckmann LS-6500 device with a scintillation cocktail from Carl Roth GmbH (Rotiszint eco plus, Karlsruhe, Germany). Experimental data was analyzed with Sigma Plot 11.0 (Systat Software GmbH, San José, California, USA) and GraphPad Prism 4.02 software (San Diego, CA, USA). Presented K_i- and $K_{b'}$-values were calculated according to the Cheng Prussoff equation[34]. In each experiment specific binding was the difference between total and nonspecific binding.

5.6.2.1   Steady state GTPase assay

Assays were performed as described in Chapter 3 (Pharmacological methods).

5.6.2.2   Histamine H_2R assay at the guinea pig atrium

Experiments were performed as described in Chapter 3 (Pharmacological methods).

5.6.2.3   Fluorimetric Ca^{2+} assay on U-373 MG cells

Experiments were performed as depicted in chapter3.

5.6.2.4   Radioligand binding assay on HEK293-FLAG-hH$_3$R-His$_6$ cells

Determination of K_i-values was done as described in chapter 3

5.6.2.5   Determination of ligand affinity on HEK293-hH$_2$R-qs5-HA cells by flow cytometry

Competition binding experiments with **5.10** using **6.23** as standard fluorescent ligand (c: 200 nM) were done as described in chapter 3.

5.6.2.6   The fura-2 assay with HEK293-hH$_2$R-qs5-HA cells

General

Used chemicals and solvents were from commercial suppliers as described in chapter 3.

The Fura-2 assay

Cell culture, preparation of HEK293-hH$_2$R-qs$_5$-HA cells for the assay, loading of the cells with fura-2/AM and investigations of H$_2$R ligands on the GENios Pro^{TM} (Tecan Salzburg, Austria) plate reader were done as described previously[20]. In brief: 89 µl of the fura-2/AM loaded cells (1 million cells /ml) were added to the cavities of a 384-well plate. After addition of one microliter of 100-fold concentrated feed solutions (in DMSO) of the ligands of interest, the plate was incubated for 15 min under light protection at rt. Kinetics was measured at an excitation wavelength of 340 nm and 380 nm before and after eliciting of calcium transients with 10 µl of histamine in PBS (10 µM, final c.). Emission was measured at 510 nm. The blank value was measured with the solvent instead of the ligand. A 50 – and 100 % suppression of the Ca signal as control was performed using famotidine in concentrations of 500 nM and 50 µM (final c.). Investigations were performed with 120 measurement cycles. Data analysis was done according to the procedure described previously[20] and the plots were created with the multiple scatter error bars option in SigmaPlot® 9.0 (curve fitting: standard curves, four parameter logistic function). As EC$_{50}$ value for HIS, used in the Cheng Prusoff equation, 1.4 µM were assumed.

5.6.2.7   5.10a ([^{3}H] De257) binding assay

Radioligand binding experiments were performed in analogy to described methods[16, 5]. They were conducted with Sf9 insect cell membranes expressing the hH$_2$R-G$_{s\alpha S}$ fusion protein. Membranes were thawed and centrifuged for 10 min at 4 °C and 13,000 rpm before suspension in binding buffer (12.5 mM MgCl$_2$, 1mM EDTA and 75 mM Tris/HCl, pH 7.4). Each tube contained 150 µl binding buffer, 25 µl BSA 2% (m/v), and 25 µl of the radioligand in the respective concentrations, dissolved in binding buffer. Additionally the tubes for total binding contained 25 µl H$_2$O (millipore), whereas the tubes for unspecific binding contained 25 µl of a 1 mM or 500 µM solution of famotidine in H$_2$O (millipore). Experiments were started by addition of 25 µl membrane suspension to each tube (total volume in reaction tube: 250 µl, final concentration: 50 -100 µg protein (hH$_2$R-G$_{s\alpha S}$).The radioligand was diluted with unlabelled ligand due to economic reasons.

In saturation experiments 4/5 of 5.10 + 1/5 of 5.10a and 3/5 of 5.10 + 2/5 of 5.10a in competition binding experiments were employed.

Saturation binding experiments were conducted with radioligand concentrations (final conc.) between 0.75 nM and 200 nM, whereas competition binding experiments were performed with 25 nM radioligand (final conc.) and increasing concentrations of the unlabelled ligands. Unspecific binding was determined for both kinds of experiments with 50 or 100 µM famotidine. Incubations were done for 90 min at 22 °C and shaking at 250 rpm (saturation and competition). Then bound radioligand was separated from free radioligand by filtration through GF/C filters followed by three washing steps with 2 ml of binding buffer (4 °C) using a Brandel Harvester. GF/C filters were pretreated with 0.3 % (m/v) polyethyleneimine to reduce binding of free radioligand to the filter material. After an equilibration period of 12 h filter bound radioactivity was measured in 3 ml of Rotiszint eco plus by scintillation counting.

5.6.2.8   5.10a ([^{3}H] De257) kinetic experiments

In kinetic experiments the membranes were prepared as described for the binding assays in 5.7.2.7. Each tube contained 150 µl binding buffer (12.5 mM $MgCl_2$, 1 mM EDTA and 75 mM Tris/HCl, pH 7.4), 2 µl BSA 2 % (m/v), and 25 µl of the suspended membrane (hH_2R-$G_{s\alpha S}$,50-100 µg/tube) in binding buffer. Association and dissociation kinetic experiments were started by addition of 5.10a (c = 25 nM for each tube). The dilution of the radioligand contained 3/5 of unlabelled ligand and 2/5 of tritiated radioligand leading to an end concentration of 25 nM in each reaction tube. During incubation all tubes were shaken (250 rpm) at 22 °C.

The tubes for total binding in association experiments additionally contained 25 µl H_2O (millipore), the tubes for unspecific binding 25 µl of a 1 mM or 500 µM solution of famotidine in H_2O (millipore). The respective radioligand was added at different time points (0-180 min) to the membrane containing tubes (two tubes for each time point to get the results in duplicate). At certain time points (e.g. 6, 13, 20, 50, 70, 80, 100 and 120 min) famotidine (final conc.: 100 µM/ tube) was added simultaneously with **5.10a** to determine the amount of unspecific binding. After the last addition of radioligand (after 180 min) bound radioligand was separated from free radioligand by filtration through GF/C filters (see 5.7.2.7), pretreated with 0.3 % (m/v) PEI solution, immediately. Three washing steps with 2 ml binding buffer (4 °C) followed. Thus the last time point (last addition of radioligand) represented the shortest incubation time (0 min), whereas the first time point (first addition of radioligand) represents the longest incubation time

(180 min). After an equilibration period of 12 h filter-bound radioactivity was measured in 3 ml of Rotiszint eco plus by liquid scintillation counting.

In dissociation experiments all tubes (containing binding buffer, BSA 2 % and membrane suspension) were preincubated with **5.10a** (25 µl, final concentration: 25 nM in each tube) for 60 min, before starting dissociation by addition of famotidine (25 µl, final concentration: 100 µm/tube). Preincubation was started for each data set at different time points (e.g. at: 0 min, 10 min, 15 min, ...). Dissociation kinetics was measured over 90 min. Bound radioligand was separated instantly from free radioligand by filtration through GF/C filters (see 5.7.2.7). Filter-bound radioactivity was determined after a 12 h equilibration phase by liquid scintillation counting. For non-specific binding **5.10a** was incubated 90 min in the presence of famotidine (100 µM).

References

1.	Repke, H., Liebmann, C. *Membranrezeptoren und ihre Effektorsysteme*. Akademie Verlag Berlin: **1987**; p 55-79.

2.	Rising, T. J.; Norris, D. B.; Warrander, S. E.; Wood, T. P. High affinity ^{3}H-cimetidine binding in guinea-pig tissues. *Life Sci.* **1980,** 27, 199-206.

3.	Smith, I. R.; Cleverley, M. T.; Ganellin, C. R.; Metters, K. M. Binding of [^{3}H]cimetidine to rat brain tissue. *Agents Actions* **1980,** 10, 422-6.

4.	Gajtkowski, G. A.; Norris, D. B.; Rising, T. J.; Wood, T. P. Specific binding of ^{3}H-tiotidine to histamine H_2 receptors in guinea pig cerebral cortex. *Nature* **1983,** 304, 65-7.

5.	Kelley, M. T.; Burckstummer, T.; Wenzel-Seifert, K.; Dove, S.; Buschauer, A.; Seifert, R. Distinct interaction of human and guinea pig histamine H_2-receptor with guanidine-type agonists. *Mol. Pharmacol.* **2001,** 60, 1210-25.

6.	Wenzel-Seifert, K.; Kelley, M. T.; Buschauer, A.; Seifert, R. Similar apparent constitutive activity of human histamine $H_{(2)}$-receptor fused to long and short splice variants of $G_{(salpha)}$. *J. Pharmacol. Exp. Ther.* **2001,** 299, 1013-20.

7.	Ruat, M.; Traiffort, E.; Bouthenet, M. L.; Schwartz, J. C.; Hirschfeld, J.; Buschauer, A.; Schunack, W. Reversible and irreversible labeling and autoradiographic localization of the cerebral histamine H_2 receptor using [^{125}I]iodinated probes. *Proc. Natl. Acad. Sci. U. S. A.* **1990,** 87, 1658-62.

8.	Leurs, R.; Smit, M. J.; Menge, W. M.; Timmerman, H. Pharmacological characterization of the human histamine H_2 receptor stably expressed in Chinese hamster ovary cells. *Br. J. Pharmacol.* **1994,** 112, 847-54.

9.   Preuss, H.; Ghorai, P.; Kraus, A.; Dove, S.; Buschauer, A.; Seifert, R. Constitutive activity and ligand selectivity of human, guinea pig, rat, and canine histamine H_2 receptors. *J. Pharmacol. Exp. Ther.* **2007,** 321, 983-95.

10.   Hirschfeld, J.; Buschauer, A.; Elz, S.; Schunack, W.; Ruat, M.; Traiffort, E.; Schwartz, J. C. Iodoaminopotentidine and related compounds: a new class of ligands with high affinity and selectivity for the histamine H_2 receptor. *J. Med. Chem.* **1992,** 35, 2231-8.

11.   Yellin, T. O.; Buck, S. H.; Gilman, D. J.; Jones, D. F.; Wardleworth, J. M. ICI 125,211: a new gastric antisecretory agent acting on histamine H_2-receptors. *Life Sci.* **1979,** 25, 2001-9.

12.   Igel, P.; Schnell, D.; Bernhardt, G.; Seifert, R.; Buschauer, A. Tritium-labeled N(1)-[3-(1H-imidazol-4-yl)propyl]-N(2)-propionylguanidine ([(^{3})H]UR-PI294), a high-affinity histamine H($_3$) and H($_4$) receptor radioligand. *ChemMedChem* **2009,** 4, 225-31.

13.   Keller, M.; Pop, N.; Hutzler, C.; Beck-Sickinger, A. G.; Bernhardt, G.; Buschauer, A. Guanidine-acylguanidine bioisosteric approach in the design of radioligands: synthesis of a tritium-labeled N(^{G})-propionylargininamide ([^{3}H]-UR-MK114) as a highly potent and selective neuropeptide Y Y_1 receptor antagonist. *J. Med. Chem.* **2008,** 51, 8168-72.

14.   Keller, M. Guanidine-acylguanidine bioisosteric approach to address peptidergic receptors: pharmacological and diagnostic tools for the NPY Y_1 receptor and versatile building blocks based on arginine substitutes. *Doctoral Thesis*, University of Regensburg, Germany, http://epub.uni-regensburg.de/12092/, **2008**.

15.   Kracht, J. Bestimmung der Affinität und Aktivität subtypselektiver Histamin- und Neuropeptid Y-Rezeptorliganden an konventionellen und neuen pharmakologischen In-vitro-Modellen. *Doctoral thesis*, University of Regensburg, **2001**.

16.   Seifert, R.; Wenzel-Seifert, K.; Burckstummer, T.; Pertz, H. H.; Schunack, W.; Dove, S.; Buschauer, A.; Elz, S. Multiple differences in agonist and antagonist pharmacology between human and guinea pig histamine H_1-receptor. *J. Pharmacol. Exp. Ther.* **2003,** 305, 1104-15.

17.   Ghorai, P.; Kraus, A.; Keller, M.; Gotte, C.; Igel, P.; Schneider, E.; Schnell, D.; Bernhardt, G.; Dove, S.; Zabel, M.; Elz, S.; Seifert, R.; Buschauer, A. Acylguanidines as bioisosteres of guanidines: NG-acylated imidazolylpropylguanidines, a new class of histamine H_2 receptor agonists. *J. Med. Chem.* **2008,** 51, 7193-204.

18.   Nordemann, U. *Personal communication*. In Department of Pharmaceutical and Medicinal Chemistry II, University of Regensburg (Germany), **2009**.

19.   Schnell, D. *Personal communication*. In Department of Pharmacology and Toxicology, University of Regensburg (Germany), **2008**.

20.   Mosandl, J. Radiochemical and luminescence-based binding and functional assays for human histamine receptors using genetically engineered cells. *Doctoral thesis*, University of Regensburg, Germany, http://epub.uni-regensburg.de/12335/, **2009**.

21.   Lazareno, S. Quantification of receptor interactions using binding methods. *J. Recept. Signal Transduct. Res.* **2001,** 21, 139-65.

22.   Kenakin, T.; Jenkinson, S.; Watson, C. Determining the potency and molecular mechanism of action of insurmountable antagonists. *J. Pharmacol. Exp. Ther.* **2006,** 319, 710-23.

23.   Lopuch, M. *Personal communication*. In Department of Pharmaceutical and Medicinal Chemistry II, University of Regensburg (Germany), **2010**.

24.   Birnkammer, T. Personal communication. *Department of Pharmaceutical & Medicinal Chemistry II, University Regensburg (Germany)* **2010**.

25.   Apodaca, R.; Dvorak, C. A.; Xiao, W.; Barbier, A. J.; Boggs, J. D.; Wilson, S. J.; Lovenberg, T. W.; Carruthers, N. I. A new class of diamine-based human histamine H_3 receptor antagonists: 4-(aminoalkoxy)benzylamines. *J. Med. Chem.* **2003,** 46, 3938-44.

26.   Buyniski J.P., R. L. C., R.L., Pircio, A.W. Algieri A.A., Crenshaw R.R. . Highlights in Receptor Chemistry. *Melchiorre, C, Gianella, M, eds. Structure- activity relationships among newer histamine H_2-receptor antagonists, Amsterdam: Elsevier Sciences,* **1984**, 195-215.

27.   Cavanagh, R. L.; Buyniski, J. P. Effect of BMY-25368, a potent and long-acting histamine H_2-receptor antagonist, on gastric secretion and aspirin-induced gastric lesions in the dog. *Aliment. Pharmacol. Ther.* **1989,** 3, 299-313.

28.   Torchiana, M. L.; Pendleton, R. G.; Cook, P. G.; Hanson, C. A.; Clineschmidt, B. V. Apparent irreversible H_2-receptor blocking and prolonged gastric antisecretory activities of 3-N-(3-[3-(1-piperidinomethyl)phenoxy]propyl) amino-4-amino-1,2,5-thiadiazole-1-oxide (L-643, 441). *J. Pharmacol. Exp. Ther.* **1983,** 224, 514-9.

29.   Brittain, R. T.; Jack, D.; Reeves, J. J.; Stables, R. Pharmacological basis for the induction of gastric carcinoid tumours in the rat by loxtidine, an insurmountable histamine H_2-receptor blocking drug. *Br. J. Pharmacol.* **1985,** 85, 843-7.

30.   Stables, R.; Daly, M. J.; Humphray, J. M. Comparison of antisecretory potency and duration of action of the H_2-receptor antagonists AH 22216, cimetidine, ranitidine and SK & F 93479 in the dog. *Agents Actions* **1983,** 13, 166-9.

31.   Vauquelin, G.; Van Liefde, I.; Vanderheyden, P. Models and methods for studying insurmountable antagonism. *Trends Pharmacol. Sci.* **2002,** 23, 514-8.

32.   Vauquelin, G.; Van Liefde, I.; Birzbier, B. B.; Vanderheyden, P. M. New insights in insurmountable antagonism. *Fundam. Clin. Pharmacol.* **2002,** 16, 263-72.

33.   Monczor, F.; Fernandez, N.; Legnazzi, B. L.; Riveiro, M. E.; Baldi, A.; Shayo, C.; Davio, C. Tiotidine, a histamine H2 receptor inverse agonist that binds with high affinity to an inactive G-protein-coupled form of the receptor. Experimental support for the cubic ternary complex model. *Mol. Pharmacol.* **2003,** 64, 512-20.

34.   Cheng, Y.; Prusoff, W. H. Relationship between the inhibition constant (K1) and the concentration of inhibitor which causes 50 per cent inhibition (I50) of an enzymatic reaction. *Biochem. Pharmacol.* **1973,** 22, 3099-108.

Chapter 6

Fluorescent H$_2$-receptor ligands

6   Fluorescent H₂-receptor ligands

6.1   Introduction

Nowadays there is high demand for fast and reliable methods to pharmacologically characterize receptor ligand interactions, for example by quantification of receptor affinity, functional activity and selectivity. Thereby, fluorescence based binding assays offer an attractive option. Fluorescence detection (confocal microscopy, flow cytometry) is very sensitive, allowing investigations on living cells under equilibrium conditions and enables multiparametric measurements[1-2]. There is a high demand for appropriate fluorescent probes for high throughput screening[3] of large compound libraries as well as for detailed pharmacological studies on affinity, agonistic/antagonistic activity and for the detection of receptors on the cellular level.

Compared to radioligands the use of fluorescent probes is more convenient and less expensive in terms of safety precautions and waste disposal, respectively. Additionally, in binding studies, time consuming steps like separation of free from bound ligand (radioligand binding assays) can be omitted, as measurements can be performed under equilibrium conditions without the need of washing steps[1]. Furthermore, ligand internalization processes[2] can be monitored and techniques like FRET or BRET are applicable.

Many fluorescent ligands have been synthesized in the last decades[2, 4], among them are fluorescently labelled peptides/peptide analogues (e. g. for formyl peptide[5], insulin[6], epidermal growth factor[7], NPY[8-9] receptors) as well as small molecules like fluorescence ligands of aminergic receptor (e. g. histamine[10-11], 5-HT₄[12], β-adrenergic[13], adenosine A₁[14] receptors). One of the challenges in this field of research is the maintenance of receptor affinity and activity despite the introduction of the mostly large and bulky fluorophoric residues, especially, when small low molecular weight ligands are labelled. In the histamine receptor field the agonist histamine is commercially

w radioligands

sosomes. Fluorescence labelled histamine receptor antagonists, emitting at wavelengths below 600 nm (NBD, fluorescein, dansyl, TAMRA....), including work from our laboratory, are described in the literature for the H₁R[10], the H₂R[-11, 15] and the H₃R[16-18]. The previous results from our group on H₂R antagonists demonstrate that, in principle, coupling to fluorophores is possible without dramatic decrease or complete loss of activity and affinity. Ligands labelled with nitrobenzoxadiazole (NBD) or carboxyfluorescein[11] (see Figure 6.1) proved to be the most potent H₂R antagonists (guinea pig right atrium: pA₂ values in the range of 5 to 8)[11], but with drawbacks due to

unfavorable fluorescence properties. In both cases, the labelled ligands were inappropriate for flow cytometry or confocal microscopy due to interference of the emission with cellular auto-fluorescence resulting in unsatisfactory signal-to-noise ratios.
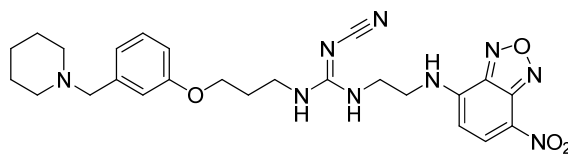
Compound **UR-LLT21** (with NBD as fluorophore)
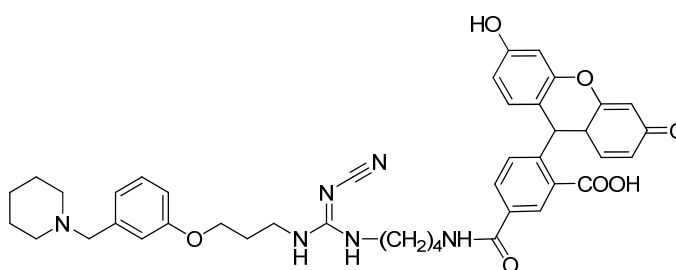
Compound **UR-LLT40** (with Carboxyfluorescein as fluorophore)

Figure 6.1: Selected fluorescent H$_2$R antagonists from previous investigations[11]

Recent results from our work group in the neuropeptide Y (NPY)[1, 9, 19] and histamine receptor field[20] prove the applicability of red-emitting dyes to avoid the aforementioned problems. Aiming at more potent and selective fluorescent ligands and improving the signal-to-noise ratio, the H$_2$R antagonists described in chapter 3 of this thesis were coupled to different fluorophoric moieties emitting at wavelengths > 590 nm .

6.2   Chemistry

Different cyanine dyes like S0536, S0535, S0586 and Dyes like Dy 630 and Dy 675 with a ben-zopyrane moiety (Scheme 6.1), a bodipy ("*boron-dipyrromethene*") dye, Bodipy 650/665-X, as well as the small pyrylium dyes Py1 and Py5 were employed. The cyanine- and bodipy fluoropho-res are excitable with the red diod laser (633 nm), often used in flow cytometry and confocal microscopy, and their fluorescence properties do not strongly depend on the pH of the solvent or the used solutions and buffers. Their emission is detected above 650 nm. The pyrylium dyes, originally developed for staining of small amounts of protein [21], are coupled to a primary amino group resulting in pyridinium compounds, which are excitable with a 488 (Argon) laser, a stan-dard component of flow cytometers and confocal microscopes. They have high stokes shifts resulting in emissions > 600 nm. As we use low molecular weight H_2R antagonists for labelling, introducing bulky, high molecular weight fluorophores could considerably impair H_2R activ-ity/affinity. In this regard the use of the lower molecular weight pyrylium dyes should be advan-tageous. Although carboxyfluorescein is not a ideal fluorophore, this dye was used to label one of the squaramide derivatives for pharmacological investigations, i. e. to compare its activities with known carboxyfluorescein coupled H_2R antagonists[11].

5-SFX - SE ("succinimidyl" ester)

Py-1

Py-5

Bodipy 650/665-X- SE

S₀₅₃₆/S₀₅₈₆/S₀₅₃₅ - SE

Dy630,- SE

Dy675- SE
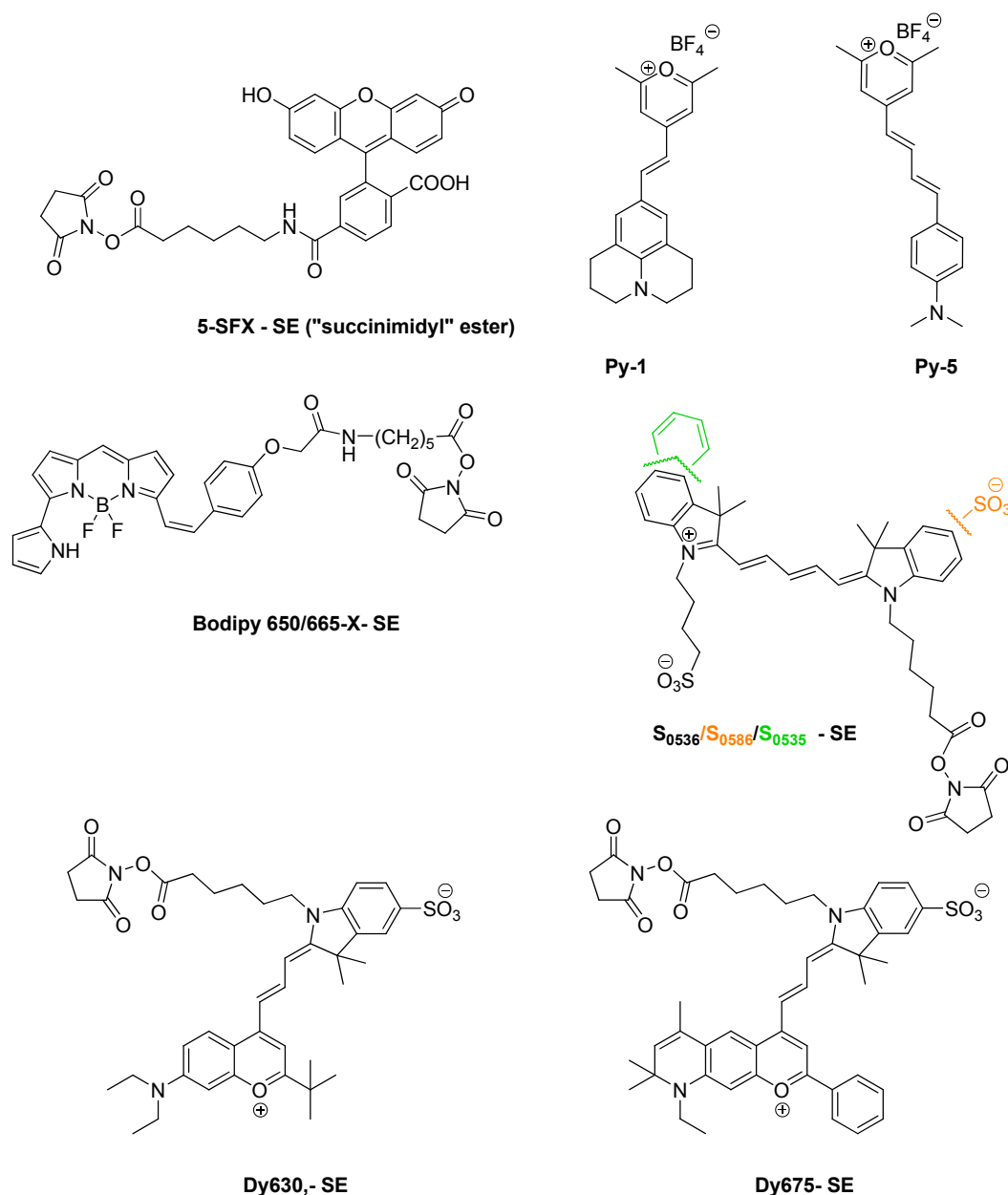
Scheme 6.1: Structures of fluorescent dyes (corresponding succinimidyl esters) used for labeling of H₂-receptor antagonists

The pyrylium (Py) dyes, also called chameleon dyes, undergo a rapid reaction with primary amines at a pH of 8-9 at rt. Due to the ring transformation resulting in positively charged pyridinium compounds the absorption maximum is shifted about 100 nm (hypsochromic shift) from around 600 nm to 500 nm[22]. This is visible by a change in color from dark blue to red. Coupling was carried out with the amine precursors from chapter 3 and the Py dyes Py1 and Py5 in a mixture of DMF (solvent for Py dye) and methanol at rt in the dark (Scheme 6.2).
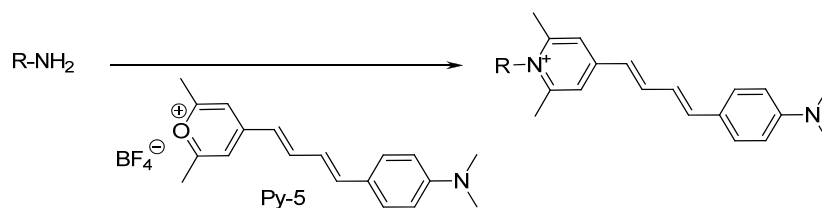
Scheme 6.2: Schematic coupling reaction of a Pyrylium dye (Py5 as example) to a primary amine containing compound; R stands for H_2R antagonistic moiety.

Dyes (cyanine, Bodipy and carboxyfluorescein) were linked to the compounds via a ω-aminoalkylspacer, which is already present in the new ligands described in chapter 3. The coupling reaction was performed with the active esters of the fluorophores and the respective primary amines at rt in an organic solvent (mainly MeCN or MeOH) at a pH of 8-9 in the dark. Purification of all fluorescently labelled compounds was done by preparative HPLC, followed by lyophilisation to give the products as colored semi solids.
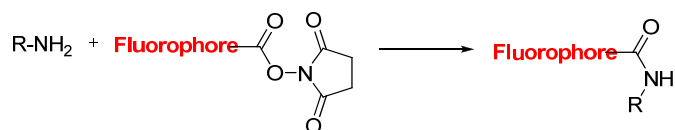
Scheme 6.3: Principle of the reaction of fluorescent active esters with primary amines; R stands for H_2R antagonistic moiety.

Aminopotentidine related compounds (cyanoguanidines, amides)

Compound **6.3**, known from our workgroup[20], was resynthesized for pharmacological characterization and supplemented by new cyanoguanidine-like ligands bearing different fluorophores and different spacers. Additionally, the roxatidine-like amides were labelled with S0536.

Compd.	n	X	Fl
6.1	2	-NHCO-	S0536
6.2	5	-NHCO-	S0536
6.3	2	-NHC(NCN)NH-	S0536
6.4	6	-NHCN(CN)NH-	S0536
6.5	2	-NHCN(CN)NH-	Bodipy[a]
6.6	2	-NHCN(CN)NH-	Py1
6.7	2	-NHCN(CN)NH-	Dy675
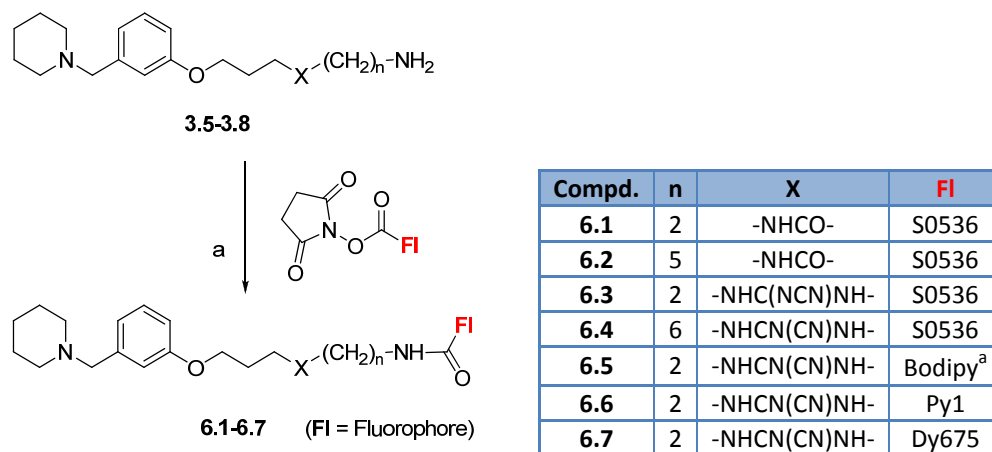
Scheme 6.4: Synthesis of fluorescent ligands **6.1-6.7**. Reagents and conditions: (a) organic solvent (see exp. data) Et$_3$N, rt, light protection, 30 min-3 h,[a] Bodipy 650/665, X-SE

From the squaramide building blocks (chapter 3) compounds **3.4** and **3.9-3.15** were coupled to a number of different fluorophores (Scheme 6.5) as they were considered the most promising precursors, expected to retain H$_2$R affinity after coupling. Actually, maintained or even increased activity was achieved (see results). Therefore, rather weak H$_2$R antagonists (e.g. cimetidine-like compounds) were also labelled in order to get information on the contribution of the fluorophore to H$_2$R affinity, when combined with different pharmacophoric groups (Scheme 6.6)

Compd.	n	Fluorophore	Compd.	n	Fluorophore
6.8	-	S0535	**6.17**	4	Dy675
6.9	2	S0536	**6.18**	6	Dy675
6.10	3	S0536	**6.19**	5	Bodipy 650/665-X
6.11	4	S0536	**6.20**	6	Bodipy 650/665-X
6.12	5	S0536	**6.21**	6	5-SFX
6.13	6	S0536	**6.22**	6	S0535
6.14	7	S0536	**6.23**	4	Py5
6.15	8	S0536	**6.24**	4	Py1
6.16	4	S0586			
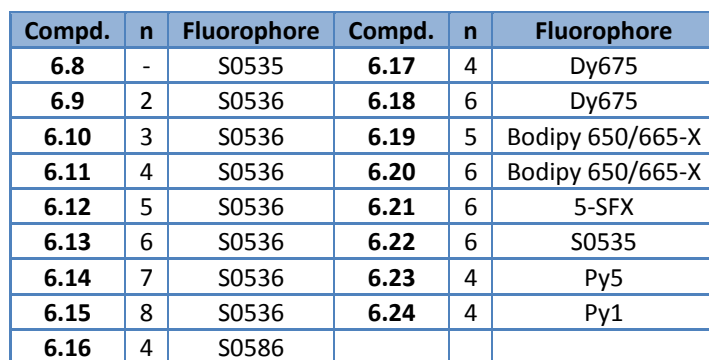
Scheme 6.5: Coupling of primary amines **3.4** and **3.9-3.15** to fluorophores. Reagents and conditions: (a) Et$_3$N, MeCN, light protection, rt, 3 h, (b) Et$_3$N, organic solvent (see exp.data) light protection, rt, 30 min-3 h, (c) Et$_3$N, MeOH/DMF, light protection, rt, 30 min -3 h;

Scheme 6.6: Synthesis of compounds **6.26-6.29,** Reagents and conditions: Et$_3$N, organic solvent (see exp.data), light protection, rt, 30 min-3 h

6.3 Pharmacological results

6.3.1 H$_2$-receptor antagonism

GTPase assay at the guinea pig and human histamine H$_2$-receptor

The fluorescent H$_2$R antagonists were investigated for H$_2$R antagonism in the steady state GTPase assay at the gpH$_2$R-G$_{s\alpha S}$ and hH$_2$R-G$_{s\alpha S}$ fusion proteins[23]. All fluorescent ligands were able to decrease GTPase activity (antagonist mode) in a concentration dependent manner, achieving K$_{b'}$-values in the lower nanomolar to lower micromolar range. Low inverse agonistic effects (E$_{max}$) were determined ranging from -0.3 to 0.0.

The partial agonistic effect of **6.3** (Lit: [20]) could not be confirmed. Our results revealed antagonistic activities in the low micromolar range (K$_{b'}$ = 2738 nM). There was no significant intrinsic activity (-0.07). The newly synthesized ligands **6.4, 6.6** and **6.7,** coupled to cyanine dyes, exerted antagonistic effects in the same range as **6.3,** whereas the Py-labelling resulted in a drop (4-5 fold

of activity). The most potent antagonist in this series was compound **6.5**, bearing a bodipy dye, which showed a tremendous increase in activity (8 fold) compared to the cyanine linked compounds ($K_{b'}$ = 132 nM). The same tendency in activity was obvious for roxatidine-like ligands **6.1** and **6.2** linked to S0536, which achieved $K_{b'}$-values in the low micromolar range. The named ligands (except **6.5**) showed a drop in activity compared to the parent compounds or only slightly increased activity (1.5 to 2 fold, for **6.1** and **6.2**).

Highest H_2R antagonistic activities with $K_{b'}$-values in the low nanomolar range were obtained by labelling of squaramide-type precursors. Activities between 72 and 195 nM were achieved in the series of ligands linked to the cyanine dye S0536 and covering a spacer length between 2 and 8 methylene groups. A slight increase in activity, depending on the spacer length, was observed (except for **6.14**). Exchanging the fluorophoric moiety with different cyanine dyes, maintaining the spacer at 4-6 methylene groups, gave highly active substances (**6.17, 6.18** and **6.22**). By contrast introduction of the cyanine dye S0586, with an additional sulfonate moiety, as well as the use of carboxyfluorescein as fluorophore (**6.21**) resulted in a drop in activity (**6.16**). Like ligand **6.5**, the Bodipy-labelled compounds **6.19** and **6.20**, with $K_{b'}$-values around 27 nM, showed high H_2R antagonistic activity, superior to the S0536 coupled ligands. The labelling with pyrylium dyes gave active compounds such as **6.24** ($K_{b'}$ =136 nM) and led to the most potent squaramide type H_2R antagonist **6.23** in this series (together with Bodipy-labelled compounds **6.18** and **6.19**) ($K_{b'}$ =22 nM).

Coupling of the cimetidine-like precursor yielding compounds **6.26** and **6.27**, resulted in up to 17 fold increase in activity ($K_{b'}$ = 490 nM for **6.27** respectively) compared to the parent compound, even though activity at the H_2R was still lower than those of the squaramide-type substances. Cyanine-labelling of H_2R antagonist moieties lacking the "urea equivalent" gave only one moderately active compound (**6.8,** $K_{b'}$ = 635 nM), whereas the ligands **6.28** and **6.29** had only micromolar activities. Selected highly active fluorescent ligands were also investigated at the $gpH_2R\text{-}G_{s\alpha S}$ fusion protein; the determined H_2R antagonistic activities at guinea pig and human receptor were in the same range.

Table 6.1: Activities and efficacies of fluorescent ligands (squaramides) in GTPase assays [a]

Compd.	gpH$_2$R-G$_{s\alpha s}$ K$_{b'}$ [nM]	hH$_2$R-G$_{s\alpha s}$ K$_{b'}$ [nM]	E$_{max}$
Histamine	EC$_{50}$ 850 ± 340[b]	EC$_{50}$990 ± 92[b]	1.00
6.1	n.d.	2486 ± 691	-0.04
6.2	n.d.	1054 ± 229	-0.03
6.3	n.d.	2738 ± 849	-0.07 ± 0.02
6.4	n.d.	1151 ± 4	-0.1 ± 0.03
6.5	200 ± 24.7	132 ± 34	-0.22 ± 0.03
6.6	n.d.	5450 ± 51	-0.05 ± 0.02
6.7	n.d.	1276 ± 127	-0.13 ± 0.07
6.8	n.d.	635 ± 326	-0.29 ± 0.04
6.9	161 ± 27	176 ± 3	-0.02 ± 0.03
6.10	81 ± 0.6	195 ± 10	-0.05 ± 0.03
6.11	73 ± 15	113 ± 1.2	-0.03 ± 0.0
6.11	49 ± 2	115 ± 27	-0.01 ± 0.01
6.13	66 ± 10	87 ± 15	0.00 ± 0
6.14	n.d.	175 ± 37	0.00 ± 0
6.15	n.d.	72 ± 13	-0.11 ± 0.04
6.16	2462 ± 36	1835 ± 151	0.19 ± 0.01
6.17	n.d.	162 ± 51	-0.06 ± 0.03
6.18	n.d.	183 ± 82	-0.24 ± 0.00
6.19	n.d.	80 ± 53	-0.006 ± 0.08
6.20	n.d.	30 ± 0.01	-0.23 ± 0.00
6.22	n.d.	238 ± 90	-0.24 ± 0.00
6.21	n.d.	1411 ± 395	-0.16 ± 0.01
6.23	33 ± 14	22 ± 2	-0.08 ± 0.03
6.24	n.d.	136 ± 23	-0.1 ± 0.1
6.26	n.d.	1429	-0.12 ± 0.012
6.27	n.d.	490 ± 202	-0.17 ± 0.06
6.28	n.d.	1485 ± 138	-0.19 ± 0.00
6.29	n.d.	> 5000	-0.19 ± 0.01

[a] steady state GTPase assay on Sf9 cell membranes; c. ligands: 1 nM - 100 µM; typical GTPase activities (stimulation with 1 µM HIS (gpH$_2$R/hH$_2$R): 3.5-7 pmol x mg^{-1} x min^{-1}; E$_{max}$= efficacy relative to histamine, E$_{max}$ HIS=1 (c. ligands: 10 µM), Mean values ± S.E.M. (n = 2-4, performed in duplicate); n.d.: not determined; [b] cf. ref.[24]

6.3.2   Receptor selectivity

Activity on human H_1-, H_3- and H_4-receptors in GTPase assays

The compounds were investigated for inverse agonism at the H_1R[25] and H_4R[26] GTPase assays on Sf9 cell membranes bearing hH_1R + RGS4 and hH_4R-RGS19+ $Gi_{\alpha2}+G_{\beta1\gamma2}$. Intrinsic activities at the H_1R were negligible, ranging from -0.13 to -0.01 (see appendix), except for **6.8**, which showed an intrinsic activity of -0.29. Investigations at the H_4R revealed in general low inverse agonistic activities of -0.2 to -0.02 (see appendix). Exceptions were **6.4**, **6.12** and **6.24** with E_{max} values between approx. -0.3 to -0.4. Most of the fluorescent ligands were tested in the antagonist mode for antagonism at the H_4R, where the majority of compounds, including **6.4**, **6.12** and **6.28,** had low activity ($K_{b'}$ > 1000-4000 nM). Exceptions were **6.18** and **6.19** with activities in the three-digit nanomolar range ($K_{b''}$= 449 nM and 632 nM, respectively, see appendix).

As found for the corresponding non-fluorescent H_2R antagonists the fluorescence labelled compounds had also activities at the H_3R in the nanomolar to micromolar range, depending on the pharmacophoric and fluorophoric moieties, with highly variable intrinsic activities (inverse agonism) between -1 and -0.1. For potentidine-like cyanoguanidines even an activity increase at the H_3R compared to the H_2R was detected. Activities of the amides **6.1** and **6.2** at the H_3R were in the same range as at the H_2R.

All compounds of the squaramide series labelled with cyanine dyes were almost equipotent at the H_3R and H_2R, with activities ranging from 44 to 400 nM. By contrast, Bodipy and Py coupled ligands had the highest selectivity for the H_2R, for instance **6.23** had 12 fold preference for the H_2R. With compounds **6.27** and **6.28** 3 to 5 fold selectivity versus the H_3R was achieved, whereas **6.26** and **6.29** showed activity in the nanomolar range.

Affinities at the H_3-receptor in radioligand binding experiments

In order to verify the results from GTPase assays, selected substances were investigated in radioligand binding studies on HEK-293-FLAG-hH_3R-His$_6$ cells expressing the human H_3R. These studies were performed with [^{3}H]N^α-methylhistamine ([^{3}H]NAMH) as radioligand at a concentration of 1 nM (K_D= 5.1 nM). The fluorescent compounds displaced the radioactive tracer [^{3}H]NAMH in a concentration dependent manner. The K_i-values substantiated the results from functional experiments.

Table 6.2: H_3R antagonistic activity and binding of selected compounds, determined on Sf9 cell membranes (GTPase[a]) and on HEK-293-FLAG-hH$_3$R-His$_6$cells[b]

Compd.	GTPase assay hH$_3$R+ G$_{i\alpha2}$ +β$_1$γ$_2$ + RGS4[a]		Binding assay HEK-293 FLAG hH$_3$R His$_6$ cells[b]
	K$_{b'}$ [nM]	E$_{max}$	K$_i$ (K$_D$) [nM]
Histamine	EC$_{50}$ 25 ± 3[c]	1.00	
[^{3}H]NAMH	-	-	(5.1)[d]
JNJ5207852	4.3 ± 0.64	-0.88 ± 0.12	n.d
Thioperamide	97 ± 18	-0.66 ± 0.1	n.d
6.1	n.d.	n.d.	n.d.
6.2	1756 ± 872	-1.01 ± 0.3	425 ± 87
6.3	249	-1.18 ± 0.13	247 ± 15
6.4	210	-0.24	96 ± 75
6.5	222 ± 98	-1.34 ± 0.15	104 ± 73
6.6	n.d.	n.d.	923 ± 402
6.7	657 ± 308	-1.2 ± 0.12	32 ± 12
6.8	9742	-0.34 ± 0.04	n.d
6.9	223 ± 121	-1.08 ± 0.25	n.d
6.10	779 ± 445	-1.07 ± 0.28	n.d
6.11	223 ± 53	-0.95 ± 0.34	276 ± 68
6.12	44 ± 8	-1.16	175 ± 29
6.13	313 ± 173	-1.06 ± 0.14	168 ± 30
6.14	73 ± 33	-0.93 ± 0.27	n.d
6.15	225 ± 60	-1.13	n.d
6.16,	320 ± 124	-0.87 ± 0.04	n.d
6.17,	228 ± 188	-1.04 ± 0.28	586 ± 152
6.18	n.d.	n.d.	n.d
6.19	396 ± 80	-0.93 ± 0.25	100 ± 24
6.20,	244 ± 177	n.d.	126 ± 79
6.21,	1362 ± 2	-0.73 ± 0.14.	n.d
6.22	n.d.	n.d.	n.d
6.23	264 ± 112	-0.82 ± 0.06	600 ± 36
6.24	692 ± 498	-0.2 ± 0.08	1046 ± 160
6.26	720.2	n.d.	1414 ± 39
6.27	4411	-0.16	836 ± 83
6.28	5319	-0.14 ± 0.05	903 ± 273
6.29	140 ± 100	n.d.	n.d

[a] steady state GTPase assay on Sf9 cell membranes; c. ligands: 1 nM - 100 µM; typical GTPase activities (stimulation with 100 nM HIS (hH$_3$R): 2.5-6.0 pmol x mg^{-1} x min^{-1}; E$_{max}$= efficacy relative to histamine; E$_{max}$ HIS=1 (c. ligands: 10 µM), mean values ± S.E.M. (n = 1-3, performed in duplicate);

[b] c. ligands: 1 nM - 100 µM, c. [^{3}H]NAMH: 1 nM, 2-5 million cells/well; Mean values ± S.E.M. (n = 1-2) performed in duplicate; n.d.: not determined; [b, d] cf. ref.[27]; [c] cf. ref.[28]

6.3.3   Fluorescence based methods on HEK293 -hH$_2$R-qs5-HA and HEK293 FLAG-hH$_2$R-His$_6$ cells

6.3.3.1   Fluorescence properties of labelled antagonists

Fluorescence properties of a selection of the synthesized ligands are summarized in Table 6.3. The quantum yield is defined as the number of emitted photons relative to the number of absorbed photons. Determination of quantum yields (Φ) was performed in three different solutions, phosphate buffered saline (PBS, pH 7.4), PBS containing 1 % bovine serum albumin (BSA) and in ethanol. By investigating the quantum yield in the presence of 1 % BSA (in PBS), the influence of proteins on fluorescence properties could be studied and assay conditions could be simulated. Selected compounds, especially those with high affinity in flow cytometric binding assays, were investigated (Table 6.3). The fluorescence properties were not remarkably influenced by the H$_2$R antagonist pharmacophoric groups or by the chain length of the spacer. As examples for compounds having different chain lengths, three squaramides, all bearing S0536 as fluorphore, are included in Table 6.3 (**6.4, 6.11** and **6.14**).

The highest quantum yields were detected for the cyanine dyes S0536 and S0535 in PBS with 1 % BSA (Φ= 28 -78 %) and in ethanol (Φ= 27 -51 %). In PBS the quantum yields were decreased to 9 to 30 % (2 to 5 fold compared to PBS + 1 % BSA). In case of the dyomics dyes (Dy675 and Dy630) low quantum yields (e. g. 10 % in the case of **6.19**) in ethanol were measured, whereas the quantum yields in PBS and PBS + 1 % BSA were comparable or slightly increased. For the bodipy labelled H$_2$R antagonist the quantum yields increased by more than a factor of 28 when BSA was added to the solution. Compound **6.23** displayed extremely low quantum yields in PBS (2 %). Addition of BSA increased the quantum yield by a factor of 3.5 to 7 %, still being very low compared to the other ligands. Electrostatic interactions of fluorophores with proteins and/or rigidization effects can lead to an increase in the quantum yield and in a shift of the emission wavelengths. Increased quantum yields in buffers containing BSA was observed for all fluorophores, indicating that - to a certain extent - such effects could play a role, although these effects were not as pronounced as for fluorescent NPY receptor ligands bearing similar fluorophores synthesized in our laboratory[29].

Table 6.3: Spectroscopic properties of selected fluorescent compounds in PBS (pH 7,4), 1 % BSA in PBS and ethanol

Compd	(Dye)	PBS		PBS+ 1 % BSA		EtOH	
		$\lambda_{ex}/\lambda_{em}$	Φ [%]	$\lambda_{ex}/\lambda_{em}$	Φ [%]	$\lambda_{ex}/\lambda_{em}$	Φ [%]
6.2	S0536	643/666	22 ± 0.7	666/672	38 ± 3	650/670	31 ± 3
6.4	S0536	643/666	31 ± 2	666/672	78	650/671	51 ± 4
6.5	"Bodipy"	652/667	0.7	661/671	27 ± 2	600/664	8 ± 3
6.11	S0536	643/666	31 ± 2	666/673	62 ± 5	650/670	41 ± 5
6.14	S0536	643/666	21 ± 4	666/ 675	64 ± 6	650/670	45 ± 4
6.17	Dy675	675/703	28	677/702	37 ± 5	678/701	10 ±1
6.19	"Bodipy"	651/669	1 ±0.2	663/670	28 ± 2	652/665	40 ± 3
6.23	Py5	450/695	2 ± 0.1	487-505/641	7 ± 4	500/700	3 ± 0.3
6.27	Dy630	630/654	9 ± 0.4	640/654	35	638/658	8 ± 0.7
6.26	S0536	647/664	18 ± 1	666/676	40 ± 3	650/670	40 ± 3
6.29	S0535	n.d.	n.d.	684/697	70 ± 9	674/694	26 ± 3
6.28	S0535	665/684	9 ± 1	684/700	48 ± 6	670/694	27 ± 3

$\lambda_{ex}/\lambda_{em}$: excitation/emission maxima, Φ: quantum yield (reference: cresyl violet perchlorate)

6.3.3.2   *Flow cytometric saturation and competition binding experiments*

Saturation binding

Flow cytometric measurements were performed according to a previously described procedure[30] using HEK293-hH$_2$R-qs5-HA cells. These investigations showed that, in principle, saturation curves can be constructed when the ligands have K$_{b'}$-values below 1000 nM (see Table 6.2) in the GTPase assay. From the potentidine-like cyanoguanidine and amide series four substances (**6.2, 6.3, 6.5 and 6.7**) were selected for saturation binding studies. Compound **6.7** showed a high extent of unspecific binding (no K$_D$-value calculated). By contrast, despite moderate activity at the H$_2$R in the functional assay, **6.2** and **6.3** gave saturation curves with a low extent of unspecific binding; the affinities were around 400 nM. Compound **6.5** had high affinity to the H$_2$R, but the shape of the curve indicated cellular uptake of the fluorescent ligand at concentrations above 200 nM (see appendix). This was confirmed by confocal microscopy (see appendix). For **6.8** and **6.27** saturation curves were constructed, which revealed a tendency for internalisation and displayed high unspecific binding at concentrations above 200 and 400 nM, respectively (see appendix).

Table 6.4: Saturation binding experiments of fluorescent ligands on HEK293 -hH$_2$R-qs5-HA cells

Compd.	Saturation HEK293 -hH$_2$R-qs5-HA cells K$_D$ [nM]	Compd.	Saturation HEK293 -hH$_2$R-qs5-HA cells K$_D$ [nM]
6.1	n.d.	6.15	322 ± 95
6.2	397 ± 68	6.16	h.u.b.
6.3	357 ± 117	6.17	90 ± 17
6.4	n.d.	6.18	146 ± 46
6.5	43 ± 14	6.19	49 ± 14
6.6	-	6.20	35 ± 9
6.7	h.u.b.	6.21	h.u.b.
6.8	276 ± 72	6.22	1783
6.9	461 ± 222	6.23	181 ± 38
6.10	353 ± 59	6.24	>3000
6.11	804 ± 53	6.26	h.u.b.
6.12	331 ± 9	6.27	1481 ± 695
6.13	166 ± 39	6.28	n.d.
6.14	358 ± 66	6.29	n.d.

[a]c. ligands: 1 nM - 300 nM to 100 µM, 2-3 million cells/ml; Mean values ± S.E.M. (n = 2-3); n.d.: not determined, h.u.b.= high unspecific binding, therefore no K$_D$ calculated

As shown in Table 6.4 for the majority of squaramide based fluorescent ligands K$_D$-values in the two- to three-digit nanomolar range were determined from saturation curves, and unspecific binding was low (10-30 %). Exceptions in terms of unspecific binding were **6.16** (linked to S0586) and **6.21** (linked to carboxyfluorescein) (**6.21**: cf. appendix). The K$_D$-values of compounds labelled with the cyanine dye Dy675 (**6.9**, **6.18**) or the Bodipy dye (**6.19, 6.20**), respectively, were in good accordance with the activities determined in GTPase assays. Fluorescent compound **6.17** for example had a low K$_D$-value (K$_D$= 90 nM) and an excellent ratio of specific binding to unspecific binding (22 % unspecific binding at concentraton between 80 - 100 nM; cf. Figure 6.2).
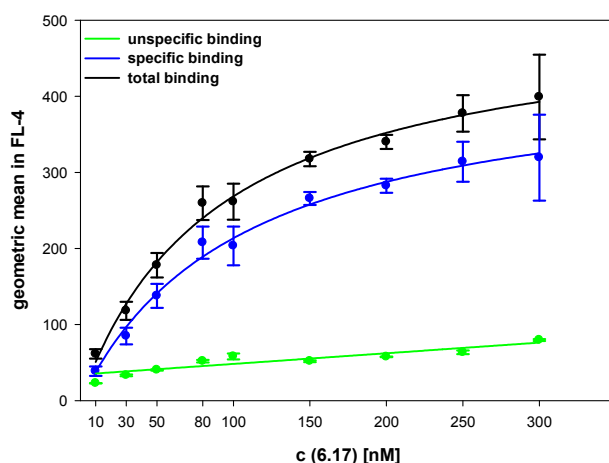
Compd.	K_D [nM]
6.17	90 ±17

Figure 6.2: Saturation binding of **6.17** on HEK293 -hH$_2$R-qs5-HA cells (mean values ± S.E.M, n=3), unspecific binding determined in the presence of famotidine (c final: 30 µM), incubation time: 37 min, rt

Results for **6.19** and **6.20** were in the same order of magnitude regarding K_D-values and specific/unspecific binding. Cyanine dye S0536 coupled ligands and the Py-5 coupled compound showed a lower affinity than expected from the GTPase assays, but regardless of that, affinity was sufficiently high to get reliable results (e.g. K_D = 166 nM for **6.13,** K_D = 181 nM for **6.23**). As demonstrated by three saturation curves (Figs. 6.2, 6.3), representative of this series of compounds, specific binding concentrations around the K_D-value were high with a small percentage of unspecific binding (10 to 30 %), especially in case of **6.15**.
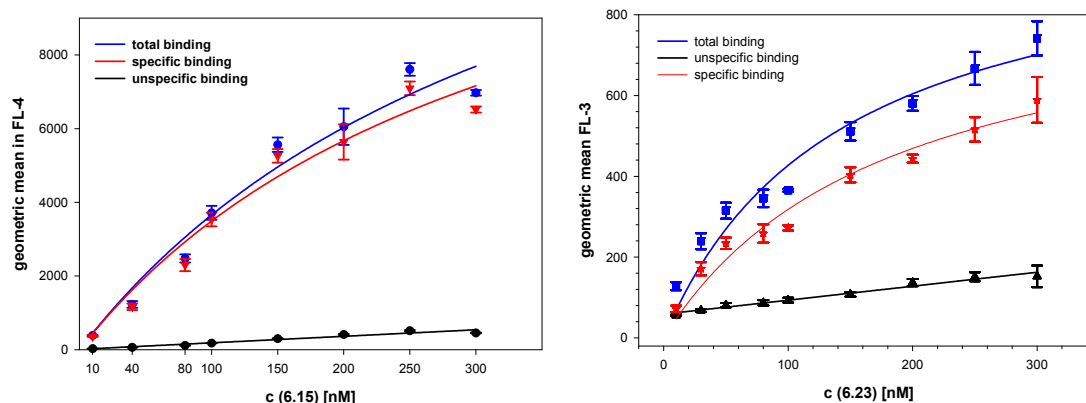
Compd.	K_D [nM]	Compd.	K_D [nM]
6.15	322± 95	**6.23**	181 ± 38

Figure 6.3: Saturation binding of **6.15** and **6.23** on HEK293 -hH$_2$R-qs5-HA cells (mean values ± S.E.M, n=3), unspecific binding determined in the presence of famotidine (c final: 30 µM); incubation time: 37 min, rt

Despite $K_{b'}$-values below 200 nM (GTPase assays) compounds **6.22** and **6.24** had only low affinities (see Table 6.1). The applicability of ligands with low affinity in flow cytometry is limited due to economic reasons and due to high unspecific binding (e.g. **6.7** and **6.27**). Therefore, only substances with determined $K_{D'}$-values in the two- to three-digit nanomolar range were used for further detailed investigations.

Competition binding

The suitability of selected fluorescent ligands (**6.13**, **6.17** and **6.23**) as reference compounds for the determination of H$_2$R ligand affinity was explored in competition binding experiments. The fluorescent compounds were used at concentrations around their K_D-value. H$_2$R ligands, such as cimetidine, famotidine or histamine, decreased specific binding of the fluorescent compounds in a concentration-dependent manner. Calculated K_i-values (Table 6.5) were in agreement with data from radioligand binding experiments with [³H]tiotidine[30] performed in our laboratory, using the same cell type. Anyway, the affinities of histamine, dimaprit and arpromidine were different from data determined on cell membranes (radioligand binding)[31]. The displacement of **6.17** by several standard ligands is depicted in Figure 6.4.

Table 6.5: K_i-values calculated from flow cytometric competition binding on HEK293 -hH$_2$R-qs5-HA cells, compared to data from literature

Labelled ligand Compd.	HEK293 -hH$_2$R-qs5-HA cells, K$_i$ [µM]			
	6.23 [a]	6.13 [b]	6.17 [c]	Lit. Data [d]
Histamine	138 ± 15	11.6 ± 3.3	40 ± 7	118 ± 54 [a]
Arpromidine	9.0 ± 1.9	3.5 ± 1.3	11.2 ± 3	5.4 ± 1.3 [a]
Dimaprit	116 ± 39	305 ± 48	350 ± 26	67 ± 20 [a]
Cimetidine	1.9 ± 0.4	0.26 ± 0.097	0.85 ± 0.25	-
Ranitidine	0.60 ± 0.16	0.41 ± 0.07	0.46 ± 0.09	0.17± 0.01 [a]
Famotidine	0.13 ± 0.01	0.08 ± 0.02	0.12 ± 0.05	-

c. ligands: 1 nM - 10 mM, 2-3 million cells/ml; mean values ± S.E.M. (n = 2-3); n.d.: not determined, unspecific binding determined in the presence of famotidine (c final 100 µM); K$_D$ (**6.23**)= 181 nM, K$_D$ (**6.13**)= 166 nM, K$_D$ (**6.17**)= 90 nM; [a] c: 200 nM; [b] c: 200 nM, 150 nM; [c] c: 90 nM; [d]cf. ref. [30], radioligand: [³H]tiotidine, c: 5/ 10 nM, K$_D$= 0.073 ± 0.013, see[30]
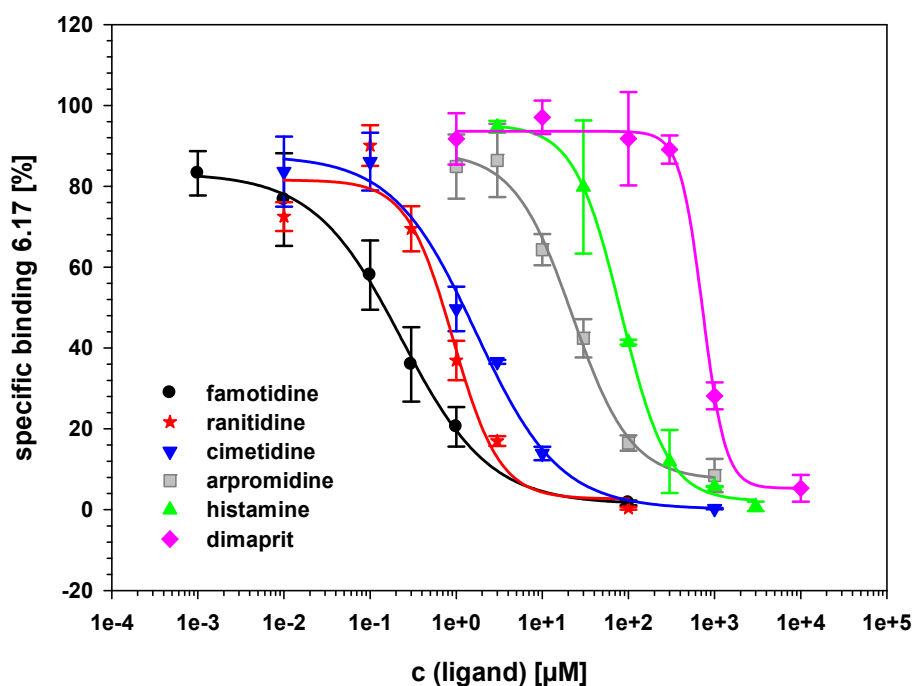
Figure 6.4: Concentration dependent displacement of **6.17** (c: 90 nM) on HEK293 -hH$_2$R-qs5-HA cells by various standard ligands; unspecific binding determined in the presence of famotidine (c final 100 µM); incubation time: 37 min, rt

6.3.3.3   *Confocal microscopy*

Visualization of ligand binding by confocal microscopic measurements was possible with a wide range of fluorescent ligands. Binding studies performed on HEK293 -hH$_2$R-qs5-HA cells (see also flow cytometry) and on HEK293 FLAG-hH$_2$R-His$_6$ cells (cells kindly provided by Dietmar Gross) gave comparable results. The fluorescent compounds were used at a concentration around the respective K$_D$- or K$_{b'}$-values and unspecific binding was detected in the presence of 10 µM famotidine. Images were taken for the binding of the squaramides **6.13**, **6.14**, **6.19** and **6.23** (K$_D$ < 200 nM). Compounds **6.13** (Figure 6.6**,** A1-A2), **6.14** (Figure 6.6, B1-B2) and **6.23** (Figure 6.7, C1-C1) showed a clear difference between total and unspecific binding as also determined by flow cytometry.
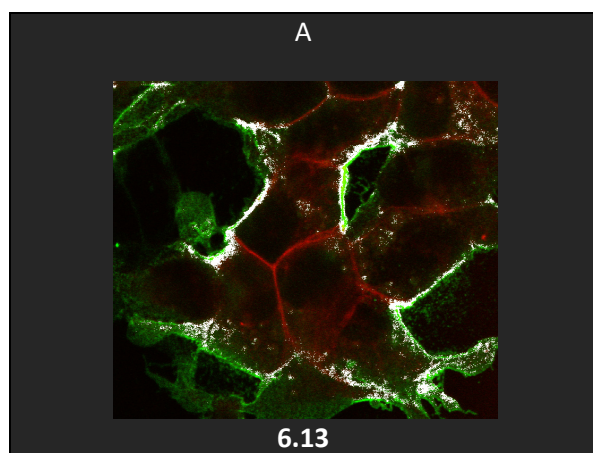
Figure 6.5: Colocalisation experiments (**6.13**); HEK293 FLAG-hH$_2$R-His$_6$ cells were fixed with 4 % PFA as previously described (hH$_2$R-immunostaining: rabbit-anti-FLAG-Antibody, Cy2-conj. 2nd antibody); Cy2-conj. 2nd antibody attached to the hH$_2$R in green (488/LP505, 71 µm); in red: **6.13** (633 nm/LP650, 90 µm); in white: colocalisation, C-Apochromat 40x/1. 2W

After fixation (fixed cells kindly provided by Dietmar Gross[32]) of the cells binding the fluorescent ligand and staining with a Cy2 conjugated antibody against H$_2$R, colocalisation of bound fluorescent ligand and stained receptor was observed (Figure 6.6, colocalisation visible as white regions). To compare binding to HEK293-FLAG-hH$_2$R-His$_6$ cells and to HEK293-hH$_2$R-qs5-HA cells **6.13** was investigated at both cell lines (Figure 6.6, A3-A4). High total binding was detected on HEK293-hH$_2$R-qs5-HA cells with a slightly higher unspecific binding than on HEK293 FLAG-hH$_2$R-His$_6$ cells.

A1

Total binding of **6.13** (c: 80 nM), 30 min

A2

unspecific binding of **6.13** (c: 80 nM), in the presence of 10 µM famotidine, 30 min

A3

Total binding of **6.13** (c: 80 nM), 30 min

A4

unspecific binding of **6.13** (c: 80 nM), in the presence of 10 µM famotidine, 30 min

B1

Total binding of **6.17** (c: 100 nM), 30 min

B2

unspecific binding of **6.17** (c: 100 nM), in the presence of 10 µM famotidine, 30 min
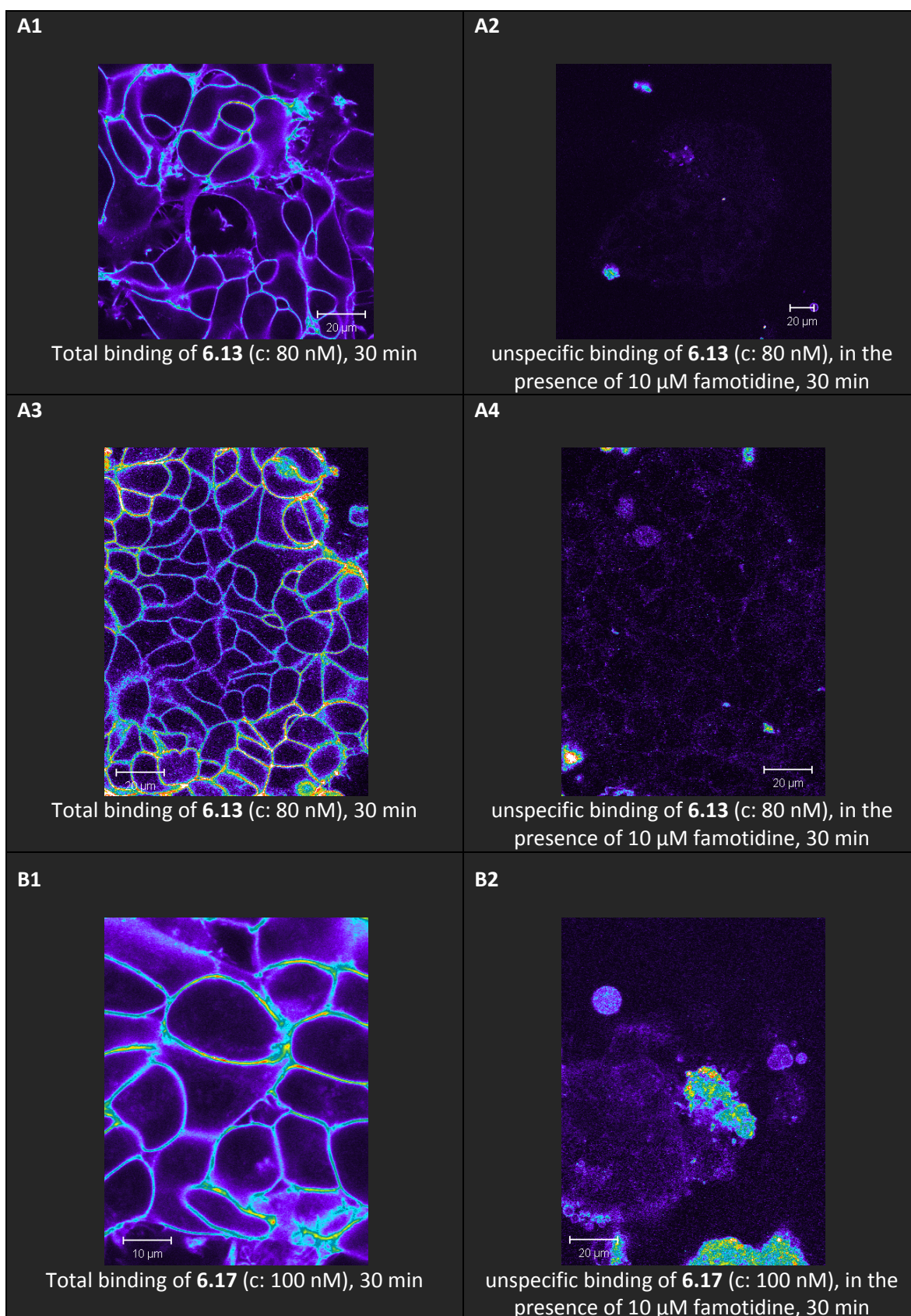
Figure 6.6: Binding of **6.13** and **6.17** to the H_2R expressed in HEK293 FLAG-hH_2R-His_6 cells and HEK293 - hH_2R-qs5-HA (A3-A4); cells were incubated in Leibovitz L15 culture medium with 1 % FCS for 30 min at 37 °C; C-Apochromat 40x/1.2W, 633 nm/LP650;

C1

Total binding of **6.23** (c: 80 nM),20min

C2

uspecific binding of **6.23** (c: 80 nM), in the presence of 10 μM famotidine, 20 min, right panel: autofluorescence

D1

Total binding of **6.19** (c: 100 nM),16 min

D2

unspecific binding of**6.19** (c: 100 nM), in the presence of 10 μM famotidine, 11 min

D3

Total binding of **6.19** (c: 100 nM),60 min

D4

unspecific binding of **6.19** (c: 100 nM), in the presence of 10 μM famotidine, 60 min
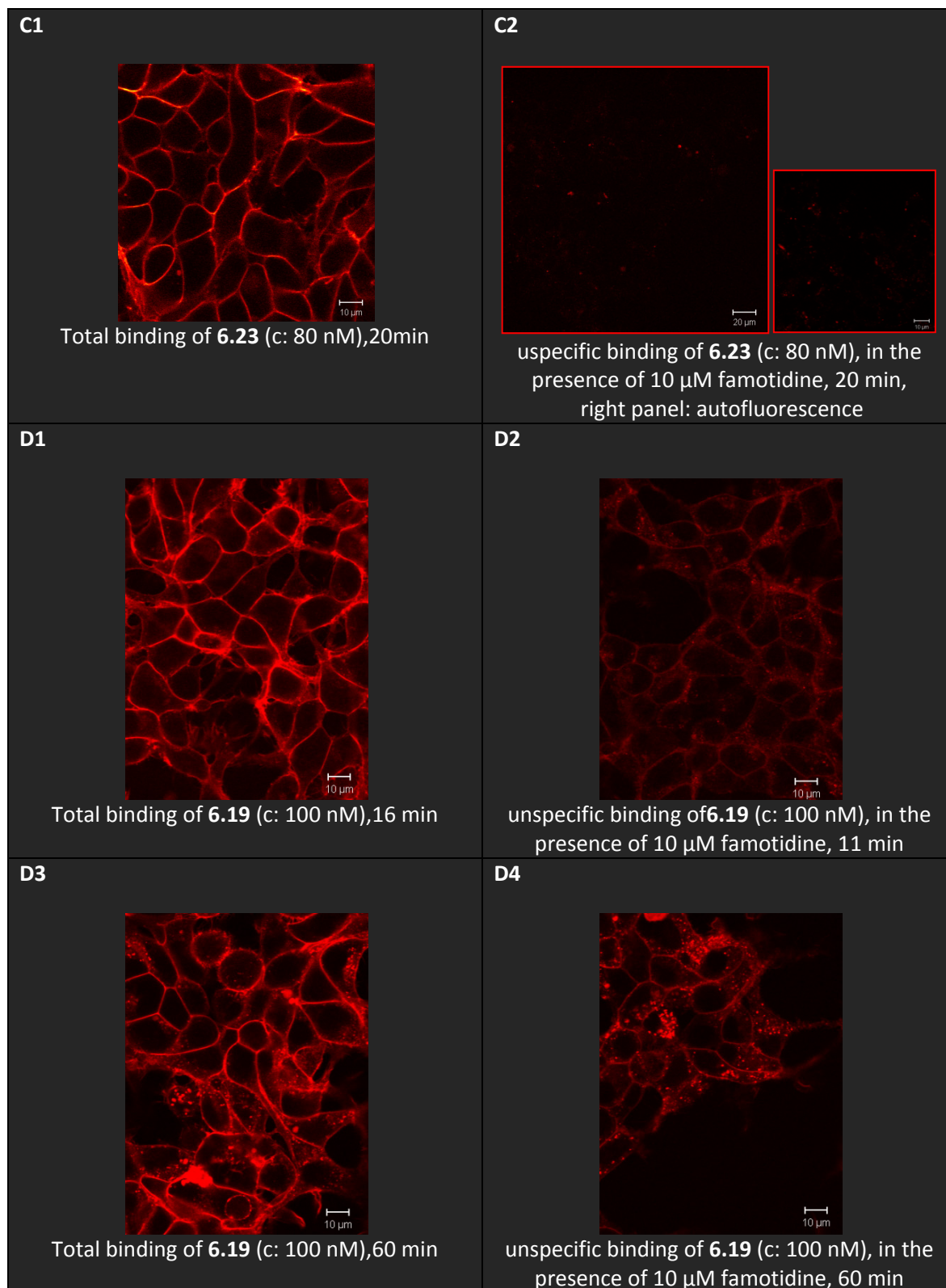
Figure 6.7: Binding of **6.13** and **6.17** to the H_2R expressed in HEK293-FLAG-hH_2R-His$_6$ cells; cells were incubated in Leibovitz L15 culture medium with 1 % FCS for 30 min at 37 °C; C-Apochromat 40x/1.2W, 633 nm/LP650;for C1 and C2 488 nm, LP 615nm;

In case of compound **6.19** cellular uptake was detectable already after incubation periods >16 min (Figure 6.7, D1-D2) and became obvious to a high extent after 1 h (Figure 6.7, D3-D4). Additionally, unspecific binding was remarkable higher compared to the other ligand.

Regarding the fluorescent ligands with moderate to low affinity, selected compounds (**6.2**, **6.3** and **6.7**) were investigated for detectable total binding. Under the same conditions as described above, differences between total and unspecific binding were obvious, however, the concentrations (>200 nM) and incubation periods had to be increased (from 30 to 60 min) (cf. **6.7** as an example in appendix). In case of **6.5**, bearing the same fluorophore as **6.19**, enrichment of the compound in the cells was observed after 20 min (see appendix). The same phenomenon was detected for **6.8** but to a lower extent. Consequently, for these ligands the difference between total and unspecific binding was lower as for the squaramide derivatives (data not shown).

6.4 Discussion

The fluorescent compounds proved to have moderate to high potency at the H_2R, with generally high selectivity over the H_1R and H_4R and a moderate selectivity regarding the H_3R. For the potentidine-like cyanoguanidines and amides a, decrease (max 2-6 fold) in potency, often observed for fluorescent ligands, did not occur. On the contrary, with ligand **6.5** even an increase (7 fold) in activity was accomplished. However, this increase in activity is accompanied by cellular uptake as detected by confocal microscopy. In case of the cyanoguanidine **6.3** a partial agonistic activity reported in the literature[20] was not confirmed. Cleavage of the cyanoguanidine to a guanidine might be an explanation for the previously detected partial agonism. Therefore, during purification and handling of cyanoguanidines strongly acidic conditions were strictly avoided. Variations in the pharmacophoric moieties and the use of H_2R antagonist core structures lacking the urea equivalent as building blocks resulted in only moderately active antagonists. However, for these substances even increased potency compared to the parent compounds was detected (e.g. **6.27**). Although characterization of these compounds was possible by flow cytometry and confocal microscopy, the application is limited due to very low affinity and intracellular accumulation (e.g. **6.5**).

The most potent ligands were the fluorescently labelled squaramides with activities in the two- to three-digit nanomolar range. Compared to the corresponding building blocks there was a 2.6- 16 fold decrease in potency. The remaining H_2R antagonistic potency was still remarkably high

due to the pronounced binding affinity of the pharmacophoric moiety which is superior to that of the other H_2R antagonist classes. As fluorophoric moieties all cyanine dyes, except S0586 and Bodipy and Py dyes turned out to be favourable as labels. By contrast the fluorescein linked compound, a moderate antagonist, with high unspecific binding was inapplicable to fluorescence based methods, thus substantiating results from previous studies[10-11].

In the S0536 coupled set of compounds a tendency towards higher potency at the hH_2R with spacer lengths of 4-8 methylene groups was observed (GTPase assays, exception: **6.14**). This phenomenon was less pronounced than for the parent compounds, and not obvious in the cellular assay, suggesting a minor contribution of the spacer length to potency. Comparing the potentidine-like amides, cyanoguanidines and squaramides, in general, all used dyes (except S0586 and carboxyfluorescein) could be used to obtain potent fluorescent H_2R antagonists. As the major difference in the pharmacophoric moiety of these compounds is the chemical nature of the urea equivalent, obviously this group is crucial in maintaining affinity for the H_2R when fluorophores are introduced. The squaramides were superior to the other urea equivalents. Furthermore, it may be speculated that fluorophores bearing charged groups are beneficial, as the corresponding labelled compounds did not or only to a low extent (**6.8**) enter the cells. A clear preference in potency for one of the fluorophores was not observed. The bulky cyanine and bodipy dyes as well as the small Py dyes were tolerated.

Looking more closely at the most potent ligands **6.13, 6.16, 6.17, 6.19** and **6.23,** all of them were applicable at concentrations below 200 nM to flow cytometric competition binding and confocal microscopy. High quantum yields in buffers containing small amounts of protein suggest with high signal-to-noise ratios for all examined compounds. The cyanine and Py bearing ligands were superior to the bodipy coupled ligands, as they were not accumulated in the cells when investigated by confocal microscopy. Bodipy linked ligands had higher unspecific binding. Additionally, compound **6.19** was found to bind to the H_4R with K_i-values in the nanomolar range. Application of **6.13**, **6.17** and **6.23** as standard ligands in competition binding experiments (flow cytometry) led to K_i-values for the various agonists and antagonists, which were in the same rank order as in radioligand competition binding experiments with [^{3}H]tiotidine using the same cell line. Anyway, the affinity of the agonists histamine, arpromidine and dimaprit was lower than reported for GTPase assays (Sf9 cell membranes expressing the hH_2R $G_{s\alpha S}$ fusion protein[24]) and radioligand binding assays ([^{125}I]IAPT; CHO cells expressing the H_2R[31]). These test sytems differ with respect to conditions (solvents, volumes, incubation times, whole cells versus membranes) and receptor expression systems. For example, the artificial fusion proteins are used in the GTPase assays.

These differences could account for the diverging data. Another explanation might be different association and dissociation kinetics of competitor and fluorescent ligand.

6.5 Summary and conclusion

The aim of this work was to design and synthesize fluorescent ligands on the basis of potentidine like H_2R antagonists with different alkyl spacers. The fluorophores were attached to primary amino groups by acylation with succinimidyl esters or by reaction with pyrylium dyes. The synthesized derivatives proved to be potent and selective for the H_2R compared to the H_1R and H_4R. Cyanine, bodipy, as well as Py dyes were suited to create highly active compounds ($K_{b'} < 200$ nM). Compounds **6.13, 6.17** and **6.23** turned out to be the most potent new entities, and were successfully applied to determine the affinity of agonists and antagonists (flow cytometry) and to detect receptor binding by confocal microscopy. The cyanine dye coupled ligands (with S0536) had the advantage of relatively high quantum yields in the used buffers. This facilitated measurements due to a favorable signal-to-noise ratio. Anyway both kinds of dyes (cyanine and Py dyes) were appropriate for the preparation of fluorescent H_2R ligands, which turned out to be valuable H_2R ligands for optical detections of the respective receptors on living cells and tissues. Furthermore, we have ligands in hand, which can be excited either with the argon (Py dye coupled ligands) or the red diode laser (Cyanine dye coupled ligands). These ligands might be useful as reference compounds and pharmacological tools for fluorescence based screening of new H_2R ligands as well as for detailed pharmacological characterisations. Future work in this field should be focused on improving the H_2R selectivity profile in order to eliminate the additional H_3R antagonistic activity.

6.6 Experimental section

6.6.1 Chemistry

6.6.1.1 General conditions

Chemicals and solvents were purchased from commercial suppliers Merck KGaA (Darmstadt, Germany), Acros Organics (Geel, Belgium) and Sigma Aldrich GmbH (Munich, Germany) and used without further purification unless otherwise stated. DMF was stored over 3 Å molecular sieves. Pyrylium dyes Py-1 and Py-5 (tetrafluoroborate salts) were kindly provided by the Institute of Analytical Chemistry, Chemo- and Biosensors at the University of Regensburg (Prof. Dr. O. S.

Wolfbeis). These dyes are also commercially available from Active Motif Chromeon (www.activemotif.com). The succinimidyl esters of fluorescent dyes S0536, S0535, and S0586 were obtained from FEW Chemicals (Bitterfeld-Wolfen, Germany), Dy630 and Dy675 from Dyomics (Jena, Germany). The succinimidyl ester of Bodipy650/665-X (SE) and 6-(fluorescein-5-carboxamido)hexanoic acid *single isomer* (5-SFX) were purchased from Molecular Probes (now Invitrogen; Darmstadt, Germany). Methods for preparative HPLC and other analytical methods see chapter 3.

UV- and VIS spectra were recorded on a Cary 100 UV/VIS photometer (Varian Inc., Mulgrave, Victoria, Australia).

General conditions like HPLC conditions see chapter 3.

6.6.1.2   *Preparation of fluorescent ligands*

General procedure 1: Coupling of primary amines with succinimidyl esters of fluorescent dyes

Primary amines (1.2-3.7 eq) were solved in 0.3-1 ml of solvent, depending on solubility (MeCN, MeOH, EtOH or DMSO) under addition of 2-3 drops of Et$_3$N to adjust to a pH of 8-9. A pH of 8-9 was necessary to prevent protonation of the amino group, which would hinder the reaction. The succinimidyl esters of the fluorescent dyes (1 eq) were dissolved in 0.5 - 1.5 ml of the appropriate solvent (MeCN, MeOH, EtOH, DMSO) and added to the amine containing solution. The reaction was performed in small flasks at rt under stirring in the dark overnight. Purification was performed by preparative HPLC. The reaction mixtures for preparative HPLC were adjusted with MeCN and TFA (0.05 or 0.1 %) to a volume of 4-5 ml, containing the same amount of MeCN /TFA as the starting eluent mixture or a maximum of MeCN corresponding to the two-fold concentration of MeCN in the starting eluent. MeCN was removed under reduced pressure and the remaining water was removed by lyophilisation. The fluorescent compounds were obtained as yellow or blue semi solids.

Compound 3.7 coupled to S0536 (6.1)

Compound **3.7** (1.13 mg, 3.7 µmol, 1.9 eq) and S0536 (1.32 mg, 1.9 µmol, 1 eq) in 0.9 ml MeCN + Et$_3$N (pH 8-9); preparative HPLC (system 1, 254 nm, B: 0.5 % TFA); product as blue semi solid,

yield 0.28 mg,(13 %); <u>RP-HPLC </u>(210 nm, gradient 1): 96.8%, (t_R= 19.4 min, k= 6.6); <u>ESMS</u>: m/z 892 [MH$^+$], 447 [(M+2H)$^{2+}$]; $C_{52}H_{69}N_5O_6S$ x $C_4H_2F_6O_4$ (1120)

Compound 3.8 coupled to S0536 (6.2)

Compound **3.8** (1.5 mg, 4.1 µmol, 3.7 eq) in 1 ml ethanol + Et$_3$N (pH 8-9); S0536 (0.78 mg, 1.1 µmol, 1 eq) in 1 ml ethanol; preparative HPLC (system 1, 254 nm); product as blue semi solid, yield 0.56 mg, 43 %; <u>RP-HPLC (</u>210 nm, gradient 1,): 98.1 %, (t_R= 20.37 min, k= 7.0); <u>ESMS:</u> (CH$_2$Cl$_2$/MeOH/10 mM NH$_4$OAc) m/z 948.7 [MH$^+$], 479.9 [(M+2H)$^{2+}$]; $C_{56}H_{77}N_5O_4S$ x $C_4H_2F_6O_4$ (1176)

Compound 3.5 coupled to S0536 (6.3)

Compound **3.5** (1.8 mg, 5 µmol, 3 eq) in 0.6 ml MeCN + Et$_3$N (pH 8-9) and S0536 (1.15 mg, 1.6 µmol, 1 eq) in 0.6 ml MeCN preparative HPLC (system 1, 254 nm); product as blue semi solid, yield: 0.29 mg (16 %); <u>RP-HPLC</u>: (gradient 1, 210 nm): 99.5 % (t_R= 19.00 min, k= 6.5); <u>ESMS</u>: (CH$_2$Cl$_2$/MeOH/10 mM NH$_4$OAc) m/z 945.5 [MH$^+$]; $C_{54}H_{72}N_8O_5S$ x $C_4H_2F_6O_4$ (1173)

Compound 3.6 coupled to S0536 (6.4)

Compound **3.6** (1.47 mg, 3.5 µmol, 1.8 eq) in 0.4 ml MeCN + Et$_3$N (pH 8-9) and S0536 (1.32 mg, 1.9 µmol, 1 eq) in 0.9 ml MeCN; preparative HPLC (system 1, 254 nm, B: 0.5 %TFA); product as blue semi solid, yield 0.75 mg (33 %); <u>RP-HPLC</u> (gradient 1, 210 nm): 99 % (t_R=20.7 min, k= 7.2); <u>ESMS</u>: m/z 1001.4 [MH$^+$], 501.3 [(M+2H)$^{2+}$]; $C_{58}H_{80}N_8O_5S$ x $C_4H_2F_6O_4$ (1229)

Compound 3.5 coupled to Bodipy 650/665-X, SE (6.5)

Compound **3.5** (1.3 mg, 3.6 µmol, 2 eq) in 1 ml MeOH + Et$_3$N (pH 8-9) and Bodipy 650/665-X, SE (1.12 mg, 1.7 µmol, 1 eq) in 1.5 ml DMSO; preparative HPLC (system 1, 220 nm, B: 0.5 % TFA); green to blue semi solid, yield 0.52 mg (31 %); <u>RP-HPLC 1. (</u>210 nm, gradient 1) 98 %, (t_R = 21.46 min, k = 7.5); and 2. (210 nm) gradient: 0 min: 45/55, 20 min: 90/10 30 min 90/10): (t_R = 16.94

min, k = 5.67); <u>ESMS</u>: (MeOH/10 mM NH$_4$OAc) m/z 888 [MH$^+$], 524 [(M+2H)$^{2+}$]; C$_{48}$H$_{57}$BF$_2$N$_8$O$_6$S x C$_2$HF$_3$O$_2$ (1001)

Compound 3.5 coupled to Dy675 (6.7)

Compound **3.5** (1.2 mg, 3.3 µmol, 2.8 eq), Dy 675 (1 mg, 1.2 µmol, 1 eq) in 2.5 ml MeOH + Et$_3$N (pH 8-9); preparative HPLC (system 1, 220 nm, B: 0.5 % TFA); blue semi solid, yield 0.88 mg (59 %); <u>RP-HPLC </u>(210 nm, gradient 0 min: 45/55, 20 min: 90/10 30 min: 90/10): > 99 %, (t$_R$= 14.4 min, k= 4.7); <u>ESMS</u>: (MeOH/10 mM NH$_4$OAc) m/z 1048 [MH$^+$], 524 [(M+2H)$^{2+}$]; C$_{61}$H$_{74}$N$_8$O$_6$S x C$_4$H$_2$F$_6$O$_4$ (1275)

Compound 3.4 coupled to S0535 (6.8)

Compound **3.4** (2 mg, 8 µmol, 2.9 eq) in 1 ml MeCN + Et$_3$N (pH 8-9); S0535 (2 mg, 2.8 µmol, 1 eq) in 1 ml MeCN; semi blue solid, yield 1.1 mg (37 %); preparative HPLC (system 2-1, 220 nm); <u>RP-HPLC 1. </u>(210 nm, gradient 1,): 91.4 %, (t$_R$= 22.8 min, k= 8.0), 2. (gradient: 0 min: 35/65, 90, 25 min 90/10, 35 min 95/10, 210 nm) 97 % (t$_R$= 22.3 min, k= 7.8); <u>ESMS</u>: m/z 885.6 [MH$^+$], 443.2 [(M+2H)$^{2+}$]; C$_{54}$H$_{68}$N$_4$O$_5$ x C$_4$H$_2$F$_6$O$_4$ (1113)

Compound 3.10 coupled to S0536 (6.9)

Compound **3.9** (1.78, 4.6 µmol) in 0.6 ml MeCN + Et$_3$N (pH 8-9) and S0536 (2 mg, 2.8 µmol, 1.6 eq) in 0.6 ml MeCN; preparative HPLC (system 1, 254 nm); product as blue semi solid, yield: 0.62 mg, (18 %); <u>RP-HPLC</u>: (gradient 1, 210 nm): 99.0 % (t$_R$ =19.05 min, k = 6.5); <u>ESMS:</u> (MeCN/MeOH 10 mM NH$_4$OAc) 973.6 [MH+], 487.4 [(M+2H)$^{2+}$]; C$_{56}$H$_{72}$N$_6$O$_7$S x C$_4$H$_2$F$_6$O$_4$ (1201)

Compound 3.10 coupled to S0536 (6.10)

Compound **3.10** (1.2 mg, 3 µmol, 2.7 eq) in 1 ml EtOH + Et$_3$N (pH 8-9) and S0536 (0.78 mg, 1.1 µmol, 1 eq) in 1.1 ml EtOH; preparative HPLC (system 1, 220 nm); blue semi solid 0.33 mg (25 %);

RP-HPLC (210 nm, gradient 1,): 91 %, (t_R = 19.9 min, k = 6.8); ESMS: (CH_2Cl_2/ MeOH 10mM NH_4OAc) 987.6 [MH^+], 494.5 [$(M+2H)^{2+}$]; $C_{57}H_{74}N_6O_7S$ x $C_4H_2F_6O_4$ (1215)

Compound 3.11 coupled to S0536 (6.11)

Compound **3.11** (1.5 mg, 3.6 µmol, 1.8 eq) in 0.3 ml MeOH + Et_3N (pH 8-9), S0536 (1.6 mg, 2 µmol, 1 eq) in 0.5 ml MeCN; preparative HPLC (system 1, 254 nm); blue semi solid, yield 1.22 mg (50 %); RP-HPLC (210 nm, gradient 1,): 98.4 %, (t_R = 19.75 min, k = 6.78); ESMS: (MeCN, TFA) m/z 1001.8 [MH^+], 501.4 [$(M+2H)^{2+}$]; $C_{58}H_{76}N_6O_7S$ x $C_4H_2F_6O_4$ (1229)

Compound 3.12 coupled to S0536 (6.12)

Compound **3.12** (1.14 mg, 2.6 µmol, 1.5 eq) in 1 ml MeOH + Et_3N (pH 8-9); S0536 (1.2 mg, 1.7 µmol, 1 eq) in 0.5 ml MeCN, preparative HPLC (system 1, λ= 254 nm); product as blue semi solid, yield 0.82 mg, (39 %); RP-HPLC (210nm, gradient 1,): 98.4 %, (t_R = 19.6 min, k = 6.7); ESMS: (MeCN/ MeOH 10 mM NH_4OAc) m/z 1015.7 [MH^+], 508.4 [$(M+2H)^{2+}$]; $C_{59}H_{78}N_6O_7S$ x $C_4H_2F_6O_4$ (1243)

Compound 3.13 coupled to S0536 (6.13)

Compound **3.13** (1.4 mg, 3.2 µmol, 1.9 eq) in 0.3 ml MeOH + Et_3N (pH 8-9) and S0536 (1.2 mg, 1.7 µmol, 1 eq) in 0.5 ml MeCN; preparative HPLC (system1, 254 nm); blue semi solid, yield 0.65 mg (31 %); RP-HPLC (210 nm, gradient 1,): 98.9 %, (t_R = 20.4 min, k = 7.0); ESMS: (MeCN/ MeOH 10mM NH_4Ac) 1029.7 [MH^+], 515.4 [$(M+2H)^{2+}$]; $C_{60}H_{80}N_6O_7S$ x $C_4H_2F_6O_4$ (1257)

Compound 3.14 coupled to S0536 (6.14)

Compound **3.14** (0.9 mg, 2 µmol, 2 eq) in 0.5 ml MeOH + Et_3N (pH 8-9); S0536 (0.63 mg, 0.9 µmol, 1 eq) in 1 ml MeOH; preparative HPLC (system 1, 254 nm); product as blue semi solid, yield 0.36 mg, 32 %; RP-HPLC (210 nm, gradient1,): 99 %, (t_R = 20.9 min, k = 7.2); ESMS: (CH_2Cl_2/

MeOH, 10 mM NH$_4$OAc) 1043.7 [MH$^+$], 522.5 [(M+2H)$^{2+}$], 533.9 [(MH+Na)$^{2+}$]; C$_{61}$H$_{82}$N$_6$O$_7$S x C$_4$H$_2$F$_6$O$_4$ (1271)

Compound 3.15 coupled to S0536 (6.15)

Compound **3.15** (0.6 mg, 1.3 µmol, 1.4 eq) in 0.75 ml MeOH + Et$_3$N (pH 8-9); S0536 (0.64 mg, 0.9 µmol, 1 eq) in 0.75 ml MeOH; preparative HPLC (system 1, 254 nm); product as blue semi solid, yield 0.44 mg (38 %); <u>RP-HPLC</u> (220 nm, gradient 1,): 98.7 %, (t$_R$ = 20.9 min, k = 7.2); <u>ESMS</u>: (CH$_2$Cl$_2$/ MeOH 10 mM NH$_4$Ac) 1057.6 [MH$^+$], 529.4 [(M+2H)$^{2+}$]; C$_{62}$H$_{84}$N$_6$O$_7$S x C$_4$H$_2$F$_6$O$_4$ (1285)

Compound 3.11 coupled to S0586 (6.16)

Dye S0586 (1 mg, 1.24 µmol, 1eq), **3.11** (1 mg, 2.4 µmol, 1.9 eq), 2 ml MeOH, preparative HPLC (system 1, flow 38 ml/min, 254 nm); product as blue semi solid, yield 1.4 mg (78 %); <u>RP-HPLC</u> (210 nm, gradient 1,): 99.4 %, (t$_R$ = 14.4 min, k = 4.7); <u>ESMS</u>: (MeCN/TFA) m/z 1081.5 [M$^+$], 541.5 [(M+H)$^{2+}$]; C$_{58}$H$_{75}$N$_6$O$_{10}$S$_2^-$ x C$_6$H$_3$F$_9$O$_6$ (1422.5)

Compound 3.11 coupled to Dy675 (6.17)

Compound **3.11** (1.3 mg, 3.1 µmol, 1.9 eq) in 1 ml MeOH + Et$_3$N (pH 8-9); Dy675 (1.3 mg, 1.6 µmol, 1 eq) in 1 ml MeOH; preparative HPLC (system 1, 220 nm); product as blue semi solid, yield 0.77 mg (37 %); RP-HPLC: (210 nm, gradient: A/B 0min 35/66, 20min 90/90, 30 min 90/10) 94.4 % (t$_R$= 19.8 min, k= 6.8); <u>ESMS</u>: (MeOH/10 mM NH$_4$OAc) m/z 1103.7 [MH$^+$], 552.5 [(M+2H)$^{2+}$]; C$_{65}$H$_{78}$N$_6$O$_8$S x C$_4$H$_2$F$_6$O$_4$ (1331.5)

Compound 3.13 coupled to Dy675 (6.18)

Compound **3.13** (3.7 mg, 8.3 µmol, 2.3 eq) in 1 ml MeOH + Et$_3$N (pH 8-9) and Dy675 (2.9 mg, 3.6 µmol, 1 eq) in 1 ml MeOH; preparative HPLC (system 1, 220 nm); product as semi blue solid, yield 0.77 mg (16 %); RP-HPLC (gradient: A/B 0min 40/60, 20min 90/90 30min90/90) flow: 0.7) 97.2% (t$_R$= 21.2 min, k= 7.35); <u>ESMS</u>: (CH$_2$Cl$_2$/MeOH/10 mM NH$_4$OAc) m/z 1131.7 [MH$^+$], 566.4 [(M+2H)$^{2+}$]; C$_{67}$H$_{82}$N$_6$O$_8$S x C$_4$H$_2$F$_6$O$_4$ (1359.5)

Compound 3.12 coupled to Bodipy 650/665-X,SE (6.19)

Compound **3.12** (1.8 mg, 4.2 µmol, 1.8 eq) and Bodipy (1.5 mg, 2.3 µmol, 1 eq) in 2 ml MeOH + Et$_3$N (pH 8-9); preparative HPLC (system 2-1, 220 nm); product as green to blue semi solid, yield 0.55 mg (22 %); RP-HPLC (210 nm, gradient 0 min: 45/55, 30 min: 90/10): 93.2 %, (t$_R$= 19.6 min, k= 6.7); ESMS: m/z 957.4 [MH$^+$], 479.0 [(M+2H)$^{2+}$]; C$_{53}$H$_{64}$BF$_2$N$_8$O$_6$ x C$_2$HF$_3$O$_2$ (1072)

Compound 3.13 coupled to Bodipy 650/665-X,SE (6.20)

Compound **3.13** (0.8 mg, 1.8 µmol, 1.2 eq) and Bodipy 650/665-X,SE (1.0 mg, 1.5 µmol, 1 eq) in 2.5 ml MeOH + Et$_3$N (pH 8-9); preparative HPLC (system 2-1, 220 nm); product as green to blue semi solid, yield 0.15 mg (11 %); RP-HPLC: 1. (gradient 1, 210nm): 98 % (t$_R$= 23.2 min, k= 8.1); 2. (210nm, gradient 0 min: 35/65, 25 min: 90/10, 35 min 95/5): 99 % % (t$_R$= 21.3 min, k= 7.4); ESMS: m/z 971.5 [MH$^+$], 486.2 [(M+2H)$^{2+}$]; C$_{54}$H$_{65}$BF$_2$N$_8$O$_6$ x C$_2$HF$_3$O$_2$ (1085)

Compound 3.13 coupled to 5-SFX (6.21)

Compound **3.13** (1.3 mg, 2.9 µmol, 1.7 eq), 5-SFX (1 mg, 1.7 µmol, 1 eq) in 1.3 ml MeOH + Et$_3$N (pH 8-9), preparative HPLC (system 1, 254 nm, B: 0.5 %TFA); product as yellow semi solid, yield 1.48 mg (85 %); RP-HPLC (210 nm, gradient 1,): 96.4 %, (t$_R$= 16.2 min, k= 5.4); ESMS: (MeCN/TFA) m/z 914.4 [MH$^+$], 457.7 [(M+2H)$^{2+}$]; C$_{52}$H$_{59}$N$_5$O$_{10}$ x C$_2$HF$_3$O$_2$ (1027.5)

Compound 3.13 coupled to S0535 (6.22)

Compound **3.13** (1.0 mg, 2.2 µmol, 1.4 eq), S0535 (1.23 mg, 1.6 µmol, 1 eq) in 1.5 ml MeOH + Et$_3$N (pH 8-9; preparative HPLC (system 1, 254 nm); product as blue semi solid 1.37 mg (65 %); RP-HPLC (210 nm, gradient 1,): 91.4 %, (t$_R$= 22.8 min, k= 8.0); ESMS: (MeCN/TFA) m/z 1079.8 [M$^+$], 540.3 [(M+H)$^{2+}$]; C$_{64}$H$_{82}$N$_6$O$_7$S$_2$ x C$_4$H$_2$F$_6$O$_4$ (1307.5)

Compound 3.28 coupled to S0536 (6.26)

Compound **3.28** (0.81mg, 2.7 µmol, 2 eq) and S0536 (0.97 mg, 1.38 µmol, 1 eq) in 1.5 ml MeCN /200µl DMSO + Et$_3$N (pH 8-9); preparative HPLC (system 2-1, 220 nm); blue semi solid, yield 0.28

mg (19 %); RP-HPLC: (gradient: 1, 220 nm) 98 % (t_R= 16.9 min, k= 5.6); ESMS: m/z 882.7 [MH$^+$], 441.7 [(M+2H)$^{2+}$]; $C_{47}H_{63}N_9O_4S_2$ x $C_4H_2F_6O_4$ (1110.2)

Compound 3.28 coupled to Dy630 (6.27)

Compound **3.28** (1.6 mg, 5.4 µmol, 3.9 eq) in MeCN 2.5 ml + Et$_3$N (pH 8-9); Dy630 (1 mg, 1.37 µmol, 1 eq) in 300 µl DMF; preparative HPLC (system 2-1, 220 nm); product as blue semi solid, yield 0.62 mg (41 %); RP-HPLC: (gradient: 1, 220 nm) 92 % (t_R= 19.7 min, k= 6.8); ESMS: m/z 912.7 [MH$^+$], 456.7 [(M+2H)$^{2+}$], 614.8 [(2M+2H+NH$_4$)$^{3+}$],609.1 [(2M+3H)$^{3+}$]; $C_{48}H_{65}N_9O_5S_2$ x $C_4H_2F_6O_4$ (1140.3)

Compound 3.26 coupled to S0535 (6.28)

Ligand **3.26** x 2 HCl (1.6 mg, 5.3 µmol, 1.1 eq) in 1 ml MeOH + Et$_3$N (pH 8-9), S0535 (3.5 mg, 4.7 µmol, 1 eq) in 1 ml MeCN ; preparative HPLC (system 2-1, 220 nm); product as blue semi solid, yield 3.74 mg (73 %); RP-HPLC: (gradient: 1, 220 nm) 99.7 % (t_R= 20.4 min, k= 7.03); ESMS: m/z 912.7 [MH$^+$], 456.7 [(M+2H)$^{2+}$], 614.8 [(2M+2H+NH$_4$)$^{3+}$],609.1 [(2M+3H)$^{3+}$]; $C_{46}H_{57}N_7O_4S_3$ x $C_4H_2F_6O_4$ (1095.4)

Compound 6.25 coupled to S0535 (6.29)

Compound **6.25** x HBr (6 mg, 22.4 µmol, 13.9 µmol, 2.2 eq) in 1ml MeOH + Et$_3$N (pH 8-9); S0535 (4.7 mg, 6.3 µmol, 1 eq) in 1ml MeOH + Et$_3$N (pH 8-9); product as semi blue solid, yield 3.3 mg (45 %), preparative HPLC (system 2-1, 220 nm); RP-HPLC (210 nm, gradient 1,): 98 %, (t_R= 18.5 min, k= 6.4); ESMS: m/z 905.5 [MH$^+$], 604.3 [(2M+3H)$^{3+}$], 453.2 [(M+2H)$^{2+}$]; $C_{52}H_{68}N_6O_4S$ x $C_4H_2F_6O_4$ (1133.2)

General procedure 2: Coupling of primary amines with pyrylium dyes

Primary amines (1.5-2 eq) were dissolved in 1-1.5 ml MeOH under addition of Et$_3$N to ensure a pH of 8-9. Py1 or Py5 (1 eq) were dissolved in 0.15-0.4 ml DMF plus 0-0.4 ml MeOH and added to

the amine containing solution. The reaction was performed in small flasks at rt under stirring in the dark for 3 h (solution turns from blue to red). Purification was done by preparative HPLC as described above. MeCN was removed from the product fractions under reduced pressure and the remaining water was eliminated by lyophilisation. The fluorescent compounds were obtained as red semi solids.

Compound 3.5 labelled with Py1 (6.6)

Compound **3.5** (1.8 mg, 5 µmol, 2 eq) in 1.5 ml MeOH + Et_3N (pH 8-9) and Py1 (1 mg, 2.5 µmol, 1 eq) in DMF 0.4 ml; product as semi red solid, yield 0.75 mg (34 %); preparative HPLC (system 1, 254 nm); <u>RP-HPLC</u> (210 nm, gradient 1,): 97.3 % (t_R= 18.7 min, k= 6.4); <u>ESMS</u>: (MeOH) m/z 646.3 [M^+], 323.6 [$(M+H)^{2+}$]; $^+$]; $C_{40}H_{52}N_7O^+$ x $C_2HF_3O_2$ (874.4)

Compound 3.11 labelled with Py5 (6.23)

Compound **3.11** (1.87 mg, 4.5 µmol, 1.5 eq) in 1.8 ml MeOH + Et_3N (pH 8-9) and Py5 (1.1 mg, 3 µmol, 1eq) inDMF 150 µl preparative HPLC (system 1, 254 nm, B: 0.5 % TFA); product as red semi solid, yield 1.43 mg (53 %); <u>RP-HPLC</u> (254nm, gradient 1,): 98 %, (t_R= 15.8 min, k= 5.2); <u>ESMS</u>: (MeCN/MeOH/10 mM NH_4OAc) m/z 676.4 [M^+]; $C_{52}H_{42}N_5O_3^+$ x $C_4H_2F_6O_4$ (904.96)

Compound 3.11 labelled with Py1 (6.24)

Compound **3.11** (3.3 mg, 4.5 µmol, 1.2 eq) in 1.8 ml MeOH + Et_3N (pH 8-9), Py1 (1.5 mg, 3.8 µmol, 1 eq) in DMF 200 µl + 300 µl MeOH, preparative HPLC (system 1, 254 nm, B: 0.5 % TFA); red semi solid, yield 1.17 mg (33 %); <u>RP-HPLC</u> (210nm, gradient 1,): 97.8 %, (t_R= 18.6 min, k= 6.3); <u>ESMS</u>: m/z 702.4 [M^+], 351.6 [$(M+H)^{2+}$]; $C_{44}H_{56}N_5O_3^+$ x $C_4H_2F_6O_4$ (931)

6.6.2   Pharmacological methods

6.6.2.1   *Steady state GTPase assay*

See chapter 3

6.6.2.2   *Fluorimetric Ca²⁺ assay on U373-MG cells*

See chapter 3

6.6.2.3   *Radioligand binding assay on HEK293-FLAG-hH₃R-His₆ cells*

See chapter 3

6.6.2.4   *Quantum yield determination*

General

All chemicals, solvents and culture media were purchased from commercial suppliers. BSA was from Serva GmbH (Heidelberg, Germany). Quantum yields were determined with a Cary Eclipse spectrofluorimeter and a Cary 100 UV/VIS photometer (Varian Inc., Mulgrave, Victoria, Australia). Cresyl violet perchlorate was used as red fluorescent standard (Acros Organics, Geel, Belgium) with a quantum yield of 54 % in ethanol[33]. Determination of the spectra was performed in acryl cuvettes (10 × 10 mm, Ref. 67.755, Sarstedt, Nümbrecht, Germany).

Determination of quantum yields

The quantum yields were determined by analogy with the methods described previously with cresyl violet as red fluorescent standard[29, 34]. Quantum yields were determined in three different solvents: ethanol, PBS (pH= 7.4) and PBS + 1 % BSA. The fluorescent ligands were employed at a concentration range of 0.5-6 µM, ensuring absorbances between 0.05 and 0.2 at the respective excitation wavelength. As excitation wavelength the absorption maximum (e.g. Py-labelled ligands) or the absorption at a plateau of the absorption spectrum (e.g. with S0535/S0536 labelled ligands labelled compounds) can be chosen. The dilutions of the fluorescent compounds were freshly prepared from 1 mM, 500 µM or 100 µM stock solutions in DMSO or 10 % DMSO, respectively, before the experiment. Blank spectra were recorded with samples containing the respective solvent and the same amount of DMSO as those containing the fluorescent ligands. To avoid bleaching effects, the samples were protected from light between measurements. The used instrument settings are shown in Table 6.6.

Table 6.6: Instrument settings at the Cary Eclipse spectrofluorimeter

Instrument settings		Instrument settings	
Photomultiplier voltage	400 V	**Temperature**	22 °C
Excitation spectra: Slit: excitation / emission	5 nm/10 nm	**Emission starting point**	10-20 nm above excitation wavelength
Emission spectra: Slit: excitation / emission	10 nm/10 nm and 10 nm/5 nm	**Scan rate**	Medium
Filter settings: Excitation Emission	auto open		

After recording excitation and emission spectra (including reference spectra) the absorption – and reference spectra (at the UV-spectrometer) were measured within 15-30 min (T= 22 °C, same solution in the same cuvettes).

Analysis

Quantum yield

Quantum yields were calculated according to the following equation[33]:

$$\Phi_{F(X)} = \left(\frac{A_S}{A_x}\right) \times \left(\frac{F_X}{F_S}\right) \times \left(\frac{n_X}{n_S}\right)^2 \times \Phi_{F(S)}$$

A: absorbance of the corrected absorption spectrum at the excitation wavelength
F: area under the corrected emission spectrum
N: refraction index of the solvent
Φ_F: quantum yield [%]
x: investigated fluorescent ligand
s: cresyl violet standard
quantum yield [%] of cresyl violet in ethanol: 54 %

6.6.2.5   *Flow cytometric saturation and competition binding experiments*

General

Used chemicals and solvents were from commercial suppliers unless otherwise noted (see also 7.5.2.5 and 7.5.2.6).. Cell culture and preparation of HEK293-hH$_2$R-qs5-HA cells was done as described in literature[30]. For flow cytometric measurements the FACS Calibur^{TM} flow cytometer

(Becton Dickinson, Heidelberg, Germany) was used according to the following settings (Table 6.7)

Table 6.7: Instrument settings at the FACS Calibur[TM]

Instrument settings		compounds labelled with
Excitation:	488 nm (argon laser)	Py1/Py5
	633 nm (red diode laser)	Cyanine, Bodipy dyes
Emission:	Fl-3:650, λ =670 nm LP	
	Fl4: 800, λ= 661±8 nm	
Threshold:	Forward scatter light (FSC)	
	and sideward scatter light (SSC): **52**	
Secondary parameters	None	
FSC:	E-1	
SSC:	320	
Gated events:	10000	

All fluorescent ligands (stock solution in DMSO) were diluted in a solution of 30 % DMSO (in PBS v/v), famotidine and ranitidine were dissolved in DMSO. Given concentrations in parentheses are final concentrations.

In competition binding experiments, **6.13** (200 nM), **6.15** (350 nM), **6.17** (90 nM) and **6.23** (200 nM) were used as standard ligands at a fixed concentration.

Flow cytometry

HEK293-hH$_2$R-qs5-HA cells were cultured and prepared as described previously[30]. Briefly: In saturation binding experiments each tube contained 196 µl of the cell suspension (cell suspension 1-2 x 10^6 cells/ml) in Leibovitz L15 medium without phenol red. The samples for total binding contained 2 µl of the fluorescent ligand of interest (1) in different concentrations (1 nM-1 µM) and 2 µl of 30 % DMSO (in PBS v/v, 2), whereas the samples for unspecific binding contained 2 µl of the fluorescent ligand (1) plus 2 µl of famotidine (3, final c: 100 µM). Unspecific binding was determined for each concentration of fluorescent ligand. Both solutions (1 and 2 or 1 and 3) were added simultaneously to the cell containing tubes and incubated for 37 min at rt under light protection. Flow cytometric measurements were done as depicted in Table 6.8. Competition binding experiments were done using the same conditions as for saturation binding experiments. Each tube contained 196 µl of the cell suspension. For total binding the samples contained 2 µl of the fluorescent tracer (e.g. **6.23** c: 200 nM) and 2 µl of the ligand of interest (c: 1 nM - 10 mM). Unspecific binding was determined with 2 µl of fluorescent tracer (e.g. **6.23**, c: 200 nM) plus 2 µl of famotidine (c: 100 µM). Data was analyzed with WinMDI 2.8 (details cf. ref[30]).

The geometric means were calculated and curve fitting was done with SigmaPlot® 9.0 (multiple scatter -error bars option). In saturation analysis specific binding was calculated subtracting unspecific binding (geometric mean) from the geometric mean of the sample representing total binding (fluorescent ligand). Unspecific binding was determined with the standard curves, linear curve option. Curve fitting for total and specific binding was done according to ligand binding, one site saturation option to calculate the K_D-value. Competition binding experiments were analyzed subtracting the geometric mean of the samples for unspecific binding from the geometric mean of the investigated ligand (total binding) to get specific binding. IC_{50} values of the investigated ligand were calculated from the resulting competition binding curves using SigmaPlot®9.0. K_i-values could be determined with the Cheng Prussoff equation[35].

6.6.2.6   *Confocal microscopy*

General

All chemicals, solvents and culture media were purchased from commercial suppliers (Sigma Aldrich GmbH, Munich, Germany). The used chambered coverglasses (8 chambers) were Nunc LabTek™ II (Nunc GmbH & Co.KG, Wiesbaden, Germany) and 1 µ-Slides 8 well ibiTreat sterile glasses (ibidi GmbH, Munich, Germany). Cells were cultured in selective culture medium, (DMEM + 10 % FBS + 400 µg / ml G418 + 100 µg / ml hygromycin B) or in Leibovitz' L-15 medium without phenol red (Invitrogen GmbH, Darmstadt, Germany) containing 1 % FBS. Confocal microscopic experiments were performed with a Zeiss Axiovert 200 M microscope, using a LSM 510 laser scanner combined with the C-Apochromat 40 x / 1.2 W corr. The most important settings for the detection of fluorescent ligands are shown in Table 6.7.

Table 6.8: Conditions used in confocal microscopy

Compd.	Excitation (laser transmission)	Filter	Pinhole [µm]
with dyes S0536/S0535/S0586, Dy630/ Dy675, Bodipy650/665-X, SE	633 nm (5-15 %)	LP 650	90
with dyes Py1/Py5 (Cy2 conj antibody)	488 nm (5 %)	LP 615 or LP 505 (LP 505)	90 (71)
Colocalisation experiment with fixed cells	488 nm (5 %)/633 (15 %)	LP505/LP650	71/90

Confocal microscopy

HEK293-hH$_2$R-qs5-HA cells and HEK293-FLAG-hH$_2$R-His$_6$ were cultured according the method described by J. Mosandl [30]. 2- 3 days prior to microscopy, approx. 40,000 cells, cultured in selective culture medium (200 µl, DMEM + 10 % FBS + 400 µg/ml G418 + 100 µg/ml hygromycin B), were seeded per cavity on chambered cover glasses (200 µl in each cavity). The culture medium was replaced by 200 µl of L15, containing 1 % FBS (Biochrom AG, Berlin, Germany), on the day of the investigation. Subsequently 200 µl of L15, including the fluorescent compound (2-fold concentrated), were added to determine total binding. For unspecific binding (different cavity) 200 µl L15 with 1 % FBS, consisting of the fluorescent compound (2-fold concentrated) and the competing agent (famotidine, final concentration 10 µM), were added. Cells were incubated at rt or at 37 °C and images of total and unspecific binding were taken after 5-80 min. A part of the experiments was done with different chamber slides (1 µ-Slide 8 well ibiTreat), containing only a final volume of 250 µl. As 200 µl of the adherent cells in L15 medium were used, the compounds for specific and unspecific binding were added 5-fold concentrated, dissolved in 50 µl L-15, following the same conditions as described above.

References

1.   Schneider, E.; Mayer, M.; Ziemek, R.; Li, L.; Hutzler, C.; Bernhardt, G.; Buschauer, A. A simple and powerful flow cytometric method for the simultaneous determination of multiple parameters at G protein-coupled receptor subtypes. *ChemBioChem* **2006,** 7, 1400-9.

2.   McGrath, J. C.; Arribas, S.; Daly, C. J. Fluorescent ligands for the study of receptors. *Trends Pharmacol. Sci.* **1996,** 17, 393-9.

3.   Haupts, U.; Rüdiger, M.; Pope, A. J. Macroscopic versus microscopic fluorescence techniques in (ultra)-high-throughput screening. *Drug Discov. Today* **2000,** 5, 3-9.

4.   Middleton, R. J.; Kellam, B. Fluorophore-tagged GPCR ligands. *Curr. Opin. Chem. Biol.* **2005,** 9, 517-25.

5.   Finney, D. A.; Sklar, L. A. Ligand/receptor internalization: A kinetic, flow cytometric analysis of the internalization of N-formyl peptides by human neutrophils. *Cytometry* **1983,** 4, 54-60.

6.   Ciencialová, A.; Žáková, L.; Jiráček, J.; Barthová, J.; Barth, T. Preparation and characterization of two LysB29 specifically labelled fluorescent derivatives of human insulin. *J. Pept. Sci.* **2004,** 10, 470-478.

7.   Whitson, K. B.; Beechem, J. M.; Beth, A. H.; Staros, J. V. Preparation and characterization of Alexa Fluor 594-labeled epidermal growth factor for fluorescence resonance energy transfer studies: application to the epidermal growth factor receptor. *Anal. Biochem.* **2004,** 324, 227-236.

8.   Dumont, Y.; Gaudreau, P.; Mazzuferi, M.; Langlois, D.; Chabot, J. G.; Fournier, A.; Simonato, M.; Quirion, R. BODIPY-conjugated neuropeptide Y ligands: new fluorescent tools to tag Y_1, Y_2, Y_4 and Y_5 receptor subtypes. *Br. J. Pharmacol.* **2005,** 146, 1069-81.

9.   Ziemek, R.; Brennauer, A.; Schneider, E.; Cabrele, C.; Beck-Sickinger, A. G.; Bernhardt, G.; Buschauer, A. Fluorescence- and luminescence-based methods for the determination of affinity and activity of neuropeptide Y_2 receptor ligands. *Eur. J. Pharmacol.* **2006,** 551, 10-8.

10.   Li, L.; Kracht, J.; Peng, S.; Bernhardt, G.; Buschauer, A. Synthesis and pharmacological activity of fluorescent histamine H_1 receptor antagonists related to mepyramine. *Bioorg. Med. Chem. Lett.* **2003,** 13, 1245-8.

11.   Li, L.; Kracht, J.; Peng, S.; Bernhardt, G.; Elz, S.; Buschauer, A. Synthesis and pharmacological activity of fluorescent histamine H_2 receptor antagonists related to potentidine. *Bioorg. Med. Chem. Lett.* **2003,** 13, 1717-20.

12.   Berque-Bestel, I.; Soulier, J. L.; Giner, M.; Rivail, L.; Langlois, M.; Sicsic, S. Synthesis and characterization of the first fluorescent antagonists for human 5-HT_4 receptors. *J. Med. Chem.* **2003,** 46, 2606-20.

13.   Heithier, H.; Hallmann, D.; Boege, F.; Reilander, H.; Dees, C.; Jaeggi, K. A.; Arndt-Jovin, D.; Jovin, T. M.; Helmreich, E. J. Synthesis and properties of fluorescent beta-adrenoceptor ligands. *Biochemistry (Mosc).* **1994,** 33, 9126-34.

14.   Baker, J. G.; Middleton, R.; Adams, L.; May, L. T.; Briddon, S. J.; Kellam, B.; Hill, S. J. Influence of fluorophore and linker composition on the pharmacology of fluorescent adenosine A1 receptor ligands. *Br. J. Pharmacol.* **2010,** 159, 772-86.

15.   Malan, S. F.; van Marle, A.; Menge, W. M.; Zuliana, V.; Hoffman, M.; Timmerman, H.; Leurs, R. Fluorescent ligands for the histamine H_2 receptor: synthesis and preliminary characterization. *Bioorg. Med. Chem.* **2004,** 12, 6495-503.

16.   Amon, M.; Ligneau, X.; Camelin, J. C.; Berrebi-Bertrand, I.; Schwartz, J. C.; Stark, H. Highly potent fluorescence-tagged nonimidazole histamine H_3 receptor ligands. *ChemMedChem* **2007,** 2, 708-16.

17.   Cowart, M.; Gfesser, G. A.; Bhatia, K.; Esser, R.; Sun, M.; Miller, T. R.; Krueger, K.; Witte, D.; Esbenshade, T. A.; Hancock, A. A. Fluorescent benzofuran histamine $H_{(3)}$ receptor antagonists with sub-nanomolar potency. *Inflammation Res.* **2006,** 55 Suppl 1, S47-8.

18.   Kuder, K. J.; Kottke, T.; Stark, H.; Ligneau, X.; Camelin, J. C.; Seifert, R.; Kiec-Kononowicz, K. Search for novel, high affinity histamine H_3 receptor ligands with fluorescent properties. *Inflammation Res.* **2010,** 59 Suppl 2, S247-8.

19.   Schneider, E.; Keller, M.; Brennauer, A.; Hoefelschweiger, B. K.; Gross, D.; Wolfbeis, O. S.; Bernhardt, G.; Buschauer, A. Synthesis and characterization of the first fluorescent nonpeptide NPY Y_1 receptor antagonist. *ChemBioChem* **2007,** 8, 1981-8.

20.   Xie, S. X.; Petrache, G.; Schneider, E.; Ye, Q. Z.; Bernhardt, G.; Seifert, R.; Buschauer, A. Synthesis and pharmacological characterization of novel fluorescent histamine H_2-receptor ligands derived from aminopotentidine. *Bioorg. Med. Chem. Lett.* **2006,** 16, 3886-90.

21.   Wetzl, B. K.; Yarmoluk, S. M.; Craig, D. B.; Wolfbeis, O. S. Ein Chamäleon-Marker zur Anfärbung und quantitativen Bestimmung von Proteinen. *Angew. Chem.* **2004,** 116, 5515-5517.

22.   Höfelschweiger, B., K. The pyrylium dyes: A new class of biolabels. Synthesis, spectroscopy, and application as labels and in general protein assay, . *Doctoral thesi*s, **2005**.

23.   Kelley, M. T.; Burckstummer, T.; Wenzel-Seifert, K.; Dove, S.; Buschauer, A.; Seifert, R. Distinct interaction of human and guinea pig histamine H_2-receptor with guanidine-type agonists. *Mol. Pharmacol.* **2001,** 60, 1210-25.

24.   Preuss, H.; Ghorai, P.; Kraus, A.; Dove, S.; Buschauer, A.; Seifert, R. Constitutive activity and ligand selectivity of human, guinea pig, rat, and canine histamine H_2 receptors. *J. Pharmacol. Exp. Ther.* **2007,** 321, 983-95.

25.   Seifert, R.; Wenzel-Seifert, K.; Burckstummer, T.; Pertz, H. H.; Schunack, W.; Dove, S.; Buschauer, A.; Elz, S. Multiple differences in agonist and antagonist pharmacology between human and guinea pig histamine H_1-receptor. *J. Pharmacol. Exp. Ther.* **2003,** 305, 1104-15.

26.   Ghorai, P.; Kraus, A.; Keller, M.; Gotte, C.; Igel, P.; Schneider, E.; Schnell, D.; Bernhardt, G.; Dove, S.; Zabel, M.; Elz, S.; Seifert, R.; Buschauer, A. Acylguanidines as bioisosteres of guanidines: NG-acylated imidazolylpropylguanidines, a new class of histamine H_2 receptor agonists. *J. Med. Chem.* **2008,** 51, 7193-204.

27.   Nordemann, U. *Personal communication*. In Department of Pharmaceutical and Medicinal Chemistry II, University of Regensburg (Germany), **2009**.

28.   Schnell, D. *Personal communication*. In Department of Pharmacology and Toxicology, University of Regensburg (Germany), **2008**.

29.   Keller, M. Guanidine-acylguanidine bioisosteric approach to address peptidergic receptors: pharmacological and diagnostic tools for the NPY Y_1 receptor and versatile building blocks based on arginine substitutes. *Doctoral Thesis*, University of Regensburg, Germany, http://epub.uni-regensburg.de/12092/, **2008**.

30.   Mosandl, J. Radiochemical and luminescence-based binding and functional assays for human histamine receptors using genetically engineered cells. *Doctoral thesis*, University of Regensburg, Germany, http://epub.uni-regensburg.de/12335/, **2009**.

31.   Leurs, R.; Smit, M. J.; Menge, W. M.; Timmerman, H. Pharmacological characterization of the human histamine H_2 receptor stably expressed in Chinese hamster ovary cells. *Br. J. Pharmacol.* **1994,** 112, 847-54.

32.   Gross, D. New Approaches to the Chemotherapy of Glioblastoma: investigations on doxorubicin nanoparticles, inhibition of PDGF receptors and kinesin Eg5, with emphasis on confocal laser-scanning microscopy. *Doctoral thesis*, University of Regensurg (Germany), http://epub.uni-regensburg.de/10466/, **2006**.

33.   Magde, D. B., J. H.; Cremers, T. L.; Olmsted, J., III,. Absolute luminescence yield of

cresyl violet. *J. Phys. Chem.* **1979,** 83, 696-699.

34.   Fery-Forgues, S. Are Fluorescence Quantum Yields So Tricky to Measure? A Demonstration Using Familiar Stationery Products. *J. Chem. Educ.* **1999,** 76 1260.

35.   Cheng, Y.; Prusoff, W. H. Relationship between the inhibition constant (K1) and the concentration of inhibitor which causes 50 per cent inhibition (I50) of an enzymatic reaction. *Biochem. Pharmacol.* **1973,** 22, 3099-108.

Chapter 7
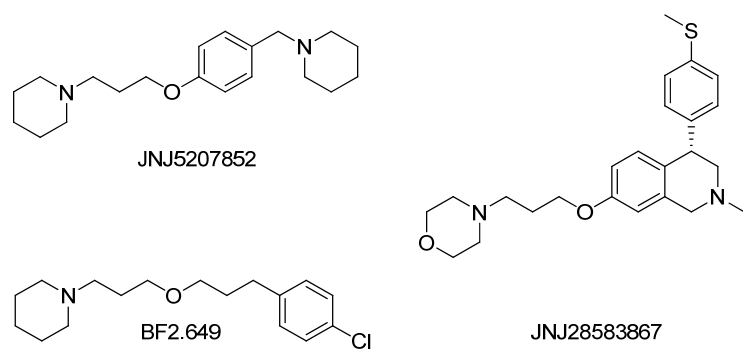
3[4(Piperidinomethyl)phenoxy]alkylamine derivatives as histamine H$_3$- receptor ligands

7 3-[4-(Piperidinomethyl)phenoxy]alkylamine derivatives as histamine H_3 -receptor ligands

7.1 Introduction

Considering the blockbuster drug status that the H_1R- and H_2R- antagonists had reached in the past, the expectations in the therapeutic potential of H_3R- targeting drugs are high. The H_3R acts as a presynaptic autoreceptor in the CNS, regulating the synthesis and release of histamine. As a heteroreceptor, the H_3R regulates the release of other neurotransmitters (e.g. acetylcholine, dopamine, norepinephrine)[1]. Antagonists for the H_3R are regarded as potential drugs for the treatment of neuronal diseases, for example, sleep and wake disorders, cognitive dysfunction or schizophrenia[2-3]. Numerous potential H_3R- antagonists from several pharmaceutical companies (e.g. Bioprojet, Johnson & Johnson, Merck, Glaxo Smith Kline, Pfizer, Abott and others) are currently under clinical investigations (see reviews [3-5]) or in preclinical evaluation processes[6], but to date there exists no clear proof of concept. In the last 10 years many ligands without imidazole moiety became available. Among them are several H_3R - ligands comprising, for example, a phenoxyalkylamine[7-9] and/or 3-aminopropoxy moiety (for a overview cf. ref.[10]). Examples of highly potent H_3R- antagonists with these structural motifs are JNJ5207852[11], BF2.649 (tiprolisant[5, 12]) and JNJ28583867[13] (Figure 7.1). The latter combines H_3R- antagonistic properties with the blockade of serotonin re-uptake with the intention to treat depression[3, 13].

Figure 7.1: Selected examples for H_3R antagonists with phenoxyalkylamine/ 3-aminopropoxy moiety

Evaluations of a pharmacophore model for this kind of ligands started from imidazole-based compounds, refining the model for non-imidazole H_3R- ligands[4] (Figure 7.2). Most of these "non-imidazoles" consists of a basic moiety, connected via a spacer to a (phenyl-like) core structure and a more variable region, i. e. a polar group, second basic moiety or lipophilic residue[4] (for variations cf. ref.[9]). Most potent ligands are varied in the "eastern part" of the molecule. The phenoxyalkylamine portion is also present in the H_2R antagonists described in chapter 3, but

with a different substitution pattern (meta at the phenyl ring for H_2R- ligands, para for H_3R-ligands).
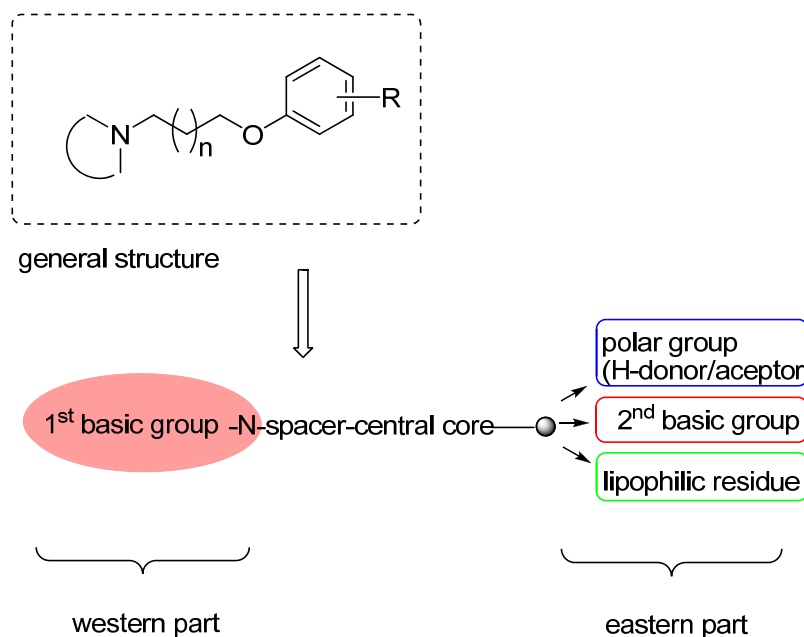
Figure 7.2: Refined pharmacophore model for non-imidazole H_3R antagonists[4]

As the squaramides described in chapter 3 turned out to have additional H_3R- antagonistic properties, H_3R- ligands structurally related to these H_2R- igands were synthesized with the aim to gain more insight into the structure-activity and structure-selectivity relationships. For this purpose, the "western part" of the general structure was modified. JNJ5207852 was used as a starting point, and the piperidine ring was replaced by flexible alkylamine spacers, aminopiperidines and by squaramide derivatives combined with alkylamines. Ligands bearing primary amino groups were synthesized with respect to future preparation of new fluorescent and radiolabeled ligands. To explore the suitability as radioligands the "cold" forms of such antagonists were synthesized by coupling of the primary amines to propionic or 4-F-benzoic acid.

7.2 Chemistry

The benzylpiperidine **7.3** was obtained from p-hydroxybenzaldehyde by analogy with the synthesis of the H_2R potentidine-like compounds. The Leuckart Wallach reaction using formic acid and piperidine[14]. Reductive amination with piperidine and $NaBH(OAc)_3$ (as described in litera-

ture[15]) afforded compound **7.3** as well. Both synthetic routes afforded the product in 80-87 % yield and comparable purity as pale brown to yellow solids.
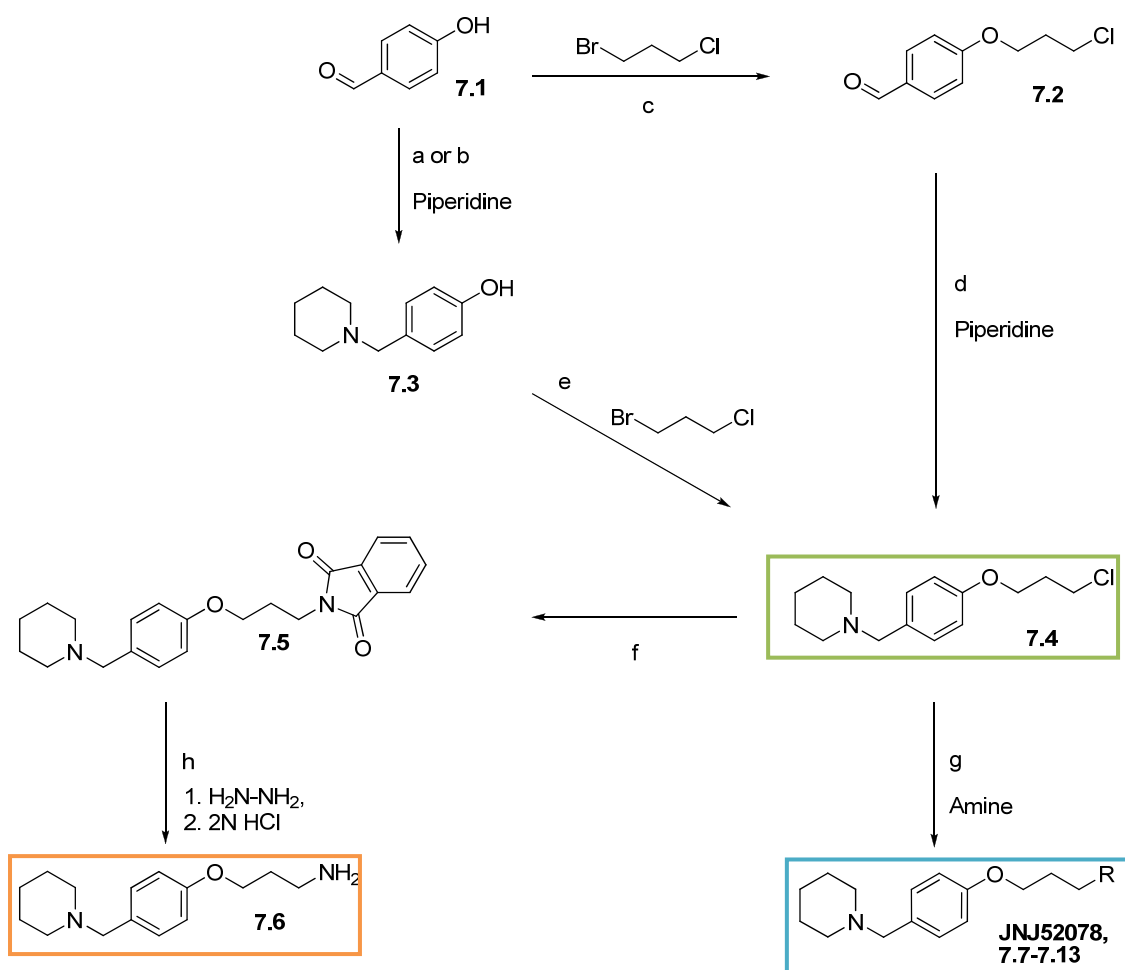
residue	JNJ5207852	7.7	7.8	7.9	7.10	7.11	7.12	7.13
R			$-NH_2(CH_2)_nNH_2$					
n	-	-	3,	4	-	2	-	2

Scheme 7.1: Synthesis of building blocks for the preparation of 3-[4-(piperidin-1-ylmethyl)phenoxy]-propylamine-type H_3R antagonists. Reagents and conditions: (a) HCOOH, reflux, 2 h, (b) dichloro-methane, $NaBH(OAc)_3$, rt, overnight, (c) acetone, K_2CO_3, reflux, 20 h, (d)) dichloromethane, $NaBH(OAc)_3$, rt, 30 h (e) acetone, K_2CO_3, reflux, 48 h, (f) isoindoline-1,3-dione, K_2CO_3, DMF, reflux 18 h , (g) butanol, KI, K_2CO_3, reflux, 18-48 h, (h) 1.hydrazine hydrate, rt, 48 h, 2. 2N HCl;

Alkylation of the hydroxygroup with 1-bromo-3-chloropropane and K_2CO_3 in acetone yielded **7.4** (50 % yield, Scheme 7.1). The synthesis of **7.4** was also accomplished via intermediate **7.2**, pre-pared by alkylation of **7.1** with 1-bromo-3-chloropropane (50 % yield) and subsequent reductive

amination of the aldehyde group in **7.2**. Compound **7.4** served as key intermediate for the prep-aration of the H$_3$R ligand JNJ 5207852[11] as well as for the synthesis of **7.7, 7.8** and **7.9** by nucleo-philic displacement at the alkyl halide functionality (Scheme 7.1).
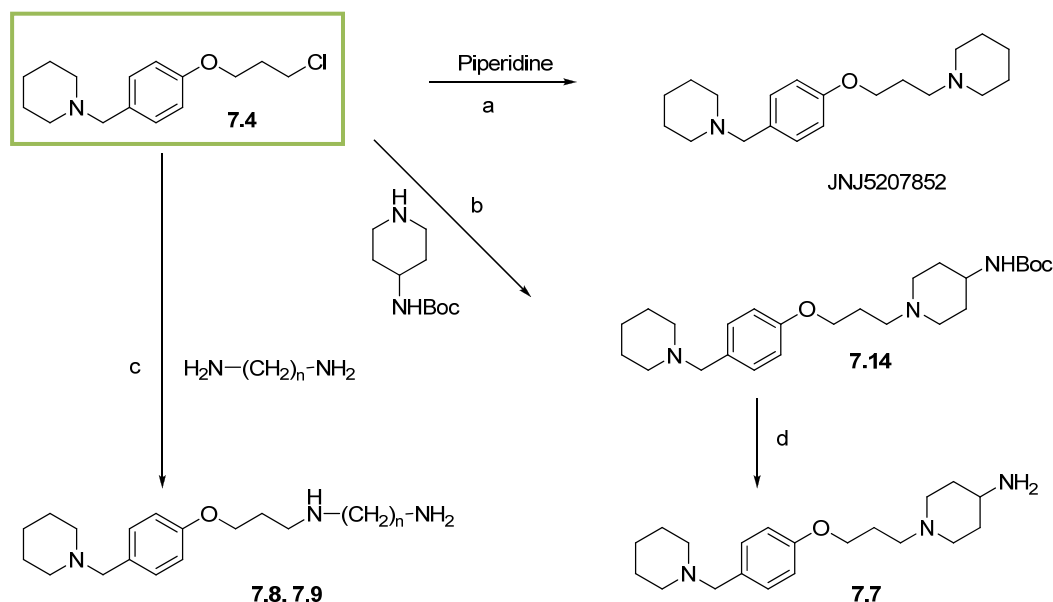

Compd.	n	Compd.	n
7.8	3	**7.9**	4

Scheme 7.2: Synthesis of 3-[4-(piperidin-1-ylmethyl)phenoxy]alkylamine derivatives, Reagents and conditions (a) KI, K$_2$CO$_3$, butanol, reflux 18 h, (b) see a, (c) see a, (d) 10 % TFA in CH$_2$Cl$_2$, 2.5 h, rt

A mixture of **7.4**, dissolved in butanol, potassium carbonate, sodium iodide and the respective amine was heated to 105 °C for 18 - 24 h giving the desired products (**7.8, 7.9, 7.14**, and JNJ5207852) in 30 to 90 % yield (after extraction and purification). Reductive amination, O-alkylation and nucleophilic displacement of the alkyl halide were performed by analogy with described procedures[8]. Ligand **7.7** was obtained by cleavage of the Boc- protecting group with 10 % TFA in CH$_2$Cl$_2$, followed by preparative HPLC (Scheme 7.2). Introduction of a protected ami-no group via N-alkylation of phthalimide and subsequent cleavage of the phthaloyl residue by hydrazinolysis afforded **7.6**, which was purified by preparative HPLC, giving yellow oil (Scheme 7.1).
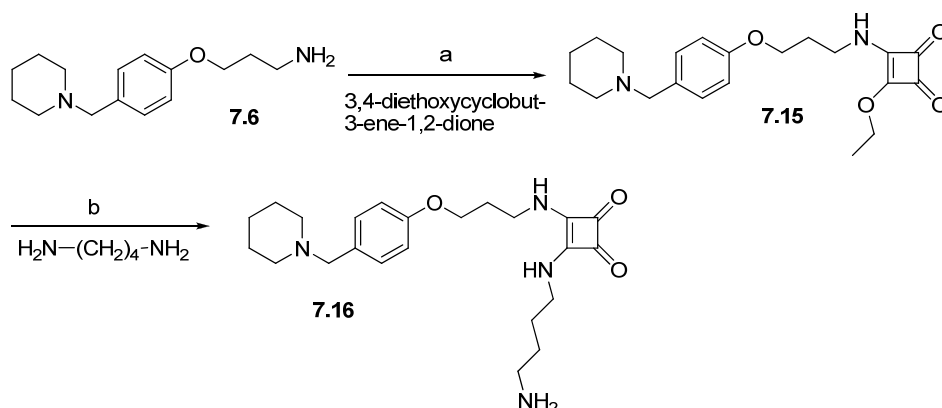
Scheme 7.3: Synthesis of squaramide **7.16**. Reagents and conditions: (a) Ethanol, rt, 48 h, (b) ethanol, rt, overnight

Squaramide **7.15** was prepared from **7.6** according to the same procedure as described for the synthesis of squaramides in chapter 3.

The "cold" forms of potential new H$_3$R radioligands were synthesized by acylation of amines **7.8** and **7.9** using the succinimidyl esters of propionic- and 4-F-benzoic acid (**7.17, 7.18**) according to the procedure described for the H$_2$-receptor radioligands in chapter 3 (see Scheme 7.4). Labelling with **7.18** afforded the two fold acylated products **7.10** and **7.11**. With respect to radiolabelling conditions, this procedure has to be optimized for instance, by using an excess of compound **7.8** and **7.9**, probably resulting in mono propionylated compounds. By contrast, the bulkier succinimidyl 4-fluorobenzoate gave only the monosubstituted compounds

Compd	R^1	R^2	n	Compd	R^1	R^2	n
7.10			3	**7.12**	H		3
7.11			4	**7.13**	H		4

Scheme 7.4: Synthesis of potential H$_3$-receptor ligands. Reagents and conditions: (a) MeCN/MeOH, Et$_3$N, rt, overnight

7.12 and **7.13**, which were isolated by preparative HPLC as yellow to brown oils.

7.3 Pharmacological results

7.3.1 H$_3$- receptor antagonism and binding

H$_3$R- antagonism was determined in a steady state GTPase assay on Sf9 cell membranes express-
ing the hH$_3$R (hH$_3$R+ G$_{i\alpha2}$ +β$_1$γ$_2$ + RGS4[16]). The synthesized ligands were potent hH$_3$R- antagonists
with K$_{b'}$- values in the low nanomolar range (5.2 – 121 nM) except for **7.6**. This class of com-
pounds (derived from JNJ5207852) showed intrinsic activities ranging from almost full inverse
agonistic activity (at a concentration of 10 µM) to low inverse agonistic activity relative to hista-
mine (Table 7.1). This was also true for standard ligands such as thioperamide and JNJ7753707.
The H$_3$R- antagonistic activity of the most potent substance **7.13** (K$_{b'}$ = 5.2 nM, K$_i$ = 3.4 nM), bear-
ing a tetramethylene spacer and a fluorobenzoyl residue, was in the same range as that of
JNJ5207852 (K$_{b'}$ = 4 nM). The results from GTPase assays were essentially confirmed by data
from binding studies on HEK293-FLAG-hH$_3$R-His$_6$ cells using [^{3}H]NAMH as radioligand.

Table 7.1: H$_3$R- antagonism and binding determined on Sf9 cell membranes (GTPase[a]) and HEK-293-FLAG-
hH$_3$R-His$_6$cells[b]

Compd.	GTPase assay hH$_3$R+ G$_{i\alpha2}$ +β$_1$γ$_2$ + RGS4[a]		Binding assay HEK293-FLAG-hH$_3$R-His6 cells[c]
	K$_{b'}$ [nM]	E$_{max}$	Ki (K$_D$) [nM]
Histamine	EC$_{50}$ 25 ± 3 [b]	1.00	-
[^{3}H]NAMH	-	-	(5.1)[c]
JNJ5207852	4.3 ± 0.6	-0.88 ± 0.12	2.3
JNJ7753707	4 ± 2	-0.9	0.33
Thioperamide	97 ± 18	-0.66 ± 0.1	n.d.
7.6	773 ± 327	-0.12 ± 0.02	1709 ± 930
7.7	70 ± 14	-0.18	77 ± 14
7.8	49 ± 16	-0.92 ± 0.02	70 ± 15
7.9	60 ± 16.6	-0.85 ± 0.0	45 ± 16
7.10	51 ± 32	-0.2 ± 0.01	132 ± 42
7.11	32 ± 3	-0.22 ± 0.01	111 ± 34
7.12	36 ± 25	-0.22 ± 0.02	89 ± 21
7.13	5.2 ± 0.6	-0.24 ± 0.02	3.4 ±0.9
7.16	121 ± 110	-0.17 ± 0.02	197 ±19

[a] steady state GTPase assay on Sf9 cell membranes; concentrations of ligands: 1 nM - 100 µM; typical
GTPase activities (stimulation with 100 nM HIS (hH$_3$R): 2.5-6.0 pmol x mg^{-1} x min^{-1}; E $_{max}$= efficacy relative
to histamine = 1 (E$_{max}$ HIS=1) (c. ligands: 10 µM, for efficacy), Mean values ± S.E.M. (n = 1-3; performed in
duplicate).

[b]concentrations of ligands: 1 nM - 100 µM, c. [^{3}H]NAMH: 1 nM, 2-5 million cells/well; Mean values ±
S.E.M. (n = 1-2) performed in duplicate; n.d.: not determined, [b] cf. ref.[17] [c] cf. ref.[18]

7.3.2   Histamine receptor subtype selectivity

The receptor subtype selectivity of the compounds was functionally investigated in GTPase assays on human H_1-, H_2- and H_4- receptors. In addition, the affinity at the H_4R was determined in radioligand binding studies. According to the literature 4-(aminoalkoxy)benzylamine-type H_3R-antagonists such as JNJ5207852 exhibit more than 1000-fold selectivity over the other histamine receptors[8]. In the present study the synthesized compounds turned out to have a high preference for the hH_3R, compared to the hH_1R, hH_2R and hH_4R. Ca^{2+} assays (spectrofluorimetric) on U-373 MG cells revealed low hH_1R antagonistic properties (IC_{50} values 3.6 - 100 µM; data cf. appendix). In GTPase assays on Sf9 cells expressing the hH_1R + RGS4, there were no significant inverse agonistic activities (E_{max}= -0.06 - 0.00). The same holds for efficacies at hH_4R-RGS19 (+ $G_{i\alpha2}$ +$\beta_1\gamma_2$)[16] (E_{max}= -0.09 - 0.02) and hH_2R-$G_{s\alpha s}$. At the hH_2R, as well as at the hH_4R, $K_{b'}$ values above 1000 - 10000 nM were determined (cf. table 7.2 and appendix). The only exception was the squaramide compound **7.16** with a 2 fold increase in activity at the hH_2R.

Tabelle 7.2: Activity and Affinity of selected compounds on Sf9 cell membranes (GTPase[a]) and on HEK-293-FLAG-hH_4R-His_6 cells[b]

Compd.	GTPase assay hH_2R-$G_{s\alpha s}$		GTPase assay hH_4R-RGS19+ $G_{i\alpha2}$+$G_{\beta1\gamma2}$	Binding assay HEK293-FLAG-hH_4R-His6 cells[c]
	$K_{b'}$ [nM]	$K_{b'}$ [nM]	Ki (K_D) [nM]	Ki (K_D) [nM]
Histamine	EC_{50}: 990 ± 92[b]	1.00	EC_{50}: 12 ± 3[d]	-
[^{3}H]UR-PI294	-	-	-	(7.5)[c]
7.6	>5000	-0.2 ± 0.07	>3000	n.d
7.8	>5000	0.01 ±0.03	>5000	>5000
7.9	>5000	0.01 ±0.04	>5000	>5000
7.7	>5000	-0.19 ± 0.11	>5000	>5000
7.11	n.d	-0.19 ± 0.08	>1000	>1000
7.10	n.d	-0.1 ±0.03	>5000	n.d
7.12	n.d	0.01 ±0.03	>5000	n.d
7.13	n.d.	0.06 ±0.02	>5000	n.d
7.16	61 ±20	-0.20 ± 0.01	>2500	>2500

[a] steady state GTPase assay on Sf9 cell membranes; concentrations of ligands: 1 nM - 100 µM; typical GTPase activities (stimulation with 100 nM HIS (hH_4R), with 1 µM HIS (hH_2R): 2.5-7.0 pmol x mg^{-1} x min^{-1}; E_{max}= efficacy relative to histamine =1, E_{max} HIS=1 (c. ligands: 10 µM, for efficacy), Mean values ± S.E.M. (n = 1-3, performed in duplicate);

[b] concentrations of ligands: 1 nM - 100 µM, c. [^{3}H]UR-PI294: 5nM, 2-5 million cells/well; mean values ± S.E.M. (n = 1-2, performed in duplicate); n.d.: not determined, [c] see[18], [d] see[19]

7.4   Discussion

Variations in the western part of 4-(aminoalkoxy)benzylamine-type H_3R- antagonists, aiming at building blocks bearing primary amino groups for the coupling to fluorophores and radiolabels, resulted in compounds with nanomolar antagonistic activities and affinities at the hH_3R. All primary amines revealed showed a 10-30 fold decrease in H_3R- antagonistic activity compared to JNJ5207852. Flexible ω-aminoalkyl spacers as well as more rigid spacers were tolerated, giving activities around 50 to 120 nM. Although potencies were lower than that of the reference compound, coupling to fluorophores is promising as demonstrated for H_2R- antagonists in chapter 6. This is also supported by 4-F-benzamides and propionamides. Compound **7.13** proved to be comparable in activity H_3R- antagonistic to the JNJ substance. Thus, the ^{18}F-labelled form of **7.13** might be suitable as a radiotracer for PET imaging. Except for the squaramide **7.16** all investigated H_3R- antagonists exhibited high selectivity for the hH_3R over the other histamine receptors. Squaramide **7.16** differs from the squaramides presented in chapter 3 (e.g. **3.11**) only in the substitutional pattern: para substitution for the H_3R- ligand, meta substitution for the H_2R- ligand. The two ligands (**3.11, 7.16**) had comparable activities at the hH_3R and hH_2R. The para substitution is characteristic of H_3R selective antagonistic 4-(aminoalkoxy)benzylamine derivatives (see above). Therefore, the loss of selectivity is attributed to the squaramide moiety

7.5   Summary and conclusion

Our aim to get appropriate building blocks for the synthesis of fluorescent H_3R- ligands resulted in potent H_3R- antagonists with high selectivity over the other histamine receptor subtypes, except for the squaramides. Additionally, compounds **7.10-7.13** revealed that the 4-F-benzoyl and the propionyl residue are tolerated as substituents at the amino group. This paves the way to the development of potential radio/PET ligands.

7.6 Experimental section

7.6.1 Chemistry

7.6.1.1 General conditions

See chapter 3

4-(Piperidin-1-ylmethyl)phenol (7.3)

Fresh piperidine (9 g, 106 mmol, 2.6 eq), formic acid (5.2 g, 0.113 mol, 2.8 eq) and 4-hydroxybenzaldehyde (5 g, 41 mmol, 1 eq) were allowed to react as described in chapter 3 for **3.2**. The isolated compound (pale light brown crystals) was dried in vacuo (6.8 g, 87 %) and used without further purification. Mp 136 °C

$\underline{^1\text{H-NMR: (300 MHz, DMSO-d}_6\text{):}}$ δ (ppm) 1.25-1.96 (m, 6H, **C3,4,5-H** Pip), 2.27 (m, 4H, **C2,6-H** Pip), 3.29 (s, 2H, Pip**CH₂**), 6.68 (d, 2H, ^{3}J=8.4 Hz, **C2,6-H** phenoxy), 7.04 (d, 2H, ^{3}J= 8.4 Hz, **C3,5-H** phenoxy), 9.25 (s, 1H, **OH);** $\underline{^1\text{H-NMR: (300 MHz, CDCl}_3\text{):}}$ δ (ppm) 1.44-1.61 (m, 6H, **C3,4,5-H** Pip), 2.49 (m, 4H, **C2,6-H** Pip), 3.42 (s, 2H, Pip**CH₂**), 6.59 (d, 2H, ^{3}J=8.5 Hz, **C2,6-H** phenoxy), 7.08 (d, 2H, ^{3}J=8.4 Hz, **C3,5-H** phenoxy); $\underline{^{13}\text{C-NMR (75.5 MHz, CDCl}_3\text{):}}$ δ (ppm) 24.01 (**C4**-Pip), 25.01 (2C, **C3,5**-Pip), 54.12 (2C, **C2,6**-Pip), 63.17 (Pip-**CH₂**), 115.76 (2C **C2,6**-phenoxy), 126.76 (q, **C4**-phenoxy), 131.83 (2C, **C3,5**-phenoxy), 156.38(q, **C1**-phenoxy); $\underline{\text{CIMS}}$: (NH₃) m/z 192.2 [MH$^+$] 100 %; $C_{12}H_{17}NO$ (191)

Preparation of 3-chloropropyl phenyl ethers - general procedure 1[8]

4-Hydroxybenzaldehyde or 4-(piperidin-1-ylmethyl)phenol (1 eq) was suspended in 100 ml of acetone. After addition of 1-bromo-3-chloropropane (2 eq) and K_2CO_3 (2.9-3.0 eq), the suspension was refluxed for 20-30 h. Insoluble material was filtered off, and the solvent was evaporated to give orange or yellow oils. The crude product was purified by flash chromatography (silica gel) with ethyl acetate/hexane.

4-(3-Chloropropoxy)benzaldehyde (7.2)

4-Hydroxybenzaldehyde (4.08 g, 33.4 mmol, 1 eq), 1-bromo-3-chloropropane (10.27 g, 65.2 mmol, 2 eq) and K_2CO_3 (13.65 g, 97.8 mmol, 2.9 eq) were used as described in procedure 1 (20 h

reflux). 6.4 g of crude product were obtained (orange oil). From 3.9 g of the crude product, puri-fied by flash chromatography (ethyl acetate/hexane= 1/4, silica gel), resulted 1.96 g (49 %) pure compound (colorless oil).

^{1}H-NMR: (300 MHz, CDCl$_3$): δ (ppm) 2.34-2.32 (OCH$_2$**CH$_2$**CH$_2$Cl), 3.76 (t, 2H, ^{3}J=6.2 Hz, -OCH$_2$CH$_2$CH$_2$Cl), 4.21 (t, 2H, ^{3}J=5.9 Hz, -OCH$_2$CH$_2$CH$_2$Cl) 7.01 (d, 2H, ^{3}J=8.7 Hz, **C2,6-H** phenoxy), 7.83-7.86 (m, 2H, **C3,5-H** phenoxy), 9.89 (s, 1H, OH); ^{13}C-NMR (75.5 MHz, CDCl$_3$): δ (ppm) 31.99, 41.23, 64.61 (OCH$_2$CH$_2$**CH$_2$**NH-), 114.77 (2C **C2,6**-phenoxy), 130.1 (q, **C4**-phenoxy), 132.03 (2C, **C3,5**-phenoxy), 163.73 (q, **C1**-phenoxy), 190.83; CIMS: (NH$_3$) m/z 216.0 [MNH$_4^+$] 100 %, 198.9 [MH$^+$] 98 %; C$_{10}$H$_{11}$ClO$_2$ (199)

Preparation of 1-[4-(3-chloropropoxy)benzyl]piperidine (7.4) according to procedure 1

Compound **7.3** (3 g, 15.7 mmol, 1 eq), 1-bromo-3-chloropropane (3.1 ml, 31 mmol, 2 eq) and K$_2$CO$_3$ (6.5 g, 47 mmol, 3 eq) were refluxed for 30 h as described in procedure 1. Evaporation of the solvent gave 4.5 g of yellow oil. 1.8 g were purified by flash chromatograpy on silica gel with ethyl acetate/hexane = 1.5/1, yielding the product as pale yellow oil (810 mg, 48 %).

^{1}H-NMR and ^{13}C-NMR see preparation of **7.4** according to method b; CIMS: (NH$_3$) m/z 268.1 [MH$^+$] C$_{15}$H$_{22}$ClNO (268)

Reductive amination - general procedure 2

Synthesis was performed as described in literature[8]. The aldehyde (1 eq) and piperidine (1.1 eq) were dissolved in dichloroethane (50 ml) before addition of 1.4 eq sodium triacetoxyboro-hydride (NaBH(OAc)$_3$). The solution was stirred for 18-48 h and then treated with 10 % aqueous sodium hydroxide (10-100 ml). Extraction of the aqueous phase was done with CHCl$_3$ or di-chloromethane. The organic phases were combined, washed with water and dried over magne-sium sulphate. The solvent was evaporated and the product dried in vacuo to give yellow oils or solids.

Synthesis of 4-(piperidin-1-ylmethyl)phenol (7.3) according to procedure 2

4-Hydroxybenzaldehyde (2.99 g, 24.45 mmol, 1 eq), piperidine (2.26 g, 26.3 mmol, 1.1 eq) and NaBH(OAc)$_3$ (7.17 g, 33.8 mmol, 1.4 eq) were allowed to react as described in general procedure 2 for 18 h. 100 ml of 10 % aqueous sodium hydroxide were used. As the extraction of the aqueous phase with dichloromethane (50 ml) was incomplete, ammonia solution (32 %) was added to the aqueous phase, and the extraction was completed with diethyl ether. The organic layers were treated as described yielding 3.8 g (81 %) of a yellow solid. Mp: 136 °C

^{1}H-NMR: ^{13}C-NMR see **7.3** prepared according to method a; CIMS: (NH$_3$) m/z 192.1 [MH$^+$] 86.1 (C$_5$H$_{12}$N$^+$, 100 %); C$_{12}$H$_{17}$NO (191)

Synthesis of 1-[4-(3-chloropropoxy)benzyl]piperidine (7.4) according to procedure 2

Compound **7.2** (1.1 g, 5.5 mmol, 1 eq), piperidine (0.52 g, 6.1 mmol, 1.1 eq) and NaBH(OAc)$_3$ (1.65 g, 7.8 mmol, 1.4 eq) were used as described in general procedure 2 (48 h). Sodium hydroxide (10 %) at a volume of 20 ml was used. Extraction of the product: dichloroethane under addition of sodium chloride solution for phase separation. The combined phases were treated as described, yielding 1.13 g of the product (76 %).

^{1}H-NMR: (300 MHz, CDCl$_3$): δ (ppm) 1.42-1.60 (m, 6H, **C3,4,5-H** Pip), 2.19-2.27 (m, 2H, -OCH$_2$**CH$_2$**CH$_2$Cl), 2.35 (m, 4H, **C2,6-H** Pip), 3.41 (s, 2H, PipCH$_2$), 3.75 (t, 2H, ^{3}J=6.4 Hz, -OCH$_2$CH$_2$CH$_2$Cl), 4.1 (t, 2H, ^{3}J=5.8 Hz, -OCH$_2$CH$_2$CH$_2$Cl) 6.85 (d, 2H, ^{3}J=8.6 Hz, **C2,6-H** phenoxy), 7.2 (m, 2H, ^{3}J=8.6 Hz, **C3,5-H** phenoxy), 9.89 (s, 1H, OH); ^{13}C-NMR (75.5 MHz, CDCl$_3$): δ (ppm) 24.41, 25.96, 32.34 (OCH$_2$**CH$_2$**CH$_2$Cl), 41.26 (-OCH$_2$CH$_2$CH$_2$Cl), 54.35, 63.23 (OCH$_2$CH$_2$CH$_2$Cl), 64.23, 114.07 (2C, **C2,6**-phenoxy), 130.49 (2C, **C3,5**-phenoxy), 130.78 (q, **C4**-phenoxy), 157.71 (q, **C1**-phenoxy); CIMS: (NH$_3$) m/z 268.1 [MH$^+$] 100 %; C$_{15}$H$_{22}$ClNO (268)

2-{3-[4-(Piperidin-1-ylmethyl)phenoxy]propyl}isoindoline-1,3-dione (7.5)

Ligand **7.4** (400 mg, 1.49 mmol, 1 eq), isoindoline-1,3-dione (219.8 mg, 1.49 mmol, 1 eq) and potassium carbonate (206 mg, 1.49 mmol, 1 eq) were suspended in 40 ml of DMF and refluxed for 18 h. Ice water was added and the organic layer was extracted with CHCl$_3$. The CHCl$_3$ phase was dried over magnesium sulphate, filtered and the solvent evaporated under reduced pres-

sure. The compound was purified by flash chromatography (silica gel) using CH_2Cl_2 to remove impurities and the methanol as eluent. The product was obtained as yellow oil (260 mg, 46 %).

^{1}H-NMR: (300 MHz, CDCl$_3$): δ (ppm) 1.41-1.59 (m, 6H, **C3,4,5-H** Pip), 2.12-2.22 (m, 2H, -OCH$_2$**CH$_2$**CH$_2$Cl), 2.35 (m, 4H, **C2,6-H** Pip), 3.40 (s, 2H, PipCH$_2$), 3.90 (t, 2H, ^{3}J=6.9 Hz, -OCH$_2$CH$_2$CH$_2$Cl), 4.01 (t, 2H, ^{3}J=6.1 Hz, -OCH$_2$CH$_2$CH$_2$Cl) 6.75 (d, 2H, ^{3}J=8.6 Hz, **C2,6-H** phenoxy), 7.16 (m, 2H, ^{3}J=8.6 Hz, **C3,5-H** phenoxy), 7.69-7.72 (m, 2H, phthalimido), 7.82-7.85 (m, 2H, phthalimido); ^{13}C-NMR (75.5 MHz, CDCl$_3$): δ (ppm) 24.35 (**C4** Pip), 25.85 (2C, **C3,5** Pip), 28.36 (-OCH$_2$**C**H$_2$CH$_2$-), 35.54 (-OCH$_2$CH$_2$CH$_2$-), 54.25 (2C, **C2,6** Pip), 63.14, 64.23 114.05 (2C, **C2,6-**phenoxy), 123.26 (2C, phthalimido), 130.3 (q) 130.47 (2C, **C3,5**-phenoxy), 132.17 (q), 133.94 (2C, phthalimido), 157.78 (q, C1-phenoxy), 168.40 (2C, **C**O); ESMS: m/z 379.9 [MH$^+$]; $C_{23}H_{26}N_2O_3$ (379)

3-[4-(Piperidin-1-ylmethyl)phenoxy]propan-1-amine (7.6)

To **7.5** (230 mg, 608 μmol, 1 eq), dissolved in 25 ml of ethanol, hydrazine hydrate (0.15 g, 3.1 mmol, 5 eq) were added and stirred at rt for 48 h. The solvent was concentrated and the precipitate was filtered off. Subsequently, the solvent was evaporated and the crude product was obtained as yellow oil (170 mg, 60 %). From the crude product 50 mg were purified by preparative HPLC (system 2, flow 16 ml/min). After evaporation of MeCN and lyophilisation, the product was obtained as yellow oil (43 mg, 86 % from the crude product).

RP-HPLC (220 nm, gradient 1): 99 % (t$_R$= 4.6 min, k=0.8); ^{1}H-NMR: (300 MHz, methanol-d$_4$): δ (ppm) 1.45-1.95 (m, 6H, **C3,4,5-H** Pip), 2.17-2.20 (m, 2H, -OCH$_2$**CH$_2$**CH$_2$NH-), 2.86-2.95 (m,4H, **C2/6-H** Pip), 3.15 (t, 2H, ^{3}J=7.4 Hz, , -OCH$_2$CH$_2$**CH$_2$**NH-), 3.4-3.44 (m, 2H, **C2/6-H** Pip) 4.14 (t, 2H, ^{3}J=5.8 Hz, -O**CH$_2$**CH$_2$CH$_2$NH) 4.2 (s, 2H, Pip**CH$_2$**), 7.05 (d, 2H, ^{3}J=8.7 Hz, **C2,6-H** phenoxy), 7.42 (d, 2H, ^{3}J=8.7 Hz, **C3,5-H** phenoxy); ^{13}C-NMR (100.6 MHz, methanol-d$_4$): δ (ppm) 22.79 (**C4-Pip**), 24.13 (2C, **C3,5**-Pip), 28.36 (-OCH$_2$**CH$_2$**CH$_2$NH-), 38.5 (OCH$_2$CH$_2$**CH$_2$**NH-), 53.71(2C, **C2,6**-Pip), 61.26 (Pip-**CH$_2$**), 66.36 (-O**CH$_2$**CH$_2$CH$_2$NH-), 116.16 (2C **C2,6**-phenoxy), 122.69 (q, **C4**-phenoxy), 133.94 (2C, **C3,5**-phenoxy), 161.38 (q, **C1**-phenoxy); HRMS: (EI) m/z calcd. for $C_{15}H_{24}N_2O$ 248.1889 [M$^+$], found: 248.1882; $C_{15}H_{24}N_2O$ x $C_4HF_6O_4$ (476)

Amination of 3-chloropropyl ethers - General procedure 3 [8]

The 3-chloropropyl ether (1 eq), the respective amine (1.3-1.5 eq), K_2CO_3 (1-1.1 eq) and KI (0.05 eq) were suspended in 20 ml of butanol and heated to reflux for 18-48 h. Insoluble material was filtered off and the solution was treated as described below to give the products as yellow oils or as white solids.

tert-Butyl 1-{3-[4-(piperidin-1-ylmethyl)phenoxy]propyl}piperidin-4-ylcarbamate (7.14)

General procedure 3: **7.4** (128 mg, 478 µmol, 1 eq), tert-butyl piperidin-4-ylcarbamate (0.14 g, 699 µmol, 1.5 eq), K_2CO_3 (0.1 g, 723 µmol, 1 eq), and KI (4 mg, 24 µmol, 0.05 eq), reflux for 18 h. Insoluble material was filtered off and the solvent was evaporated (sticky yellow solid). The compound was purified by flash chromatography (silica gel) with CH_2Cl_2/methanol = 8/2, then 6/4, then 1/1 to give 59 mg (29 %) of the product.

<u>^{1}H-NMR: (600 MHz, methanol-d$_4$):</u> δ (ppm) 1.42 (s, 6H, **CH$_3$**), 1.46-1.63 (m, 6H,**C3,4,5-H** Pip), 1.85-1.88 (m, 2H, **CH$_2$** piperidin-4-amine), 1.89 (s, 3H, **CH$_3$**), 1.94-1.99 (m, 2H, OCH$_2$**CH$_2$**CH$_2$NH-), 2.13 (t, 2H, ^{3}J=11.1 Hz, **C2/6-H** Pip), 2.49 (m, 2H, **CH$_2$** piperidin-4-amine), 2.54-2.57 (m, 2H, -OCH$_2$CH$_2$**CH$_2$**NH-), 2.65 (s, 3H, CH$_3$), 2.93-2.95 (m, 2H, **C2/6-H** Pip) 3.51 (s, 2H, Pip**CH$_2$**), 4.00 (t, 2H, ^{3}J=6.1 Hz, -O**CH$_2$**CH$_2$CH$_2$NH) 6.87 (d, 2H, ^{3}J=8.6 Hz, **C2,6-H** phenoxy), 7.32 (d, 2H, ^{3}J=8.6 Hz, **C3,5-H** phenoxy); <u>^{13}C-NMR (150.95 MHz, methanol-d$_4$):</u> δ (ppm) 24.18 (2C, **CH$_3$**), 24.89 (**C4-Pip**), 26.1 (2C, **C3,5**-Pip), 27.67 (-OCH$_2$**CH$_2$**CH$_2$NH-), 28.77, 32.31, 32.70, 40.43 (2C), 53.55 (2C, **C2,6**-Pip), 54.93, 56.37 (OCH$_2$CH$_2$**CH$_2$**NH-), 63.70 (Pip-**CH$_2$**), 64.30, 67.23 (-O**CH$_2$**CH$_2$CH$_2$NH-), 79.97, 115.31 (2C, **C2,6**-phenoxy), 129.09 (q, **C4**-phenoxy), 132.44 (2C, **C3,5**-phenoxy), 160.05 (q, **C1**-phenoxy), 170.37 (q,), 180.39 (q, **C**O); <u>ESMS:</u> (EI) m/z 432.2 [MH$^+$] ; $C_{25}H_{41}N_3O_3$ (432)

N1-{3-[4-(piperidin-1-ylmethyl)phenoxy]propyl}propane-1,3-diamine (7.8)

Compound **7.4** (280 mg, 1.1 mmol, 1 eq), propane-1,3-diamine (340 mg, 4.6 mmol, 4.4 eq), sodium carbonate (97 mg, 915 µmol, 0.9 eq) and KI (5 mg, 30 µmol, 0.03 eq) were dissolved in 20 ml of butanol and refluxed for 10 h. The solution was filtered, the filtrate dried over sodium sulfate and the solvent evaporated. The white solid was dissolved in a small amount of methanol

and crystallized after addition of diethyl ether/ethyl acetate= 3/1. The compound was isolated as a yellow to white solid (306 mg, 96 %). Mp 125-130 °C.

RP-HPLC (220 nm): 0.00 min 7/93, 20.00 min 40/60, 99.7 % (t_R=11.3 min, k=3.44); ^{1}H-NMR: (300 MHz, DMSO-d$_6$): δ (ppm) 1.36-1.48 (m, 6H, **C3,4,5-H**), 1.63-1.72 (m, 2H, -NHCH$_2$**CH$_2$**CH$_2$NH$_2$) 1.82-1.91 (m, 2H, -OCH$_2$**CH$_2$**CH$_2$NH-), 2.27 (m, 4H, **C2/6-H** Pip), 2.6-2.75 (m, 4H, -OCH$_2$CH$_2$**CH$_2$**NH-, NHCH$_2$CH$_2$**CH$_2$**NH$_2$), 2.77 (t, 2H, ^{3}J=7.1 Hz, -NH**CH$_2$**CH$_2$CH$_2$NH$_2$), 3.32 (s, 2H, Pip-**CH$_2$**), 3.99 (t, 2H, ^{3}J=6.4 Hz, -O**CH$_2$**CH$_2$CH$_2$NH-) 6.85 (d, 2H, ^{3}J=8.6 Hz, **C2,6-H** phenoxy), 7.42 (d, 2H, ^{3}J=8.6 Hz, **C3,5-H** phenoxy); ^{13}C-NMR (150.95 MHz, DMSO-d$_6$): δ (ppm) 24.67 (**C4**-Pip), 25.91 (2C, **C3,5**-Pip), 26.64 (**C**-butyl), 27.33 (**C**-butyl), 28.97 (-OCH$_2$**CH$_2$**CH$_2$NH-), 40.72 (**C**-butyl), 47.17 (-OCH$_2$CH$_2$**CH$_2$**NH-), 49.4 (**C**-butyl) 53.83 (2C, **C2,6**-Pip), 63.44 (Pip-**CH$_2$**), 66.86 (-O**CH$_2$**CH$_2$CH$_2$NH-), 115.40 (2C **C2,6**-phenoxy), 128.69 (q, **C4**-phenoxy), 132.63 (2C, **C3,5**-, phenoxy), , 159.99 (q, **C1**-phenoxy), HRMS: (EI) m/z calcd. for C$_{18}$H$_{31}$N$_3$O 305.2467 [M$^+$], found: 305.2470; C$_{18}$H$_{31}$N$_3$O (306)

N1-{3-[4-(Piperidin-1-ylmethyl)phenoxy]propyl}butane-1,4-diamine (7.9)

Ligand **7.4** (150 mg, 560 μmol, 1 eq), butane-1,4-diamine (248 mg, 2.8 mmol, 5 eq), potassium carbonate (100 mg, 724 μmol, 1.3 eq) and KI (5 mg, 30 μmol, 0.05 eq) were dissolved in 20 ml of butanol and refluxed for 18 h. The solution was filtered, the filtrate dried over sodium sulfate and the solvent evaporated. The white solid was dissolved in a small amount of methanol and crystallized after addition of diethyl ether to yield a white solid (66 mg, 37 %). Mp >130 °C (de-comp.)

RP-HPLC (220 nm): 0.00 min 7/93, 20.00 min 40/60, 99 % (t_R=10.8 min, k=3.3); ^{1}H-NMR: (300 MHz, methanol-d$_4$): δ (ppm) 1.45-1.62 (m, 2H, **C4-H**), 1.64-1.73 (m, 8H, **C3,5-H**, -NHCH$_2$**CH$_2$**CH$_2$NH$_2$), 2.04-2.12 (m, 2H, -OCH$_2$**CH$_2$**CH$_2$NH-), 2.57 (m, 4H, **C2/6-H** Pip), 2.80-2.87 (m, 2H, -NCH$_2$CH$_2$CH$_2$CH$_2$NH-), 2.87-2.92 (m, 2H, -NCH$_2$CH$_2$CH$_2$CH$_2$NH$_2$), 2.97 (t, 2H, ^{3}J=7.4 Hz, -NH**CH$_2$**CH$_2$CH$_2$NH$_2$), 3.6 (s, 2H, Pip-**CH$_2$**), 4.08 (t, 2H, ^{3}J=6.0 Hz, -O**CH$_2$**CH$_2$CH$_2$NH-), 6.92 (d, 2H, ^{3}J=8.6 Hz, **C2,6-H** phenoxy), 7.28 (d, 2H, ^{3}J=8.6 Hz, **C3,5-H** phenoxy); ^{13}C-NMR (150.95 MHz, methanol-d$_4$): δ (ppm) 24.07 (**C4**-Pip), 25.53 (2C, **C3,5**-Pip), 27.73 (**C**-propyl), 28.65 (-OCH$_2$**CH$_2$**CH$_2$NH-), 37.74 (**C**-propyl), 45.64 (-OCH$_2$CH$_2$**CH$_2$**NH-), 46.31 (**C**-propyl), 53.73 (2C, **C2,6**-Pip), 62.25 (Pip-**CH$_2$**), 65.67 (-O**CH$_2$**CH$_2$CH$_2$NH-), 113.99 (2C **C2,6**-phenoxy), 129.95 (2C, **C3,5**-, phenoxy), 130.29 (q, **C4**-phenoxy), 157.52 (q, **C1**-phenoxy); HRMS: (EI) m/z calcd. for C$_{19}$H$_{33}$N$_3$O, 319.2624 [M$^+$], found: 319.26258; C$_{19}$H$_{33}$N$_3$O (320)

3-Ethoxy-4-{3-[4-(piperidin-1-ylmethyl)phenoxy]propylamino}cyclobut-3-ene-1,2-dione (7.15)

Compound **7.6** (88 mg, 184 µmol, 1 eq) and 3,4-diethoxycyclobut-3-ene-1,2-dione (33 mg, 191 µmol, 1 eq) were dissolved in ethanol under addition of 2-3 drops of Et_3N and stirred at rt for 48 h. The solvent was evaporated. The sticky oil was dissolved in a small amount of ethanol. Crystals precipitated after addition of diethyl ether were filtered off and dried in vacuo yielding a yellow semi solid (60 mg, 87 %).

<u>^{1}H-NMR: (300 MHz, methanol-d_4):</u> δ (ppm) 1.29-1.34 (t, 3H, CH$_2$**CH$_3$**), 1.36-1.46 (m, 2H, **C-H** Pip), 1.79-1.90 (m, 4H, **C-H** Pip), 2.04-2.12 (m,2H, -OCH$_2$**CH$_2$**CH$_2$NH), 2.93 (m, 2H, **C2/6-H** Pip), 3.18-3.25 (m, 2H, **-CH$_2$**CH$_3$), 3.4 (m, 2H, **C2/**6-H Pip), 3.79-3.83 +3.62-3.67 2x (m, 1H, -OCH$_2$**CH$_2$**CH$_2$NH-), 4.10-4.14 (m, 2H, O**CH$_2$**CH$_2$CH$_2$NH-), 4.21 (s, 2H, PipCH$_2$), 6.97-7.00 (m, 2H, **C2,6-H** phenoxy), 7.40-7.45 (m, 2H, **C3,5-H** phenoxy); <u>^{13}C-NMR (100.6 MHz, methanol-d_4):</u> δ (ppm) 16.16 (C, **CH$_3$**), 22.80 (**C4-Pip**), 24.16 (2C, **C3,5-Pip**), 31.18 (-OCH$_2$**CH$_2$**CH$_2$NH-), 43.08 (OCH$_2$CH$_2$**CH$_2$**NH-), 53.71 (2C, **C2,6-Pip**), 61.26 (Pip-**CH$_2$**), 66.40 (-O**CH$_2$**CH$_2$CH$_2$NH-), 70.70 (-**CH$_2$**CH$_3$), 116.02 (2C **C2,6**-phenoxy), 122.36 (q, **C4**-phenoxy), 133.99 (2C, **C3,5**-phenoxy), 161.61 (q, **C1**-phenoxy), 175.5 (C, cyclobutenyl), 184.4 (C, **C**O cyclobutenyl); <u>ESMS:</u> m/z 372.9 [MH$^+$]; $C_{21}H_{28}N_2O_4$ (373)

3-(4-Aminobutylamino)-4-{3-[4-(piperidin-1-ylmethyl)phenoxy]propylamino}cyclobut-3-ene-1,2-dione (7.16)

Ligand **7.15** (50 mg, 134 µmol, 1 eq) was dissolved in 15 ml of methanol. Butane-1,4-diamine (240 mg, 2.7 mmol, 20 eq), dissolved in 5 ml of methanol, was added and the solution was stirred overnight. Subsequently the solution was concentrated and diethyl ether was added to get crystals. As the formed yellow crystals contained impurities, 46 mg of the crude product were purified by preparative HPLC (system 2, 220 nm). After evaporation of acetonitrile and lyophilisation 19.19 mg (22 %) of the product were obtained as yellow oil.

<u>RP-HPLC (220 nm, gradient 1):</u> 99.6 % (t_R=8.7 min, k=2.4); <u>^{1}H-NMR: (600 MHz, methanol-d_4):</u> δ (ppm) 1.46-1.68 (m, 10H, **C3,4,5-H** Pip, 2x CH$_2$ butyl), 2.08 (qui, 2H, ^{3}J=6.3 Hz -OCH$_2$**CH$_2$**CH$_2$NH-), 2.44 (m, 4H, **C2/6-H** Pip), 2.78-2.8 (m, 2H, -OCH$_2$CH$_2$**CH$_2$**NH-), + 2.83-2.86 (m, 2H, **CH$_2$**-butyl), 3.47 (s, 2H, Pip-**CH$_2$)**, 3.61 (m, 2H, **CH$_2$**-butyl), 3.81 (m, 2H, -OCH$_2$CH$_2$**CH$_2$**NH), 4.08 (t, 2H, ^{3}J=5.9 Hz, -O**CH$_2$**CH$_2$CH$_2$NH-) 4.2 (s, 2H, Pip**CH$_2$**), 7.05 (d, 2H, ^{3}J=8.7 Hz, **C2,6-H** phenoxy), 7.42 (d, 2H, ^{3}J=8.7 Hz, **C3,5-H** phenoxy); <u>^{13}C-NMR (150.95 MHz, methanol-d_4):</u> δ (ppm) 25.04 (**C4-**Pip), 26.26 (2C,

C3,5-Pip), 27.25 (**C**-butyl), 28.58, 29.36 (**C**-butyl), 31.84 (-OCH$_2$**CH$_2$**CH$_2$NH-), 40.86 (**C**-butyl), 41.2, 42.52 (-OCH$_2$CH$_2$**C**H$_2$NH-), 44.56 (**C**-butyl), 55.05 (2C, **C2,6**-Pip), 63.87 (Pip-**CH$_2$**), 66.04 (-O**CH$_2$**CH$_2$CH$_2$NH-), 115.29 (2C **C2,6**-phenoxy), 122.69 (q, **C4**-phenoxy), 130.57 (2C, **C3,5**-, phenoxy), 159.78 (q, **C1**-phenoxy), 172.64 (q, cyclobutenyl), 183.54 (q, cyclobutenyl); <u>LSIMS</u>: (glycerol) m/z calcd. for C$_{23}$H$_{35}$N$_4$O$_3$ 415.2709 [MH$^+$], found: 415.2708; C$_{23}$H$_{34}$N$_4$O$_3$ x C$_4$HF$_6$O$_4$ (643)

1-{3-[4-(Piperidin-1-ylmethyl)phenoxy]propyl}piperidin-4-amine (7.7)

Compound **7.14** (50 mg, 116 mmol) was stirred in 20 ml of 10 % TFA (v/v) in CH$_2$Cl$_2$ at rt for 2.5 h (green solution). The solvent was evaporated and the residue was purified by preparative HPLC (system 2-1, 220 nm). After evaporation of acetonitrile and lyophilisation the product was obtained as yellow oil (50 mg, 77 %)

<u>RP-HPLC</u> (220 nm, gradient 1): 95 % (t$_R$=4.5 min, k=0.8); <u>^{1}H-NMR: (600 MHz, methanol-d$_4$)</u>: δ (ppm) 1.47-1.83 (m, 4H, 2x **CH$_2$** Pip), 1.91-2.02 (m, 4H, 2x **CH$_2$** Pip), 2.24-2.29 (m, 4H, -OCH$_2$**CH$_2$**CH$_2$NH-, **CH$_2$** piperidin-4-amine), 2.89-2.92 (m, 2H, **C2/6-H** Pip), 3.33 (m, 2H, **CH$_2$** piperidin-4-amine), 3.34 (m, 6H, -OCH$_2$CH$_2$**CH$_2$**NH-, **CH$_2$** piperidin-4-amine), 3.4-3.42 (m, 2H, **C2/6-H** Pip) 3.48 (m, 1H, **CH** piperidin-4-amine), 3.74 (m, 2H, **CH$_2$** piperidin-4-amine), 4.13 (t, 2H, ^{3}J=5.8 Hz, -O**CH$_2$**CH$_2$CH$_2$NH) 4.2 (s, 2H, Pip**CH$_2$**), 7.02 (d, 2H, ^{3}J=8.7 Hz, **C2,6-H** phenoxy, 7.41 (d, 2H, ^{3}J=8.7 Hz, **C3,5-H** phenoxy); <u>^{13}C-NMR (150.95 MHz, methanol-d$_4$)</u>: δ (ppm) 22.74 (**C4**-Pip), 24.09 (2C, **C3,5**-Pip), 25.32 (-OCH$_2$**CH$_2$**CH$_2$NH-), 28.7, 46.83, 49.85, 51.99, 53.69 (2C, **C2,6**-Pip), 55.71 (OCH$_2$CH$_2$**C**H$_2$NH-), 61.23 (Pip-**CH$_2$**), 66.08 (-O**CH$_2$**CH$_2$CH$_2$NH-), 116.13 (2C **C2,6-**phenoxy), 122.7 (q, **C4**-phenoxy), 133.91 (2C, **C3,5**-phenoxy), 161.27 (q, **C1**-phenoxy), 162.66 (q); <u>HRMS</u>: (EI) m/z calcd. for C$_{20}$H$_{33}$N$_3$O 331.2624 [M$^+$], found: 331.2625; C$_{20}$H$_{33}$N$_3$O x C$_4$HF$_6$O$_4$ (560)

Preparation of propionic and 4-fluorobenzoic amides

General procedure 4

The amines **7.8/7.9** (1 eq) were dissolved in acetonitrile/methanol (1/1, v/v, approx. 1 ml) under addition of Et$_3$N (pH 8-9), to prevent protonation of the amino group. Succinimidyl propionate (1.1 eq), dissolved in 1 ml of acetonitrile, was added and the solution was stirred overnight at rt. Subsequently, the solution was filtered (0.2 μm), adjusted to an appropriate volume (acetonitrile/0.1 % TFA 20/80) for preparative HPLC analysis (3-7 ml) and purified on a RP column (sys-

tem 2). The products were obtained as yellow oils in 15-37 % yield as TFA salts after lyophilisation.

N-{3-[4-(Piperidin-1-ylmethyl)phenoxy]propyl}-N-(3-propionylaminopropyl)propionamide (7.10)

Compound **7.8** (22.8 mg, 74.7 µmol, 1 eq) and succinimidyl propionate (14.3 mg, 83.6 µmol, 1.1 eq) were used to synthesise compound **7.10** according to procedure 4. The solution containing **7.10** was adjusted to a volume of 6 ml with MeCN /0.1 % TFA (20/80) and purified by preparative HPLC (system 2). After evaporation of acetonitrile and lyophilisation the product was obtained as beige oil (7.32 mg, 37 %).

RP-HPLC (220 nm, gradient 1): 99.5 % (t_R=13.99 min, k=4.5); ^{1}H-NMR: (600 MHz, methanol-d_4): δ (ppm) 1.04-1.12 (m, 6H, **CH$_3$**), 1.46-1.53 (m, 1H, CH$_2$ Pip), 1.67-1.83 (m, 5H CH$_2$ Pip, -NCH$_2$**CH$_2$**CH$_2$NHCO-), 1.92-1.95 (m, 2H, CH$_2$ Pip), 2.00-2.09 (m, 2H, -OCH$_2$**CH$_2$**CH$_2$-), 2.19 (qua, 2H, ^{3}J=7.6 Hz, -**CH$_2$**CH$_3$), 2.39 (m, 2H, -**CH$_2$**CH$_3$), 2.89-3.13 (m, 2H, **C2/6-H** Pip), 3.13-3.18 (m, 1H, -NHCH$_2$CH$_2$CH$_2$NCO-), 3.19-3.20 (m, 1H, -NHCH$_2$CH$_2$**CH$_2$**NCO-), 3.35-3.39 (m, 2H, -NHCH$_2$CH$_2$CH$_2$NCO-), 3.41-3.43 (m, 2H, **C2/6-H** Pip), 3.50-3.52 (m, 1H, -OCH$_2$CH$_2$**CH$_2$**-), 3.54-3.57 (m, 1H, -OCH$_2$CH$_2$**CH$_2$**-), 4.02 (t, 1H, ^{3}J=6.1 Hz, -O**CH$_2$**CH$_2$CH$_2$NH-), 4.05 (t, 2H, ^{3}J=5.7 Hz, -O**CH$_2$**CH$_2$CH$_2$NH-) 4.2-4.21 (m, 2H, Pip-**CH$_2$**), 7.02 (dd, 2H, ^{3}J=5.8 Hz, ^{3}J=11.6 Hz, **C2,6-H** phenoxy), 7.4 (dd, 2H, ^{3}J=5.8 Hz, ^{3}J=11.6 Hz, **C3,5-H** phenoxy); ^{13}C-NMR (150.95 MHz, methanol-d_4): δ (ppm) 10.03 (C, CH$_3$), 10.52 (C, CH$_3$), 22.74 (**C4-Pip**), 24.12 (2C, **C3,5**-Pip), 27.08 + 27.20 (**C,-CH$_2$**CH$_3$), 28.49+ 28.49 (C, -OCH$_2$CH$_2$CH$_2$NH-, -N-CH$_2$CH$_2$CH$_2$NHCO-), 29.34 (C, -OCH$_2$CH$_2$CH$_2$NH-), 29.9 (C, -N-CH$_2$CH$_2$CH$_2$NHCO-), 30.22 + 30.29 (**C,-C**H$_2$CH$_3$), 37.78 + 37.89 (C, -N-CH$_2$CH$_2$CH$_2$NHCO-), 44.46+ 44.49 (C, -OCH$_2$CH$_2$**CH$_2$**NH-, -N-CH$_2$CH$_2$CH$_2$NHCO-), 45.87 (C, -OCH$_2$CH$_2$**CH$_2$**NH-), 47.13 (C, -N-CH$_2$CH$_2$CH$_2$NHCO-), 53.7 (2C, **C2,6**-Pip), 61.36 (Pip-**CH$_2$**), 66.11+ 67.1 (-O**CH$_2$**CH$_2$CH$_2$NH-), 116.8 (2C, **C2,6**-phenoxy), 122.13 (q, **C4**-phenoxy), 133.84 (2C, **C3,5**-, phenoxy), 161.53 (q, **C1**-phenoxy), 176.27-177.21 (q, 2x **C**O); HRMS: (EI) m/z calcd. for $C_{24}H_{39}N_3O_3$ 417.2991 [M$^+$], found: 417.2993; $C_{24}H_{39}N_3O_3$ x $C_2HF_3O_3$ (532)

N-{3-[4-(Piperidin-1-ylmethyl)phenoxy]propyl}-N-(4-propionylaminobutyl)propionamide (7.11)

Compound **7.9** (23.8 mg, 74.5 µmol, 1 eq) and succinimidyl propionate (14.3 mg, 83.6 mmol, 1.1 eq) were used as described in procedure 4. The solution containing **7.11** was adjusted to a vol-

ume of 4.5 ml with acetonitrile /0.1 % TFA (20/80) and purified by preparative HPLC (system 2). After evaporation of acetonitrile and lyophilisation the product was obtained as beige oil (5.5 mg, 24 %).

RP-HPLC (220 nm, gradient 1): 99.9 % (t_R=14.8 min, k=4.8); ^{1}H-NMR: (600 MHz, methanol-d$_4$): δ (ppm) 1.04-1.11 (m, 6H, -CH$_2$**CH$_3$**), 1.44-1.63 (m, 6H, -**C3,4,5**-H Pip), 1.70-1.93 (m, 4H, -NCH$_2$**CH$_2$CH$_2$**CH$_2$-NHCO-), 2.00-2.09 (m, 2H, -OCH$_2$**CH$_2$**CH$_2$NH-), 2.15-2.20 (m, 2H, -**CH$_2$**CH$_3$) 2.39 (qua, 2H, ^{3}J=7.5 Hz, **CH$_2$**CH$_3$), 2.9 (m, 4H, **C2/6-H** Pip-NCH$_2$**CH$_2$CH$_2$**CH$_2$-NHCO-), 3.15-3.19 (m, 2H, -NCH$_2$**CH$_2$CH$_2$**CH$_2$-NHCO-), 3.34- 3.37 (m, 2H, **C2/6-H** Pip) 3.49-3.51 (m, 1H, -OCH$_2$CH$_2$**CH$_2$**NH-), 3.34-3.67 (m, 1H, -OCH$_2$CH$_2$**CH$_2$**NH-), 4.02 (t, 1H, ^{3}J=6.1 Hz, -O**CH$_2$**CH$_2$CH$_2$-), 4.03-4.06 (m, 1H, -O**CH$_2$**CH$_2$CH$_2$-), 4.19 (s, 2H, Pip-**CH$_2$**), 7.03 (dd, 2H, ^{3}J=8.7 Hz, ^{3}J=11.9 Hz **C2,6-H** phenoxy), 7.39 (dd, 2H, ^{3}J=8.7 Hz, ^{3}J=11.4 Hz, **C3,5-H** phenoxy); ^{13}C-NMR (150.95 MHz, methanol-d$_4$): insufficient amount of substance; HSQC and COSY were performed for structural determination; HRMS: (EI) m/z calcd. for C$_{25}$H$_{41}$N$_3$O$_3$ 431.3148 [M$^+$], found: 431.3148; C$_{25}$H$_{41}$N$_3$O$_3$ x C$_2$HF$_3$O$_3$ (546)

4-Fluoro-N-(3-{3-[4-(piperidin-1-ylmethyl)phenoxy]propylamino}propyl)benzamide (7.12)

Compound **7.8** (16 mg, 52.4 μmol, 1 eq) and succinimidyl 4-fluorobenzoate. (14.1 mg, 59.44 μmol, 1.1 eq) were used to synthesise compound **7.12** according to procedure 4. The solution containing **7.12** was adjusted to a volume of 5 ml with acetonitrile/0.1 % TFA (20/80) and puri-fied by preparative HPLC (system 2). After evaporation of acetonitrile and lyophilisation the product was obtained as beige oil (11.9 mg, 34 %).

RP-HPLC (220 nm, gradient 1): 99.1 % (t_R=12.66 min, k=4.0); ^{1}H-NMR: (600 MHz, methanol-d$_4$): δ (ppm) 1.45-1.51 (m, 1H, C4-H Pip), 1.66-1.83 (m, 4H, CH$_2$ Pip), 1.91-1.93 (m, 2H, CH$_2$ Pip), 1.98-2.02 (m, 2H -NHCH$_2$**CH$_2$**CH$_2$NHCO-), 2.22-2.25 (m, 2H, -OCH$_2$**CH$_2$**CH$_2$-), 2.88-2.93 (m, 2H, **C2/6-H** Pip), 3.09 (t, 2H, ^{3}J=7.2 Hz, -NHCH$_2$CH$_2$CH$_2$NHCO-), 3.25 (t, 2H, ^{3}J=7.3 Hz, -OCH$_2$CH$_2$**CH$_2$**-), 3.4-3.42 (m, 2H, **C2/6-H** Pip), 3.5 (t , 2H, ^{3}J=6.5 Hz, -NHCH$_2$CH$_2$CH$_2$NHCO), 4.19 (t, 1H, ^{3}J=5.8 Hz, -O**CH$_2$**CH$_2$CH$_2$NH-), 4.21 (s, 2H, Pip-**CH$_2$**), 7.06 (d, 2H, ^{3}J=8.7 Hz, **C2,6-H** phenoxy), 7.18 (d, 2H, ^{3}J=8.7 Hz, 4-fluorobenzamide), 7.42 (d, 2H, ^{3}J=8.7 Hz, **C3,5-H** phenoxy), 7.86-7.88 (m, 2H, 4-fluorobenzamide), ^{13}C-NMR (150.95 MHz, methanol-d$_4$): δ (ppm) 22.74 (**C4-Pip**), 24.09 (2C, **C3,5**-Pip), 27.30 (C, -OCH$_2$**C**H$_2$CH$_2$NH-), 27.9 (-NH-CH$_2$CH$_2$CH$_2$NHCO-), 37.36 (-NH-CH$_2$CH$_2$CH$_2$NHCO-), 46.54+46.73 (2C, -OCH$_2$CH$_2$**C**H$_2$NH-, -NH-CH$_2$CH$_2$CH$_2$NHCO-), 53.71 (2C, **C2,6**-Pip), 61.24 (Pip-**CH$_2$**), 66.25 (-O**CH$_2$**CH$_2$CH$_2$NH-), 116.19+ 116.41 (2C **C2,6** phenoxy, **2C** 4-fluorobenzamide), 122.67 (q,

C4-phenoxy), 131.04, 133.9 (2C 4-fluorobenzamide),133.9 (2C, **C3,5** phenoxy)**,** 161.35 (q, **C1**-phenoxy), 165.57 8q), 167.23 (q), 169.99 (q, **C**O); <u>HRMS:</u> (EI) m/z calcd. for $C_{25}H_{34}FN_3O_2$ 427.2635 [M$^+$], found: 427.2630; $C_{25}H_{34}FN_3O_2$ x $C_4H_2F_6O_6$ (656)

4-Fluoro-N-4-{3-[4-(piperidin-1-ylmethyl)phenoxy]propylamino}butyl)benzamide (7.13)

Compound **7.9** (32.7 mg, 102.4 μmol, 1 eq) and succinimidyl 4-fluorobenzoate. (27.42 mg, 116 μmol, 1.1 eq) were used as described in procedure 4. The solution containing **7.13** was adjusted to a volume of 4.5 ml with acetonitrile/0.1 % TFA (20/80) and purified by preparative HPLC (system 2, 254 nm). After evaporation of acetonitrile and lyophilisation the product was obtained as beige oil (10.4 mg, 15 %).

<u>RP-HPLC</u> (220 nm, gradient 1): 99.1 % (t_R=13.99 min, k=4.5); <u>^{1}H-NMR: (600 MHz, methanol-d$_4$):</u> δ (ppm) 1.44-1.52 (m, 1H, C4-H Pip), 1.69-1.83 (m, 8H, CH$_2$ Pip, -NHCH$_2$**CH$_2$CH$_2$**CH$_2$NHCO-), 1.91-1.93 (m, 2H, CH$_2$ Pip), 2.19 (m, 2H -^{3}J=6.0 Hz, ^{3}J=12.4 Hz, -OCH$_2$**CH$_2$**CH$_2$), 2.88-2.93 (m, **C2/6-H** Pip), 2.96-2.97 (m, 0.5H, -NHCH$_2$CH$_2$CH$_2$CH$_2$NHCO-), 3.09-3.12 (m, 2H, -NHCH$_2$CH$_2$CH$_2$CH$_2$NHCO-), 3.22-3.24 (m, 2H, -OCH$_2$CH$_2$**CH$_2$**-), 4.4- 3.44 (m, 4H, **C2/6-H** Pip, -NHCH$_2$CH$_2$CH$_2$NHCO-), 4.14 (t, 1H, ^{3}J=5.8 Hz, -O**CH$_2$**CH$_2$CH$_2$NH-), 4.2 (s, 2H, Pip-**CH$_2$)**, 7.03 (d, 2H, ^{3}J=8.7 Hz, **C2,6-H** phenoxy), 7.18 (d, 2H, ^{3}J=8.8 Hz, 4-Fluorobenzamide), 7.41 (d, 2H, ^{3}J=8.7 Hz, **C3,5-H** phenoxy),7.86-7.88 (m, 2H, 4-Fluorobenzamide); <u>^{13}C-NMR (150.95 MHz, methanol-d$_4$):</u> δ (ppm) 22.74 (**C4-Pip**), 24.08 (2C, **C3,5**-Pip), 24.57+25.57 (-NH-CH$_2$CH$_2$CH$_2$CH$_2$NHCO-), 27.19 (C, -OCH$_2$**CH$_2$**CH$_2$NH-), 27.63 (-NH-CH$_2$CH$_2$CH$_2$CH$_2$NHCO-), 39.94 + 40.03 (-NH-CH$_2$CH$_2$CH$_2$CH$_2$NHCO-), 46.52 (C, -OCH$_2$CH$_2$**CH$_2$**NH-), 49.58 (-NH-CH$_2$CH$_2$CH$_2$CH$_2$NHCO-), 53.69 (2C, **C2,6**-Pip), 61.22 (Pip-**CH$_2$**), 66.21 (-O**CH$_2$**CH$_2$CH$_2$NH-), 116.13+ 116.34 (116.48) (2C **C2,6**-phenoxy, **2C** 4-fluorobenzamide), 122.68 (q, **C4**-phenoxy), 130.81 (2C 4-fluorobenzamide), 131.89 (q), 133.92 (2C, **C3,5** phenoxy), 161.3 (q, C1-phenoxy), 165.40 (q), 167.05 (q), 169.21 (q, **C**O); <u>HRMS:</u> (EI) m/z calcd. for $C_{26}H_{36}FN_3O_2$ 441.2792 [M$^+$], found: 441.2794; $C_{26}H_{36}FN_3O_2$ x $C_4H_2F_6O_6$ (670)

7.6.2 Pharmacological methods

7.6.2.1 Steady state GTPase assay

See chapter 3.

7.6.2.2 Fluorimetric Ca²⁺ assay on U373-MG cells

See chapter 3.

7.6.2.3 Radioligand binding assay on HEK293-FLAG-hH₃R-His₆ cells

See chapter 3

7.6.2.4 Radioligand binding assay at HEK293-FLAG-hH₄R-His₆ cells

The radioligand binding assays were performed as described in chapter 3. Radioligand [³H]UR-PI294 (K_D value 7.5 nM)[20] was used at a concentration of 5 nM[18].

References

1.   Parsons, M. E.; Ganellin, C. R. Histamine and its receptors. *Br. J. Pharmacol.* **2006,** 147 Suppl 1, S127-35.

2.   Leurs, R.; Bakker, R. A.; Timmerman, H.; de Esch, I. J. The histamine H_3 receptor: from gene cloning to H_3 receptor drugs. *Nat Rev Drug Discov* **2005,** 4, 107-20.

3.   Esbenshade, T. A.; Browman, K. E.; Bitner, R. S.; Strakhova, M.; Cowart, M. D.; Brioni, J. D. The histamine H_3 receptor: an attractive target for the treatment of cognitive disorders. *Br. J. Pharmacol.* **2008,** 154, 1166-81.

4.   Celanire, S.; Wijtmans, M.; Talaga, P.; Leurs, R.; de Esch, I. J. Keynote review: histamine H_3 receptor antagonists reach out for the clinic. *Drug Discov Today* **2005,** 10, 1613-27.

5.   Gemkow, M. J.; Davenport, A. J.; Harich, S.; Ellenbroek, B. A.; Cesura, A.; Hallett, D. The histamine H_3 receptor as a therapeutic drug target for CNS disorders. *Drug Discov Today* **2009,** 14, 509-15.

6.   Letavic, M. A.; Aluisio, L.; Atack, J. R.; Bonaventure, P.; Carruthers, N. I.; Dugovic, C.; Everson, A.; Feinstein, M. A.; Fraser, I. C.; Hoey, K.; Jiang, X.; Keith, J. M.; Koudriakova, T.; Leung, P.; Lord, B.; Lovenberg, T. W.; Ly, K. S.; Morton, K. L.; Motley, S. T.; Nepomuceno, D.; Rizzolio, M.; Rynberg, R.; Sepassi, K.; Shelton, J. Pre-clinical characterization of aryloxypyridine amides as histamine H_3 receptor antagonists: identification of candidates for clinical development. *Bioorg. Med. Chem. Lett.* **2010,** 20, 4210-4.

7.   Dvorak, C. A.; Apodaca, R.; Barbier, A. J.; Berridge, C. W.; Wilson, S. J.; Boggs, J. D.; Xiao, W.; Lovenberg, T. W.; Carruthers, N. I. 4-phenoxypiperidines: potent, conformationally restricted, non-imidazole histamine H_3 antagonists. *J. Med. Chem.* **2005,** 48, 2229-38.

8.   Apodaca, R.; Dvorak, C. A.; Xiao, W.; Barbier, A. J.; Boggs, J. D.; Wilson, S. J.; Lovenberg, T. W.; Carruthers, N. I. A new class of diamine-based human histamine H$_3$ receptor antagonists: 4-(aminoalkoxy)benzylamines. *J. Med. Chem.* **2003,** 46, 3938-44.

9.   Swanson, D. M.; Wilson, S. J.; Boggs, J. D.; Xiao, W.; Apodaca, R.; Barbier, A. J.; Lovenberg, T. W.; Carruthers, N. I. Aplysamine-1 and related analogs as histamine H$_3$ receptor antagonists. *Bioorg. Med. Chem. Lett.* **2006,** 16, 897-900.

10.   Wijtmans, M.; Denonne, F.; Celanire, S.; Gillard, M.; Hulscher, S.; Delaunoy, C.; Van houtvin, N.; Bakker, R. A.; Defays, S.; Gerard, J.; Grooters, L.; Hubert, D.; Timmerman, H.; Leurs, R.; Talaga, P.; de Esch, I. J. P.; Provins, L. Histamine H$_3$ receptor ligands with a 3-cyclobutoxy motif: a novel and versatile constraint of the classical 3-propoxy linker. *MedChemComm* **2010,** 1, 39-44.

11.   Barbier, A. J.; Berridge, C.; Dugovic, C.; Laposky, A. D.; Wilson, S. J.; Boggs, J.; Aluisio, L.; Lord, B.; Mazur, C.; Pudiak, C. M.; Langlois, X.; Xiao, W.; Apodaca, R.; Carruthers, N. I.; Lovenberg, T. W. Acute wake-promoting actions of JNJ-5207852, a novel, diamine-based H$_3$ antagonist. *Br. J. Pharmacol.* **2004,** 143, 649-61.

12.   Ligneau, X.; Landais, L.; Perrin, D.; Piriou, J.; Uguen, M.; Denis, E.; Robert, P.; Parmentier, R.; Anaclet, C.; Lin, J. S.; Burban, A.; Arrang, J. M.; Schwartz, J. C. Brain histamine and schizophrenia: potential therapeutic applications of H$_3$-receptor inverse agonists studied with BF2.649. *Biochem. Pharmacol.* **2007,** 73, 1215-24.

13.   Barbier, A. J.; Aluisio, L.; Lord, B.; Qu, Y.; Wilson, S. J.; Boggs, J. D.; Bonaventure, P.; Miller, K.; Fraser, I.; Dvorak, L.; Pudiak, C.; Dugovic, C.; Shelton, J.; Mazur, C.; Letavic, M. A.; Carruthers, N. I.; Lovenberg, T. W. Pharmacological characterization of JNJ-28583867, a histamine H($_3$) receptor antagonist and serotonin reuptake inhibitor. *Eur. J. Pharmacol.* **2007,** 576, 43-54.

14.   Buschauer, A.; Postius, S.; Szelenyi, I.; Schunack, W. [Isohistamine and homologs as components of H$_2$-antagonists. 22. H$_2$-antihistaminics]. *Arzneimittelforschung.* **1985,** 35, 1025-9.

15.   Abdel-Magid, A. F.; Carson, K. G.; Harris, B. D.; Maryanoff, C. A.; Shah, R. D. Reductive Amination of Aldehydes and Ketones with Sodium Triacetoxyborohydride. Studies on Direct and Indirect Reductive Amination Procedures(1). *J. Org. Chem.* **1996,** 61, 3849-3862.

16.   Ghorai, P.; Kraus, A.; Keller, M.; Gotte, C.; Igel, P.; Schneider, E.; Schnell, D.; Bernhardt, G.; Dove, S.; Zabel, M.; Elz, S.; Seifert, R.; Buschauer, A. Acylguanidines as bioisosteres of guanidines: NG-acylated imidazolylpropylguanidines, a new class of histamine H$_2$ receptor agonists. *J. Med. Chem.* **2008,** 51, 7193-204.

17.   Schnell, D. *Personal communication*. In Department of Pharmacology and Toxicology, University of Regensburg (Germany), **2008**.

18.   Nordemann, U. *Personal communication*. In Department of Pharmaceutical and Medicinal Chemistry II, University of Regensburg (Germany), **2009**.

19.   Schneider, E. *Personal communication*. In Department of Pharmacology and Toxicology, University of Regensburg, **2008**.

20.   Igel, P.; Schnell, D.; Bernhardt, G.; Seifert, R.; Buschauer, A. Tritium-labeled N(1)-[3-(1H-imidazol-4-yl)propyl]-N(2)-propionylguanidine ([(^{3})H]UR-PI294), a high-affinity histamine H($_3$) and H($_4$) receptor radioligand. *ChemMedChem* **2009,** 4, 225-31.

Chapter 8

Fluorescent H₃-receptor ligands

8   Fluorescent H₃-receptor ligands

8.1   Introduction

The approach described in chapter 6 to fluorescent H₂R ligands was considered promising with respect to the design and synthesis of labelled H₃R ligands, too. So far, only fluorophores emitting at wavelengths below 600 nm were introduced into H₃R antagonistic structures. These po-

tent ligands are bearing fluorophores such as NBD, Dansyl, TAMRA or cyanoisoindoles (Figure 8.1)[1-4]. Compounds related to ABT-239 [5-7] and (3-phenoxypropyl)piperidine derivatives were employed as building blocks. To the best of our knowledge no H₃R fluorescent ligands emitting at wavelengths above 600 nm are reported in the literature. The aim of this work was to synthesize and characterise such fluorescent probes and to explore whether more bulky red-emitting fluorophores are tolerated in terms of H₃R affinity. For this purpose we used the new H₃R

Figure 8.1: Representative examples for fluorescent H₃R ligands (**8.1a** Abt-239 related, **8.1b** (3-phenoxypropyl)piperidine derivative**)**

ligands described in chapter 7 and coupled them to cyanine, bodipy and pyrylium (Py) dyes (structures of fluorophores see chapter 6). A squaramide-type H₃R ligand was included in this series despite its additional activity at the H₂R to evaluate the impact of the fluorophore on affinity and selectivity.

8.2 Chemistry

Pyridinium compounds were prepared in a mixture of DMF and MeOH at rt under light protection. The reactions took place within 30 min to 3 h, visible by a change in color from dark blue to red (see chapter 7). Preparative HPLC, followed by lyophilisation afforded the products as red semi solids. H_3R ligands were coupled to cyanine dyes, Bodipy and carboxyfluorescein via the active esters of the fluorescent dyes resulting in the corresponding amides.

Compd.	X	Fluorophore	Compd.	X	Fluorophore
8.1	-NH(CH$_2$)$_3$-	S0536	8.5	-NH(CH$_2$)$_4$-	5-SFX
8.2	-NH(CH$_2$)$_4$-	S0536	8.6	-NH(CH$_2$)$_4$-	Py5
8.3	-NH(CH$_2$)$_4$-	Dy675	8.7	-	Py1
8.4	-NH(CH$_2$)$_4$-	Bodipy 650/665, X-SE	8.8	-	S0535
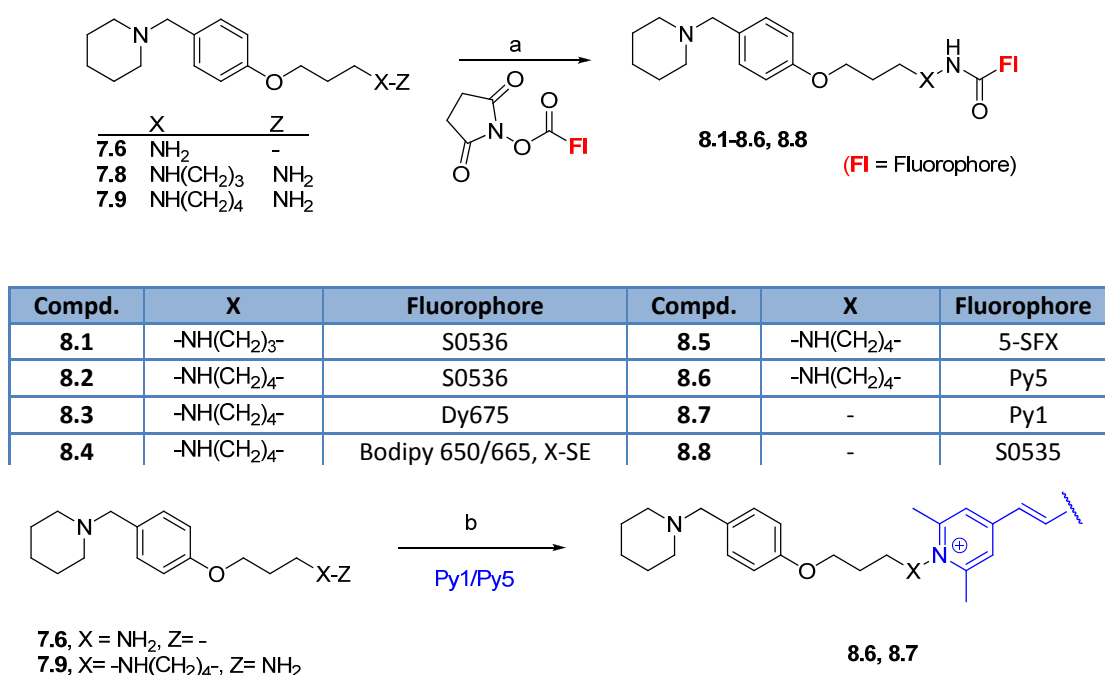
Scheme 8.1: Synthesis of fluorescent ligands **8.1-8.8**. Reagents and conditions: (a) organic solvent (see exp.data,) Et$_3$N, rt, light protection, 30 min - 3 h, (b) MeOH, rt, 30 min to 3 h, light protection.

The coupling reactions with succinimidyl esters were performed overnight at rt in an organic solvent (mainly MeCN or MeOH) at a pH of 8-9 under light protection. Purification was done by preparative HPLC, followed by lyophilisation to give the products as colored semi solids (schematic reactions see chapter 6).

Compounds **7.6**, **7.8** and **7.9** were coupled to a range of different fluorophores (Scheme 8.1), including Py, bodipy and cyanine dyes. The fluorophore S0535-NHS was coupled to **UR-Fp-05** and to compound **7.7,** whereas ligand **7.16** was coupled to S0535 and Dy630 (Scheme 8.2).
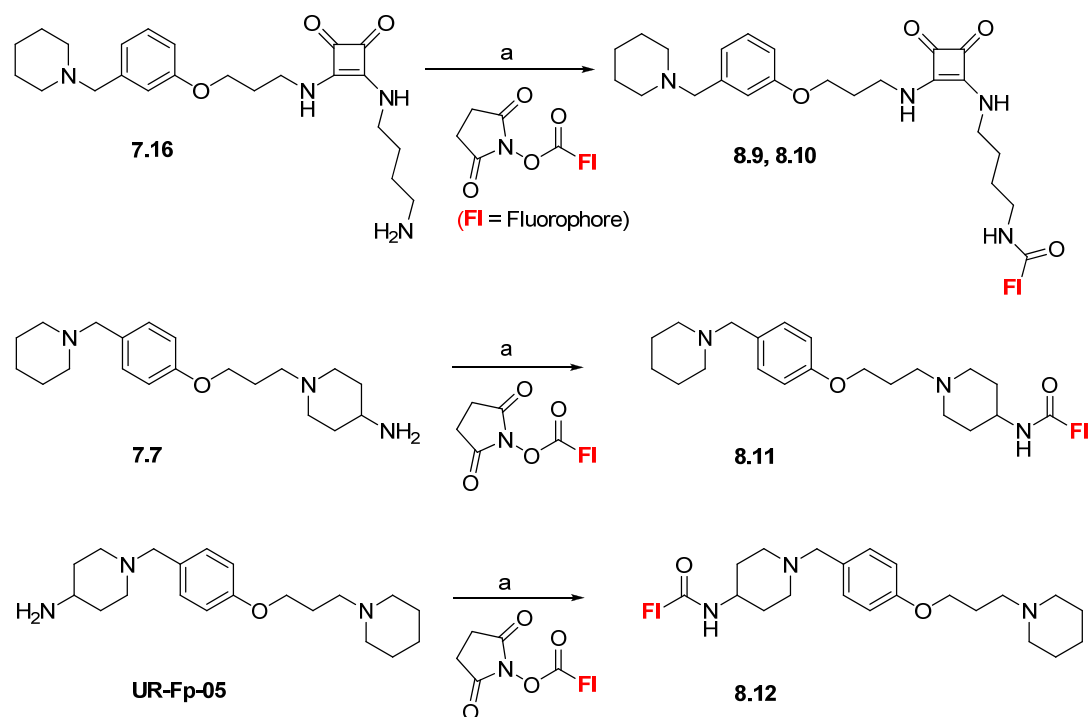
Scheme 8.2: Synthesis of ligands **8.9** - **8.12**. Reagents and conditions: (a) Et$_3$N, MeCN/MeOH, light protection, rt, 30 min to 3 h.

8.3 Pharmacological results

8.3.1 H$_3$ receptor antagonism and binding

The fluorescent H$_3$R ligands were investigated for H$_3$R antagonism versus histamine in a steady state GTPase assay on Sf9 cell membranes expressing the hH$_3$R plus G$_{i\alpha2}$, $\beta_1\gamma_2$ and RGS4[8]. Moreover, H$_3$R binding was determined on HEK293-FLAG-hH$_3$R-His$_6$ cells. The results are summarized in Table 8.1. Histamine stimulated GTP hydrolysis was inhibited by all test compounds (K$_{b'}$-values: 5.8 -123 nM), except for compound **8.5** (K$_{b'}$ > 1900 nM). Thus, except for carboxyfluorescein, all fluorophores were tolerated. Inverse H$_3$R agonism was detected, mostly with intrinsic activities slightly higher than that of thioperamide and in the same range as that of JNJ5207852. Only the squaramides and compound **8.12** showed lower inverse agonism (intrinsic activities about -0.25). Among the most potent compounds were those with fluorophores directly attached to the 3-[4-(piperidin-1-ylmethyl)phenoxy]propan-1-amine (**8.7**), as well as those bearing

flexible alkylamine spacers (**8.1-8.4, 8.6**). They all showed H$_3$R antagonistic activities with K$_{b'}$-values lower than 35 nM. In case of 3-[4-(piperidin-1-ylmethyl)phenoxy]propan-1-amine derivatives devoid of spacer groups, labelling with the pyrylium dye Py1 (**8.7**) was superior to coupling with the more bulky cyanine dye S0535. In general, the labelled ligands were more active than the corresponding parent compounds. In case of **8.6** and **8.8** even a 7 to 50 fold increase in H$_3$R antagonistic potency was observed. Labelling of aminopiperidines (**8.11, 8.12**) and aminoalkyl-squaramides (**8.9, 8.10**) resulted in K$_{b'}$-values around 30 to 60 nM (Table 8.1), which are in the same range as those of the corresponding parent ligands (see chapter 7). The results from the functional GTPase assay were confirmed by radioligand binding experiments on HEK293-FLAG-hH$_3$R-His$_6$ cells with [^{3}H]NAMH as radioligand. K$_i$-and K$_{b'}$-values were in the same order of magnitude.

Table 8.1: H$_3$R antagonism and binding of selected compounds on Sf9 cell membranes (GTPase) and on HEK-293-FLAG-hH$_3$R-His$_6$cells

Compd.	GTPase assay hH$_3$R+ G$_{i\alpha2}$ + β$_1$γ$_2$ + RGS4[a]		Binding assay HEK293-FLAG-hH$_3$R-His6 cells[c]
	K$_{b'}$ [nM]	E$_{max}$	K$_i$ (K$_D$) [nM]
Histamine	EC$_{50}$ 25± 3[b]	1.00	-
[^{3}H]NAMH	-	-	(5.1)[d]
JNJ5207852	4.3 ± 0.6	-0.88 ± 0.12	2.3
Thioperamide	97 ± 18	-0.66 ± 0.1	n.d.
8.1	21 ± 10	-1.03 ± 0.14	11 ± 2
8.2	22 ± 18	-0.98 ± 0.14	13 ± 2
8.3	5.8 ± 0.5	-0.9 ± 0.25	22 ± 1
8.4	6.4 ± 1.2	-0.85 ± 0.26	7.2 ± 1
8.5	1956 ± 763	-0.85 ± 0.15	963 ± 1 30
8.6	34 ± 14	-0.91 ± 0.29	9.2 ± 0.0
8.7	15 ± 6	-0.9 ± 0.27	4.2 ± 1.5
8.8	123 ± 36	-0.8	531 ± 58
8.9	51 ± 14	-0.25 ± 0.02	232 ± 54
8.10	54 ± 6	n.d.	239 ± 66
8.11	42 ± 27	-0.26 ± 0.02	33 ± 13
8.12	36 ± 4	-0.26 ± 0.03	100 ± 42

[a] steady state GTPase assay on Sf9 cell membranes; c. ligands: 1 nM - 100 µM; typical GTPase activities (stimulation with 100 nM HIS (hH$_3$R): 2.5-6.0 pmol x mg^{-1} x min^{-1}; E$_{max}$= efficacy relative to histamine E$_{max}$ HIS=1 (c. ligands: 10 µM), Mean values ± S.E.M. (n = 1-3, performed in duplicate); [b] cf. ref. [9]

[c] c. ligands: 1 nM - 100 µM, c. [^{3}H]NAMH: 1 nM, 2-5 million cells/well; Mean values ± S.E.M. (n = 1-2, performed in duplicate); n.d.: not determined, [c,d] cf. ref. [10]

8.3.2   Histamine receptor subtype selectivity

In GTPase assays on recombinant hH_1R^{11} (hH_1R and RGS4 co-expressed in Sf9 cells) the test compounds were devoid of agonistic or inverse agonistic activity (intrinsic activities: -0.09 to 0.01; data cf. appendix). Inverse agonistic efficacies at the hH_4R (Sf9 cell membranes expressing hH_4R-RGS19 $+G_{i\alpha2}+G\beta_1\gamma_2^8$) were moderate to low between -0.4 and -0.05 (cf. appendix). But the majority of compounds were devoid of remarkable activity at the hH_4R, determined in the antagonist mode ($K_{b'}$ values > 2000 nM). Exceptions were compounds **8.4, 8.10** and **8.11** with $K_{b'}$-values in the range between 400 and 1000 nM. The high affinity H_3R antagonist **8.4** had only six fold selectivity for the H_3R compared to the H_4R. An unfavourable influence of the bodipy fluorophore on receptor selectivity was also observed for H_2R ligands (cf. chapter 6).

Selected substances were investigated for H_4R affinity in competition binding on HEK293-FLAG-hH_4R-His$_6$ cells using $[^3H]$UR-PI294^{12} as the radioligand. For the majority of compounds the results from the functional assay were confirmed by binding data (Table 8.2). By contrast, for **8.4** and **8.11**, which were found to be moderate H_4R antagonists in the GTPase assay, there was no marked H_4R affinity detectable in the binding assay.

At the hH_2R^{13} the ligands **8.1**-**8.7** elicited no remarakable effects as agonists or inverse agonists (E_{max} values between -0.14 and 0.03). Compound **8.8** and the aminopiperidine derivatives **8.11** and **8.12** had weak inverse agonistic efficacies (-0.22 and -0.18). As expected these ligands showed the characteristics of the class of phenoxyalkylamine H_3R antagonists related to JNJ5207852, which are generally devoid of significant antagonistic activity at the H_2R. This was confirmed by GTPase assays performed in the antagonist mode, revealing $K_{b'}$-values > 700 nM. This represents more than 50 fold selectivity for the H_3R compared to the H_2R. By contrast, the squaramides (**8.9, 8.10**) were only about 3 to 5 fold more active at the H_3R compared to the H_2R (weak H_2R inverse agonism, E_{max}= -0.2).

Table 8.2: Antagonistic activity of selected fluorescent H_3R antagonists on hH_2R and hH_4R determined on Sf9 cell membranes (GTPase) and binding affinity on HEK-293-FLAG-hH_4R-His_6cells

Compd.	hH_2R GTPase[a]		hH_4R GTPase	hH_4R Binding
	hH_2R-$G_{s\alpha s}$		hH_4R-RGS19 + $G_{i\alpha 2}$+$G_{\beta 1\gamma 2}$	HEK293-FLAG-hH_4R-His6 cells[b]
	$K_{b'}$ [nM]	E_{max}	$K_{b'}$ [nM]	K_i (K_D) [nM]
Histamine	EC_{50} 990 ± 92[c]	1.00	EC_{50} 12 ± 3[d]	
[^{3}H]UR-PI294	-	-	-	(7.5)
8.1	>4000	0.03 ±0.07	5621 ± 2448	1431
8.2	1249 ±130	-0.05 ±0.07	>10000	1845
8.3	675 ±18	-0.1 ±0.02	>2000	n.d
8.4	717 ±167	-0.14 ±0.02	436 ±109	4349
8.5	2583 ±246	-0.03 ±0.03	>5000	n.d
8.6	2933 ±1569	-0.14 ±0.0	5395 ± 1693	>5000
8.7	2322±1413	-0.1 ±0.01	>10000	>5000
8.8	>2000	-0.22 ± 0.03	3684 ±392	>2500
8.9	265 ±113	-0.21 ± 0.00	2457	>2500
8.10	156 ±31	-0.20 ± 0.00	1063	n.d
8.11	>2000	-0.18 ± 0.08	879	>2500
8.12	580 ±169	-0.24 ± 0.01	>10000	n.d

[a] steady state GTPase assay on Sf9 cell membranes; concentrations of ligands: 1 nM - 100 μM; typical GTPase activities (stimulation with 100 nM HIS (hH_4R), stimulation with 1 μM HIS (hH_2R): 2.5-6.0 pmol x mg^{-1} x min^{-1}; E_{max}= efficacy relative to histamine = 1 (E_{max} HIS=1) (c. ligands: 10 μM, for efficacy), Mean values ± S.E.M. (n = 1-3; performed in duplicate).

[b] concentrations of ligands: 1 nM - 100 μM, c. [^{3}H]UR-PI294: 5nM, 2-5 million cells/well; mean values ± S.E.M. (n = 1-2, performed in duplicate); n.d; not determined [c] cf. ref.[14], [d] cf. ref. [15]

8.3.3   Fluorescence based methods on HEK293-FLAG-hH₃R-His6 cells

8.3.3.1   *Fluorescence properties of labelled antagonists*

Quantum yield determination, emission and excitation spectra for selected fluorescent ligands were recorded in three solutions as described in chapter 6. In case of the cyanine, bodipy and Py dyes the fluorescence properties were not remarkably influenced by the nature of the attached H₃R antagonist moiety. An increase (2-3 fold) in quantum yields was observed by changing the solvent from PBS to PBS with 1 % BSA. In case of the Py dyes for compound **8.7** even a 27 fold increase was oberved. In solutions containing proteins intermolecular interactions, such as electrostatic or hydrophobic interactions can occur, resulting in higher quantum yields. Additionally, upon binding to proteins a kind of "rigidization" can take place enhancing the quantum yields. For compound **8.7** such effects can be assumed. The observed changes of the quantum yield by the addition of BSA to solutions of bodipy, cyanine and Py5 coupled ligands in PBS were obviously not as pronounced as for the Py1 derived compound **8.7**, but to a certain extent such effects also seem to play a role. In principle, the moderate to good quantum yields in PBS + 1 % BSA make these ligands applicable to confocal microscopy and flow cytometry.

Table 8.3: Spectroscopic properties of selected fluorescent compounds in PBS (pH 7,4), 1 % BSA in PBS andethanol

Compd	(Dye)	PBS		PBS+ 1 % BSA		EtOH	
		$\lambda_{ex}/\lambda_{em}$	Φ [%]	$\lambda_{ex}/\lambda_{em}$	Φ [%]	$\lambda_{ex}/\lambda_{em}$	Φ [%]
8.1	S0536	644/668	14 ± 1	664/670	34	650/670	29 ± 2
8.3	Dy675	675/702	31 ± 2	675/703	26 ± 3	675/700	10 ± 1
8.4	"Bodipy"	652/665	21 ± 4	659/ 669	36 ± 3	600/669	37 ± 10
8.6	Py5	455/705	11 ± 8	530/ 637	25 ± 4	500/700	10 ± 5
8.7	Py1	459/646	1 ± 0.2	531/605	27 ± 1	511/625	1.5
8.8	S0535	645/666	17 ± 2	662/686	58 ± 7	600/665	39 ± 19
8.11	S0535	647/683	17 ± 2	666/675	55 ± 5	669/694	48 ± 6
8.12	S0535	645/685	8 ± 1	666/686	27 ± 5	669/693	15 ± 2

$\lambda_{ex}/\lambda_{em}$: excitation/emission maxima, Φ: quantum yield (reference: cresyl violet perchlorate)

8.3.4 Flow cytometric saturation binding experiments

Flow cytometry was essentially performed as previously described[16], using HEK293-FLAG-hH$_3$R-His6 cells (kindly provided by David Schnell, Department of Pharmacology and Toxicology, University of Regensburg) instead of H$_2$R expressing cells (cf. experimental section). The most potent compounds (**8.1-8.4, 8.6** and **8.7**) were investigated in saturation binding experiments. High specific binding (70- 80 %) in the range of the K$_D$-value was determined for compounds **8.1** and **8.2** (with S0536 as fluorescent dye) and for **8.6** (Py5 labelled; data see Table 8.4). The determined K$_D$-values were in agreement with data from radioligand binding and from functional GTPase assays. In the case of **8.3, 8.4** and **8.7** no K$_D$-values were calculated as the percentage of unspecific binding exceeded specific binding. Obviously, the applicability of the ligands to flow cytometry does not mainly depend on the fluorescent dye used for labelling. Cyanine dyes as well as Py dyes proved to be useful to obtain suitable fluorescent probes. As an example the saturation binding curve of compound **8.6** is depicted in Figure 8.2.
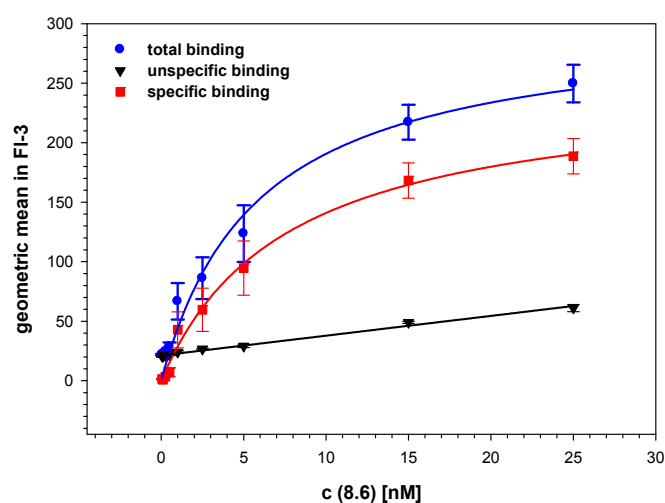
Compd.	K$_D$ [nM]
8.6	15 ±4

Figure 8.2: Saturation binding of **6.17** on HEK293–FLAG-hH$_3$R-His$_6$ cells (mean values ± S.E.M, n=3), unspecific binding determined in the presence of thioperamide (c final: 10 µM), incubation time: 15 min, rt

Table 8.4: Saturation binding of selected H$_3$R fluorescent ligands on HEK293 –FLAG-hH$_3$R-His$_6$ cells[a]

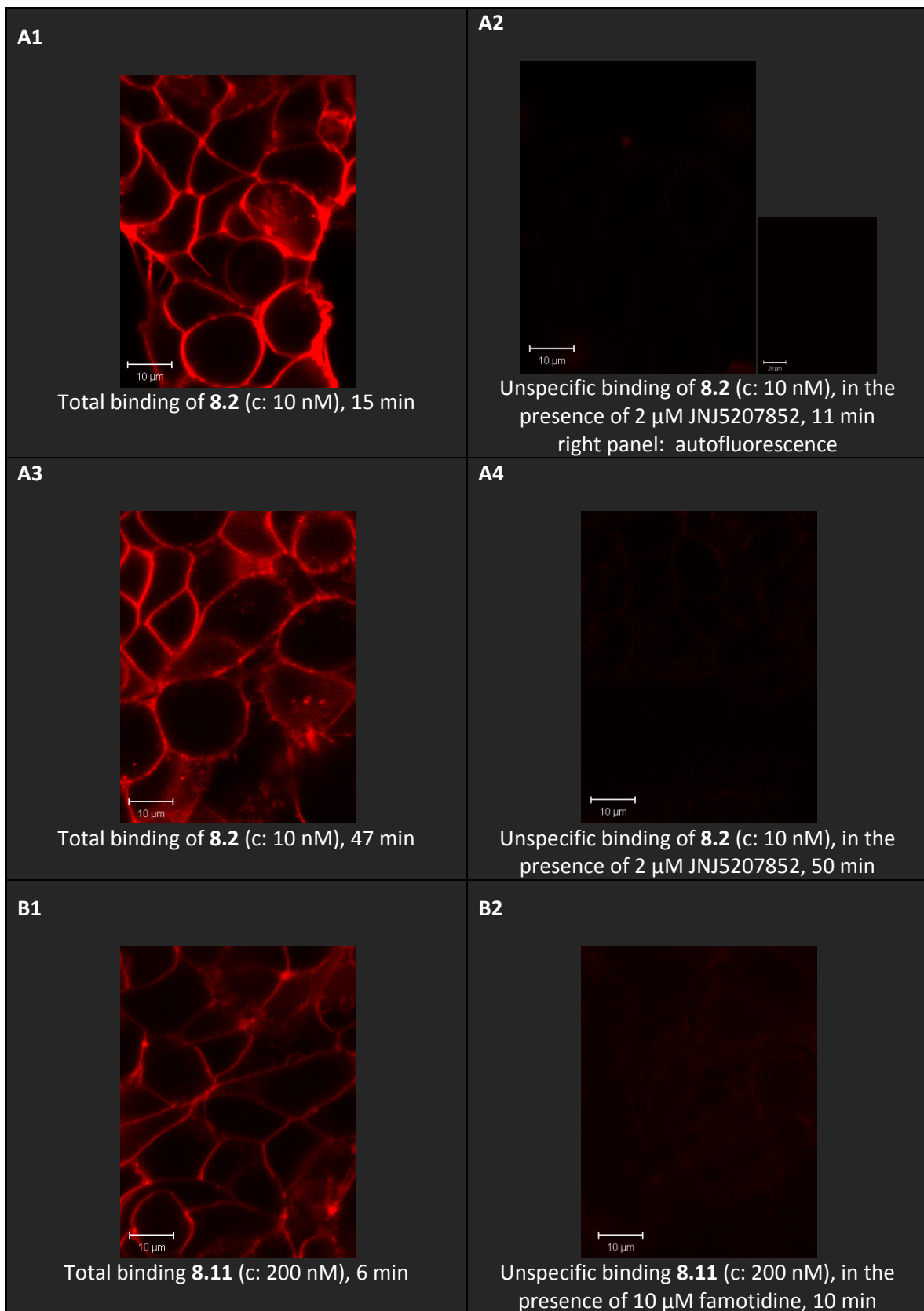| Compd.	HEK293 –FLAG-hH$_3$R-His$_6$ cells K$_D$ [nM]
8.1, 199	8.5 ± 2
8.2, 200	8 ± 3 [b]
8.6, 178	15 ± 4

[a] c. ligands: 1 nM-50 nM, 1-2 million cells/ml; Mean values ± S.E.M. (n = 2-3 unless otherwise indicated);
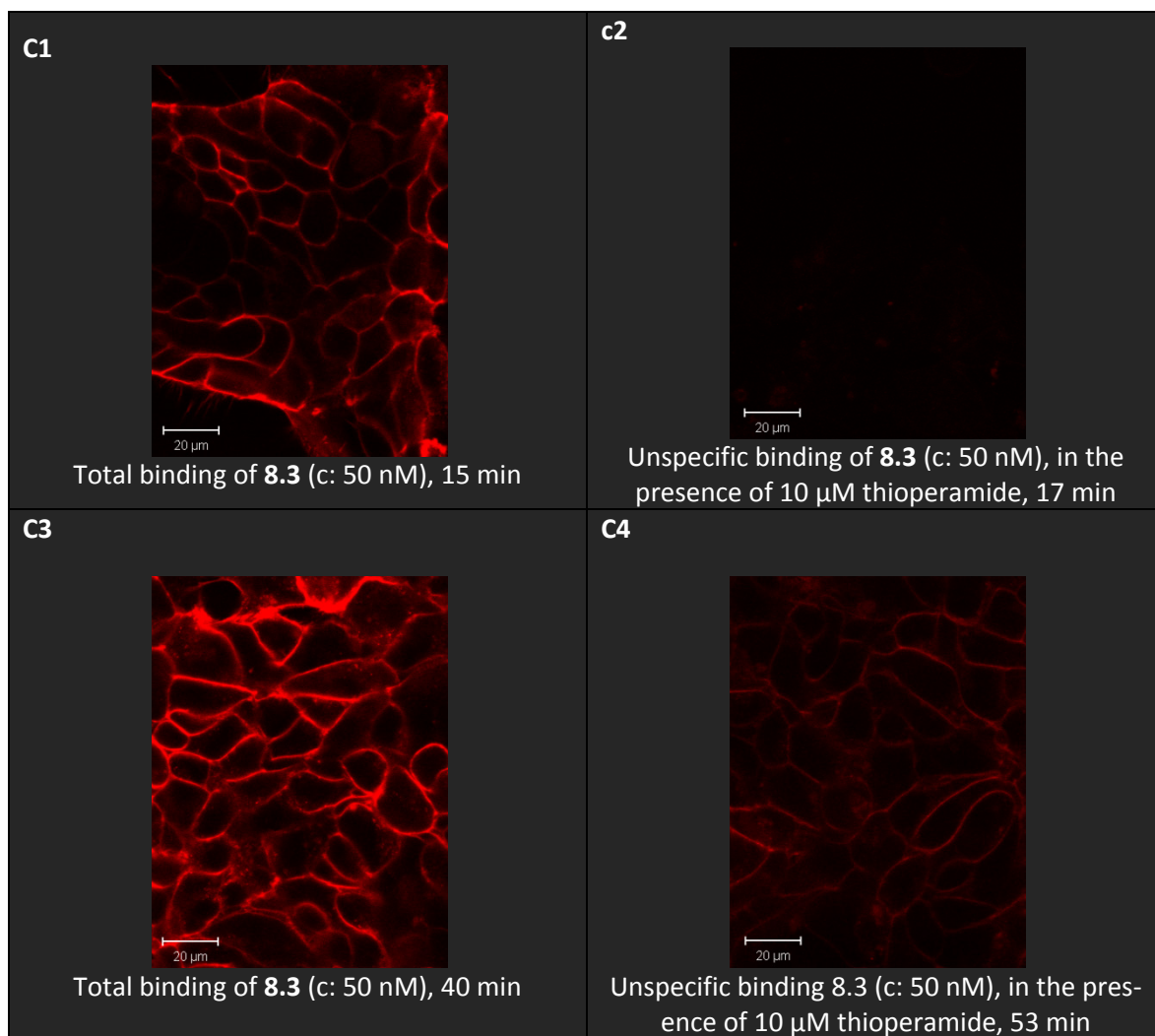[a] n=1.

8.3.4.1   Confocal microscopy

Ligand binding was detected by confocal microscopy on HEK293 –FLAG-hH$_3$R-His$_6$ cells by anal-ogy with the method described in chapter 6 for H$_2$R fluorescent ligands. Investigated compounds were used at concentrations around the determined K$_D$- /K$_{b'}$-value and unspecific binding was determined in the presence of 10 µM thioperamide or 2 µM JNJ5207852. Ligands investigated in flow cytometry were selected for confocal microscopy with respect to comparison of the results from both methods. Despite high specific binding affinity no difference between total and un-specific binding could be determined at the confocal microscope for pyridinium compound **8.6.** By contrast, ligands bearing S0536 (**8.1** and **8.2**) showed a clear difference between total and unspecific binding within a time period of 15 min (as an example: see binding of **8.2** in Figure 8.3, A1-A4). This is in accordance with flow cytometric measurements. After 47 min the pictures indi-cate only a slight tendency toward cellular uptake of the ligand (Figure 8.3, A3/4). Stimulated by these results compound **8.11,** which is bearing a structurally very similar fluorophore (S0535, only differing from S0536 in one additional aromatic group), was also successfully applicated to visualize binding to the H$_3$R. However, it has to be taken into account that a higher concentra-tion of the ligand was used; this could explain the observed higher unspecific binding.

Images were also acquired for compounds **8.3** and **8.4**, despite the lack of specific binding in flow cytometry. For ligand **8.4** binding was detected at a concentration of 10 nM, but the incu-bation period had to be extended, and the compound was taken up by the cells. A similar effect was already observed for H$_2$R fluorescent ligands bearing the same fluorophore (bodipy, data not shown). Ligand **8.3** had to be used at a concentration as high as 50 nM to clearly discrimi-nate between specific and unspecific binding (Figure 8.4, C1 and C2). The tendency for high un-specific binding, already observed in flow cytometry, was evident in pictures taken at extended incubation periods (Figure 8.4, C3 and C4). Anyway it has to be taken into consideration that the concentration of 50 nM (final c) was five fold higher than the K$_{i'}$-value from radioligand binding. This may be the major reason for relatively high unspecific binding under these conditions.

Figure 8.3: Binding of **8.2 and 8.11** to the H_3R expressed in HEK293 FLAG-hH_3R-His_6 cells; cells were incubated in Leibovitz culture medium with 1 % FCS for 15-50 min at 37 °C; C-Apochromat 40x/1.2W, 633 nm/LP650; pinhole 268 μm

C1

Total binding of **8.3** (c: 50 nM), 15 min

c2

Unspecific binding of **8.3** (c: 50 nM), in the presence of 10 µM thioperamide, 17 min

C3

Total binding of **8.3** (c: 50 nM), 40 min

C4

Unspecific binding **8.3** (c: 50 nM), in the presence of 10 µM thioperamide, 53 min

Figure 8.4: : Binding of **8.3** to the H_3R expressed in HEK293 FLAG-hH$_3$R-His$_6$ cells; cells were incubated in Leibovitz L15 culture medium with 1 % FCS for 15-50 min at 37 °C; C-Apochromat 40x/1.2W, 633 nm/LP650;pinhole 268 µm

8.4 Discussion

The phenoxyalkyl-substituted piperidine ring (in blue, see Figure 8.5) in JNJ5207852 was re-
placed with an amino group or an aminoalkyl residue
allowing for coupling of these new H_3R receptor ligands
to different types of fluorophores. The resulting deri-
vates turned out to be potent and selective H_3R fluores-
cent antagonists. Usually, labelling of small ligands with
bulky fluorophores results in a decrease in binding affin-
ity (for examples cf. chapter 6 or fluorescent NPY recep-

JNJ5207852

Figure 8.5: JNJ5207852

tor ligands[17]). By contrast, in this series of compounds structurally diverse more and less bulky
fluorophores were tolerated. The H_3R affinity was maintained or even increased (e.g. **8.7, 8.8**),
suggesting the fluorophore to contribute to affinity by interaction with additional binding sites.
Substances lacking an additional spacer or having flexible alkyl linkers turned out to be the most
potent H_3R antagonists. There was no clear preference for one of the fluorophores. However, as
already observed for H_2R ligands, carboxyfluorescein-labeled compounds were not suited as
pharmacological tools due to low receptor affinity and unfavourable fluorescence properties.
Fluorescent squaramide derivatives turned out to be combined H_2R/H_3R antagonists, as ex-
pected from the selectivity data of the precursor. Thus, the nature of the fluorophore did not
change the selectivity profile of this kind of ligands. The observation that ligands coupled to
bodipy dyes were taken up by the cells and displayed lower receptor subtype selectivity (here:
towards the H_4R) was evident in this series of compounds as well as the example of the squara-
mide type H_2R fluorescent ligands. S0536 labeled (**8.1, 8.2**) and the Py5 coupled ligands (**8.6**)
proved to be suitable as pharmacological tools in flow cytometry. These compounds displayed a
high degree of specific binding at concentrations in the range of the K_D-value. This was con-
firmed for compound **8.2** by confocal microscopy.
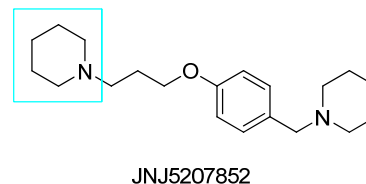
8.5 Summary and conclusion

The aim to synthesize new fluorescent H_3R ligands with high affinity and selectivity versus the
other receptor subtypes resulted in potent H_3R antagonists. Three ligands, **8.1**, **8.2** and **8.6** were
succesfully applied in fluorescence based methods, i. e. in flow cytometry (**8.1**, **8.2** and **8.6**) and
confocal microscopy (**8.2**). To our knowledge these compounds are currently the most potent
H_3R fluorescent ligands emitting at wavelengths above 600 nm. These labelled antagonists could
be valuable pharmacological tools, for instance, to determine ligand affinities at the H_3R with the

aid of fluorescence based methods, to detect H_3Rs on the cellular level in tissues, to study recep-
tor trafficking and to extend the spectrum of methods with the perspective of applications in
high throughput screening.

8.6   Experimental section

8.6.1   Chemistry

8.6.1.1   *General conditions*

See chapter 3, especially conditions for HPLC analysis.

8.6.1.2   *Preparation of fluorescent ligands*

General procedure 1 - Labelling of amines with succinimidyl esters of fluorescent dyes

Primary amines (1-2 eq) were dissolved in 0.3-1 ml of solvent (depending on solubility: MeCN,
MeOH, EtOH or DMSO) under addition of 2-3 drops of Et_3N to ensure a pH of 8-9. This pH was
necessary to prevent protonation of the amino group, which would impair the reaction. The
succinimidyl esters of the fluorescent dyes (1 eq) were dissolved in 0.5-1.5 ml of the appropriate
solvent (MeCN, MeOH) and added to the amine containing solution. The reaction was per-
formed in small flasks at rt under stirring in the dark overnight. Purification was performed by
preparative HPLC. Prior to preparative HPLC the mixtures were adjusted to a volume of 4-5 ml,
containing the same amount of MeCN/TFA as the starting eluent mixture The product containing
fractions were collected, MeCN was evaporated under reduced pressure and the remaining wa-
ter was removed by lyophilisation. The fluorescent compounds were obtained as yellow or blue
semi solids.

Labelling of amines with Py- dyes

Primary amines (1-2.5 eq) were dissolved in 1.2 ml MeOH and Et_3N was added to ensure a pH of
8-9. Py1 or Py5 (1 eq) were dissolved in 0.4 ml DMF plus 0-0.4 ml MeOH and added to the amine
containing solution. The reaction was performed in small flasks at rt with stirring in the dark for
3 h (solution turns from blue to red). Purification was done by preparative HPLC as described
above. MeCN was evaporated from the product fractions under reduced pressure and residual

water was removed by lyophilisation. The fluorescent compounds were obtained as red semi solids.

Compound 7.8 labelled with S0536 (8.1)

Ligand **7.8** (1.1 mg, 3.6 mmol, 1.9 eq) in 0.4 ml MeOH, + Et$_3$N (pH 8-9), S0536 (1.32 mg, 1.9 µmol, 1 eq) in 0.9 ml MeCN; preparative HPLC (system 1, 220 nm); product as blue semi solid, yield 1.35 mg (59 %); <u>RP-HPLC</u> (220 nm, gradient 1,): > 99 %, (t$_R$= 18.9 min, k= 6.44); <u>ESMS</u>: m/z 892.5 [MH$^+$], 446.6 [(M+2H)$^{2+}$]; C$_{53}$H$_{73}$N$_5$O$_5$S x C$_6$H$_3$F$_9$O$_6$ (1234)

Compound 7.9 labelled with S0536 (8.2)

Compound **7.9** (1.1 mg, 3.4 µmol, 1.8 eq) in 0.4 ml MeOH, + Et$_3$N (pH 8-9) and S0536 (1.3 mg, 1.9 µmol, 1 eq) in 0.9 ml MeCN; preparative HPLC (system 1, 220 nm); product as blue semi solid, yield 0.39 mg (17 %); <u>RP-HPLC</u> (220 nm, gradient 1): 92 %, (t$_R$= 17.1 min, k= 5.73); <u>ESMS</u>: m/z 906.5 [MH$^+$], 453.7 [(M+H)$^{2+}$]; C$_{54}$H$_{75}$N$_5$O$_5$S x C$_6$H$_3$F$_9$O$_6$ (1248)

Compound 7.9 labelled with Dy675 (8.3)

Ligand **7.9** (0.9 mg, 2.8 µmol, 1.9 eq) and Dy675 (1.2 mg, 1.5 µmol, 1 eq) in 1.4 ml MeOH, + Et$_3$N (pH 8-9); preparative HPLC (system 1, 254 nm, B: 0.5 % TFA); product as blue semi solid, yield 0.61 mg (31 %); <u>RP-HPLC</u> 1.(220 nm, gradient 1,): 97.9 %, (t$_R$= 26.5 min, k= 9.43), 2.(gradient: 0 min: 35/65, 90, 25 min 90/10, 35 min 95/10, 210 nm) 97.2 % (t$_R$= 21.2 min, k= 7.3); <u>ESMS</u>: (MeOH/0.1 % TFA) m/z 1008.5 [MH$^+$], 504.8 [(M+H)$^{2+}$]; C$_{61}$H$_{77}$N$_5$O$_6$S x C$_6$H$_3$F$_9$O$_6$S (1350)

Compound 7.9 labelled with Bodipy 650/665-X, SE (8.4)

Compound **7.9** (0.4 mg, 1.2 µmol, 2 eq) and Bodipy 650/665-X, SE (0.4 mg, 0.6 µmol, 1 eq) in 1.5 ml MeOH + Et$_3$N (pH 8-9), preparative HPLC (system 1, 254 nm); product as green to blue semi solid, yield 0.32 mg (50 %) <u>RP-HPLC</u> (210 nm, gradient 1): 99 %, (t$_R$= 19.18 min, k= 6.55); <u>ESMS</u>: m/z 848.6 [MH$^+$], 424.6 [(M+2H)$^{2+}$]; C$_{48}$H$_{60}$BF$_2$N$_7$O$_4$ x C$_4$H$_2$F$_6$O$_4$ (1076)

Compound 7.9 labelled with 5-SFX (8.5)

Compound **7.9** (0.95 mg, 2.98 µmol, 2 eq) and 5-SFX (0.9 mg, 1.5 µmol, 1 eq) in 1.2 ml MeOH, +
Et_3N (pH 8-9); preparative HPLC (system 1, 254 nm); product as yellow semi solid, yield 1.01 mg
(66 %); RP-HPLC (210 nm, gradient 1): > 99 %, (t_R= 13.7 min, k= 4.37); ESMS: (MeOH/0.1 % TFA)
m/z 791.3 [MH^+], 396.2 [$(M+2H)^{2+}$]; $C_{46}H_{54}N_4O_8$ x $C_4H_2F_6O_6$ (1019)

Compound 7.9 labelled with Py5 (8.6)

Ligand **7.9** (2.6 mg, 8.1 µmol, 2 eq) in 1.2 ml MeOH, + Et_3N (pH 8-9) and Py5 (1.5 mg, 4.1 µmol, 1
eq) in 400 µl DMF + 0.4 ml MeOH; preparative HPLC (system 1, 254 nm, B: 0.5 % TFA), red semi
solid, yield 1.07 mg (28 %); RP-HPLC (210 nm, gradient 1) 98.3 %, (t_R= 13.5 min, k= 4.3); ESMS:
m/z 581.3 [M^+], 291.1 [$(M+H)^{2+}$]; $C_{38}H_{53}N_4O^+$ x $C_6H_3F_9O_6$, (924)

Compound 7.6 labelled with Py1 (8.7)

Ligand **7.6** (5.5 mg, 11.6 µmol, 2.5 eq) in 1.2 ml MeOH + Et_3N (pH 8-9) and Py1 (1.8 mg, 4.6 µmol,
1 eq) in 400 µl DMF + 0.4 ml MeOH; preparative HPLC (system 1, 254 nm, B: 0.5 %TFA); product
as red semi solid, yield 0.98 mg (28 %); RP-HPLC (220 nm, gradient 1): 94.5 %, (t_R= 20.5 min, k=
7.1); ESMS: m/z 536.3 [M^+], 268.6 [$(M+H)^{2+}$]; $C_{36}H_{46}N_3O^+$ x $C_4H_2F_6O_4$ (765)

Compound 7.6 labelled with S0535 (8.8)

Compound **7.6** (1.8 mg, 3.8 µmol , 1.6 eq) and S0535 (1.8 mg, 2.4 µmol, 1 eq) in 2.0 ml MeCN +
Et_3N (pH 8-9); preparative HPLC (system 2-1, 220 nm); product as blue semi solid, yield 2.27 mg
(85 %); RP-HPLC 1. (220nm, gradient 1): 99 %, (t_R= 22.4 min, k= 7.82), 2. (gradient: 0 min: 35/65,
90, 25 min 90/10, 35 min 95/10, 210 nm) 99 % (t_R= 21.2 min, k= 7.3); ESMS: m/z 885.7 [MH^+],
443.2 [$(M^++H)^{2+}$]; $C_{54}H_{68}N_4O_5S$ x $C_4H_2F_6O_4$ (1113)

Compound 7.16 labelled with S0535 (8.9)

Compound **7.16** (2 mg, 3.1 µmol, 1.5 eq) in 0.9 ml MeOH + Et$_3$N (pH 8-9), S0535 (1.6 mg, 2.1 µmol, 1 eq) in 0.9 ml MeOH; preparative HPLC (system 2-1, 220 nm); product as blue semi solid, yield 1.11 mg (41 %); RP-HPLC: 1. (gradient 1, 220 nm) 99 % (t$_R$= 22.9 min, k= 8.0), 2. (gradient: 0 min: 35/65, 90, 20 min 90/10, 30 min 90/10, 220 nm) 99.2 % (t$_R$= 20,0 min, k= 6.87); ESMS: m/z 1051.8 [MH$^+$], 525.9 [(M+2H)$^{2+}$]; C$_{62}$H$_{78}$N$_6$O$_7$S x C$_4$H$_2$F$_6$O$_6$ (1279)

Compound 7.16 labelled with Dy630 (8.10)

Ligand **7.16** (1.7 mg, 2.6 µmol, 1.9 eq) and Dy630 (1.0 mg, 1.4 µmol, 1 eq) in 2.5 ml MeCN + Et$_3$N (pH 8-9); preparative HPLC (system 2-1, 220 nm); 2 purification steps necessary; product as blue semi solid, yield 0.15 mg (9 %) RP-HPLC 1. (220 nm, gradient 1): > 99 %, (t$_R$= 21.3 min, k= 7.39), 2. (gradient: 0 min: 35/65, 90, 25 min 90/10, 35 min 95/10, 210 nm) 99 % (t$_R$= 19.9 min, k= 6.9); ESMS: m/z 1031.8 [MH$^+$], 516.5 [(M+2H)$^{2+}$]; C$_{59}$H$_{78}$N$_6$O$_8$S x C$_4$H$_2$F$_6$O$_4$ (1259)

Compound 7.7 labelled with S0535 (8.11)

Ligand **7.7** (3.0 mg, 5.4 µmol, 1.4 eq), S0535 (2.9 mg, 3.9 µmol, 1 eq) in 2.0 ml MeCN, + Et$_3$N (pH 8-9); Preparative HPLC (system 2-1, 220 nm); blue semi solid 2.36 mg (46 %); RP-HPLC (220nm, gradient 1): 94 %, (t$_R$= 18.8 min, k= 6.4); ESMS: m/z 968.8 [MH$^+$], 484.8 [(M+H)$^{2+}$]; C$_{59}$H$_{77}$N$_5$O$_5$S x C$_6$H$_3$F$_9$O$_6$ (1310)

Compound Fp 05 labelled with S0535 (8.12)

Ligand **UR-FP 05** x 3 HCl (1-{4-[3-(piperidin-1-yl)propoxy]benzyl}piperidin-4-amine) (4 mg, 9.1 µmol, 2 eq) in 1 ml MeOH + Et$_3$N (pH 8-9), S0535 (3.48 mg, 4.6 µmol, 1 eq) in 2.0ml MeOH; pre-parative HPLC (system 2-1, 220 nm); product as blue semi solid, yield 2.2 mg (37 %), RP-HPLC: 1. (gradient 1, 220 nm) 99.5 % (t$_R$= 19.96 min, k= 6.86), 2.(gradient: 0 min: 35/65, 90, 20 min 90/10, 30 min 90/10, 220 nm) 99.5 % (t$_R$= 16.2 min, k= 5.36); ESMS: m/z 968.8 [MH$^+$], 485.0 [(M+2H)$^{2+}$], C$_{59}$H$_{77}$N$_5$O$_6$S x C$_6$H$_3$F$_9$O$_6$ (1310)

8.7   Pharmacological methods

8.7.1.1   Steady state GTPase assay

See chapter 3

8.7.1.2   Fluorimetric Ca²⁺ assay on U373-MG cells

See chapter 3

8.7.1.3   Radioligand binding assay on HEK293-FLAG-hH₃R-His6 cells

See chapter 3

8.7.1.4   Radioligand binding assay on HEK293-FLAG-hH₄R-His6 cells

See chapter 8

8.7.1.5   Quantum yield

Measurements were conducted according to the procedure described in chapter 6.

8.7.1.6   Flow cytometric saturation binding experiments

Experiments were performed on HEK-293-FLAG-hH$_3$R-His$_6$ cells (kindly provided by David Schnell, Department of Pharmacology and Toxicology, University of Regensburg). Cell culture was performed as described in chapter 3 for the radioligand binding assays on HEK-293-FLAG-hH$_3$R-His$_6$ cells. The preparation of the cells was done according to the procedure described for HEK-293-hH$_2$R-qs5-HA cells in chapter 6 with minor modifications. Cells were grown prior to the experiment to a confluency of 50-60 % and adjusted to a concentration of 1-2 mio cells/ml for the experiment. Incubation was performed for 15 min in the dark. To determine the amount of unspecific binding 10 µM thioperamide were used (final concentration).

8.7.1.7   Confocal microscopy

Confocal microscopy was performed by analogy with the procedure described in chapter 6 using HEK-293-FLAG-hH3R-His6 cells. Unspecific binding was determined in the presence of either thioperamide (10 µM, final c) or JNJ5207852 (2 µM, final c) (see microscopic pictures)

References

1.   Amon, M.; Ligneau, X.; Schwartz, J. C.; Stark, H. Fluorescent non-imidazole histamine H$_3$ receptor ligands with nanomolar affinities. *Bioorg. Med. Chem. Lett.* **2006,** 16, 1938-40.

2.   Amon, M.; Ligneau, X.; Camelin, J. C.; Berrebi-Bertrand, I.; Schwartz, J. C.; Stark, H. Highly potent fluorescence-tagged nonimidazole histamine H$_3$ receptor ligands. *ChemMedChem* **2007,** 2, 708-16.

3.   Cowart, M.; Gfesser, G. A.; Bhatia, K.; Esser, R.; Sun, M.; Miller, T. R.; Krueger, K.; Witte, D.; Esbenshade, T. A.; Hancock, A. A. Fluorescent benzofuran histamine H($_3$) receptor antagonists with sub-nanomolar potency. *Inflammation Res.* **2006,** 55 Suppl 1, S47-8.

4.   Kuder, K. J.; Kottke, T.; Stark, H.; Ligneau, X.; Camelin, J. C.; Seifert, R.; Kiec-Kononowicz, K. Search for novel, high affinity histamine H$_3$ receptor ligands with fluorescent properties. *Inflammation Res.* **2010,** 59 Suppl 2, S247-8.

5.   Cowart, M.; Faghih, R.; Curtis, M. P.; Gfesser, G. A.; Bennani, Y. L.; Black, L. A.; Pan, L.; Marsh, K. C.; Sullivan, J. P.; Esbenshade, T. A.; Fox, G. B.; Hancock, A. A. 4-(2-[2-(2(R)-methylpyrrolidin-1-yl)ethyl]benzofuran-5-yl)benzonitrile and related 2-aminoethylbenzofuran H$_3$ receptor antagonists potently enhance cognition and attention. *J. Med. Chem.* **2005,** 48, 38-55.

6.   Esbenshade, T. A.; Fox, G. B.; Krueger, K. M.; Miller, T. R.; Kang, C. H.; Denny, L. I.; Witte, D. G.; Yao, B. B.; Pan, L.; Wetter, J.; Marsh, K.; Bennani, Y. L.; Cowart, M. D.; Sullivan, J. P.; Hancock, A. A. Pharmacological properties of ABT-239 [4-(2-{2-[(2R)-2-Methylpyrrolidinyl]ethyl}-benzofuran-5-yl)benzonitrile]: I. Potent and selective histamine H$_3$ receptor antagonist with drug-like properties. *J. Pharmacol. Exp. Ther.* **2005,** 313, 165-75.

7.   Sun, M.; Zhao, C.; Gfesser, G. A.; Thiffault, C.; Miller, T. R.; Marsh, K.; Wetter, J.; Curtis, M.; Faghih, R.; Esbenshade, T. A.; Hancock, A. A.; Cowart, M. Synthesis and SAR of 5-amino- and 5-(aminomethyl)benzofuran histamine H3 receptor antagonists with improved potency. *J. Med. Chem.* **2005,** 48, 6482-90.

8.   Ghorai, P.; Kraus, A.; Keller, M.; Gotte, C.; Igel, P.; Schneider, E.; Schnell, D.; Bernhardt, G.; Dove, S.; Zabel, M.; Elz, S.; Seifert, R.; Buschauer, A. Acylguanidines as bioisosteres of guanidines: NG-acylated imidazolylpropylguanidines, a new class of histamine H$_2$ receptor agonists. *J. Med. Chem.* **2008,** 51, 7193-204.

9.   Schnell, D. *Personal communication*. In Department of Pharmacology and Toxicology, University of Regensburg (Germany), **2008**.

10.   Nordemann, U. *Personal communication*. In Department of Pharmaceutical and Medicinal Chemistry II, University of Regensburg (Germany), **2009**.

11.   Seifert, R.; Wenzel-Seifert, K.; Burckstummer, T.; Pertz, H. H.; Schunack, W.; Dove, S.; Buschauer, A.; Elz, S. Multiple differences in agonist and antagonist pharmacology between human and guinea pig histamine H$_1$-receptor. *J. Pharmacol. Exp. Ther.* **2003,** 305, 1104-15.

12.   Igel, P.; Schnell, D.; Bernhardt, G.; Seifert, R.; Buschauer, A. Tritium-labeled N(1)-[3-(1H-imidazol-4-yl)propyl]-N(2)-propionylguanidine ([(^{3})H]UR-PI294), a high-affinity histamine H($_3$) and H($_4$) receptor radioligand. *ChemMedChem* **2009,** 4, 225-31.

13.   Kelley, M. T.; Burckstummer, T.; Wenzel-Seifert, K.; Dove, S.; Buschauer, A.; Seifert, R. Distinct interaction of human and guinea pig histamine H_2-receptor with guanidine-type agonists. *Mol. Pharmacol.* **2001,** 60, 1210-25.

14.   Preuss, H.; Ghorai, P.; Kraus, A.; Dove, S.; Buschauer, A.; Seifert, R. Constitutive activity and ligand selectivity of human, guinea pig, rat, and canine histamine H_2 receptors. *J. Pharmacol. Exp. Ther.* **2007,** 321, 983-95.

15.   Schneider, E. *Personal communication*. In Department of Pharmacology and Toxicology, University of Regensburg, **2008**.

16.   Mosandl, J. Radiochemical and luminescence-based binding and functional assays for human histamine receptors using genetically engineered cells. *Doctoral thesis*, University of Regensburg, Germany, http://epub.uni-regensburg.de/12335/, **2009**.

17.   Keller, M. Guanidine-acylguanidine bioisosteric approach to address peptidergic receptors: pharmacological and diagnostic tools for the NPY Y_1 receptor and versatile building blocks based on arginine substitutes. *Doctoral Thesis*, University of Regensburg, Germany, http://epub.uni-regensburg.de/12092/, **2008**.

Chapter 9

Summary

9 Summary

G-protein coupled receptors represent one of the largest families in the druggable human genome, targeted by a multitude of currently available drugs and are regarded as promising biological targets for the discovery of new drugs as well. Histamine receptors, as typical aminergic GPCRs, are subject of an extensive research project in our laboratory, aiming at receptor subtype (H_1R, H_2R, H_3R, H_4R) selective agonists and antagonists, including radiolabeled and fluorescence ligands. The H_2-receptor (H_2R) plays a key role in gastric acid secretion and H_2R antagonists, developed in the late 1970s, revolutionized the treatment of peptic ulcer and gastric acid related diseases. Antagonists targeting the H_3-receptor (H_3R) are regarded as potential drugs for the treatment of CNS disorders, such as sleep and wake disorders or schizophrenia.

In order to extend our knowledge about structure-activity and structure-selectivity relationships this work aimed at the synthesis and pharmacological characterization of novel histamine H_2R and H_3R taking into account the development and application of new radiolabeled or fluorescent pharmacological tools. Additionally, the application of the bivalent ligand approach was explored. The synthesized compounds were investigated in steady state GTPase assays on membranes of Sf9 cells expressing the human (or guinea pig) receptor of interest and in radioligand binding studies on Sf9 cell membranes or H_xR expressing mammalian cells. In addition, fluorescence based methods were applied such as calcium assays, flow cytometry and confocal microscopy.

Histamine H_2R antagonists: In the first series of H_2R antagonists the "urea equivalent", i.e. the cyanoguanidine group, in piperidinomethylphenoxyalkylamine-type compounds derived from potentidine, was replaced with squaramides, amides and nitroethenediamine moieties and/or coupled to ω-aminoalkyl spacers allowing for labelling reactions or bivalent ligand construction. By analogy, cimetidine- and tiotidine-like compounds were synthesized. The potentidine-derived compounds were potent antagonists with high selectivity for the H_2R over the H_1R and H_4R, but with moderate selectivity compared to the H_3R. Highest H_2R antagonist activity resided in aminoalkyl-substituted squaramides ($K_{b'}$-values ranging from 1 to 200 nM); the selectivity of these compounds versus the H_3R improved with the chain lengths of the alkyl spacers. Bivalent ligands such as N^2-[3-(3-piperidin-1-ylmethylphenoxy)propyl]squaric diamides, dimerized by alkanediyl spacers of different length attached to N^1, achieved H_2R antagonistic potencies in the one-digit nanomolar range. Highest H_2R selectivity was obtained with 8- and 10-membered alkyl chains. Coupling of the corresponding N^1-(6-aminohexyl)-substituted squaramide with [2,3-^{3}H]propionic

acid yielded a new highly potent tritiated H_2R antagonist [^{3}H]UR-DE257 ([2,3-^{3}H]-N-((3,4-dioxo-2-(3-(3-(piperidin-1-ylmethyl)phenoxy)propylamino)cyclobut-1-enylamino)hexyl)propionamide; (K_D saturation: 27 nM), which was successfully applied for the determination of H_2R ligand affinities in competition binding experiments. Aiming at fluorescent ligands several amine precursors from the H_2R antagonist series were employed and linked to different fluorophores such as, cyanine, bodipy and pyrylium (Py) dyes. Examples of the most potent compounds ($K_{b'}$-values 20 - 200 nM) were successfully applied in confocal microscopy and flow cytometric equilibrium binding studies (saturation and competition binding).

Histamine H_3R antagonists: The same approach, which led to radio- and fluorescence-labeled H_2R antagonists, was applied to H_3R ligands. Building blocks having similar structural features as the piperidinomethylphenoxyalkylamine-type H_2R ligands, but with a different substitution (para instead of meta) at the phenoxy moiety were used. Comparable structural motifs are present in potent H_3R antagonists such as JNJ5207852. Modifications by introduction of flexible alkylamine spacers, aminopiperidines, squaramides, 4-F-benzoic and propionic acid residues were carried out. Most of these variations were tolerated. The p-F-benzamide derivative turned out to be a highly potent H_3R antagonist ($K_{b'}$ 5.2 nM) and a promising lead compound for the development of potential PET ligands. The squaramides were found to be only moderately selective for the H_3R over the H_2R. Inversely, reduced selectivity was also characteristic of squaramide-typ H_2R antagonists. Thus, the squaramide residue was identified as a moiety confering affinity to both histamine receptors and accounting for the loss of selectivity. Coupling of fluorophores to the primary amine residues of the new H_3R antagonists resulted in fluorescent compounds with partly increased activity at the receptor compared to the parent compound. Among the most potent ones ($K_{b'}$ 5 - 20 nM) selected candidates proved to be suitable for the determination of H_3R binding constants by flow cytometry and for application in confocal microscopy.

In conclusion, the structural modifications of the piperidinomethylphenoxyalkylamine motif provided potent H_2R and H_3R antagonists and new insights into structure-activity and structure-selectivity relationships. In principle, the new fluorescent probes enable fluorescence based investigations to identify new H_2R or H_3R ligands. They are useful tools for more detailed pharmacological investigations and for the detection of the receptor subtypes on cells and in tissues. Additionally, a straightforward approach to the preparation of radiolabeled compounds was applied, resulting in a new H_2R radioligand ([^{3}H]UR-DE257) and paving the way to potential H_3R PET ligands.

Chapter 10

Appendix

10 Appendix

A1:

Activities at the hH$_1$R and hH$_4$R (GTPase assays)

Table 10.1: Activities and efficacies of selected substances determined in GTPase assays[a] on Sf9 cell membranes expressing the hH$_1$R[1] or the hH$_4$R[2]

Compd.	hH$_1$R +RGS4	hH$_4$R-RGS19+ G$_{i\alpha2}$+G$_{\beta1\gamma2}$	
	E$_{max}$	K$_{b'}$ [nM]	E$_{max}$
Histamine	1.0	12 ± 3	1.0
Thioperamide	-0.01		-0.61 ± 0.03
JNJ5207852	-0.02 ± 0.01	No activity	-0.09 ± 0.05
Mepyramine	-0.06 ± 0.01	n.d.	-0.06
JNJ77777	n.d.	16 ± 5	-0.05
3.5	0.019 ± 0.01	> 1000	-0.09 ± 0.02
3.6	-0.05 ± 0.00	> 1000	-0.16 ± 0.04
3.7	-0.04 ± 0.02	n.d.	-0.01 ± 0.02
3.8	0.041 ± 0.06	n.d.	-0.08 ± 0.04
3.9	0.02 ± 0.02	n.d.	0.00
3.10	-0.03 ± 0.01	n.d.	0.133 ± 0.04
3.11	-0.04 ± 0.02	n.d.	0.0
3.12	-0.2 ± 0.01	n.d.	-0.07
3.13	-0.03 ± 0.00	No activity	-0.12
3.14	-0.07 ± 0.03	n.d.	0.2 ± 0.05
3.15	-0.12 ± 0.16	n.d.	-0.28 ± 0.13
3.16	-0.04 ± 0.1	> 1000	-0.12
3.24	0.05	n.d.	n.d.
3.28	0.01 ± 0.01	No activity	0.00
4.3	-0.13 ± 0.01	No activity	-0.28 ± 0.03
4.4	-0.011 ± 0.008	n.d.	-0.1
4.5	0.032 ± 0.022	n.d.	-0.15 ± 0.03
4.6	-0.039 ± 0.02	n.d.	-0.12 ± 0.04
4.7	-0.034 ± 0.023	n.d.	-0.07 ± 0.05
4.8	0.022 ± 0.025	n.d.	-0.123
5.2	-0.03 ± 0.04	> 5000	0.004
5.4	0.002	n.d.	0.052
5.5	0.02	n.d.	-0.048 ± 0.07
5.6	-0.32 ± 0.01	n.d.	0.03 ± 0.02
5.7	-0.018 ± 0.018	n.d.	-0.04
5.8	0.13 ± 0.13	n.d.	0.007 ± 0.06
5.9	0.02 ± 0.01	n.d.	-0.16 ± 0.02
5.10	0.031 ± 0.035	No activity	0.042 ± 0.048
5.11	-0.06 ± 0.013	n.d.	-0.065 ± 0.12

| Compd. | hH$_1$R +RGS4 | hH$_4$R-RGS19+ G$_{i\alpha2}$+G$_{\beta1\gamma2}$ | |
	E$_{max}$	K$_{b'}$ [nM]	E$_{max}$
6.1	-0.05 ±0.03	> 5000	-0.21 ± 0.01
6.2	-0.07 ± 0.05	n.d.	-0.1
6.3	-0.04 ± 0.02	n.d.	-0.1
6.4	-0.8 ± 0.03	> 1000	-0.4
6.5	-0.13 ± 0.08	> 3000	-0.2
6.6	0.05	> 5000	-0.3
6.7	-0.13 ± 0.05	> 5000	-0.13
6.8	-0.29 ± 0.04	n.d.	n.d
6.9	-0.03 ± 0.01	> 2000	-0.19 ± 0.08
6.10	-0.03 ± 0.00	> 10000	-0.2 ± 0.14
6.11	-0.01 ± 0.05	> 10000	-0.09 ± 0.05
6.12	-0.06 ± 0.03	> 5000	-0.32 ± 0.27
6.13	-0.07 ± 0.1	> 5000	-0.04 ± 0.04
6.14	-0.02 ± 0.004	> 2000	-0.2 ± 0.1
6.15	-0.06 ± 0.01	> 2000	-0.2 ± 0.13
6.16	-0.05 ± 0.01	n.d.	-0.022 ± 0.06
6.17	-0.02 ± 0.02	> 2000	-0.18 ± 0.18
6.18	-0.03 ± 0.02	632 ± 107	-0.1
6.19	-0.03 ± 0.03	449	-0.1 ± 0.01
6.20	n.d.	n.d.	-0.07 ± 0.08
6.21	-0.07	> 5000	-0.05
6.22	-0.08 ± 0.04	> 5000	-0.3
6.23	-0.07 ± 0.00	> 5000	-0.2 ± 0.07
6.24	-0.02 ± 0.03	> 5000	-0.27 ± 0.06
6.26	0.0 ± 0.05	n.d.	-0.03
6.27	-0.03 ± 0.04	n.d.	-0.03
6.28	-0.08 ± 0.01	> 5000	-0.6
6.29	-0.04 ± 0.04	n.d.	n.d.
7.6	-0.09	> 3000	-0.04 ± 0.34
7.7	-0.04 ± 0.02	> 10000	-0.05 ± 0.05
7.8	-0.06 ± 0.01	> 1000	0.05 ± 0.0
7.9	-0.04 ± 0.04	> 1000	-0.05 ± 0.34
7.10	-0.01 ± 0.02	> 2000	-0.13
7.11	0.00 ± 0.03	> 2000	n.d.
7.12	0.06 ± 0.02	> 2000	-0.09
7.13	0.004 ± 0.01	> 2000	-0.18
7.16	-0.02 ± 0.02	> 1000	-0.07 ± 0.0
8.1	-0.05 ± 0.04	> 3000	-0.13 ± 0.01
8.2	-0.06 ± 0.05	> 5000	-0.05 ± 0.03
8.3	-0.08 ± 0.01	> 2000	-0.31 ± 0.17
8.4	-0.06 ± 0.03	436 ± 10	-0.32 ± 0.2
8.5	0.01 ± 0.00	> 5000	-0.1 ± 0.07
8.6	-0.09 ± 0.04	5395 ± 1693	-0.31 ± 0.1

Compd.	hH$_1$R +RGS4	hH$_4$R-RGS19+ G$_{i\alpha2}$+G$_{\beta1\gamma2}$	
	E$_{max}$	K$_{b'}$ [nM]	E$_{max}$
8.7	-0.042 ± 0.04	> 10000	-0.29 ± 0.18
8.8	0.001	3684 ± 392	-0.12 ± 0.18
8.9	-0.05 ± 0.03	> 2000	-0.36 ± 0.12
8.10	-0.05	> 1000	-0.4 ± 0.1
8.11	0.08	> 1000	-0.46 ± 0.14
8.12	-0.06 ± 0.02	> 4000	-0.44

[a] steady state GTPase assay on Sf9 cell membranes; ; ligands were used at concentrations from 1 nM to 100 µM; typical GTPase activities (stimulation with 100 nM HIS (hH$_4$R): 2.5-5.0 pmol x mg^{-1} x min^{-1}; intrinsic activity, relative to histamin, E$_{max}$: HIS=1 (c. ligands: 10 µM, f. efficacy), Mean values ± S.E.M. (n = 1-3) performed in duplicate; n.d.: not determined

A2

Antagonism at the hH$_1$R, determined on U-373 MG cells (Ca^{2+} assay)

Table 10.2: hH$_1$R antagonism of compounds designed as H$_2$R and H$_3$R ligands in the fluorimetric Ca^{2+} assay[a] (fura-2 assay) on U-373 MG cells[3]

Compd.	U-373 MG cells IC$_{50}$ [µM]	Compd.	U-373 MG cells IC$_{50}$ [µM]
3.5	> 150	5.2	> 100
3.6	75	5.4	39
3.7	81	5.5	100
3.8	> 30	5.6	> 100
3.9	> 100	5.7	> 100
3.10	> 100	5.8	> 100
3.11	> 100	5.9	> 100
3.12	> 100	5.10	> 100
3.13	> 100	5.11	34
3.14	35	7.6	> 50
3.15	>10	7.7	> 50
3.24	>50	7.8	> 50
3.28	48	7.9	> 50
4.3	> 5	7.11	28
4.4	> 50	7.10	> 100
4.5	> 100	7.12	>50
4.6	> 50	7.13	3.6
4.7	25	7.16	> 50
4.8	> 100		

[a]c. ligands: 1 µM-100 µM, c. HIS: 30 µM; Mean values (n = 2-4) performed in duplicate; n.d.: not determined

B1

Flow cytometric measurements on HEK293-hH$_2$R-qs5-HA cells (saturation binding[4])
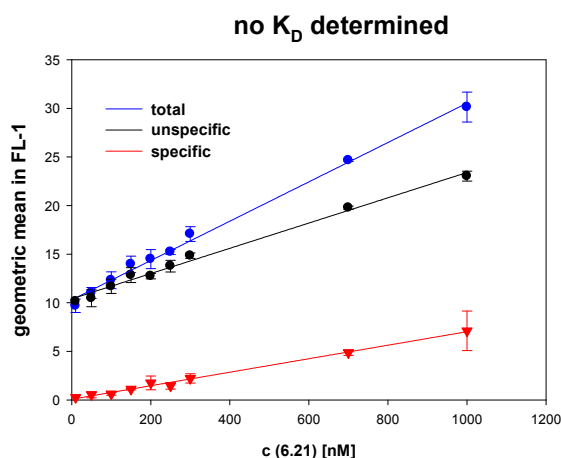
K$_D$ = 44 +/- 14 nM
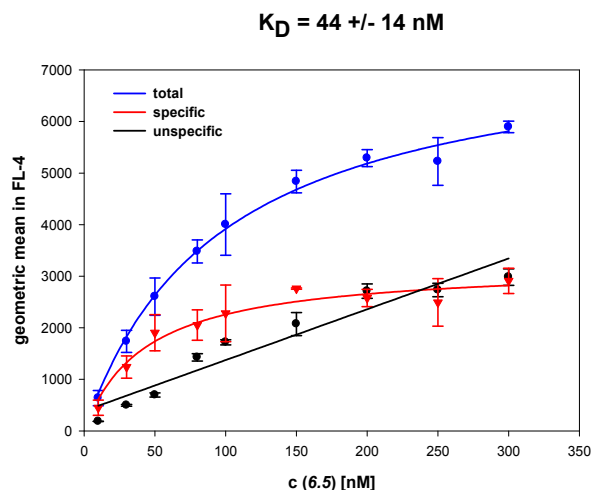
Figure 10.1: Saturation binding of **6.5** on HEK293-hH$_2$R-qs5-HA cells (mean values ± S.E.M, n=3), unspecific binding determined in the presence of famotidine (c final: 30 µM), incubation time: 37 min, rt

K$_D$ = 276 +/- 72 nM
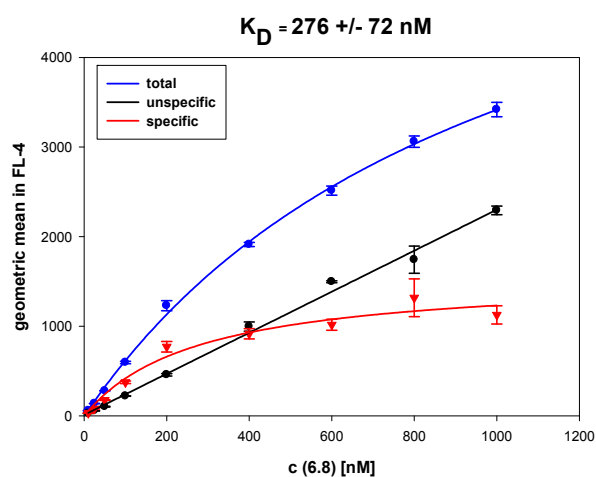
Figure 10.2: Saturation binding of **6.8** on HEK293 -hH$_2$R-qs5-HA cells (mean values ± S.E.M, n=3), unspecific binding determined in the presence of famotidine (c final: 30 µM), incubation time: 37 min, rt

K$_D$ = 351+/- 8 nM
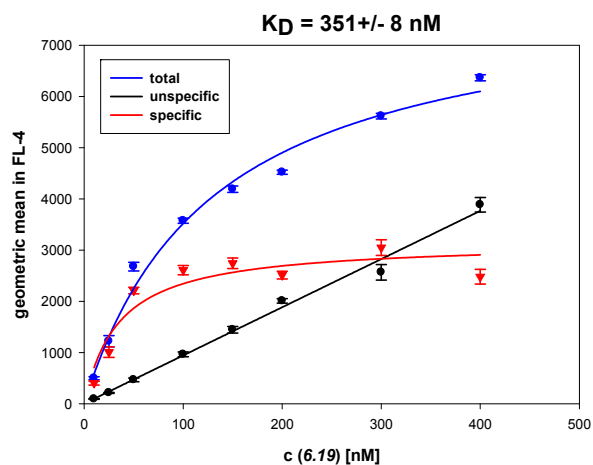
Figure 10.3: Saturation binding of **6.19** on HEK293-hH$_2$R-qs5-HA cells (mean values ± S.E.M, n=3), unspecific binding determined in the presence of famotidine (c final: 30 µM), incubation time: 37 min, rt

no K$_D$ determined

Figure 10.4: Saturation binding of **6.21** on HEK293-hH$_2$R-qs5-HA cells (mean values ± S.E.M, n=3), unspecific binding determined in the presence of famotidine (c final: 30 µM), incubation time: 37 min, rt

B2

Confocal microsopy with H$_2$R fluorescent ligands on HEK293-FLAG-hH$_2$R-His$_6$ cells

E1 — Total binding of **6.7** (c: 300nM), 48 min

E2 — Unspecific binding of **6.7** (c: 300nM), + 10 µM famotidine, 50 min
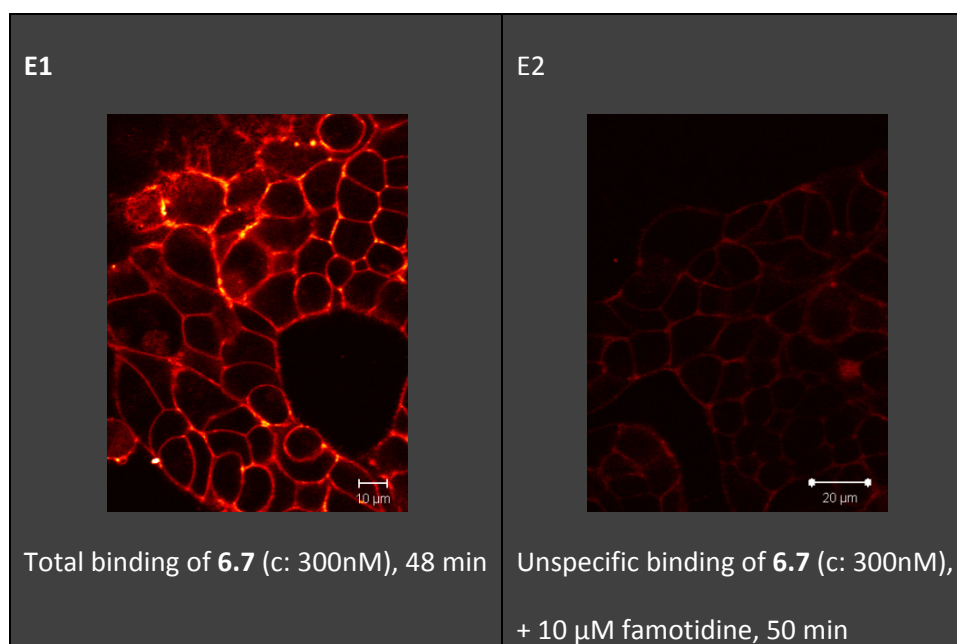
Figure 10.5: Binding of **6.7** to the H$_2$R expressed in HEK293 FLAG-hH$_2$R-His$_6$ cells; cells were incubated in Leibovitz culture medium with 1 % FCS for 30 min at 37 °C; C-Apochromat 40x/1.2W, 633 nm/LP650 (pinhole 90 µm
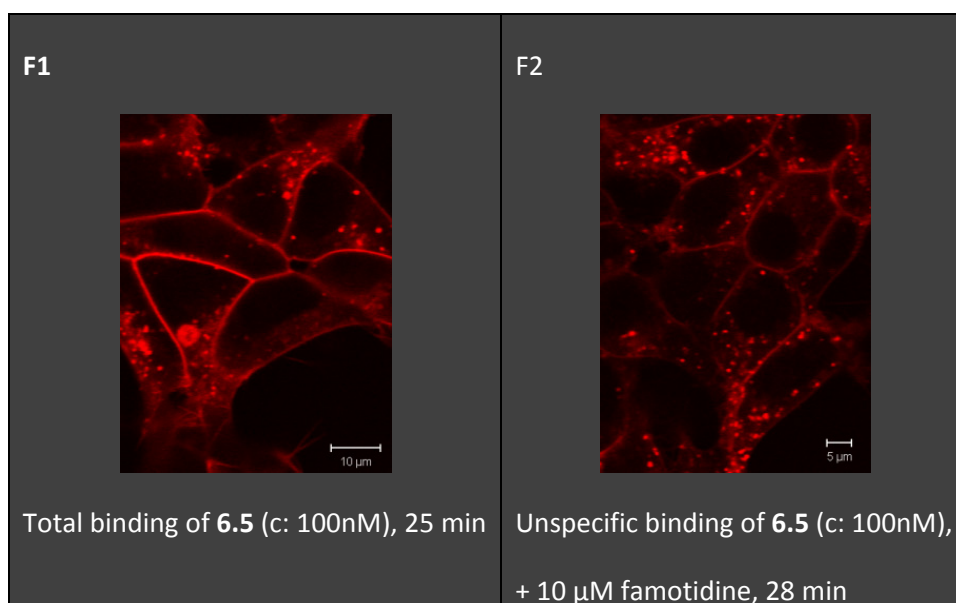
Figure 10.6: Binding of **6.5** to the H_2R expressed in HEK293 FLAG-hH_2R-His$_6$ cells; cells were incubated in Leibovitz culture medium with 1 % FCS for 30 min at 37 °C; C-Apochromat 40x/1.2W, 633 nm/LP650 (pinhole 90 µm

References

1.   Seifert, R.; Wenzel-Seifert, K.; Burckstummer, T.; Pertz, H. H.; Schunack, W.; Dove, S.; Buschauer, A.; Elz, S. Multiple differences in agonist and antagonist pharmacology between human and guinea pig histamine H1-receptor. *J. Pharmacol. Exp. Ther.* **2003,** 305, 1104-15.

2.   Ghorai, P.; Kraus, A.; Keller, M.; Gotte, C.; Igel, P.; Schneider, E.; Schnell, D.; Bernhardt, G.; Dove, S.; Zabel, M.; Elz, S.; Seifert, R.; Buschauer, A. Acylguanidines as bioisosteres of guanidines: NG-acylated imidazolylpropylguanidines, a new class of histamine H_2 receptor agonists. *J. Med. Chem.* **2008,** 51, 7193-204.

3.   Kracht, J. Bestimmung der Affinität und Aktivität subtypselektiver Histamin- und Neuropeptid Y-Rezeptorliganden an konventionellen und neuen pharmakologischen In-vitro-Modellen. *Doctoral thesis*, University of Regensburg, **2001**.

4.   Mosandl, J. Radiochemical and luminescence-based binding and functional assays for human histamine receptors using genetically engineered cells. *Doctoral thesis*, University of Regensburg, Germany, http://epub.uni-regensburg.de/12335/, **2009**.

Ich erkläre hiermit an Eides statt, dass ich die vorliegende Arbeit ohne unzulässige Hilfe Dritter und ohne Benutzung anderer als der angegebenen Hilfsmittel angefertigt habe; die aus anderen Quellen direkt oder indirekt übernommenen Daten und Konzepte sind unter Angabe des Literaturzitats gekennzeichnet.

Regensburg,

_____

Daniela Erdmann